

Aus dem Institut für Laboratoriumsmedizin, Klinische Chemie und
Pathobiochemie der Medizinischen Fakultät
Charité – Universitätsmedizin Berlin

DISSERTATION

Modifikation der Expression von Sialinsäuren auf der
Zelloberfläche mit *N*-Acetylmannosamin-Analoga

zur Erlangung des akademischen Grades

Doctor medicinae (Dr. med.)

vorgelegt der Medizinischen Fakultät
Charité – Universitätsmedizin Berlin

von

Paul Robin Wratil

aus Bergisch Gladbach

Datum der Promotion: 25.06.2017

Inhaltsverzeichnis

Zusammenfassung.....	3
Abstract	3
Einführung.....	4
Methodik	7
Ergebnisse	13
Diskussion.....	17
Literaturverzeichnis.....	21
Eidesstattliche Versicherung.....	23
Anteilserklärung an den erfolgten Publikationen	23
Druckexemplare der ausgewählten Publikationen	25
A novel approach to decrease sialic acid expression in cells by a C-3-modified <i>N</i> -acetylmannosamine	25
Mouse siglec-1 mediates trans-infection of surface-bound murine leukemia virus in a sialic acid <i>N</i> -acyl side chain-dependent manner	51
Inhibition of the key enzyme of sialic acid biosynthesis by C6-Se modified <i>N</i> -acetylmannosamine analogs	66
Lebenslauf.....	99
Publikationsliste	100
Danksagung.....	101

Zusammenfassung

Abstract

Sialinsäure ist eine Monosaccharid-Einheit, die typischerweise an den nicht-reduzierenden Enden von Glykanen vorkommt. Sie ist direkt an einer Vielzahl von physiologischen und pathophysiologischen Zellfunktionen beteiligt. In dieser Arbeit wurden verschiedene Substrat-Analoga des Schlüsselenzyms der Sialinsäurebiosynthese, der UDP-*N*-Acetylglucosamin-2-Epimerase/*N*-Acetylmannosamin-Kinase (GNE/MNK), auf ihre Fähigkeit hin untersucht, die Zelloberflächensialylierung zu modifizieren. Ein C3-methyliertes *N*-Acetylmannosamin (ManNAc)-Derivat und ein C6-ManNAc-Diselenid-Dimer erwiesen sich als Inhibitoren der MNK-Aktivität *in vitro*. Es zeigte sich, dass die chemische Struktur der C3- und C6-Modifikationen die Hemmwirkung stark beeinflusste. Die Bindungskinetiken zwischen dem C3-methylierten ManNAc-Derivat und der MNK wurden mittels Oberflächenplasmonenresonanzspektroskopie näher untersucht. Mithilfe von Sialinsäure-bindenden Lektinen wurde gezeigt, dass die neuartigen Substratanaloga- die Zelloberflächensialylierung von Jurkat-Zellen hemmten. Hochleistungs-Flüssigkeits-Chromatographie (HPLC)-Experimente offenbarten die Reduzierung der Konzentration von Sialinsäure auf der Zelloberfläche und im Zytosol nach einer Behandlung mit dem C3-methylierten ManNAc-Analogon. C2-modifizierte ManNAc-Analoga werden von Zellen zu *N*-Acyl-modifizierten unnatürlichen Sialinsäuren verstoffwechselt. Mittels HPLC wurden die Konzentrationen von unnatürlichen Sialinsäuren auf der Zelloberfläche von 293T-Zellen gemessen. Die neu entstandenen Sialinsäure-Spezies wurden danach mithilfe der Massenspektroskopie weiter untersucht. Die hier vorgestellten Methoden zur Modifikation der Expression von Sialinsäure auf der Zelloberfläche könnten in Zukunft dafür verwendet werden, Sialinsäure-abhängige Prozesse in der Medizin und Biologie gezielt zu beeinflussen und näher zu erforschen.

Sialic acid, a monosaccharide-unit that is typically found at the non-reducing termini of glycans, is directly involved in a myriad of physiological and pathophysiological cell functions. In this work, different analogs of the key enzyme of sialic acid biosynthesis, *i.e.* the UDP-*N*-acetylglucosamine-2-epimerase/*N*-acetylmannosamine-kinase (GNE/MNK), were tested as modulators of cell surface sialylation. A C3-methyl bearing *N*-acetylmannosamine (ManNAc) derivative and a C6-ManNAc-diselenide dimer were proved to be inhibitors of MNK-activity *in vitro*. The chemical structure of the C3- and C6-modifications strongly influences their inhibitory potency. The binding kinetics between the C3-methyl ManNAc-analog and MNK were analyzed

via surface plasmon resonance. Sialic acid binding lectins were used to verify that the novel substrate analogs are capable of reducing the expression of sialic acid on the surface of Jurkat cells. Treatment of Jurkat cells with the C3-methyl ManNAc analog lead to reduced concentrations of sialic acid on the cell surface and in the cytosol, shown by high performance liquid chromatography (HPLC). In treated cells, ManNAc derivatives bearing C2-modifications are metabolized to unnatural *N*-acyl-modified sialic acids. The concentrations of unnatural sialic acids on the cell surface of 293T cells were measured via HPLC. Novel sialic species were further analyzed by mass spectrometry. The herein introduced methods to modulate the expression of sialic acid on the cell surface could be applied in future experiments to evaluate and investigate sialic acid-dependent interactions in medicine and biology.

Einführung

Glykane sind als essentieller Bestandteil der Natur allgegenwärtig. Sie bestehen aus einer oder mehreren Monosaccharid-Einheiten, die kovalent mit anderen chemischen Spezies verknüpft sind. Glykane kommen beispielsweise in Glykoproteinen, Proteoglykanen oder Glykolipiden vor. Die Glykane dieser und anderer Glykokonjugate bilden die sog. Glykokalyx – eine Schicht aus Mono-, Oligo- und Polysacchariden, welche die Zelle umgibt. Glykane nehmen an einer Vielzahl von biologischen Ereignissen teil, z.B. an Zell-Zell-, Zell-Pathogen- und Zell-Matrix-Interaktionen sowie am Zusammenspiel von Glykoproteinen mit deren Rezeptoren. Für Glykan-vermittelte biologische Prozesse sind die terminalen Monosaccharid-Einheiten der Zuckerketten von besonderer Bedeutung. Eine Monosaccharid-Einheit, die sich typischer Weise an den nicht-reduzierenden Enden von Glykanen befindet, ist Sialinsäure.^{1,2}

Sialinsäure hat ein Grundgerüst aus 9 Kohlenstoffatomen. Sie besitzt eine Carboxylgruppe an der C2-Position, die unter physiologischen Bedingungen negativ geladen ist, sowie eine Aminogruppe an der C5-Position. Die Hydroxylgruppen an den Positionen C4 und C7 – C9 können durch Acetyl-, Lactolyl-, Sulfonyl-, Phosphonyl- oder Methyl-Substituenten modifiziert sein. Es wurden über 50 verschiedene natürliche Derivate der Sialinsäure beschrieben.³ Das bedeutendste und besonders beim Menschen prädominante Sialinsäure-Derivat ist *N*-Acetylneuraminsäure (Neu5Ac).⁴

Begründet durch ihre terminale Position in Glykanen nimmt Sialinsäure an einer großen Anzahl von intermolekularen und interzellulären Interaktionen teil. Dabei kann Sialinsäure prinzipiell zwei verschiedene Funktionen einnehmen: Entweder sie dient direkt als Erkennungsstruktur für bestimmte Liganden oder Rezeptoren (Erkennung) oder sie schirmt durch ihre Größe und ihre

negative Ladung darunterliegende Monosaccharideinheiten in Glykanen ab und verhindert dadurch deren Erkennung (Anti-Erkennung).¹

Säugetierzellen exprimieren verschiedene Rezeptoren, die spezifisch an Sialinsäure binden, z.B. Selectine (C-Typ-Lektine) und Siglecs (*sialic acid-binding Ig-like lectins*, I-Typ-Lektine). Als Zelloberflächenbestandteil von Leukozyten, Thrombozyten und Endothelzellen vermitteln Selectine Sialinsäure-abhängig sog. *Tethering* und Leukozyten-*Rolling* sowie die Migration von Zellen durchs Endothel.^{5,6} Siglecs spielen eine wichtige Rolle bei der Modulation des Immunsystems.⁷ Siglec-1 kommt eine große Bedeutung bei der sog. *trans*-Infektion von bestimmten Retroviren, z.B. dem Humanen Immundefizienz-Virus (HIV), zu. Hierbei binden Sialinsäure-Reste der viralen Membranen an Siglec-1, das von dendritischen Zellen (DC) exprimiert wird.⁸ Die DC vermitteln daraufhin die *trans*-Infektion der gebundenen Viren auf die eigentlichen Zielzellen. Es wurde postuliert, dass dieser Infektionsweg deutlich effektiver ist als die direkte Infektion von T-Lymphozyten durch HIV, besonders bei Exposition gegenüber kleineren Virusmengen.⁹ Auch die Infektion durch andere pathogene Erreger läuft Sialinsäure-vermittelt ab. Ein prominentes Beispiel ist der Influenzavirus A, der mithilfe seines Kapselproteins, Hämagglutinin, an Neu5Ac auf der Wirtszelloberfläche bindet.¹⁰ Einige Bakterienspezies, u.a. *Helicobacter pylori* und *Streptococcus spp.*, exprimieren Neu5Ac-spezifische Adhäsine, die zur Bindung an Zielzellen dienen.^{11,12}

Der Anti-Erkennungs-Effekt von Sialinsäure spielt u.a. eine wichtige Rolle für die Lebenszeit von Serumglykoproteinen.¹³ Low Density Lipoproteine und Chylomikronen-Remnants beispielsweise, verlieren mit zunehmender Zirkulationsdauer ihre Sialinsäure-Reste, sodass darunterliegende Galaktose-Reste frei werden. Nach dem Verlust der schützenden Sialinsäuren werden die Glykoproteine vom sog. Ashwell-Morell-Rezeptor gebunden, der sich auf Leber-Makrophagen befindet. Dies führt zur Internalisierung und damit letztlich zur Beseitigung der Glykoproteine aus dem Plasma.¹⁴ Viele Arten von Tumorzellen zeigen eine verstärkte Expression von Sialinsäure sowie ein aberrantes Sialinsäure-Expressionsmuster auf ihrer Zelloberfläche. Dadurch wird die Erkennung dieser Zellen durch das Immunsystem erschwert.^{15,16}

Als Substrat für die Biosynthese von Sialinsäure dient UDP-*N*-Acetylglukosamin (UDP-GlcNAc). In einer 4-schrittigen Reaktionsabfolge wird UDP-GlcNAc zu Neu5Ac metabolisiert.¹⁷ Neu5Ac wird daraufhin im Nucleus zu CMP-Neu5Ac aktiviert – ein einzigartiger Schritt in der Zuckerbiochemie.¹⁸ Mithilfe eines CMP-abhängigen Antiporters wird CMP-Neu5Ac in den Golgi-Apparat verbracht.¹⁹ Dort angekommen wird Neu5Ac auf Glykokonjugat-Akzeptoren (z.B. Membranglykoproteine) transferiert, katalysiert durch Enzyme aus der Gruppe der

Sialyltransferasen.²⁰ Das Schlüsselenzym der Sialinsäure-Biosynthese ist die UDP-*N*-Acetylglucosamin-2-Epimerase/*N*-Acetylmannosamin-Kinase (GNE/MNK).²¹ Dieses bifunktionelle Enzym katalysiert die ersten beiden Reaktionen auf dem Biosyntheseweg der Sialinsäure, nämlich die Epimerisierung von UDP-GlcNAc zu *N*-Acetylmannosamin (ManNAc) und danach die ATP-abhängige Phosphorylierung von ManNAc zu ManNAc-6-Phosphat.^{22,23} Eine Änderung der Expression von Sialinsäuren in Glykanen wird folgerichtig Sialinsäure-vermittelte Interaktionen beeinflussen. Dies kann dazu eingesetzt werden, um Sialinsäure-abhängige Prozesse näher zu untersuchen, sie auf molekularbiologischer Ebene zu analysieren und neue, bisher unbekannte Sialinsäure-vermittelte Interaktionen aufzuspüren. Langfristig könnte dies eventuell zur Entwicklung therapeutischer Konzepte beitragen, mit deren Hilfe krankheitsrelevante, Sialinsäure-abhängige Prozesse beeinflusst werden können. Es existieren verschiedene Methoden zur Modifikation der Expression von Sialinsäuren: Sialidasen (Sialinsäure-spezifische Glukosidasen) können verwendet werden um Sialinsäuren aus Glykanen abzuspalten.²⁴ Ein Knock-down von Enzymen der Sialinsäure-Biosynthese führt zur verminderten Expression von Sialinsäuren auf der Zelloberfläche.²¹ Zwei weitere Methoden zur Beeinflussung der Sialinsäure-Expression sind die Inhibition der Sialinsäure-Biosynthese und das sog. metabolische Glycoengineering (MGE).²⁵ Zur Hemmung der Sialinsäure-Biosynthese werden Substratanaloga verwendet, die bestimmte Enzyme des Stoffwechselweges inhibieren. Beim MGE werden ebenfalls Substratanaloga eingesetzt. Diese werden jedoch von den Zellen zu unnatürlichen Sialinsäuren metabolisiert und anschließend auf neu synthetisierte Glykokonjugate übertragen.²⁶

Für das Schlüsselenzym der Sialinsäurebiosynthese, die GNE/MNK, wurden bereits Inhibitoren entwickelt, die in ihrer Struktur die natürlichen Substrate, UDP-GlcNAc und ManNAc, nachahmen.²⁷⁻²⁹ Diese bisherigen GNE/MNK-Inhibitoren haben den Nachteil, dass sie membranimpermeabel und ungeeignet für Versuche *in cellula* sowie *in vivo* sind. Die Gruppe der Sialyltransferasen bildet ein weiteres vielversprechendes Ziel für die Inhibition der Sialinsäure-Biosynthese. Mit einem C3-fluorinierten Neu5Ac-Analogon beispielsweise, lässt sich die Sialinsäure-Expression *in cellula* und *in vivo* vermindern.^{30,31}

Die erste Substanz, die für MGE eingesetzt wurde, ist *N*-Propionylmannosamin (ManNProp). Es konnte gezeigt werden, dass dieses C2-modifizierte ManNAc-Analogon von Zellen metabolisiert und anschließend als *N*-Propionylneuraminsäure (Neu5Prop) auf der Zelloberfläche exprimiert wird.³² Andere unnatürliche Mannosamin-Derivate, wie z.B. *N*-Butanoylmannosamin (ManNBut) oder *N*-Hexanoylmannosamin, können in gleicher Weise für MGE eingesetzt werden.³³ Benutzt man C2-modifizierte ManNAc-Analoga, die reaktive Gruppen (z.B.

Ketogruppen oder Azide) tragen, können die neu entstehenden, unnatürlichen Sialinsäuren für weitere chemische Modifikationen genutzt werden. Diese Methode ermöglicht es u.a., sialylierte Glykane mit Fluoreszenzfarbstoffen zu kuppeln.^{34,35}

Im Rahmen dieser Arbeit sollte überprüft werden, inwieweit sich die Expression von Sialinsäuren auf der Zelloberfläche (Sialylierung) mit Substratanaloga des Schlüsselenzyms der Sialinsäure-Biosynthese, der GNE/MNK, beeinflussen lässt. Sowohl zur Hemmung des Stoffwechselweges, als auch für MGE wurden hierbei verschiedene, chemisch modifizierte Derivate von ManNAc verwendet.

Als mögliche Inhibitoren der Sialinsäure-Expression wurden verschiedene C3- und C6-modifizierte ManNAc-Analoga getestet. Es wurde überprüft, ob diese Substanzen dazu in der Lage sind, die Aktivität der MNK-Domäne des Schlüsselenzyms der Sialinsäure-Biosynthese zu hemmen. Die C3-Position von ManNAc wurde zuvor als wichtiges Bindeeptop für die MNK beschrieben.³⁶ ManNAc-Analoga mit C6-Modifikationen können von der MNK nicht phosphoryliert werden und sind daher falsche Substrate für das Enzym.²⁹ Des Weiteren sollte festgestellt werden, ob die getesteten MNK-Inhibitoren ebenfalls dazu fähig sind, die Sialinsäure-Expression von Zellen zu reduzieren.

Für MGE wurden C2-modifizierte ManNAc-Analoga eingesetzt. Innerhalb dieser Arbeit sollte überprüft werden, ob Virus-produzierende Zellen diese ManNAc-Derivate zu unnatürlichen Sialinsäuren metabolisieren und anschließend auf Zelloberflächen-Glykanen exprimieren. Mithilfe von *in vitro*-Experimenten konnte zuvor durch unsere Kooperationspartner gezeigt werden, dass behüllte Viruspartikel des murinen Leukämievirus (MLV) aus Zellen, die zuvor mit C2-modifizierten ManNAc-Derivaten behandelt wurden, z.T. in wesentlich geringerem Maße für die Siglec-1-abhängige *trans*-Infektion von DC zu Lymphozyten bereitstehen.³⁷

Methodik

ManNAc-Analoga – Alle getesteten ManNAc-Analoga sind in Abbildung 1 dargestellt. Die verwendeten C2-modifizierten ManNAc-Derivate wurden bereits in anderen Arbeiten erfolgreich für MGE eingesetzt.^{32,33,38-40} Die übrigen ManNAc-Analoga wurden neu synthetisiert: C3-modifizierte Derivate von Stephan Rigol (AG Prof. Giannis, Universität Leipzig), C6-modifizierte Substanzen von Olaia Nieto-Garcia (AG Prof. Hackenberger, Leibniz-Institut f. molekulare Pharmakologie Berlin).^{41,42} Für Zellexperimente wurden die ManNAc-Derivate C2-4, C3-1 – 4 sowie C6-4 – 5 durch die Kooperationspartner peracetyliert, um deren Membranpermeabilität zu erhöhen (peracetylierte Substanzen sind nachfolgend mit „*“

markiert). Im Zytosol werden die Acetylgruppen von unspezifischen Esterasen abgespalten, sodass die aktiven Monosaccharide frei werden.^{43,44}

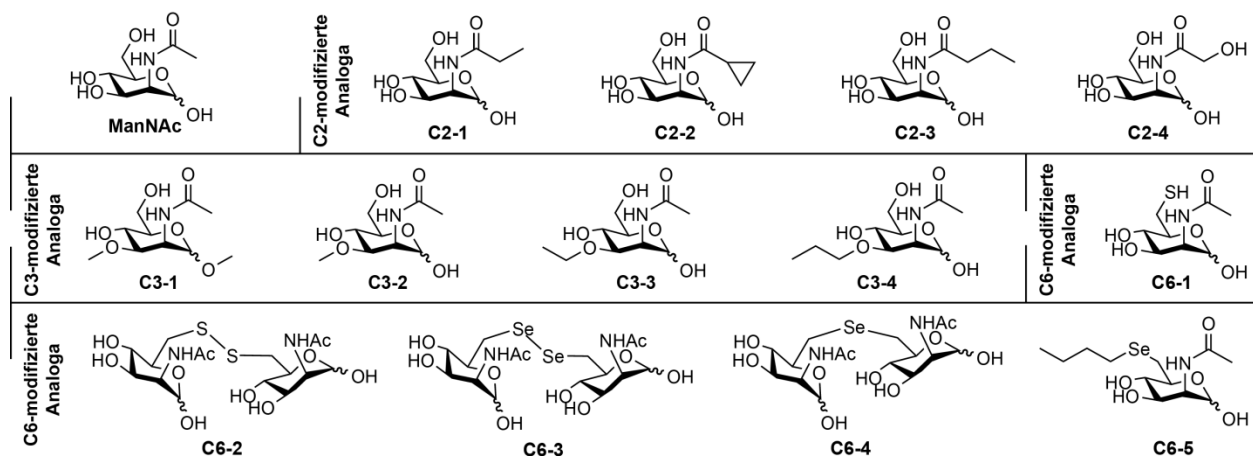


Abbildung 1. Darstellung der verwendeten ManNAc-Analoga. Zur Vereinheitlichung und Vereinfachung sind in dieser Abbildung alle ManNAc-Derivate in ihrer deacetylierten Form dargestellt. ManNAc ist zum Vergleich abgebildet (links oben). Bei der Substanz C3-1 handelt es sich um ein C3-modifiziertes ManNAc-Derivat, das zusätzlich eine C1-Modifikation trägt.

Proteinexpression und -aufreinigung – Die MNK-Domäne des Schlüsselenzyms der Sialinsäurebiosynthese wurde nach etablierten Methoden exprimiert und aufgereinigt.²⁹ Hierbei wurde humane, Hexahistidin-Tag-tragende MNK in BL21-CodonPlus(DE3)-RIL *Escherichia coli* (Stragene) exprimiert. Die Proteinaufreinigung erfolgte mithilfe von Ni-Nitrilotriacetat-Affinitäts-Chromatographie und anschließender Gel-Permeations-Chromatographie auf einer SuperdexTM HighLoad 16/600-Säule (GE Healthcare).

Mit einem Glutathion-S-Transferase-Tag versehene, humane *N*-Acetylglucosamin Kinase (GNK) wurde in BL21-CodonPlus(DE3)-RIL *E. coli* (Stragene) exprimiert, ebenfalls nach etablierten Methoden.⁴⁵ Durch Glutathion-Affinitätschromatographie und Gel-Permeations-Chromatographie auf einer SuperdexTM HighLoad 16/600-Säule (GE Healthcare) wurde das Protein aufgereinigt.

Bestimmung der Proteinkonzentration – Die Konzentration von aufgereinigten Proteinen und die Proteinkonzentration in Zelllysaten wurden mithilfe eines photometrischen Bicinchoninsäure (BCA)-Assays bestimmt. Hierzu wurde der PierceTM BCA Protein Assay Kit (Thermo Scientific) nach Herstellerangaben verwendet: Jeweils 100 µl der zu testenden Proben wurden 10 µl eines Gemisches aus BCA Reagenz A und B (50:1) hinzugefügt. Die Proben wurden für 30 min bei 37 °C inkubiert. Anschließend wurden die Absorptionen der jeweiligen Proben mit einem MultiskanTM GO Mikrotiterplatten-Spektrophotometer (Thermo Scientific) bei einer

Wellenlänge von 562 nm bestimmt. Als Standards dienten Proben mit verschiedenen Konzentrationen an bovinem Serumalbumin (BSA, Thermo Scientific).

Bestimmung von Enzymaktivitäten – Die Effekte der C3- und C6-modifizierten ManNAc-Analoga auf die Enzymaktivität der MNK wurden mithilfe eines gekoppelt optischen Tests untersucht. 55 µl Reaktionslösung enthielten die folgenden Puffer und Reagenzien: 39 µl Puffer A (65 mM MgCl₂, 200 mM Tris-HCl, pH 8,1), 5 µl ATP (unterschiedliche Konzentrationen), 3,5 µl NADH (30 mM), 2 µl Phosphoenolpyruvat (100 mM), 0,5 µl Pyruvat-Kinase/Laktat-Dehydrogenase (jeweils 2 U), 5 µl ManNAc (verschiedene Konzentrationen). Jeweils 10 µl der zu testenden ManNAc-Derivate wurden in unterschiedlichen Konzentrationen hinzugegeben. Die Reaktion wurde gestartet, indem 0,6 µg rekombinant hergestellte MNK in 35 µl Puffer B (10 mM Tris-HCl, 150 mM NaCl, pH 8,0) hinzugefügt wurden. Die Proben wurden bei 37 °C inkubiert und die Konzentration von NADH wurde mit einem Mikrotiterplatten-Spektrophotometer bei 340 nm bestimmt. Die Ergebnisse wurden mit einer Leerprobe (55 µl Reaktionslösung, 10 µl H₂O, 35 µl Puffer B ohne MNK) verglichen.

Um die Spezifität der MNK-Inhibitoren zu überprüfen, sollte bestätigt werden, dass diese weder die Enzymaktivität der GNK noch der Hexokinase (HK) hemmen. Hierzu wurden 39 µl Puffer A, 5 µl ATP (50 mM), 3,5 µl NADH (30 mM), 2 µl Phosphoenolpyruvat (100 mM), 0,5 µl Pyruvat-Kinase/Laktat-Dehydrogenase (jeweils 2 U), 5 µl GlcNAc (7,5 mM, für GNK-Experimente) oder 5 µl Glukose (5 mM, für HK-Experimente) und 10 µl des zu testenden ManNAc-Analogons entweder mit 1 µg GNK oder mit 0,2 µg HK (aus Hefe, Sigma Aldrich) in 35 µl Puffer B inkubiert. Die NADH Konzentration wurde spektrophotometrisch bestimmt (siehe oben).

Dynamische Lichtstreuungs (DLS)-Experimente – Um zu überprüfen, ob C3-2 eine Substanz ist, welche die MNK-Aktivität durch unspezifische Aggregation hemmt, wurden DLS-Experimente mit einem Laser Spector Scatter 201 (RiNA) durchgeführt. Die Küvetten wurden jeweils mit 30 µl MNK (10 µM) in Puffer B und 5 mM C3-2 oder 5 mM ManNAc präpariert. Die Messungen wurden bei 21 °C durchgeführt und die Ergebnisse mit Negativkontrollen, die unbehandelte MNK enthielten, sowie mit Positivkontrollen, die für 10 min bei 45 °C inkubierte und dadurch aggregierte MNK enthielten, verglichen.

Oberflächenplasmonenresonanzspektroskopie (SPR) – Die Experimente wurden mit einem Biacore® T100 Biosensor Instrument (GE Healthcare) und einem Nitrilotriacetat-Sensor-Chip

(NTA-Chip, GE Healthcare) durchgeführt. Dabei wurden Laufpuffer (10 mM HEPES, 150 mM NaCl, 0,05 mM EDTA, 0,005% Tween 20, pH 7,4) und Regenerationslösung (10 mM Taurodeoxycholsäure, 100 mM Tris-HCl, pH 9,0) verwendet.

Die rekombinant hergestellte MNK wurde kovalent auf dem Sensor-Chip immobilisiert bis zu einem Level von 12.000 Resonanzeneinheiten (RU, 1 RU = 1 pg/mm²). Hierbei wurde der NTA-Chip zunächst mit 0,5 mM NiCl₂ aktiviert. Eine etablierte Methode wurde verwendet, um das Hexahistidin-Tag-tragende Protein zu binden und anschließend kovalent mit dem NTA-Chip zu kuppeln.⁴⁶ Die Beschichtungsprozedur wurde durch Injektion von 350 mM EDTA in Laufpuffer vollendet. Drei der vier auf dem Chip zur Verfügung stehenden Flusszellen wurden auf diese Weise mit MNK gekuppelt. Bei der vierten Flusszelle wurde die gleiche Beschichtungsprozedur durchgeführt, jedoch in Abwesenheit von Protein. Sie diente bei den anschließenden Messungen als Referenzflusszelle.

Alle Bindestudien wurden bei 25 °C und einer Flussrate von 20 µl/min durchgeführt. Zu analysierende Substanzen wurden in verschiedenen Konzentrationen für 180 s injiziert, gefolgt von einer Dissoziationsphase von 1000 s Dauer. Für ManNAc und seine Analoga wurde die Regeneration mit zwei Injektionen von Regenerationslösung (10 µl/min, 60 s) vorgenommen. Bei Bindungsstudien mit Nukleosiden wurde die Regeneration mit 10 mM ManNAc in Laufpuffer und anschließend mit 100 mM EDTA (jeweils 10 µl/min, 60 s) durchgeführt. Die Datenauswertung erfolgte nach Subtraktion der Referenzflusszelle und der Puffer-Injektionen mithilfe von BIAevaluation (Version 4.1, GE Healthcare) unter Zuhilfenahme eines 1:1 Langmuir-Bindungsmodels.

Zytotoxizitätsstudien – Die Zytotoxizität der peracetylierten C3- und C6-modifizierten ManNAc-Analoga in Jurkat-Zellen (ATCC) wurde mithilfe des AlamarBlue[®]-Assays (AbD Serotec) bestimmt. Hierfür wurden ca. 20.000 Jurkat-Zellen für 72 h in 100 µl RPMI 1640 Medium (Pan-Biotech) kultiviert, das 10 % fetales Kälberserum (FBS), 2 mM L-Glutamin (Gln) und verschiedene Konzentrationen der zu testenden Substanzen enthielt. 10 µl AlamarBlue[®]-Lösung wurden hinzugefügt und danach wurden die Zellen für weitere 4 h inkubiert. Anschließend wurden die Proben spektrophotometrisch bei Wellenlängen von 570 und 620 nm analysiert. Die Ergebnisse wurden anhand von unbehandelten Zellen (100 % Viabilität) und Leerproben ohne Zellen (gesetzt als 0 % Viabilität) verglichen.

Bestimmung der Zelloberflächensialylierung mithilfe von Lektinen – Ca. 20.000 Jurkat-Zellen wurden zunächst für 72 h in 100 µl RPMI 1640 Medium (10 % FBS, 2 mM Gln) kultiviert, das

die peracetylierten C3- und C6-modifizierten ManNAc-Derivate in verschiedenen Konzentrationen enthielt. Danach wurden die Zellen dreimal in phosphatgepufferter Salzlösung (PBS) mit 0,5 % BSA gewaschen und anschließend für 1 h bei 4 °C entweder mit FITC-konjugiertem *Polyporus squamosus* Lektin (PSL, 0,1 µg/ml, ein Geschenk von H.J. Gabius, TU München), alkalische Phosphatase-konjugiertem *Sambucus nigra* Agglutinin (SNA, 3 µg/ml, EY Laboratories) oder alkalische Phosphatase-konjugiertem *Arachis hypogaea* Agglutinin (PNA, 2 µg/ml, EY Laboratories) inkubiert. Nach anschließendem dreimaligen Waschen mit PBS + 0,5 % BSA wurden die Jurkat-Zellen analysiert: PSL-gefärzte Zellen mithilfe eines FACSCanto™ II Durchflusszytometers (BD Biosciences), SNA- sowie PNA-behandelte Zellen wurden für 15 min mit 200µl p-Nitrophenylphosphat-Lösung (Sigma-Aldrich) behandelt und die Ergebnisse wurden anschließend spektrophotometrisch bei einer Wellenlänge von 405 nm ausgewertet. Die Proben wurden mit unbehandelten Zellen (100 % Oberflächensialylierung) und Zellen, die für 60 min mit 0,2 U/ml Sialidase aus *Clostridium perfringens* (Sigma Aldrich) behandelt wurden (gesetzt als 0 % Oberflächensialylierung) verglichen.

Die Datenauswertung der Durchflusszytometer-Experimente erfolgte mithilfe von FACSDiva 8.0 (BD Biosciences). Bei den Experimenten mit C6-modifizierten ManNAc-Analoga wurden tote Zellen mittels *Gating*, aus der Datenanalyse ausgeschlossen (siehe Nieto-Garcia *et al.* 2016: Abbildungen S5, S6)⁴². Hierzu wurde eine Probe unbehandelter Zellen verwendet, in der die toten Zellen zuvor mit Propidium Iodid (PI) gefärbt wurden.

Quantifizierung von Sialinsäure und deren unnatürlichen Derivaten in Zelllysaten – Die Konzentrationen von membrangebundenen Sialinsäuren sowie von freiem Neu5Ac und CMP-Neu5Ac wurden mithilfe von Hochleistungs-Flüssigkeits-Chromatographie (HPLC) bestimmt.⁴⁷ Für MGE wurden ca. 100.000 293T-Zellen (ATCC) in DMEM (Pan-Biotech) mit 10 % FBS, 2 mM Gln, 2 mM Natriumpyruvat und ManNAc oder C2-modifizierten ManNAc-Analoga (5 mM ManNAc, 0,3 mM Ac₄ManNAc, 5 mM C2-1 – C2-3, oder 0,3 mM C2-4*) kultiviert. Das Zellkulturmedium wurde am fünften Tag erneuert und nach 7 Tagen wurden die Zellen geerntet. Um die Inhibition der Sialinsäure-Expression zu testen, wurden ca. 1.500.000 Jurkat-Zellen in RPMI 1640 Medium (+ 10 % FBS, + 2 mM Gln) mit 500 µM C3-2* für 3 Tage kultiviert, anschließend geerntet und die Zellkonzentrationen mithilfe einer Neubauer-Improved Zählkammer (Marienfeld-Superior) ausgezählt.

Alle geernteten Zellen wurden dreimal mit PBS gewaschen und danach durch Ultraschall in eisgekühltem Lyse-Puffer (150 mM NaCl, 10 mM Tris, 5 mM EDTA, 1 mM PMSF, 40 µM Leupeptin, 1.5 µM Aprotinin, pH 8,0) homogenisiert. Durch Zentrifugation bei 21.000 g und

4 °C für 2 h wurden die Membran- von den zytosolischen Fraktionen getrennt. Bei einem Teil der Proben wurde eine mehrschrittige Chloroform/Methanol-Präzipitation durchgeführt, um die Glykolipid- von der übrigen Membranfraktion zu trennen.⁴⁸ Im zytosolischen Kompartiment wurde die Proteinkonzentration mittels eines BCA-Assays (siehe oben) bestimmt. Daraufhin wurde auch dieses Kompartiment einer Chloroform/Methanol-Präzipitation unterzogen, um den Proteinanteil zu reduzieren. Anschließend wurde das zytosolische Kompartiment durch einen 3 kDa Größenausschlussfilter filtriert, um übriggebliebene Makromoleküle zu entfernen. Ein Teil der zytosolischen Proben wurde für 12 h mit einer Natriumborhydrid-Lösung (200 mM Natriumborhydrid in 200 mM Natriumborat, pH 8,0) behandelt, wodurch nicht-CMP-konjugierte freie Neu5Ac reduziert wurde.⁴⁹ Alle Fraktionen wurden mit 1 M Trifluoressigsäure (TFA) für 4 h bei 80 °C hydrolysiert, lyophilisiert und anschließend in 5 µl TFA (120 mM) resuspendiert. Die Proben wurden für 2 h bei 56 °C mit 30 µl DMB-Lösung (6,9 mM 1,2-Diamino-4,5-Methylendioxybenzen, 0,67 mM β-Mercaptoethanol, 0,19 % Natriumbisulfit) gefärbt und mit einer Gemini-NX C18-Säule (110 Å, 3 µM Partikelgröße, 4,6 × 150 mm, Phenomenex) bei einer Flussrate von 0,5 ml/min und einem Mischverhältnis von Methanol/Acetonitril/H₂O (6:8:86) aufgetrennt. Der Fluoreszenzdetektor wurde auf Wellenlängen von 373 nm (Exzitation) und 448 nm (Emission) eingestellt. Um die verschiedenen Sialinsäure-Spezies zur quantifizieren, wurden DMB-gefärbte Standards injiziert: Neu5Ac (Sigma Aldrich), *N*-Glycolylneuraminsäure (Neu5Gc, ein Geschenk von R. Schauer, Universität Kiel) und Neu5But (ein Geschenk von C. Bertozzi, Stanford University). Die Konzentrationen von anfallender, DMB-konjugierter *N*-Propionylneuraminsäure (Neu5Prop) und *N*-Cyclopropylcarbamylneuraminsäure (Neu5Cyclo) wurden anhand des DMB-Neu5Ac-Standards abgeschätzt.

Die unbehandelten Standards sowie die einzelnen Fraktionen des HPLC-Durchflusses wurden mit LC-Elektrosprüh-Ionisations-Massenspektrometrie (ESI-MS) weiter untersucht. Hierbei wurden 20 µl gesammelter HPLC-Durchfluss oder 500 ng des entsprechenden Standards (gelöst in 20 µl H₂O) in ein Agilent 1100 LC/MSD injiziert. Als Eluent diente eine Lösung aus 79,9 % Methanol, 20 % Isopropanol und 0,1 % Ameisensäure. Die Flussrate wurde auf 0,5 ml/min, die Kapillarspannung auf 4 kV und die Kapillartemperatur auf 350 °C eingestellt.

Statistische Datenauswertung – OriginPro (Version 8.5, Perkin Elmer) wurde für die graphische Darstellung von Daten, Kurvenapproximationen sowie das Berechnen von Mittelwerten, Standardabweichungen (SD) und Standardfehlern (SEM) benutzt.

Ergebnisse

Enzyminhibition – Die mittleren inhibitorischen Konzentrationen (IC_{50}) der C3- und C6-modifizierten ManNAc-Analoga für die Hemmung der MNK-Domäne des Schlüsselenzyms der Sialinsäurebiosynthese bei Substratkonzentrationen von 0,125 mM ManNAc und 2 mM ATP sind in Tabelle 1 zusammengefasst. Die Substanzen C3-1, C3-3 und C3-4 sowie C6-1 zeigten selbst bei Konzentrationen von 10 mM keine Inhibition der MNK-Aktivität *in vitro*.

Tabelle 1. Mittlere inhibitorische Konzentrationen (IC_{50}) der getesteten C3- und C6-modifizierten ManNAc-Derivate für die Hemmung der MNK-Aktivität. Es sind die Anzahl (n) an unabhängigen Experimenten, die Mittelwerte und SEM dargestellt. N.A., nicht bestimmbar

ManNAc-Analogen	IC_{50}	SEM	
C3-1	> 10 mM	N.A.	n = 3
C3-2	1,3 mM	$\pm 0,1$ mM	n = 3
C3-3	> 10 mM	N.A.	n = 3
C3-4	> 10 mM	N.A.	n = 3
C6-1	> 10 mM	N.A.	n = 3
C6-2	4,2 mM	$\pm 0,7$ mM	n = 3
C6-3	$8,5 \times 10^{-3}$ mM	$\pm 1,9 \times 10^{-3}$ mM	n = 5
C6-4	3,0 mM	$\pm 0,7$ mM	n = 3
C6-5	1,9 mM	$\pm 0,5$ mM	n = 3

Um den Inhibitionsmodus der beiden stärksten Inhibitoren der MNK (C3-2, C6-3) näher zu charakterisieren, wurde die Enzymaktivität bei gleichbleibender Inhibitorkonzentration (C3-2 = 1,25 mM, C6-3 = 25 μ M) und unterschiedlichen ManNAc-Konzentrationen bestimmt. Die Ergebnisse wurden in einem Lineweaver-Burk-Diagramm aufgezeichnet und die Inhibitorkonstanten (K_i) wurden berechnet (Abbildung 2). Die Ergebnisse dieser Versuche legen nahe, dass C6-3 die Aktivität der MNK kompetitiv mit ManNAc hemmt ($K_i = 15,7 \mu$ M), wohingegen C3-2 das Enzym nicht-kompetitiv mit ManNAc hemmt. Daraufhin wurde die Hemmung der MNK-Aktivität von C3-2 bei unterschiedlichen Konzentrationen von ATP als Substrat der MNK bestimmt und es zeigte sich, dass C3-2 das Enzym wahrscheinlich kompetitiv mit ATP hemmt ($K_i = 649 \mu$ M).

Bei einer Konzentration von 5 mM C3-2 konnte keine Inhibition der Enzymaktivitäten der GNK oder HK *in vitro* gemessen werden. Beim ManNAc-Analogon C6-3 ergab sich eine IC_{50} für die Hemmung der GNK von 1,7 mM. Die IC_{50} von C6-3 für die Hemmung der HK-Aktivität war größer als 5 mM.

Mithilfe von DLS-Experimenten konnte gezeigt werden, dass der hydrodynamische Radius von MNK in Puffer B sich auch bei Zugabe von hohen Konzentrationen von C3-2 oder ManNAc

(beide 5 mM) nicht wesentlich vergrößerte. Die Interaktion von MNK mit C3-2 führt nicht zu einer Aggregation des Proteins (siehe Wratil *et al.* 2014: Abbildung 7)⁴¹.

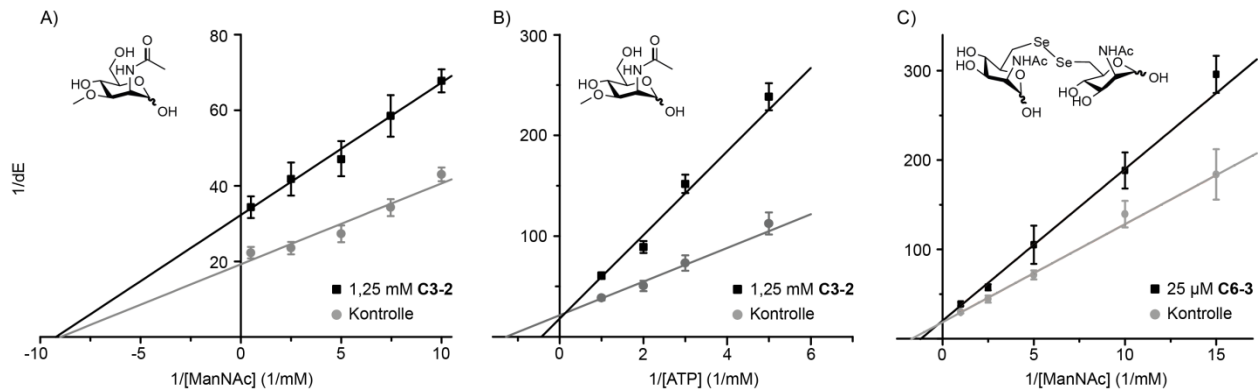


Abbildung 2. Lineweaver-Burk-Diagramme für die Hemmung der MNK mit den Substanzen C3-2 (A,B) und C6-3 (C). Die Aktivität der MNK wurde in einem gekoppelt optischen Test bei verschiedenen Substratkonzentrationen gemessen. In A) und C) wurde die ManNAc-Konzentration variiert ($cATP = 2,5$ mM). In B) wurden unterschiedliche ATP-Konzentrationen verwendet ($cManNAc = 0,5$ mM). Als Kontrollen dienten Proben ohne Inhibitor. Dargestellt sind jeweils die Mittelwerte und SEM (A: n = 5; B,C: n = 3). dE , zeitliche Änderung der Extinktion

Bindungsaffinitäten – Um die Bindungsaffinitäten zwischen MNK und C3-2 zu bestimmen, wurde SPR verwendet. Nach Immobilisierung von ca. 12.000 RU MNK wurde eine maximale Antwort von 120 RU auf die Injektion von C3-2 beobachtet. Unter Annahme einer 1:1-Langmuir-Bindung wurde eine Dissoziationskonstante (K_D) von 755 μ M für die Interaktion zwischen MNK und C3-2 berechnet. ATP und ADP banden an die MNK mit K_D -Werten von 429 μ M (ATP), bzw. 306 μ M (ADP). Der geringfügig niedrigere K_D -Wert von ADP ist durch eine höhere Dissoziationsrate (k_d) zu begründen. ManNAc sowie C3-1 und UDP, die als Kontrollen verwendet wurden, zeigten unter den experimentellen Bedingungen keine Bindung an MNK. Die Ergebnisse der SPR-Experimente sind in Tabelle 2 zusammengefasst.

Tabelle 2. Bindungsaffinitäten für die Interaktion von MNK mit verschiedenen Substanzen. Die dargestellten Daten wurden in drei unabhängigen Experimenten erhoben (n = 3). K_D , Dissoziationskonstante; k_a , Assoziationsrate; k_d , Dissoziationsrate; X^2 , Chi-Quadrat-Wert; N.A., nicht bestimmbar

	ManNAc	C3-1	C3-2	ATP	ADP	UDP
K_D (μ M)	N.A.	N.A.	755	429	306	N.A.
k_a ($M^{-1} s^{-1}$)	N.A.	N.A.	2,92	2,48	2,76	N.A.
k_d (s^{-1})	N.A.	N.A.	$2,25 \times 10^{-3}$	$1,06 \times 10^{-3}$	$8,40 \times 10^{-3}$	N.A.
X^2	N.A.	N.A.	7,65	19,20	18,87	N.A.

Zytotoxizität – Die dreitägige Behandlung mit den peracetylierten, C3-modifizierten ManNAc-Analoga (C3-1* – C3-4*) führte bis zu einer Konzentration von 1 mM im Zellkulturmedium zu keiner wesentlichen Beeinträchtigung der Zellviabilität. Die getesteten peracetylierten, C6-

modifizierten ManNAc-Derivate (C6-3*, C6-4*) zeigten bis zu einer Konzentration von 50 µM keine wesentliche Zytotoxizität. Indes führte eine Behandlung mit 100 µM C6-3* zu einer Reduktion der Zellviabilität um ca. 70 % (siehe Nieto-Garcia *et al.* 2016: Abbildung S4)⁴².

Hemmung der Zelloberflächensialylierung – Die dreitägige Behandlung von Jurkat-Zellen mit den peracetylierten ManNAc-Analoga C3-2* und C6-3* führte zu einer dosisabhängigen Reduktion der Zelloberflächensialylierung. Durch PSL-Färbung konnte gezeigt werden, dass die Expression von 6'-Sialyl-LacNAc-Resten auf der Zelloberfläche nach Applikation der beiden Substanzen um bis zu 80 % vermindert war (Abbildung 3, siehe auch Wratil *et al.* 2014: Abbildung 3)⁴¹.

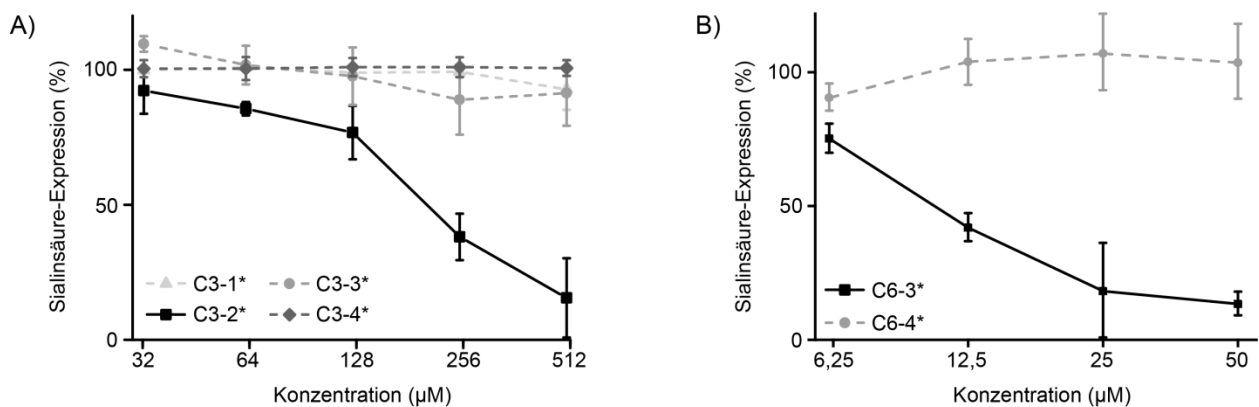


Abbildung 3. Auswirkungen auf die Zelloberflächensialylierung nach der Behandlung von Jurkat-Zellen mit den getesteten C3- (A) bzw. C6- (B) modifizierten ManNAc-Analoga. Dargestellt ist die Bindung des 6'-Sialyl-LacNAc-erkennenden PSL. Als Kontrollen dienten unbehandelte Zellen (100% Sialinsäure-Expression) sowie Zellen, die zuvor mit Sialidase behandelt wurden (gesetzt als 0% Sialinsäure-Expression). Gezeigt sind jeweils die Mittelwerte und SD aus drei unabhängigen Experimenten ($n = 3$). In B) wurden tote Zellen durch PI-Färbung ausgeschlossen.

Die Färbung mit SNA bestätigte die Hemmung der Expression von 6'-Sialyl-LacNAc-Resten durch C3-2*. PNA-Färbung zeigte, dass sich das Auftreten von nicht-sialyliertem T-Antigen (Galβ1-3GalNAcα-Ser/Thr) durch Behandlung mit C3-2* dosisabhängig steigern ließ. Daraus lässt sich auf eine Reduktion des sialylierten Epitops schließen (siehe Wratil *et al.* 2014: Abbildung 2)⁴¹. Die anderen getesteten, peracetylierten, C3- oder C6-modifizierten ManNAc-Analoga hatten unter den experimentellen Bedingungen keine Auswirkung auf die Expression von Sialinsäure auf der Zelloberfläche.

Quantifizierung von Sialinsäuren in Zelllysaten – Die dreitägige Behandlung mit dem peracetylierten ManNAc-Analogon C3-2* (0,5 mM) führte zu einer Reduktion von Neu5Ac in den getesteten Jurkat-Zellen. Nicht nur die Membran-gebundene Neu5Ac war vermindert, sondern auch die Konzentrationen von im Zytosol befindlicher freier und CMP-konjugierter

Neu5Ac (Tabelle 3). In keinem der HPLC-Chromatogramme, die bei den Messungen mit C3-2* erstellt wurden, zeigte sich ein Anhalt dafür, dass durch die Behandlung mit der Substanz eine neuartige, unnatürliche Sialinsäure entstanden wäre (siehe Wratil *et al.* 2014: Abbildung 5)⁴¹.

Tabelle 3. Konzentrationen von Membran-gebundener und im Zytosol befindlicher Neu5Ac in Jurkat-Zellen, die zuvor für drei Tage mit C3-2* (0,5 mM) behandelt wurden. Unbehandelte Zellen dienten als Kontrolle. Dargestellt sind jeweils die Mittelwerte und SD aus drei unabhängigen Experimenten ($n = 3$).

	Zytosol-Neu5Ac (nmol/ 10^6 Zellen)	CMP-Neu5Ac (nmol/ 10^6 Zellen)	Membran-Neu5Ac (nmol/ 10^6 Zellen)
Kontrolle	0,51 ($\pm 0,15$)	0,30 ($\pm 0,09$)	13,63 ($\pm 7,08$)
C3-2*	0,25 ($\pm 0,04$)	0,13 ($\pm 0,03$)	6,82 ($\pm 2,64$)

Nachweis von unnatürlichen Sialinsäuren in Zelllysaten – Nach siebentägiger Behandlung mit den C2-modifizierten ManNAc-Derivaten konnten die entsprechenden unnatürlichen Sialinsäuren in den Membran- und Glykolipidfraktionen der Zelllysate von 293T-Zellen mithilfe von HPLC nachgewiesen werden. Sowohl die Konzentrationen von N-Acyl-modifizierten Sialinsäuren als auch deren Anteil in Bezug auf Neu5Ac (und Neu5Gc) schwankten beträchtlich (Abbildung 4). In Zellen, die zuvor mit C2-1 behandelt wurden, machte der Anteil an neu entstandenen Neu5Prop 76 % aller Sialinsäuren aus (83 % in der Glykolipidfraktion). Neu5Cyclo repräsentierte 91 % aller Sialinsäuren in mit C2-2 behandelten Zellen (93 % in der Glykolipidfraktion). 23 % aller Sialinsäuren in mit C2-3 behandelten Zellen wurden als Neu5But identifiziert (48 % in der Glykolipidfraktion). Im Gegensatz zu Zellen anderer Säugetierspezies sind humane Zellen sind in der Regel nicht dazu in der Lage, Neu5Gc zu synthetisieren.⁵⁰ Trotzdem konnten in den Zelllysaten kleine Mengen von Neu5Gc festgestellt werden. Dies lässt sich am ehesten durch einen Stoffwechselweg erklären, bei dem die Zellen das im Kälberserum vorhandene Neu5Gc aufnehmen und wiederverwerten.⁵¹ Behandlung mit ManNAc oder Ac₄ManNAc führte zur vermehrten Expression von Neu5Ac, besonders in der Glykolipidfraktion, und hemmte darüber hinaus die Expression des Neu5Gc-Epitops. Die Expression von Neu5Gc ließ sich durch Behandlung mit C2-4* deutlich steigern. Zur Berechnung ihres relativen Anteils wurden die indirekt bestimmten Konzentrationen der neu entstandenen, DMB-konjugierten Sialinsäure-Spezies jeweils mit denen von DMB-Neu5Ac und DMB-Neu5Gc ins Verhältnis gesetzt.

Durch ESI-MS konnte die Reinheit der verwendeten Standards (Neu5Ac, Neu5Gc, Neu5But) bestätigt werden. Des Weiteren wurden aus den jeweiligen HPLC-Durchläufen die DMB-gekoppelten Sialinsäure-Spezies mittels Massenspektrometrie nachgewiesen (siehe Erikson *et al.* 2015: Abbildung 5)³⁷.

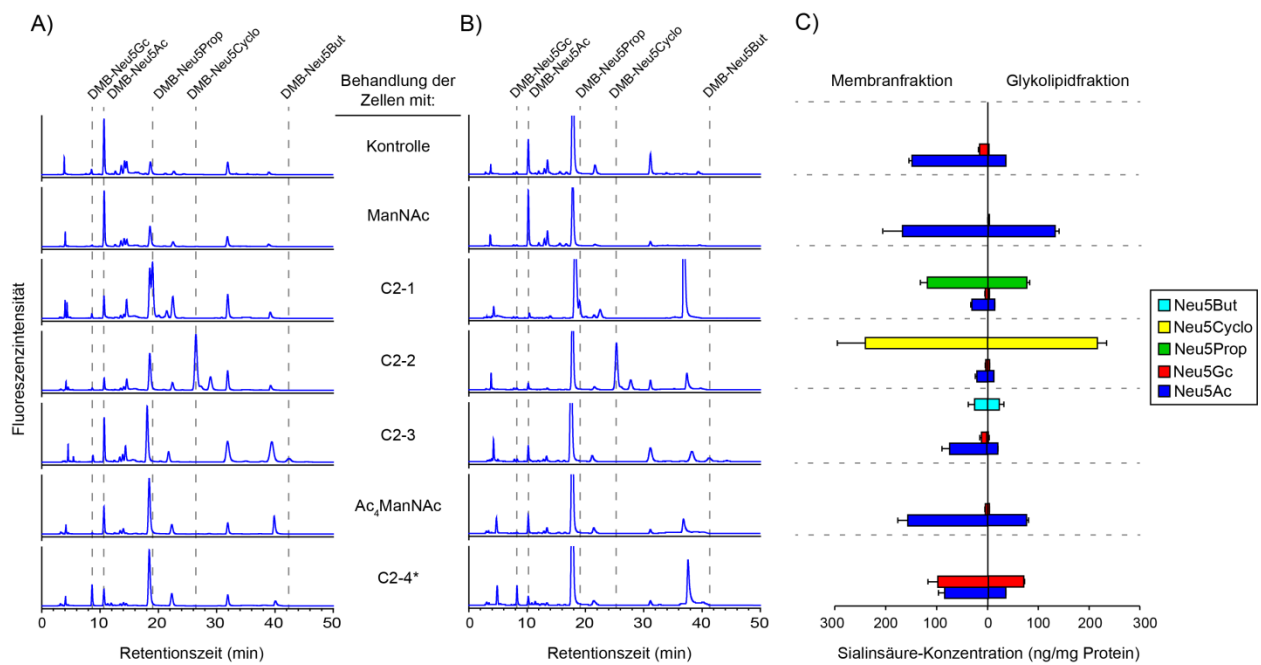


Abbildung 4. Detektion von modifizierten Sialinsäuren in Glykokonjugaten von 293T-Zellen. Es sind Chromatogramme von HPLC-Messungen abgebildet mit A) der gesammelten Membranfraktion oder B) der Glykolipidfraktion. Die Zellen wurden zuvor mit ManNAc oder den C2-modifizierten ManNAc-Analoga behandelt. Chromatogramm-Ausschläge, die nicht in der Kontrolle vorkommen, deuten auf das Vorhandensein unnatürlicher Sialinsäuren hin. Mithilfe von Standards und via ESI-MS wurden die neuen Sialinsäure-Spezies verifiziert. In C) sind Mittelwerte und SD der gemessenen Konzentrationen der verschiedenen Sialinsäure-Spezies in Bezug auf die Proteinkonzentration in den jeweiligen Zellysaten als Diagramm dargestellt ($n = 2$).

Diskussion

Sialinsäure ist an einer Vielzahl von Interaktionen zwischen Zellen und ihrer Umgebung beteiligt. Daher ist es von besonderer Bedeutung, einfache Methoden zu entwickeln, mit deren Hilfe sich die Expression von Sialinsäure auf der Zelloberfläche modifizieren lässt.

Obwohl bereits etablierte Methoden existieren, um die Expression von Sialinsäure auf der Zelloberfläche zu hemmen (z.B. Inhibition von Sialyltransferasen, Behandlung mit Sialidasen oder Knock-down der GNE/MNK *in cellula*),^{21,30,52} systemische, Zell-permeable Inhibitoren für die *de novo* Biosynthese von Sialinsäure standen bis heute nicht zur Verfügung. In dieser Arbeit wurden verschiedene C3- und C6-modifizierte ManNAc-Analoga auf ihre Fähigkeit hin untersucht, die Enzymaktivität der MNK-Domäne des Schlüsselenzyms der Sialinsäurebiosynthese *in vitro* zu inhibieren.

Von den getesteten C3-modifizierten ManNAc-Derivaten übte lediglich die Substanz C3-2 (ein ManNAc-Analogon mit einer Methylengruppe an der C3-Position) eine inhibitorische Wirkung auf die MNK-Aktivität aus. Durch das Hinzufügen einer C1-Modifikation (wie bei C3-1), oder durch den Einsatz langkettiger C3-Modifikationen wird die Hemmwirkung auf das Enzym aufgehoben. Die aktive Bindetasche der MNK scheint lediglich kleinere Substratmodifikationen an der Position C3 zu tolerieren. Diese Ergebnisse stehen im Einklang mit der Analyse einer Co-

Kristallisation von MNK und ManNAc.²⁹ Die IC₅₀ für die Hemmung der MNK-Aktivität *in vitro* durch C3-2 betrug 1,29 mM. Mithilfe von DLS-Experimenten konnte ausgeschlossen werden, dass die Inhibition der MNK-Aktivität durch C3-2 durch unspezifische Proteinaggregation hervorgerufen wird. Der Inhibitionsmodus von C3-2 ist nicht-kompetitiv mit ManNAc, dafür aber kompetitiv mit ATP (K_i , 649 µM). Es ist wahrscheinlich, dass C3-2 mit ATP um die Bindung an die aktive Bindetasche der MNK konkurriert und nicht mit ManNAc. Mittels SPR konnte die Bindung von C3-2 an die MNK bestätigt werden (K_D , 755 µM). ManNAc selbst hat nicht an das immobilisierte Protein gebunden. Dies kann durch Änderungen der Konformation der ManNAc-Bindetasche erklärt werden, die bei der Immobilisierung des Proteins aufgetreten sein könnten oder durch den technischen Versuchsaufbau. Die selektive Bindung von ADP, ATP und C3-2 deutet darauf hin, dass der Inhibitor (zumindest zum Teil) dieselbe Bindestelle wie ADP und ATP hat, auch weil ManNAc unter den gleichen Bedingungen nicht an das Enzym gebunden hat. Die Tatsache, dass strukturell ähnliche Substanzen, wie C3-1 oder UDP, im SPR nicht mit der MNK interagierten, legt nahe, dass die Bindetasche des Enzyms auch nach der Immobilisierung intakt war.

Bei den enzymatischen Hemmtests mit C6-modifizierten ManNAc-Derivaten erwies sich C6-3, ein C6-ManNAc-Analogon mit einer Diselenid-Verknüpfung und einem weiteren ManNAc-Rest als potenter Inhibitor der MNK-Aktivität *in vitro*. Mit einer IC₅₀ von 8,5 µM ist diese Substanz ein deutlich stärkerer Hemmstoff als alle anderen getesteten ManNAc-Analoga. Darüber hinaus zeigte sich, dass C6-3 die Enzymaktivität kompetitiv mit ManNAc inhibiert (K_i , 15,7 µM). C6-3 ist ein Homodimer, in dem das Grundgerüst von ManNAc doppelt vorkommt. Somit stehen in diesem Molekül theoretisch zwei Bindepartner für die Substratbindetasche der MNK bereit. Dies wiederum führt zu einem stöchiometrischen Vorteil dieser Substanz gegenüber den bekannten Inhibitoren mit Monosaccharid-Struktur.^{27,29,41,53,54} Die Versuche mit C6-3 legen nahe, dass die ManNAc-Bindetasche der MNK auch größere C6-modifizierte ManNAc-Derivate akzeptiert. Dieser Befund steht im Einklang mit der bekannten Kristallstruktur des Proteins.²⁹ Beim Vergleich der Ergebnisse aus den Inhibitionsstudien mit C6-3 und C6-4 zeigte sich, dass die Art und Länge der Selenid-Verknüpfung eine wichtige Rolle für die Hemmung der MNK spielt. Die C-Se-Se-C-Verknüpfung in C6-3 ist länger und wahrscheinlich auch flexibler als die C-Se-C-Verknüpfung in C6-4. Diese Eigenschaften könnten von Bedeutung für die Positionierung des Inhibitors in der aktiven Bindetasche der MNK sein, zusammen mit der Länge und der Winkelbeziehung der C-Se-Verbindung selbst.^{55,56} Unterschiede in den van-der-Waals- und Wasserstoffbrücken-Bindungen von Selen und Schwefel in C6-2 und C6-3 könnten eine Erklärung für die unterschiedlichen Bindungen dieser Substanzen an die MNK liefern.²⁹

Die relative Spezifität der beiden stärksten MNK-Inhibitoren (C3-2, C6-3) wurde dadurch bestätigt, dass diese Substanzen nicht oder nur in geringem Maße dazu in der Lage waren, die verwandten Zuckerkinasen GNK und HK in ihrer Aktivität zu hemmen.

Die beiden MNK-Inhibitoren C3-2 und C6-3 erwiesen sich als Hemmstoffe der Sialinsäure-Expression *in cellula*. Jurkat-Zellen, die mit diesen Substanzen in ihrer peracetylierten Form (C3-2*, C6-3*) behandelt wurden, zeigten eine Dosis-abhängige Reduktion der Sialinsäure-Konzentration auf ihrer Zelloberfläche. Die Expression von Sialinsäure konnte in diesen Zellen um bis zu 80 % reduziert werden. Eine absolute Inhibition der Zelloberflächensialylierung konnte nach Behandlung mit den Substanzen jedoch nicht beobachtet werden. Dies lässt sich am ehesten durch Aufnahme und Wiederverwertung von Sialinsäure aus dem Serumzusatz im Zellkulturmedium (FBS) begründen.⁵¹ Des Weiteren kommt ein langsamer Umsatz von sialylierten Glykoproteinen als Grund für diese Beobachtung in Frage.⁵⁷ Durch die HPLC-Analyse von Zelllysaten aus Jurkat-Zellen, die zuvor mit C3-2* behandelt wurden, konnte gezeigt werden, dass dieses ManNAc-Analogon die Neu5Ac-Konzentration sowohl auf der Zelloberfläche als auch im Zytosol reduziert. Darüber hinaus wurde eine erniedrigte Konzentration von CMP-Neu5Ac in den behandelten Zellen gemessen. Keine neuartigen, unnatürlichen Sialinsäuren wurden bei der Applikation von C3-2* *in cellula* gebildet. Diese Ergebnisse deuten darauf hin, dass C3-2* die Sialinsäure-Expression durch Inhibition ihrer *de novo* Biosynthese hemmt. Substanzen, die nicht in der Lage waren, die MNK-Aktivität effektiv zu hemmen (C3-1, C3-3, C3-4, C6-4), waren in peracetylierter Form auch keine Inhibitoren der Zelloberflächensialylierung. Die geringe Zytotoxizität von C3-2* unterstreicht die Tatsache, dass die Hemmung der Expression von Sialinsäure auf der Zelloberfläche keinen Einfluss auf die Zell-Viabilität hat.^{21,30} Das peracetylierte, C6-modifizierte ManNAc-Analogon C6-3* war in Versuchen mit Jurkat-Zellen zytotoxisch, wodurch der Einsatz dieser Substanz in Zellkultur-Experimenten auf eine maximale Konzentration von 50 µM beschränkt werden musste.

E. Erikson *et al.* konnten zeigen, dass behüllte MLV-Partikel aus Zellen, die zuvor mit bestimmten C2-modifizierten ManNAc-Analoga behandelt worden waren, deutlich in ihrer Fähigkeit gehemmt waren, Siglec-1 abhängig an DC zu binden. Darüber hinaus war auch die *trans*-Infektion von DC zu Lymphozyten eingeschränkt.³⁷ Die Tatsache, dass C2-modifizierte ManNAc-Analoga für MGE von Zelloberflächen-Sialinsäuren genutzt werden können, ist bekannt und gut erforscht.^{32,33} In dieser Arbeit sollte die Frage beantwortet werden, ob die Stärke der Inhibition der Siglec-1-abhängigen Bindung von MLV-Partikeln an DC und der anschließenden *trans*-Infektion mit dem Grad der Expression von unnatürlichen Sialinsäuren auf der Zelloberfläche in direktem Zusammenhang steht, oder ob die Art der eingeführten *N*-Acyl-

Modifikationen bedeutender für die Hemmung dieses Vorgangs ist. Hierbei interessierten besonders die sialylierten Glykolipide auf der Zelloberfläche der Virus-produzierenden Zellen, denn es konnte gezeigt werden, dass die Konzentration des Gangliosids GM3 in der Hülle von MLV- und den verwandten HIV-Partikeln erhöht ist.⁵⁸ GM3 scheint von essentieller Bedeutung für die Siglec-1/Virus-Interaktion zu sein.⁵⁹ In dieser Arbeit konnten die unnatürlichen Sialinsäuren auf der Zelloberfläche von 293T-Zellen, die zur Virusproduktion eingesetzt werden und die zuvor mit bestimmten C2-modifizierten ManNAc-Derivaten behandelt wurden, nachgewiesen werden. Die Konzentration der neu entstandenen unnatürlichen Sialinsäuren wurde mithilfe von HPLC bestimmt. Die einzelnen Sialinsäure-Spezies wurden durch ESI-MS bestätigt. Interessanterweise zeigte sich, dass besonders die Behandlung mit C2-1 und C2-2 zu einer starken Expression der jeweiligen unnatürlichen Sialinsäuren (Neu5Prop, Neu5Cyclo) auf der Zelloberfläche führte und die Expression von natürlichem Neu5Ac deutlich hemmte. In den vorangegangenen Studien hatten C2-1 und C2-2 allerdings weder einen Effekt auf die Siglec-1 abhängige Bindung von MLV-Partikeln an DC noch auf die *trans*-Infektion von Lymphozyten. C2-3 und C2-4* hatten eine geringere metabolische Effektivität, hemmten die Bindung und *trans*-Infektion der Viruspartikel jedoch deutlich.³⁷ Diese Ergebnisse legen den Schluss nahe, dass der *N*-Acyl-Rest von großer Bedeutung für die Interaktion zwischen Sialinsäure und Siglec-1 ist. Neu5Prop und Neu5Cyclo werden wahrscheinlich von diesem Lektin als Bindepartner akzeptiert, während Neu5But und Neu5Gc nicht für die Interaktion bereitstehen. Bei der Applikation aller C2-modifizierter ManNAc-Derivate war zu beobachten, dass die neu entstandenen unnatürlichen Sialinsäuren besonders in der Glykolipid-Fraktion der Zellmembran akkumulierten. Dies erklärt einerseits den Erfolg der Hemmung der MLV/Siglec-1-Interaktion durch C2-3 und C2-4*, andererseits deutet dieser Befund auf einen vermehrten Umsatz von Glykolipiden in den behandelten Zellen hin.

Diese Arbeit zeigt die Vielseitigkeit der ManNAc-Analoga zur Modifikation der Expression von Sialinsäuren auf der Zelloberfläche. Neuartige ManNAc-Derivate mit C3- oder C6-Modifikationen wurden vorgestellt. Ein C3-methyliertes ManNAc-Analogon und ein C6-modifiziertes ManNAc-Diselenid-Dimer sind die ersten membranpermeablen Inhibitoren des Schlüsselenzyms der Sialinsäurebiosynthese. Diese Substanzen können die Sialinsäure-Expression auf der Zelloberfläche von Kulturzellen reduzieren. C2-Modifizierte ManNAc-Analoga konnten erfolgreich für MGE eingesetzt werden und so zum Verständnis der Siglec-1-abhängigen *trans*-Infektion von bestimmten Retroviren beitragen. Vielleicht können die vorgestellten Substanzen und Methoden eines Tages dabei helfen, neue Sialinsäure-abhängige

Interaktionen aufzudecken, oder sogar Krankheitsprozesse, bei denen Sialinsäure eine wichtige Rolle spielt, günstig zu beeinflussen.

Literaturverzeichnis

1. Schauer R. Sialic acids as regulators of molecular and cellular interactions. *Curr Opin Struct Biol* 2009;19:507-14.
2. Varki A. Sialic acids in human health and disease. *Trends Mol Med* 2008;14:351-60.
3. Angata T, Varki A. Chemical diversity in the sialic acids and related alpha-keto acids: An evolutionary perspective. *Chem Rev* 2002;102:439-69.
4. Irie A, Koyama S, Kozutsumi Y, Kawasaki T, Suzuki A. The molecular basis for the absence of N-glycolylneuraminic acid in humans. *J Biol Chem* 1998;273:15866-71.
5. Marshall BT, Long M, Piper JW, Yago T, McEver RP, Zhu C. Direct observation of catch bonds involving cell-adhesion molecules. *Nature* 2003;423:190-3.
6. Varki A. Glycan-based interactions involving vertebrate sialic-acid-recognizing proteins. *Nature* 2007;446:1023-9.
7. Macauley MS, Crocker PR, Paulson JC. Siglec-mediated regulation of immune cell function in disease. *Nat Rev Immunol* 2014;14:653-66.
8. Izquierdo-Useros N, Lorizate M, McLaren PJ, Telenti A, Kräusslich H-G, Martinez-Picado J. HIV-1 capture and transmission by Dendritic Cells: The Role of Viral Glycolipids and the Cellular Receptor Siglec-1. *PLoS Pathog* 2014;10:e1004146.
9. Geijtenbeek TB, Kwon DS, Torensma R, van Vliet SJ, van Duijnhoven GC, Middel J, Cornelissen IL, Nottet HS, KewalRamani VN, Littman DR, Figdor CG, van Kooyk Y. DC-SIGN, a dendritic cell-specific HIV-1-binding protein that enhances trans-infection of T cells. *Cell* 2000;100:587-97.
10. Weis W, Brown JH, Cusack S, Paulson JC, Skehel JJ, Wiley DC. Structure of the influenza-virus hemagglutinin complexed with its receptor, sialic-acid. *Nature* 1988;333:426-31.
11. Mahdavi J, Sondén B, Hurtig M, Olfat FO, Forsberg L, Roche N, Angstrom J, Larsson T, Teneberg S, Karlsson KA, Altraja S, Wadström T, Kersulyte D, Berg DE, Dubois A, Petersson C, Magnusson KE, Norberg T, Lindh F, Lundskog BB, Arnqvist A, Hammarström L, Borén T. Helicobacter pylori SabA adhesin in persistent infection and chronic inflammation. *Science* 2002;297:573-8.
12. Mitchell J, Sullam PM. Streptococcus mitis phage-encoded adhesins mediate attachment to α 2-8-linked sialic acid residues on platelet membrane gangliosides. *Infect Immun* 2009;77:3485-90.
13. Ashwell G, Morell A. The dual role of sialic acid in the hepatic recognition and catabolism of serum glycoproteins. *Biochemical Society symposium* 1974;117-24.
14. Windler E, Greeve J, Levkau B, Kolbbachofen V, Daerr W, Greten H. The human asialoglycoprotein receptor is a possible binding-site for low-density lipoproteins and chylomicron remnants. *Biochem J* 1991;276:79-87.
15. Chen S, Fukuda M. Cell type-specific roles of carbohydrates in tumor metastasis. *Methods Enzymol* 2006;416:371-80.
16. Samraj A, Läubli H, Varki N, Varki A. Involvement of a non-human sialic acid in human cancer. *Front in Oncol* 2014;4.
17. Comb DG, Roseman S. The sialic acids. I. The structure and enzymatic synthesis of N-acetylneuraminic acid. *J Biol Chem* 1960;235:2529-37.
18. Münster AK, Eckhardt M, Potvin B, Mühlhoff M, Stanley P, Gerardy-Schahn R. Mammalian cytidine 5'-monophosphate N-acetylneuraminic acid synthetase: A nuclear protein with evolutionarily conserved structural motifs. *Proc Natl Acad Sci USA* 1998;95:9140-5.
19. Eckhardt M, Gotza B, Gerardy-Schahn R. Membrane topology of the mammalian CMP-sialic acid transporter. *J Biol Chem* 1999;274:8779-87.
20. Harduin-Lepers A, Vallejo-Ruiz V, Krzewinski-Recchi MA, Samyn-Petit B, Julien S, Delannoy P. The human sialyltransferase family. *Biochimie* 2001;83:727-37.
21. Keppler OT, Hinderlich S, Langner J, Schwartz-Albiez R, Reutter W, Pawlita M. UDP-GlcNAc 2-epimerase: A regulator of cell surface sialylation. *Science* 1999;284:1372-6.
22. Hinderlich S, Stäsche R, Zeitler R, Reutter W. A bifunctional enzyme catalyzes the first two steps in N-acetylneuraminic acid biosynthesis of rat liver - Purification and characterization of UDP-N-acetylglucosamine 2-epimerase/N-acetylmannosamine kinase. *J Biol Chem* 1997;272:24313-8.
23. Stäsche R, Hinderlich S, Weise C, Effertz K, Lucka L, Moormann P, Reutter W. A bifunctional enzyme catalyzes the first two steps in N-acetylneuraminic acid biosynthesis of rat liver - Molecular cloning and functional expression of UDP-N-acetyl-glucosamine 2-epimerase/N-acetylmannosamine kinase. *J Biol Chem* 1997;272:24319-24.
24. Jensen PH, Karlsson NG, Kolarich D, Packer NH. Structural analysis of N- and O-glycans released from glycoproteins. *Nat Protocols* 2012;7:1299-310.
25. Tan E, Almaraz RT, Khanna HS, Du J, Yarema KJ. experimental design considerations for in vitro non-natural glycan display via metabolic oligosaccharide engineering. *Current Protoc Chem Biol* 2010;2:171-94
26. Wratil PR, Horstkorte R, Reutter W. Metabolic Glycoengineering with N-acyl side chain modified mannosamines. *Angew Chem Int Ed* 2016;55:9482-512.
27. Al-Rawi S, Hinderlich S, Reutter W, Giannis A. Synthesis and biochemical properties of reversible inhibitors of UDP-N-acetylglucosamine 2-epimerase. *Angew Chem Int Ed* 2004;43:4366-70.
28. Stoltz F, Reiner M, Blume A, Reutter W, Schmidt RR. Novel UDP-glycal derivatives as transition state analogue inhibitors of UDP-GlcNAc 2-epimerase. *J Org Chem* 2004;69:665-79.
29. Martinez J, Nguyen LD, Hinderlich S, Zimmer R, Tauberger E, Reutter W, Saenger W, Fan H, Moniot S. Crystal structures of N-acetylmannosamine kinase provide insights into enzyme activity and inhibition. *J Biol Chem* 2012;287:13656-65.
30. Rillahan CD, Antonopoulos A, Lefort CT, Sonon R, Azadi P, Ley K, Dell A, Haslam SM, Paulson JC. Global metabolic inhibitors of sialyl- and fucosyltransferases remodel the glycome. *Nat Chem Biol* 2012;8:661-8.
31. Macauley MS, Arlian BM, Rillahan CD, Pang PC, Bortell N, Marcondes MC, Haslam SM, Dell A, Paulson JC.

- Systemic blockade of sialylation in mice with a global inhibitor of sialyltransferases. *J Biol Chem* 2014;289:35149-58.
32. Kayser H, Zeitler R, Kannicht C, Grunow D, Nuck R, Reutter W. Biosynthesis of a nonphysiological sialic acid in different rat organs, using N-propanoyl-D-hexosamines as precursors. *J Biol Chem* 1992;267:16934-8.
 33. Keppler OT, Stehling P, Herrmann M, Kayser H, Grunow D, Reutter W, Pawlita M. Biosynthetic modulation of sialic acid-dependent virus-receptor interactions of two primate polyoma viruses. *J Biol Chem* 1995;270:1308-14.
 34. Mahal LK, Yarema KJ, Bertozzi CR. Engineering chemical reactivity on cell surfaces through oligosaccharide biosynthesis. *Science* 1997;276:1125-8.
 35. Saxon E, Bertozzi CR. Cell surface engineering by a modified Staudinger reaction. *Science* 2000;287:2007-10.
 36. Benie AJ, Blume A, Schmidt RR, Reutter W, Hinderlich S, Peters T. Characterization of ligand binding to the bifunctional key enzyme in the sialic acid biosynthesis by NMR - II. Investigation of the ManNAc kinase functionality. *J Biol Chem* 2004;279:55722-7.
 37. Erikson E, Wratil PR, Frank M, Ambiel I, Pahnke K, Pino M, Azadi P, Izquierdo-Useros N, Martinez-Picado J, Meier C, Schnaar RL, Crocker PR, Reutter W, Keppler OT. Mouse siglec-1 mediates trans-infection of surface-bound murine leukemia virus in a sialic acid N-acyl side chain-dependent manner. *J Biol Chem* 2015;290:27345-59.
 38. Collins BE, Fralich TJ, Itonori S, Ichikawa Y, Schnaar RL. Conversion of cellular sialic acid expression from N-acetyl- to N-glycolylneuraminic acid using a synthetic precursor, N-glycolylmannosamine pentaacetate: inhibition of myelin-associated glycoprotein binding to neural cells. *Glycobiology* 2000;10:11-20.
 39. Chefalo P, Pan YB, Nagy N, Guo ZW, Harding CV. Efficient metabolic engineering of GM3 on tumor cells by N-phenylacetyl-D-mannosamine. *Biochemistry* 2006;45:3733-9.
 40. Wolf S, Warnecke S, Ehrit J, Freiberger F, Gerardy-Schahn R, Meier C. Chemical synthesis and enzymatic testing of CMP-sialic acid derivatives. *ChemBioChem* 2012;13:2605-15.
 41. Wratil PR, Rigol S, Solecka B, Kohla G, Kannicht C, Reutter W, Giannis A, Nguyen LD. A novel approach to decrease sialic acid expression in cells by a C-3-modified N-acetylmannosamine. *J Biol Chem* 2014;289:32056-63.
 42. Nieto-Garcia O, Wratil PR, Nguyen LD, Böhrsch V, Hinderlich S, Reutter W, Hackenberger CPR. Inhibition of the key enzyme of sialic acid biosynthesis by C6-Se modified N-acetylmannosamine analogs. *Chem Sci* 2016;7:3928-33.
 43. Sarkar AK, Brown JR, Esko JD. Synthesis and glycan priming activity of acetylated disaccharides. *Carbohydr Res* 2000;329:287-300.
 44. Jones MB, Teng H, Rhee JK, Lahar N, Baskaran G, Yarema KJ. Characterization of the cellular uptake and metabolic conversion of acetylated N-acetylmannosamine (ManNAc) analogues to sialic acids. *Biotechnol Bioeng* 2004;85:394-405.
 45. Weihofen WA, Berger M, Chen H, Saenger W, Hinderlich S. Structures of human N-acetylglucosamine kinase in two complexes with N-acetylglucosamine and with ADP/glucose: insights into substrate specificity and regulation. *J Mol Biol* 2006;364:388-99.
 46. de Mol NJ, Fischer, M. J. Surface plasmon resonance: methods and protocols. Springer Verlag GmbH 2010;Heidelberg:pp. 91-100.
 47. Inoue S, Inoue Y. Ultrasensitive analysis of sialic acids and oligo/polysialic acids by fluorometric high-performance liquid chromatography. *Methods Enzymol Academic* 2003;543-60.
 48. Smith DF, Prieto PA. Special considerations for glycolipids and their purification. *Curr Protoc Mol Bio* 2001; Chapter 17, Unit 17.13
 49. Galuska SP, Geyer H, Weinhold B, Kontou M, Röhrich RC, Bernard U, Gerardy-Schahn R, Reutter W, Münter-Kühnel A, Geyer R. Quantification of nucleotide-activated sialic acids by a combination of reduction and fluorescent labeling. *Anal Chem* 2010;82:4591-8.
 50. Brinkman-Van der Linden ECM, Sjöberg ER, Juneja LR, Crocker PR, Varki N, Varki A. Loss of N-glycolylneuraminic acid in human evolution: implications for sialic acid recognition by siglecs. *J Biol Chem* 2000;275:8633-40.
 51. Oetke C, Hinderlich S, Brossmer R, Reutter W, Pawlita M, Keppler OT. Evidence for efficient uptake and incorporation of sialic acid by eukaryotic cells. *Eur J Biochem* 2001;268:4553-61.
 52. Preidl JJ, Gnanapragassam VS, Lisurek M, Saupe J, Horstkorte R, Rademann J. Fluorescent mimetics of CMP-Neu5Ac are highly potent, cell-permeable polarization probes of eukaryotic and bacterial sialyltransferases and inhibit cellular sialylation. *Angew Chem Int Ed* 2014;53:5700-5.
 53. Blume A, Chen H, Reutter W, Schmidt RR, Hinderlich S. 2'-,3'-dialdehydo-UDP-N-acetylglucosamine inhibits UDP-N-acetylglucosamine 2-epimerase, the key enzyme of sialic acid biosynthesis. *Febs Lett* 2002;521:127-32.
 54. Zhu X, Stoltz F, Schmidt RR. Synthesis of thioglycoside-based UDP-sugar analogues. *J Org Chem* 2004;69:7367-70.
 55. Fournière V, Cumpstey I. Synthesis of non-glycosidically linked selenoether pseudodisaccharides. *Tetrahedron Letters* 2010;51:2127-9.
 56. André S, Kövér KE, Gabius H-J, Szilágyi L. Thio- and selenoglycosides as ligands for biomedically relevant lectins: Valency–activity correlations for benzene-based dithiogalactoside clusters and first assessment for (di)selenodigalactosides. *Bioorg Medl Chem Lett* 2015;25:931-5.
 57. Mendla K, Baumkötter J, Rosenau C, Ulrichbott B, Cantz M. Defective lysosomal release of glycoprotein-derived sialic acid in fibroblasts from patients with sialic-acid storage disease. *Biochem J* 1988;250:261-7.
 58. Chan R, Uchil PD, Jin J, Shui G, Ott DE, Mothes W, Wenk MR. Retroviruses human immunodeficiency virus and murine leukemia virus are enriched in phosphoinositides. *J Virol* 2008;82:11228-38.
 59. Puryear WB, Yu X, Ramirez NP, Reinhard BM, Gummuluru S. HIV-1 incorporation of host-cell-derived glycosphingolipid GM3 allows for capture by mature dendritic cells. *Proc Natl Acad Sci USA* 2012;109:7475-80.

Eidesstattliche Versicherung

„Ich, Paul Robin Wratil, versichere an Eides statt durch meine eigenhändige Unterschrift, dass ich die vorgelegte Dissertation mit dem Thema: *Modifikation der Expression von Sialinsäuren auf der Zelloberfläche mit N-Acetylmannosamin-Analoga* selbstständig und ohne nicht offengelegte Hilfe Dritter verfasst und keine anderen als die angegebenen Quellen und Hilfsmittel genutzt habe.

Alle Stellen, die wörtlich oder dem Sinne nach auf Publikationen oder Vorträgen anderer Autoren beruhen, sind als solche in korrekter Zitierung (siehe „Uniform Requirements for Manuscripts (URM)“ des ICMJE -www.icmje.org) kenntlich gemacht. Die Abschnitte zu Methodik (insbesondere praktische Arbeiten, Laborbestimmungen, statistische Aufarbeitung) und Resultaten (insbesondere Abbildungen, Graphiken und Tabellen) entsprechen den URM (s.o.) und werden von mir verantwortet.

Meine Anteile an den ausgewählten Publikationen entsprechen denen, die in der untenstehenden gemeinsamen Erklärung mit dem Betreuer, angegeben sind. Sämtliche Publikationen, die aus dieser Dissertation hervorgegangen sind und bei denen ich Autor bin, entsprechen den URM (s.o.) und werden von mir verantwortet.

Die Bedeutung dieser eidesstattlichen Versicherung und die strafrechtlichen Folgen einer unwahren eidesstattlichen Versicherung (§156,161 des Strafgesetzbuches) sind mir bekannt und bewusst.“

Datum

Unterschrift

Anteilserklärung an den erfolgten Publikationen

Paul Robin Wratil hatte folgenden Anteil an den folgenden Publikationen:

Publikation 1: Wratil PR*, Rigol S*, Solecka B, Kohla G, Kannicht C, Reutter W, Giannis A, Nguyen LD. A novel approach to decrease sialic acid expression in cells by a C-3-modified N-acetylmannosamine. *Journal of Biological Chemistry*. 2014; 289: 32056-63.

Beitrag im Einzelnen:

Die Experimente zur Bestimmung der Expression von Sialinsäuren auf der Zelloberfläche mit Lektinen sowie deren Auswertung wurden von Herrn Wratil unter Anleitung von Herrn Dr. Nguyen durchgeführt. Die Zytotoxizitätsstudien und deren Auswertung führte der Promovend selbstständig durch. Zusammen mit L.D. Nguyen bestimmte P.R. Wratil mithilfe von Durchflusszytometrie- und *Enzyme-linked-lectin*-Experimenten die Expression von Sialinsäuren auf der Zelloberfläche von behandelten Zellen und Kontrollzellen. Ebenfalls zusammen mit L.D. Nguyen präparierte Herr Wratil die Zellen für die Bestimmung der membrangebundenen und intrazellulären Sialinsäure-Konzentrationen mittels HPLC. Auch die Auswertung der Chromatographie-Daten erfolgte durch P.R. Wratil. Die Expression und Aufreinigung von Proteinen für enzymatische Tests erledigten L.D. Nguyen und P.R. Wratil gemeinsam. Die Bestimmungen der Enzymkinetiken mithilfe von spektrophotometrischen Experimenten sowie deren Auswertung wurden von Herrn Wratil durchgeführt, genauso die DLS-Experimente. Die SPR-Experimente und deren Auswertung führte der Promovend in Zusammenarbeit mit Frau Dr.

Solecka durch. Mit Ausnahme des Abschnitts über die chemische Synthese der C3-modifizierten ManNAc-Analoga im Methodenteil verfasste P.R. Wratil das gesamte Manuskript. L.D. Nguyen und W. Reutter verbesserten hierbei das Geschriebene. Der Promovend erstellte alle Abbildungen, außer Abbildung 1.

*geteilte Erstautorenschaft

Publikation 2: Erikson E, Wratil PR, Frank M, Ambiel I, Pahnke K, Pino M, Azadi P, Izquierdo-Useros N, Martinez-Picado J, Meier C, Schnaar RL, Crocker PR, Reutter W, Keppler OT. Mouse siglec-1 mediates trans-infection of surface-bound murine leukemia virus in a sialic acid N-acyl side chain-dependent manner. *Journal of Biological Chemistry*. 2015; 290: 27345-59.

Beitrag im Einzelnen:

Herr Wratil führte die Messung der Konzentrationen der verschiedenen Sialinsäure-Spezies in den Zellmembranen und im Glykolipidanteil der Zellen selbstständig durch. Er präparierte die Zellen, führte alle HPLC-Messungen durch und wertete die Daten aus. Ebenfalls selbstständig nahm der Promovend die ESI-MS-Messungen vor und wertete deren Ergebnisse aus. Im Manuskript verfasste P.R. Wratil die Absätze über die Analyse der modifizierten Sialinsäuren in den Methoden und den Teil über die Detektion von modifizierten Sialinsäuren in den Ergebnissen. Der Promovend erstellte die Abbildungen 5 und 6 im Manuskript.

Publikation 3: Nieto-Garcia O*, Wratil PR*, Nguyen LD, Böhrsch V, Hinderlich S, Reutter W, Hackenberger CPR. Inhibition of the key enzyme of sialic acid biosynthesis by C6-Se modified N-acetylmannosamine analogs. *Chemical Science*. 2016; 7: 3928-3933

Beitrag im Einzelnen:

P.R. Wratil übernahm die Expression und Aufreinigung von Proteinen aus *E. coli*. Des Weiteren führte er die Spektrophotometer-Experimente zur Bestimmung der Enzymkinetiken von MNK, GNK und HK durch und wertete deren Ergebnisse aus. Auch wertete er die Ergebnisse der Experimente zur Bestimmung der Inhibition der GNE-Aktivität aus. Herr Wratil führte die Zytotoxizitätsstudien mit den peracetylierten, C6-modifizierten ManNAc-Analoga durch. Er bestimmte selbstständig mithilfe von Durchflusszytometrie die Expression von Sialinsäuren auf der Zelloberfläche von behandelten Zellen und Kontrollzellen. Herr Wratil verfasste den Teil des Manuskripts, der sich mit biochemischen Methoden, deren Auswertung und der Interpretation hierbei gewonnener Ergebnisse befasst. Er erstellte die Abbildungen 2 und 3 sowie S1 – S6.

*geteilte Erstautorenschaft

Unterschrift, Datum und Stempel des betreuenden Hochschullehrers

Unterschrift des Doktoranden/der Doktorandin

A Novel Approach to Decrease Sialic Acid Expression in Cells by a C-3-modified N-Acetylmannosamine^{*§}

Received for publication, August 29, 2014, and in revised form, October 1, 2014. Published, JBC Papers in Press, October 2, 2014, DOI 10.1074/jbc.M114.608398

Paul R. Wratil^{†1}, Stephan Rigol^{§1}, Barbara Solecka[†], Guido Kohla[†], Christoph Kannicht[†], Werner Reutter[‡], Athanassios Giannis^{§2}, and Long D. Nguyen^{‡3}

From the [†]Institut für Laboratoriumsmedizin, Klinische Chemie, und Pathobiochemie, Charité-Universitätsmedizin Berlin, Campus Benjamin Franklin, Arnimallee 22, D-14195 Berlin-Dahlem, the [§]Institut für Organische Chemie, Universität Leipzig, Fakultät für Chemie und Mineralogie, Johannisallee 29, D-04103 Leipzig, and [‡]Octapharma R&D, Molecular Biochemistry Berlin, Walther-Nernst-Strasse 3, D-12489 Berlin, Germany

Background: Inhibitors of cellular sialic acid expression offer substantial therapeutic promise for diseases associated with oversialylation.

Results: 2-Acetylaminoo-2-deoxy-3-O-methyl-D-mannose reduces the sialic acid concentration in cells and inhibits the UDP-GlcNAc-2-epimerase/ManNAc kinase.

Conclusion: Inhibition of the key enzyme of sialic acid biosynthesis by a ManNAc analog decreases cellular sialic acid expression.

Significance: ManNAc analogs represent a new class of sialic acid inhibitors.

Due to its position at the outermost of glycans, sialic acid is involved in a myriad of physiological and pathophysiological cell functions such as host-pathogen interactions, immune regulation, and tumor evasion. Inhibitors of cell surface sialylation could be a useful tool in cancer, immune, antibiotic, or antiviral therapy. In this work, four different C-3 modified N-acetylmannosamine analogs were tested as potential inhibitors of cell surface sialylation. Peracetylated 2-acetylaminoo-2-deoxy-3-O-methyl-D-mannose decreases cell surface sialylation in Jurkat cells in a dose-dependent manner up to 80%, quantified by flow cytometry and enzyme-linked lectin assays. High-performance liquid chromatography experiments revealed that not only the concentration of membrane bound but also of cytosolic sialic acid is reduced in treated cells. We have strong evidence that the observed reduction of sialic acid expression in cells is caused by the inhibition of the bifunctional enzyme UDP-GlcNAc-2-epimerase/ManNAc kinase. 2-Acetylaminoo-2-deoxy-3-O-methyl-D-mannose inhibits the human ManNAc kinase domain of the UDP-GlcNAc-2-epimerase/ManNAc kinase. Binding kinetics of the inhibitor and human N-acetylmannosamine kinase were evaluated using surface plasmon resonance. Specificity studies with human N-acetylglucosamine kinase and hexokinase IV indicated a high specificity of 2-acetylaminoo-2-deoxy-3-O-

methyl-D-mannose for MNK. This substance represents a novel class of inhibitors of sialic acid expression in cells, targeting the key enzyme of sialic acid *de novo* biosynthesis.

Sialic acid is an essential constituent of the glycocalyx. Due to its chemical characteristics, sialic acid interacts with the environment of the cell. Its terminal position in glycoconjugates enables this amino sugar to disguise or create recognition sites for receptors or ligands and thus modulates biological cell functions (1). Sialic acid is a ligand for the selectin and the sialic family of adhesion molecules, mediating immune regulation and leukocyte rolling (2–5). Various pathogenic microorganisms, similar to the influenza virus with hemagglutinin, use sialylated glycans to recognize and bind host cells (6). Most tumor cells demonstrate hypersialylation and an alteration of their sialic acid pattern, allegedly to protect themselves from immune surveillance (7, 8). There is evidence that oversialylated tumor cells are more resistant to anti-cancer drugs (9).

The bifunctional enzyme UDP-GlcNAc-2-epimerase/ManNAc⁴ kinase is the major determinant of cell surface sialylation (10). It catalyzes the first two steps in the *de novo* biosynthesis of sialic acid, namely the epimerization of UDP-GlcNAc to ManNAc and the phosphorylation of ManNAc to ManNAc-6-phosphate. Former studies succeeded in synthesizing inhibitors of the UDP-GlcNAc-2-epimerase/ManNAc kinase (11–14). However, these inhibitors were membrane-impermeable and could not be used in cell-based assays. Consequently, we focused on developing membrane-permeable analogs of N-acetylmannosamine that inhibit sialic acid expression in intact cells.

Non-natural ManNAc analogs are well established precursors of modified sialic acid on the cell surface. They, for exam-

* This work was supported by the Wilhelm-Sander Stiftung, by the Sonnenfeld Stiftung, and the Roland und Elfriede Schauer Stiftung.

This work is dedicated to Professor Konrad Sandhoff on the occasion of his 75th birthday.

§ This article contains supplemental Methods and data.

¹ Both authors contributed equally to this work.

² To whom correspondence may be addressed: Institut für Organische Chemie, Universität Leipzig, Fakultät für Chemie und Mineralogie, Johannisallee 29, D-04103 Leipzig, Germany. Tel.: 49-341-97-36-581; Fax: 49-341-97-36-599; E-mail: giannis@uni-leipzig.de.

³ To whom correspondence may be addressed: Institut für Laboratoriumsmedizin, Klinische Chemie und Pathobiochemie, Charité - Universitätsmedizin Berlin, Campus Benjamin Franklin, Arnimallee 22, D-14195 Berlin-Dahlem, Germany. Tel.: 49-30-838-71374; Fax: 49-30-838-71541; E-mail: long-duc.nguyen@charite.de.

⁴ The abbreviations used are: ManNAc, N-acetylmannosamine; DMB, 1,2-diamino-4,5-methylenedioxobenzene; GlcNAc, N-acetyl-glucosamine; GNE, human N-acetyl-glucosamine-2-epimerase; MNK, human N-acetylmannosamine kinase; Neu5Ac, N-acetyl-neurameric acid.

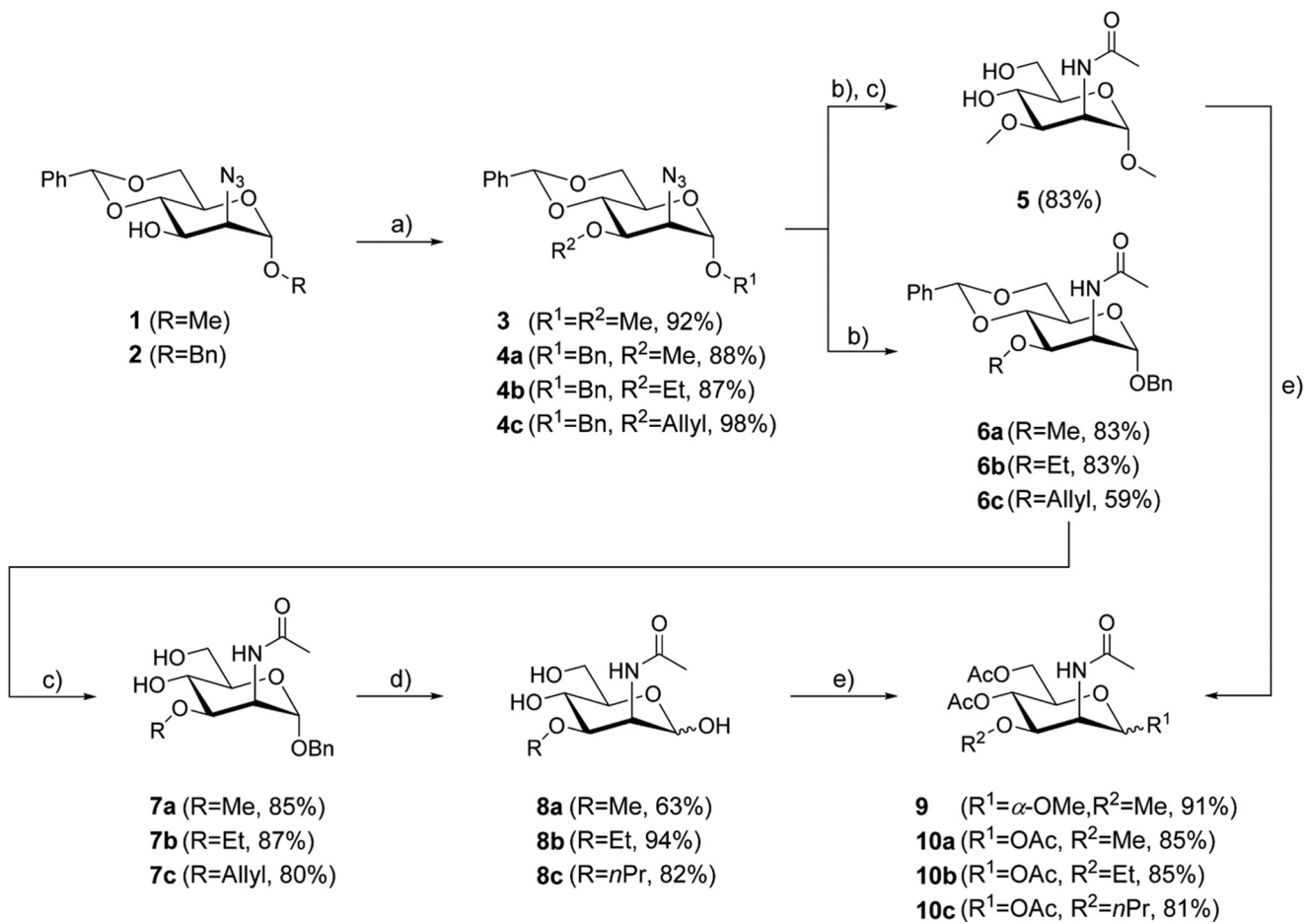


FIGURE 1. **Synthesis of C-3-modified mannosamine analogs.** 2-Acetylaminoo-2-deoxy-3-O-methyl-D-mannose (**8a**), methyl 2-acetylaminoo-2-deoxy-3-O-methyl- α -D-mannopyranoside (**5**), 2-acetylaminoo-2-deoxy-3-O-ethyl-D-mannose (**8b**), and 2-acetylaminoo-2-deoxy-3-O-propyl-D-mannose (**8c**) were prepared in three to four steps. For cell experiments, the given ManNAc analogs have been peracetylated (**9**, **10a**, **10b**, and **10c**, respectively) to increase their permeability for the plasma membrane of the cells: (a) NaH, alkyl halide (MeI, EtI, and allyl bromide), 0 °C → room temperature, dimethylformamide; (b) 1) H₂ (10% v/v), Pd/C, MeOH (for reduction of **4c**; PPh₃, THF/H₂O); 2) AcCl, NEt₃, DMAP, DCM; (c) AcOH (80%), 80 °C; (d) H₂ (11 bar), Pd/C, MeOH; and (e) Ac₂O, pyridine.

ple carrying a keto or an azido group, can be utilized to visualize sialic acid in cells (15–17). These analogs are either modified at the C-2 or the C-4 position of ManNAc (18, 19).

In our study, we introduced C-3-modified ManNAc analogs and tested their effect on cell surface sialylation. C-3 derivatives of ManNAc are not likely to be metabolized by cells into the respected sialic acids (20). Inhibition studies for the ManNAc kinase domain of the UDP-GlcNAc-2-epimerase/ManNAc kinase were performed.

EXPERIMENTAL PROCEDURES

Preparation of ManNAc Analogs

Chemical synthesis of C-3-modified *N*-acetyl-D-mannosamines (Fig. 1) started from azido mannopyranosides **1** and **2**, respectively (21, 22). Attachment of the alkoxy residue at C-3 was achieved by Williamson ether synthesis to give the alkylated derivatives **3** and **4a–c** in good to excellent yields. Reduction of the azido function with H₂-Pd/C or through Staudinger reaction and subsequent acylation under standard conditions yielded the *N*-acetylated derivatives. In the case of methyl glycoside **3** cleavage of the 4,6-O-benzylidene group by treatment with acetic acid at elevated temperature provided ManNAc analog **5**. In addition benzyl glycosides **6a–c** were also synthesized and then

subjected to acidic hydrolysis to afford derivatives **7a–c**. Cleavage of the benzyl group through palladium-catalyzed hydrogenolysis furnished the free *N*-acetyl-3-O-alkylmannosamine derivatives **8a–c**.

To increase their membrane permeability, peracetylated ManNAc analogs have been synthesized for cell experiments. In the cytoplasm, the O-acetyl groups of these molecules are removed by cytoplasmic esterases releasing the active monosaccharides (23–25). Peracetylation of **5** and **8a–c** with acetic anhydride in pyridine afforded compounds **9** and **10a–c**.

Details are included in the *supplemental data*. Identity and purity of all intermediates and final compounds were verified by spectroscopic and spectrometric methods (data not shown).

Determination of Cell Surface Sialylation

Cell Preparation—Approximately 20,000 Jurkat cells (ATCC) in 100 μ l of RPMI 1640 culture medium (PAN Biotech) with 10% FBS (PAN Biotech) and 2 mM L-glutamine, containing peracetylated ManNAc analogs in varying concentrations, were cultured for 72 h.

After incubation, cells were washed with PBS containing 0.5% bovine serum albumin (PBS + 0.5% BSA) and labeled with various lectins. Labeling was carried out for 1 h at 4 °C and

C-3-modified ManNAc Decreases Sialic Acid Expression in Cells

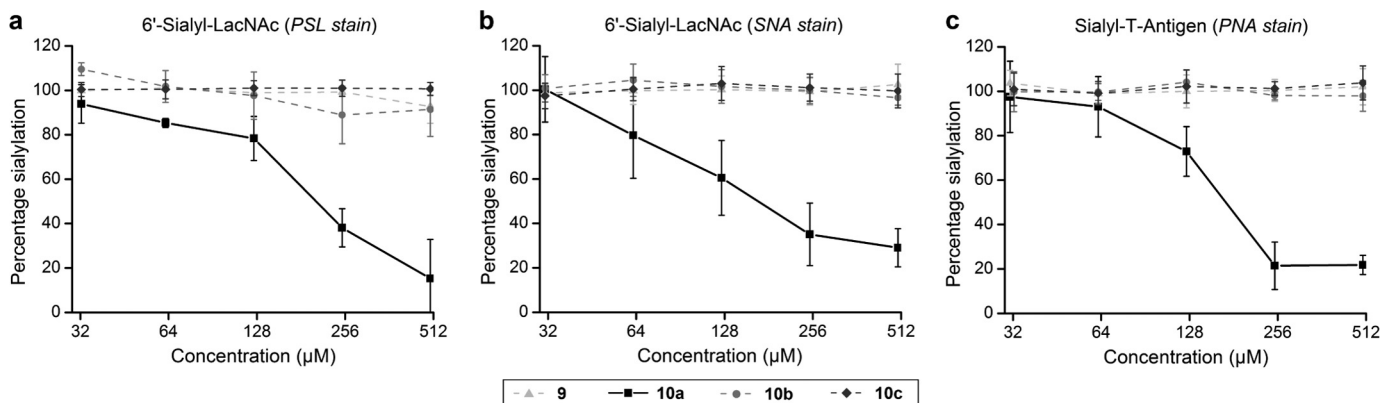


FIGURE 2. Peracetylated 2-acetylaminoo-2-deoxy-3-O-methyl-D-mannose (10a) is an inhibitor of cell surface sialylation. Jurkat cells were treated with varying concentrations of peracetylated ManNAc analogs for 72 h. Sialylated epitopes were analyzed with glycan specific lectins via flow cytometry (*a*) and in cell enzyme-linked lectin assay (*b* and *c*). Obtained data were normalized to untreated cells (100%) and cells treated for 1 h with 0.2 units/ml sialidase (0%). Data shown represent the mean values and S.D. of three independent experiments ($n = 3$). Only **10a** shows inhibition of cell surface sialylation. The peracetylated forms of methyl 2-acetylaminoo-2-deoxy-3-O-methyl- α -D-mannopyranoside (**9**), 2-acetylaminoo-2-deoxy-3-O-ethyl-D-mannose (**10b**), and 2-acetylaminoo-2-deoxy-3-O-propyl-D-mannose (**10c**) had no effects on cell surface sialylation. *PSL*, *P. squamosus* lectin; *SNA*, *S. nigra* agglutinin; *PNA*, *A. hypogaea* agglutinin.

completed by three washing steps with PBS + 0.5% BSA. Obtained data were normalized to untreated cells, and cells were treated for 1 h with 0.2 units/ml sialidase from *Clostridium perfringens* (Sigma Aldrich). All experiments were performed in triplicate.

In Cell Enzyme-linked Lectin Assay—Alkaline phosphatase-conjugated *Arachis hypogaea* agglutinin (2 μ g/ml, EY Laboratories) and alkaline phosphatase-conjugated *Sambucus nigra* agglutinin (3 μ g/ml, EY Laboratories) were used in an in cell enzyme-linked lectin assay. 200 μ l of *p*-nitrophenyl phosphate solution (Sigma-Aldrich) was added to start the reaction. Alkaline phosphatase activity was recorded at a wavelength of 405 nm.

Flow Cytometry—Flow cytometry experiments were conducted using FITC-conjugated *Polyporus squamosus* lectin (0.1 μ g/ml, a gift from Prof. H.-J. Gabius, Technische Universität München).

Cytotoxicity Assays

The cell proliferation assay AlamarBlue $^{\circ}$ (AbD Serotec) was used to determine the cytotoxicity of given peracetylated ManNAc analogs. Samples of 100- μ l cell suspension in RPMI 1640 + 10% FBS and 2 mM L-glutamine (20,000 Jurkat cells per well), containing different concentrations of peracetylated ManNAc analogs, were prepared. Cells were cultured for 72 h. Then, 10 μ l of AlamarBlue $^{\circ}$ solution was added. After 4 h of incubation, samples were analyzed at wavelengths of 570 and 620 nm. Experiments were performed in triplicate and normalized to untreated control cells.

Quantification of Cytosolic and Membrane-associated Sialic Acid

Concentrations of free, CMP-conjugated and membrane-bound sialic acid were measured by DMB HPLC (26). Jurkat cells, cultured 72 h in 5 ml of RPMI 1640 (10% FBS, 2 mM L-glutamine) containing 500 μ M **10a**, were harvested and homogenized by sonication in ice-cold lysis buffer (150 mM NaCl, 10 mM Tris, 5 mM EDTA, 1 mM PMSF, 40 μ M leupeptin, 1.5 μ M aprotinin, pH 8.0). Cytosolic fractions were separated by

centrifugation at 21,000 \times g and 4 °C for 2 h. Subsequently, a chloroform-methanol precipitation was performed to isolate the glycan moiety. The aqueous phase was filtered via a 3-kDa size exclusion filter to remove residual macromolecules. Half of the samples were subjected to sodium borohydride reduction (200 mM sodium borohydride in 200 mM sodium borate buffer, pH 8.0) for 12 h to reduce non-CMP-conjugated sialic acid.

All membrane and the cytosolic fractions were hydrolyzed with 1 M trifluoroacetic acid for 4 h at 80 °C. Hydrolyzed samples were dissolved in 2 M acetic acid. Subsequently, samples were labeled with 50 μ l of ice-cold DMB solution (6.9 mM DMB, 0.67 mM β -mercaptoethanol, 0.19% sodium bisulfide).

Labeled samples were analyzed on a Dionex Ultimate 3000 HPLC System (Thermo Scientific) using a Gemini-NX C18 column (110 Å, 3 μ m particle size, 4.6 mm \times 150 mm, Phenomenex). Probes were separated at 1 ml/min flow rate with methanol/acetonitrile/water (6:8:86) as eluent. The detector was configured with 373 nm for excitation and 448 nm for emission.

Cloning and Protein Purification

Cloning and protein purification of the MNK were performed according to an established method (27). His-tagged MNK was expressed in BL21-CodonPlus (DE3)-RIL *Escherichia coli* (Stragene), followed by nickel-nitrilotriacetic acid affinity chromatography and gel filtration with a SuperdexTM HighLoad 16/600 column (GE Healthcare) (28). Human N-acetyl-glucosamine kinase was purified as described previously (29). GST-tagged N-acetyl-glucosamine kinase was expressed in *E. coli* followed by glutathione affinity chromatography, gel filtration, and GST tag cleavage by thrombin. Human hexokinase IV was purchased from Sigma-Aldrich.

Spectrophotometric Assays (Enzyme Activity, Kinetics, and Inhibition)

Enzyme activity, kinetics, and inhibition were assessed via a coupled optical assay using purified MNK. 120 μ l of reaction mixture contained the following buffers and reagents: 66.5 μ l of buffer A (65 mM MgCl₂, 10 mM Tris-HCl, pH 8.1), 10.0 μ l of ATP (varying concentrations), 7.5 μ l of NADH (15 mM), 5.0 μ l

of phosphoenolpyruvate (100 mM), 2 units of pyruvate-kinase, 2 units of lactate dehydrogenase, 10 μ l of ManNAc of varying concentrations, and 10 μ l of ManNAc analogs of varying concentrations. The reaction was started by adding 80 μ l of MNK (1.25 μ M) in buffer B (10 mM Tris-HCl, 150 mM NaCl, pH 8.0).

All spectrophotometric experiments were performed at 37 °C, and the results obtained were normalized to blanks, consisting of 120 μ l of reaction mixture and 80 μ l of buffer B without MNK. For hexokinase IV and N-acetyl-glucosamine kinase, the activity assay was adapted using glucose or N-acetyl-glucosamine as educts, respectively.

Dynamic Light Scattering Analysis—Dynamic light scattering experiments have been performed using a Laser Spectro Scatter 201 (RiNA). Cuvettes were prepared with 30 μ l of purified MNK (10 μ M) in buffer B containing ManNAc or **8a** at concentrations of 5 mM. All measurements were performed at 21 °C. Results were compared with negative controls containing untreated MNK only and positive controls containing MNK incubated for 10 min at 45 °C to induce protein aggregation.

Surface Plasmon Resonance—Experiments were conducted using a Biacore T100 biosensor instrument (GE Healthcare) and a nitrilotriacetic acid sensor chip (GE Healthcare). The following buffers were used: (a) running buffer (10 mM HEPES, 150 mM NaCl, 0.05 mM EDTA, 0.005% Tween, pH 7.4) and (b) protein regeneration solution (10 mM taurodeoxycholic acid, 100 mM Tris-HCl, pH 9.0).

His-tagged MNK was covalently immobilized to a level of ~12,000 resonance units (1 resonance unit = 1 pg/mm²). The immobilization was carried out according to an established procedure with slight modifications, using a Biacore amine coupling kit (GE Healthcare) (30). Prior to the amine coupling procedure, the nitrilotriacetic acid sensor chip was activated with 0.5 mM NiCl₂. After covalent attachment of the protein to the surface of the sensor chip, the coating procedure was completed by injecting 350 mM EDTA in running buffer. A flow cell without immobilized protein was used as reference.

All binding experiments were performed at 25 °C and a flow rate of 20 μ l/min. Analytes of different concentrations were injected for 180 s followed by a 1000-s dissociation. In case of ManNAc and its analogs, regeneration was carried out by two injections of protein regeneration solution (10 μ l/min, 60 s). With nucleosides 10 mM ManNAc in running buffer and 100 mM EDTA were injected (each 10 μ l/min, 60 s) to assure regeneration. Each cycle was followed by a stabilization period of 1000 s. Binding data were evaluated with BIAevaluation (version 4.1, GE Healthcare), using 1:1 Langmuir binding model after reference cell and buffer injection subtraction.

RESULTS

Inhibition of Sialic Acid on the Cell Surface—**10a** decreases cell surface sialylation in a dose-dependent manner. Treatment of Jurkat cells for 72 h with **10a** led to a substantial reduction of sialic acid expression on the cell surface. The 6'-sialyl-LacNAc entity was reduced by nearly 80%, determined by *Polyporus squamosus* lectin binding (Figs. 2a and 3) and by ~70%, detected using *Sambucus nigra* agglutinin binding (Fig. 2b). The exposure of non-sialylated T antigen ($\text{Gal}\beta 1\text{-}3\text{GalNAc}-\text{Ser}/\text{Thr}$) was increased under treatment with **10a**, verified by Ara-

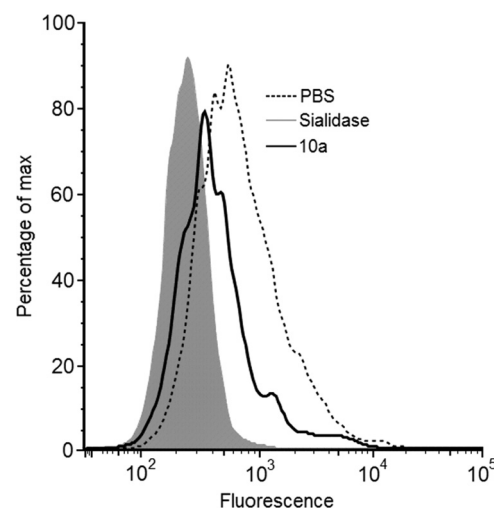


FIGURE 3. Flow cytometry analysis of Jurkat cells with FITC-conjugated *P. squamosus* lectin. Jurkat cells were treated for 72 h with peracetylated 2-acetylaminoo-2-deoxy-3-O-methyl-D-mannose (**10a**) in a concentration of 125 μ M. To evaluate their 6'-sialyl-LacNAc content, cells were labeled with *Polyporus squamosus* lectin (PSL). Results obtained were compared with untreated cells (PBS, dashed line) and cells treated for 1 h with 0.2 units/ml sialidase (gray shading).

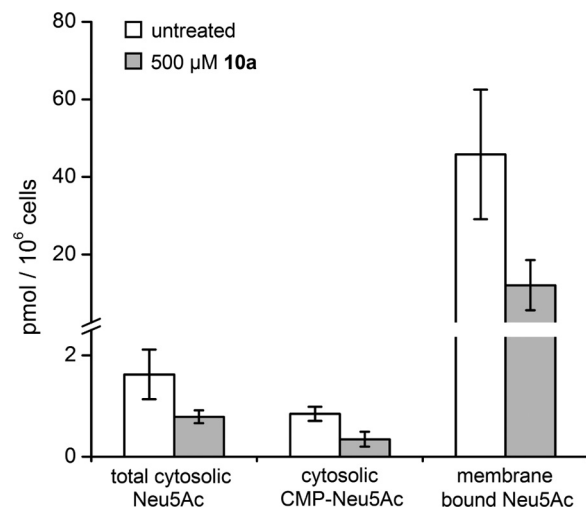


FIGURE 4. Analysis of cytosolic and membrane bound sialic acid in Jurkat cell lysates. Jurkat cells were treated for 72 h with 500 μ M peracetylated 2-acetylaminoo-2-deoxy-3-O-methyl-D-mannose (**10a**). Concentrations of Neu5Ac were measured by DMB-HPLC. CMP-activated Neu5Ac was determined after sodium borohydride reduction of the cytosolic fraction. Data shown represent the mean values and S.D. of three independent experiments ($n = 3$). **10a** inhibits the expression of cytosolic and membrane-bound Neu5Ac.

chis hypogaea agglutinin binding, which equals a reduction of the sialylated epitope of ~80% (Fig. 2c). An IC₅₀ for **10a** of 176 μ M in medium was determined. Other tested ManNAc derivatives (**9**, **10b–c**) did not influence the sialic acid expression on the cell surface, even at final concentrations of 500 μ M (Fig. 2).

Quantification of Sialic Acid in Cell Lysates—Cell lysates of Jurkat cells treated for 72 h with 500 μ M **10a** showed decreased concentrations of free, CMP-conjugated and membrane-bound N-acetyl-neurameric acid (Neu5Ac, Fig. 4). Comparing obtained HPLC chromatograms of treated cells and control cells, no additional peaks appeared, showing that **10a** was not metabolized into a modified sialic acid (Fig. 5).

Cytotoxicity of Peracetylated ManNAc analogs—The effect of tested peracetylated ManNAc analogs on cell viability was neg-

C-3-modified ManNAc Decreases Sialic Acid Expression in Cells

ligible under given conditions. The proliferation rate of Jurkat cells after 72 h of treatment with the peracetylated sugars at final concentrations of 1 mM was not significantly compromised. It is known that other peracetylated ManNAc derivatives such as peracetylated *N*-propionylmannosamine show comparable low cytotoxicity (31).

Inhibition of MNK Enzyme Activity—In spectrophotometric assays with purified MNK, the K_m values of the enzyme have been measured to be 54 μM for ManNAc (specific activity, 0.77

units/mg) and 782 μM for ATP (specific activity, 0.70 units/mg), respectively.

8a inhibits purified MNK in a dose-dependent manner with an IC_{50} value of 1.29 mM (Fig. 6*a*). Other ManNAc derivatives tested (**5**, **8b–c**) revealed no inhibition of enzyme activity, even at maximum concentrations of 10 mM. Dynamic light scattering experiments of purified MNK with **8a** demonstrated that the enzyme inhibition of this substance is not caused by unspecific protein aggregation (Fig. 7).

To evaluate the selectivity of **8a**, its inhibition was assessed for human *N*-acetyl-glucosamine kinase and hexokinase IV (29). For these two related sugar kinases, inhibition of enzyme activity could be observed only at significantly higher concentrations ($IC_{50} > 10$ mM, data not shown).

Linear curve approximation, using the Lineweaver-Burk plot for MNK activity, shows that **8a** is non-competitive for ManNAc, but competitive for ATP (Fig. 6, *b* and *c*). The K_i value of **8a** for the interaction with ATP is 649 μM . Spectrophotometric assays revealed that **5** and **8a–c** were not metabolized by the following enzymes: MNK, *N*-acetyl-glucosamine kinase, and hexokinase IV.

Binding Affinity to MNK—The binding affinity between **8a** and MNK was determined using surface plasmon resonance. The immobilization of MNK to a level of 12,000 resonance units resulted in expected maximal response of ~120 resonance units after injection of **8a** (Fig. 8*a* and Table 1). Assuming a 1:1 interaction, a dissociation constant (K_D) of 755 μM was calculated for the interaction between MNK and **8a**. Under the given experimental conditions, no binding of ManNAc to MNK could be detected. ATP and ADP bound MNK with K_D values of 429 and 306 μM , respectively (Fig. 8*b* and Table 1). The slightly lower K_D value of ADP is due to its higher off rate (k_d). UDP and **5**, which were used as controls, did not bind to MNK.

DISCUSSION

Cell surface sialic acid expression is involved in key processes between cells and their environment. Thus, having simple tools

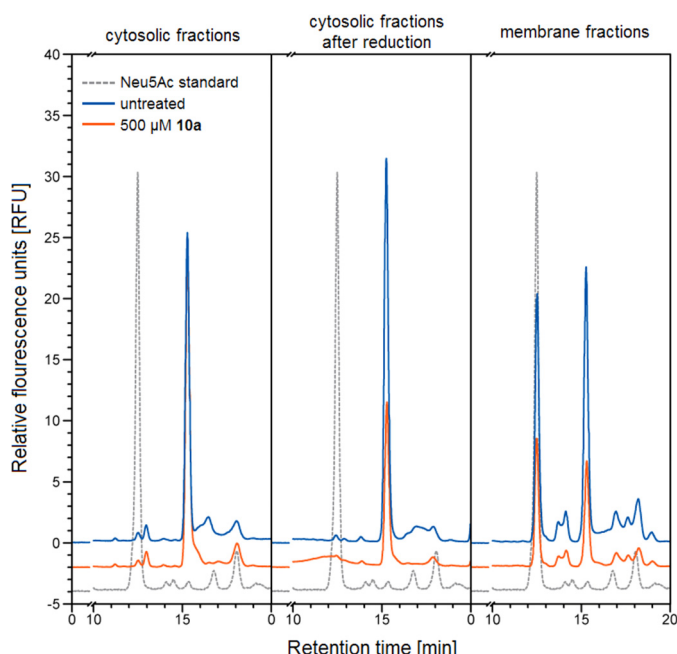


FIGURE 5. Representative chromatograms of DMB-labeled sialic acid residues from Jurkat cell lysates. Jurkat cells were treated for 72 h with 500 μM peracetylated 2-acetylamino-2-deoxy-3-O-methyl-D-mannose (**10a**). Contents of CMP-activated Neu5Ac were determined after sodium borohydride reduction of the cytosolic fraction. Chromatograms of treated cells (orange) and untreated cells (blue) are plotted against a standard of 14 ng of Neu5Ac. Comparing treated and untreated cells no additional fluorescence peak appeared, indicating that **10a** is not metabolized into a modified sialic acid.

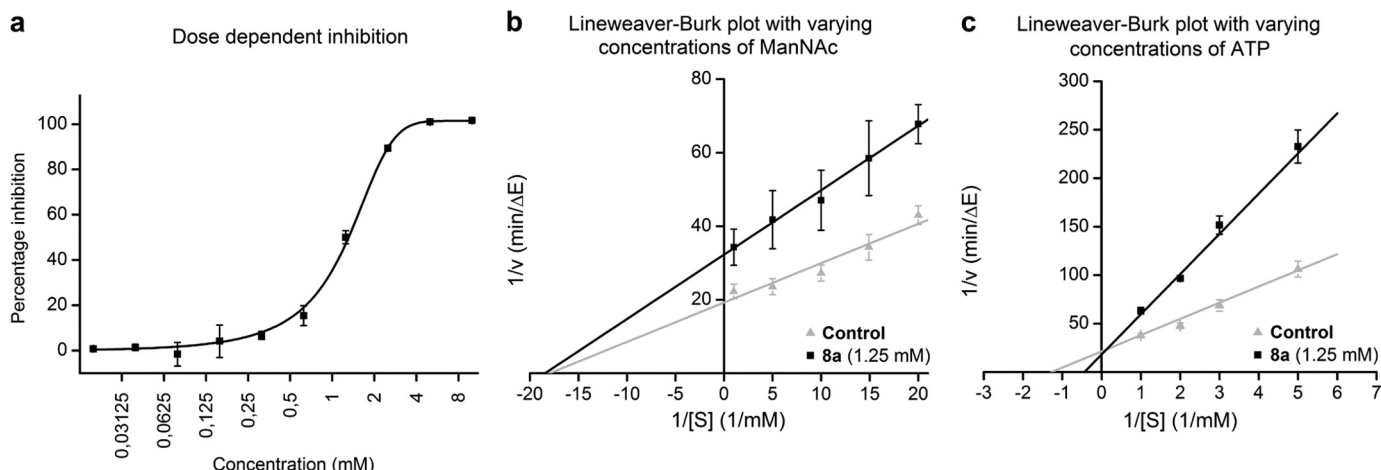


FIGURE 6. 2-Acetylaminio-2-deoxy-3-O-methyl-D-mannose (8a) inhibits purified MNK. A coupled optical assay using enzymatic consumption of NADH was performed to show the effect of **8a** on MNK activity. In *a*, purified MNK was incubated with ManNAc (125 μM), ATP (2 mM), and different concentrations of **8a**. Obtained activity data were normalized to controls without inhibitor (0%). In *b* and *c*, MNK was tested with **8a** (1.25 mM) and varying concentrations of ManNAc (*b*) or ATP (*c*), respectively. Measured data were compared with controls without inhibitor (gray triangles). Data shown represent the mean values and S.D. obtained in three independent experiments ($n = 3$) for *a* and *b* and five independent experiments ($n = 5$) in *c*. Linear (*b* and *c*) and sigmoidal dose response (*a*) curve approximations were performed to determine K_m , K_i , and IC_{50} values.

to decrease cell surface sialylation will greatly benefit research in finding roles of this sugar in biological systems and diseases. Although traditional methods are available to decrease sialic acid expression on the cell surface, e.g. sialyltransferase inhibition or UDP-GlcNAc-2-epimerase/ManNAc kinase-deficient cells (10, 32–34), a systemic inhibitor for the *de novo* biosynthesis of sialic acid is still not available.

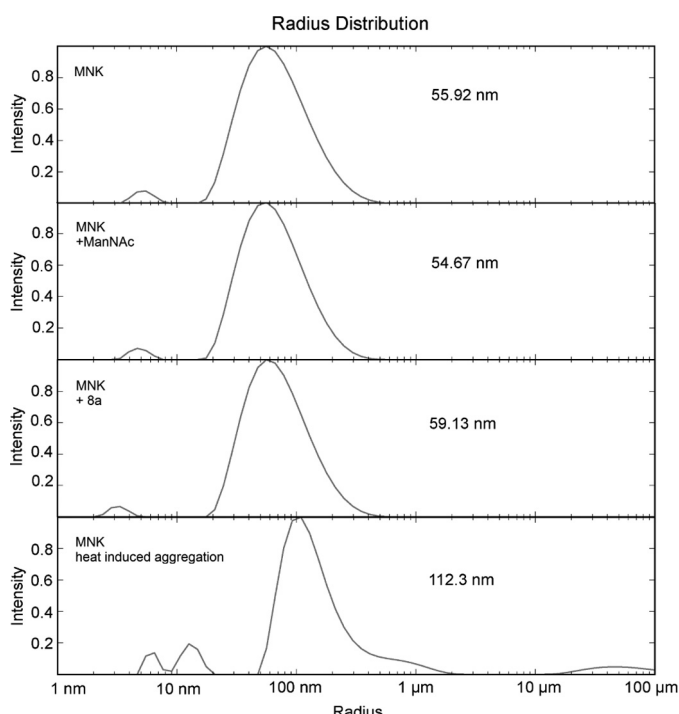


FIGURE 7. Density light-scattering experiments. Cuvettes were prepared with purified MNK ($10 \mu\text{M}$) and ManNAc or 2-acetylamino-2-deoxy-3-O-methyl-D-mannose (**8a**) at concentrations of $5 \mu\text{M}$. All measurements have been performed at 21°C . As a positive control, MNK was preincubated for 10 min at 45°C to induce protein aggregation. The radius of the highest peak for each graph is shown. Data depicted represent the mean values obtained in three independent experiments ($n = 3$). **8a** does not cause any protein aggregation under given experimental conditions.

Within this study, we presented a small molecule inhibitor of sialic acid expression, namely 2-acetylamino-2-deoxy-3-O-methyl-D-mannose (**8a**). Applying its peracetylated form (**10a**), cell surface sialic acid concentration in Jurkat cells was decreased in a dose-dependent manner (Fig. 2). At final concentrations of $500 \mu\text{M}$ in culture medium, the sialic acid concentration was reduced significantly to $\sim 20\%$. Total inhibition of cell surface sialylation could not be observed, most likely due to uptake and reutilization of sialic acid from the serum supplement (35). In addition, a slow turnover of sialylated glycoproteins could also contribute to this finding (36). The IC_{50} of the peracetylated analog (**10a**) is $176 \mu\text{M}$. With a molecular weight of 235 g/mol , **8a** has the potential for further chemical modification to improve binding affinity.

Performing DMB high-performance liquid chromatography on Jurkat cells treated with **10a** revealed that this ManNAc analog causes a substantial reduction of Neu5Ac both on the cell surface and in the cytosol. Cytosolic concentrations of free and CMP-conjugated Neu5Ac were decreased. **10a** was not metabolized into a modified sialic acid in cells (Fig. 5). These results indicate that **10a** inhibits sialic acid expression at the beginning of the *de novo* biosynthesis.

Other tested C-3-modified ManNAc analogs (**9**, **10b–c**) did not alter cell surface sialylation in treated cells. The low cytotoxicity of **10a** underlines the fact that inhibition of sialic acid biosynthesis does not cause cell viability defects (10, 32).

We suggest that the reduction of sialic acid expression achieved by **10a** is a consequence of MNK inhibition. The enzyme activity of MNK was inhibited by **8a**. The IC_{50} for the interaction is 1.29 mM . Dynamic light scattering experiments verified that the inhibition of **8a** is not due to protein aggregation. Related substances **5**, **8b**, and **8c**, which in their peracetylated forms (**9**, **10b–c**) did not alter cell surface sialylation, also showed no inhibitory effects on the MNK.

The mode of inhibition for **8a** is non-competitive for ManNAc, but competitive for ATP (K_D , $649 \mu\text{M}$). Apparently, this

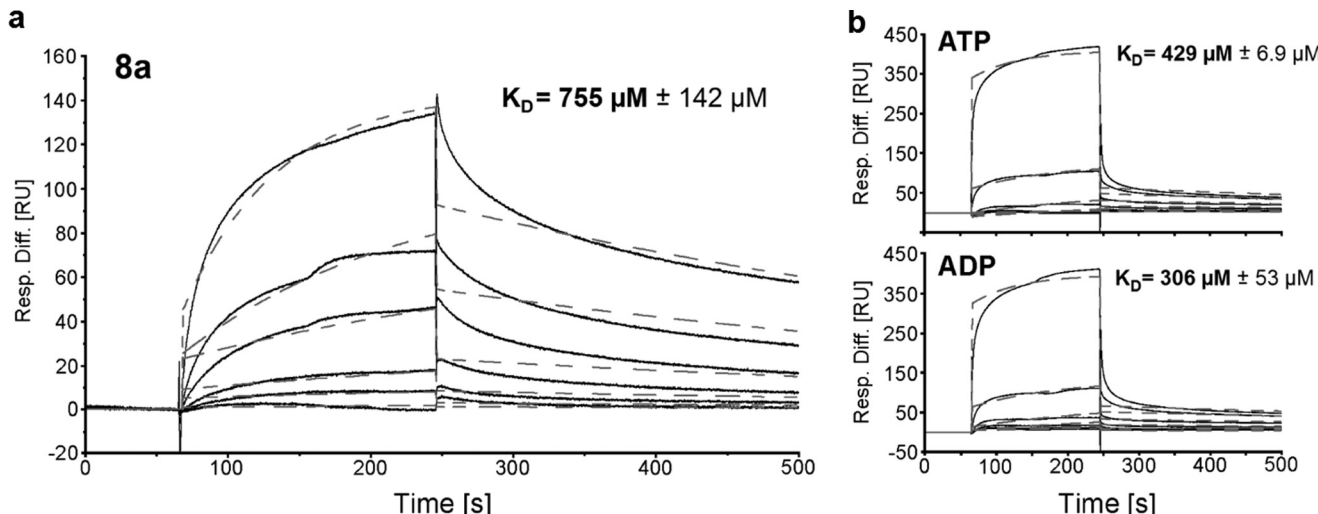


FIGURE 8. 2-Acetylamino-2-deoxy-3-O-methyl-D-mannose (8a**), ATP, and ADP binding to MNK.** In *a*, a representative sensogram of **8a** binding to MNK is depicted. The analyte was injected in a 3-fold dilution series starting from $5 \mu\text{M}$. Representative sensograms of ATP and ADP binding to MNK are shown in *b*. The analytes were injected in a 2-fold dilution series starting from $6.25 \mu\text{M}$. Obtained data (solid lines) was fitted using a 1:1 Langmuir binding model (dashed lines) and was calculated. Depicted K_D values represent means and S.D. of three independent experiments ($n = 3$). Resp. Diff., response difference; RU, response units.

C-3-modified ManNAc Decreases Sialic Acid Expression in Cells

TABLE 1

Comparison of rate constants for 2-acetylamino-2-deoxy-3-O-methyl- α -D-mannose (**8a**) binding to covalently immobilized, His-tagged MNK

SPR-binding sensorgrams were fitted using a 1:1 Langmuir binding model. Data was obtained in three independent experiments ($n = 3$) at a temperature of 25 °C. For ManNAc and methyl 2-acetylamino-2-deoxy-3-O-methyl- α -D-mannopyranoside (**5**), no binding could have been observed under given experimental conditions (NA, data not available). k_a , on rate; k_d , off rate; K_D , dissociation constant.

	ManNAc	8a	5	ATP	ADP	UDP
k_a ($M^{-1} s^{-1}$)	NA	2.92	NA	2.48	2.76	NA
k_d (s^{-1})	NA	2.25×10^{-3}	NA	1.06×10^{-3}	8.40×10^{-3}	NA
K_D (μM)	NA	755	NA	429	306	NA
X ²	NA	7.65	NA	19.20	18.87	NA

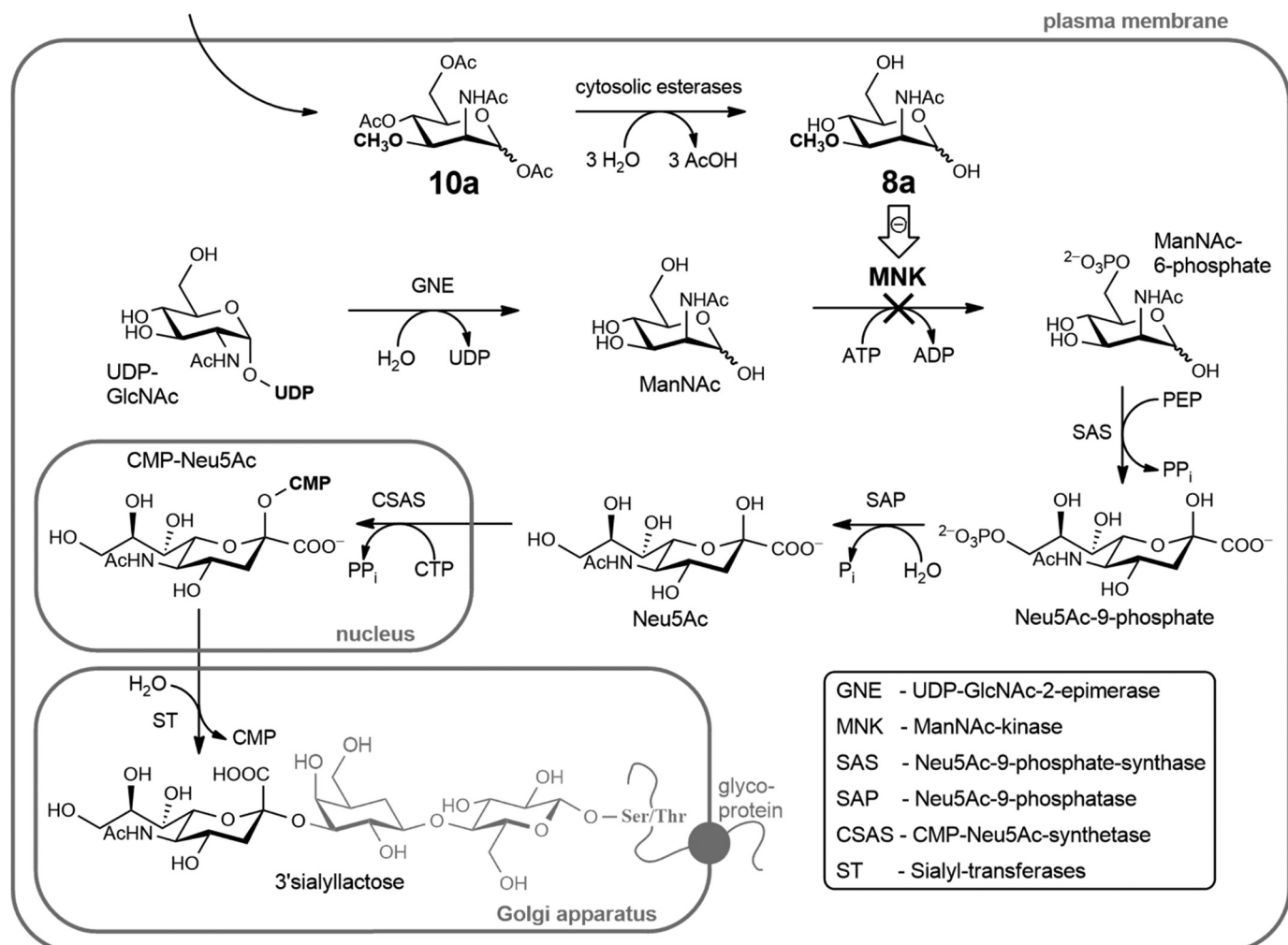


FIGURE 9. Proposed mechanism of inhibition for peracetylated 2-acetylamino-2-deoxy-3-O-methyl-D-mannose (10a**). **10a** is taken up by cells and converted to the corresponding non-peracetylated sugar (**8a**) by unspecific esterases. **8a** inhibits the kinase domain of the bifunctional UDP-GlcNAc-2-epimerase/ManNAc kinase (GNE/MNK). Inhibition of the MNK lowers the *de novo* biosynthesis of sialic acid. The depicted glycan (3'-sialyllactose) is representative for sialylated glycans in general.**

substance has its binding pocket in the ATP-binding site of MNK.

Surface plasmon resonance confirms binding of **8a** to MNK with a K_D of 755 μM . While covalently immobilized to the nitrotriacetic acid sensor chip, MNK does not bind ManNAc. This may be caused by conformational changes at the ManNAc binding site due to the immobilization procedure, or because of the technical set-up of the experiment. The selective binding of ADP, ATP and **8a** but not ManNAc also indicates that the inhibitor has the same binding site as ADP/ATP. The fact that **5** as well as UDP did not bind to MNK shows that the ATP-binding pocket of the enzyme was still intact.

The selectivity of **8a** for MNK was affirmed by evaluating its inhibitory capacity on other pyranose kinase enzymes (*N*-acetyl-glucosamine kinase, hexokinase IV). **8a** shows significantly weaker inhibitory effects on these enzymes ($IC_{50} > 10$ mM). MNK, *N*-acetyl-glucosamine kinase, and hexokinase IV did not metabolize any of the tested ManNAc analogs (**5** and **8a–c**).

Based on our results, we conclude that **10a** decreases sialic acid expression in cells by inhibiting cytosolic MNK. Being the key enzyme of sialic acid biosynthesis, its inhibition ultimately leads to the observed reduction of cell surface sialylation (10). The proposed model of sialic acid reduction in cells caused by **10a** is depicted in Fig. 9.

Peracetylated 2-acetylaminoo-2-deoxy-3-O-methyl-D-mannose (**10a**) is the first membrane permeable inhibitor of the UDP-GlcNAc-2-epimerase/ManNAc kinase described. With an inhibitor of the *de novo* biosynthesis of sialic acid, access to biological effects of global cell surface sialic acid reduction is facilitated. It paves the way for deeper understanding on the role of sialic acid in health and disease.

Acknowledgments—We thank Prof. Hans-Joachim Gabius (Technische Universität München) for providing FITC-conjugated *Polyporus squamosus* lectin. We also thank the Freie Universität Berlin for supporting our research.

REFERENCES

- Schauer, R. (2009) Sialic acids as regulators of molecular and cellular interactions. *Curr. Opin. Struct. Biol.* **19**, 507–514
- Varki, A. (2007) Glycan-based interactions involving vertebrate sialic-acid-recognizing proteins. *Nature* **446**, 1023–1029
- Lehmann, F., Tiralongo, E., and Tiralongo, J. (2006) Sialic acid-specific lectins: occurrence, specificity and function. *Cell Mol. Life Sci.* **63**, 1331–1354
- Crocker, P. R., Paulson, J. C., and Varki, A. (2007) Siglecs and their roles in the immune system. *Nat. Rev. Immunol.* **7**, 255–266
- Hakomori, S. (1989) Aberrant glycosylation in tumors and tumor-associated carbohydrate antigens. *Adv. Cancer Res.* **52**, 257–331
- Russell, C. J., and Webster, R. G. (2005) The genesis of a pandemic influenza virus. *Cell* **123**, 368–371
- Grewal, P. K. (2010) The Ashwell-Morell receptor. *Methods Enzymol.* **479**, 223–241
- Chen, S., and Fukuda, M. (2006) Cell type-specific roles of carbohydrates in tumor metastasis. *Methods Enzymol.* **416**, 371–380
- Chen, L., and Liang, J. F. (2012) Metabolic monosaccharides altered cell responses to anticancer drugs. *Eur. J. Pharm. Biopharm.* **81**, 339–345
- Keppler, O. T., Hinderlich, S., Langner, J., Schwartz-Albiez, R., Reutter, W., and Pawlita, M. (1999) UDP-GlcNAc 2-epimerase: a regulator of cell surface sialylation. *Science* **284**, 1372–1376
- Al-Rawi, S., Hinderlich, S., Reutter, W., and Giannis, A. (2004) Synthesis and biochemical properties of reversible inhibitors of UDP-N-acetylglucosamine 2-epimerase. *Angew. Chem. Int. Ed. Engl.* **43**, 4366–4370
- Stolz, F., Reiner, M., Blume, A., Reutter, W., and Schmidt, R. R. (2004) Novel UDP-glycal derivatives as transition state analogue inhibitors of UDP-GlcNAc 2-epimerase. *J. Org. Chem.* **69**, 665–679
- Zhu, X., Stolz, F., and Schmidt, R. R. (2004) Synthesis of thioglycoside-based UDP-sugar analogues. *J. Org. Chem.* **69**, 7367–7370
- Zeitler, R., Giannis, A., Danneschewski, S., Henk, E., Henk, T., Bauer, C., Reutter, W., and Sandhoff, K. (1992) Inhibition of N-acetylglucosamine kinase and N-acetylmannosamine kinase by 3-O-methyl-N-acetyl-D-glucosamine *in vitro*. *Eur. J. Biochem.* **204**, 1165–1168
- Saxon, E., and Bertozzi, C. R. (2000) Cell surface engineering by a modified Staudinger reaction. *Science* **287**, 2007–2010
- Mahal, L. K., Yarema, K. J., and Bertozzi, C. R. (1997) Engineering chemical reactivity on cell surfaces through oligosaccharide biosynthesis. *Science* **276**, 1125–1128
- Niederwieser, A., Späte, A. K., Nguyen, L. D., Jüngst, C., Reutter, W., and Wittmann, V. (2013) Two-color glycan labeling of live cells by a combination of DielsAlder and click chemistry. *Angew. Chem. Int. Ed. Engl.* **52**, 4265–4268
- Möller, H., Böhrsch, V., Bentrop, J., Bender, J., Hinderlich, S., and Hackenberger, C. P. (2012) Glycan-specific metabolic oligosaccharide engineering of C7-substituted sialic acids. *Angew. Chem. Int. Ed. Engl.* **51**, 5986–5990
- Du, J., Meledeo, M. A., Wang, Z., Khanna, H. S., Paruchuri, V. D., and Yarema, K. J. (2009) Metabolic glycoengineering: sialic acid and beyond. *Glycobiology* **19**, 1382–1401
- Tanner, M. E. (2005) The enzymes of sialic acid biosynthesis. *Bioorganic Chem.* **33**, 216–228
- Paulsen, H., Helpap, B., and Lorentzen, J. P. (1987) Bausteine von Oligosacchariden, LXXXIII. Synthese der Repeating Unit der Teichuronsäure von *Micrococcus luteus*. *Liebigs Ann.* **10.1002/jlac.198719870349**
- Hartlieb, S., Günzel, A., Gerardy-Schahn, R., Münster-Kühnel, A. K., Kirschning, A., and Dräger, G. (2008) Chemoenzymatic synthesis of CMP-N-acetyl-7-fluoro-7-deoxy-neuraminic acid. *Carbohydr. Res.* **343**, 2075–2082
- Schwartz, E. L., Hadfield, A. F., Brown, A. E., and Sartorelli, A. C. (1983) Modification of sialic acid metabolism of murine erythroleukemia cells by analogs of N-acetylmannosamine. *Biochim. Biophys. Acta* **762**, 489–497
- Sarkar, A. K., Fritz, T. A., Taylor, W. H., and Esko, J. D. (1995) Disaccharide uptake and priming in animal cells: inhibition of sialyl Lewis X by acetylated Gal β 1 \leftarrow 4GlcNAc β -O-naphthalenemethanol. *Proc. Natl. Acad. Sci. U.S.A.* **92**, 3323–3327
- Jones, M. B., Teng, H., Rhee, J. K., Lahar, N., Baskaran, G., and Yarema, K. J. (2004) Characterization of the cellular uptake and metabolic conversion of acetylated N-acetylmannosamine (ManNAc) analogues to sialic acids. *Biotechnol. Bioeng.* **85**, 394–405
- Galuska, S. P., Geyer, H., Weinhold, B., Kontou, M., Röhrich, R. C., Bernard, U., Gerurdy-Schahn, R., Reutter, W., Münster-Kühnel, A., and Geyer, R. (2010) Quantification of nucleotide-activated sialic acids by a combination of reduction and fluorescent labeling. *Anal. Chem.* **82**, 4591–4598
- Martinez, J., Nguyen, L. D., Hinderlich, S., Zimmer, R., Tauberger, E., Reutter, W., Saenger, W., Fan, H., and Moniot, S. (2012) Crystal structures of N-acetylmannosamine kinase provide insights into enzyme activity and inhibition. *J. Biol. Chem.* **287**, 13656–13665
- Reinke, S. O., Lehmer, G., Hinderlich, S., and Reutter, W. (2009) Regulation and pathophysiological implications of UDP-GlcNAc 2-epimerase/ManNAc kinase (GNE) as the key enzyme of sialic acid biosynthesis. *Biol. Chem.* **390**, 591–599
- Weihofen, W. A., Berger, M., Chen, H., Saenger, W., and Hinderlich, S. (2006) Structures of human N-acetylglucosamine kinase in two complexes with N-acetylglucosamine and with ADP/glucose: insights into substrate specificity and regulation. *J. Mol. Biol.* **364**, 388–399
- de Mol, N. J., and Fischer, M. J. (2010) *Surface Plasmon Resonance: Methods and Protocols*, pp. 91–100, Springer Verlag GmbH, Heidelberg, Germany
- Kim, E. J., Sampathkumar, S. G., Jones, M. B., Rhee, J. K., Baskaran, G., Goon, S., and Yarema, K. J. (2004) Characterization of the metabolic flux and apoptotic effects of O-hydroxyl- and N-acyl-modified N-acetylmannosamine analogs in Jurkat cells. *J. Biol. Chem.* **279**, 18342–18352
- Rillahan, C. D., Antonopoulos, A., Lefort, C. T., Sonon, R., Azadi, P., Ley, K., Dell, A., Haslam, S. M., and Paulson, J. C. (2012) Global metabolic inhibitors of sialyl- and fucosyltransferases remodel the glycome. *Nat. Chem. Biol.* **8**, 661–668
- Rillahan, C. D., Brown, S. J., Register, A. C., Rosen, H., and Paulson, J. C. (2011) High-throughput screening for inhibitors of sialyl- and fucosyltransferases. *Angew. Chem. Int. Ed. Engl.* **50**, 12534–12537
- Preidl, J. J., Gnanapragassam, V. S., Lisurek, M., Saupe, J., Horstkorte, R., and Rademann, J. (2014) Fluorescent mimetics of CMP-Neu5Ac are highly potent, cell-permeable polarization probes of eukaryotic and bacterial sialyltransferases and inhibit cellular sialylation. *Angew. Chem. Int. Ed. Engl.* **53**, 5700–5705
- Oetke, C., Hinderlich, S., Brossmer, R., Reutter, W., Pawlita, M., and Keppler, O. T. (2001) Evidence for efficient uptake and incorporation of sialic acid by eukaryotic cells. *Eur. J. Biochem.* **268**, 4553–4561
- Mendla, K., Baumkötter, J., Rosenau, C., Ulrich-Bott, B., and Cantz, M. (1988) Defective lysosomal release of glycoprotein-derived sialic acid in fibroblasts from patients with sialic acid storage disease. *Biochem. J.* **250**, 261–267

A novel approach to decrease sialic acid expression in cells by a C-3 modified N-acetyl-mannosamine

Paul R. Wratil^{‡1}, Stephan Rigol^{§1}, Barbara Solecka^{¶1}, Guido Kohla^{¶1}, Christoph Kannicht^{¶1}, Werner Reutter[‡], Athanassios Giannis[§], and Long D. Nguyen[‡]

Supplementary Information	Page(s)
Supplementary Methods	
General methods	2
General Working Procedures	2 – 3
Compounds	
Methyl 2-azido-4,6-O-benzylidene-2-deoxy-3-O-methyl- α -D-mannopyranoside (3)	3
Methyl 2-(acetylamino)-2-deoxy-3-O-methyl- α -D-mannopyranoside (5)	4
Methyl 4,6-di-O-acetyl-2-(acetylamino)-2-deoxy-3-O-methyl- α -D-mannopyranoside (9)	5
Benzyl 2-azido-4,6-O-benzylidene-2-deoxy-3-O-methyl- α -D-mannopyranoside (4a)	6
Benzyl 2-(acetylamino)-4,6-O-benzylidene-2-deoxy-3-O-methyl- α -D-mannopyranoside (6a)	6 – 7
Benzyl 2-(acetylamino)-2-deoxy-3-O-methyl- α -D-mannopyranoside (7a)	7 – 8
2-(Acetylamino)-2-deoxy-3-O-methyl-D-mannose (8a)	8
1,4,6-Tri-O-acetyl-2-(acetylamino)-2-deoxy-3-O-methyl-D-mannopyranose (10a)	9
Benzyl 2-azido-4,6-O-benzylidene-2-deoxy-3-O-ethyl- α -D-mannopyranoside (4b)	10
Benzyl 2-(acetylamino)-4,6-O-benzylidene-2-deoxy-3-O-ethyl- α -D-mannopyranoside (6b)	10 – 11
Benzyl 2-(acetylamino)-2-deoxy-3-O-ethyl- α -D-mannopyranoside (7b)	11 – 12
2-(Acetylamino)-2-deoxy-3-O-ethyl-D-mannose (8b)	12
1,4,6-Tri-O-acetyl-2-(acetylamino)-2-deoxy-3-O-ethyl-D-mannopyranose (10b)	13
Benzyl 2-azido-4,6-O-benzylidene-2-deoxy-3-O-prop-2-en-1-yl- α -D-mannopyranoside (4c)	14
Benzyl 2-(acetylamino)-4,6-O-benzylidene-2-deoxy-3-O-prop-2-en-1-yl- α -D-mannopyranoside (6c)	15
Benzyl 2-(acetylamino)-2-deoxy-3-O-prop-2-en-1-yl- α -D-mannopyranoside (7c)	16
2-(Acetylamino)-2-deoxy-3-O-propyl- α -D-mannose (8c)	17
1,4,6-Tri-O-acetyl-2-(acetylamino)-2-deoxy-3-O-propyl-D-mannopyranose (10c)	17 – 18

SUPPLEMENTARY METHODS

General methods

All reactions were run under an atmosphere of argon unless otherwise indicated. Room temperature refers to 22 °C, ambient pressure to 1013 hPa. Reagents and anhydrous solvents were transferred via oven-dried syringe or cannula. Flasks were flame-dried under vacuum and cooled under a constant stream of argon. Tetrahydrofuran (THF) was distilled under argon from potassium, dichloromethane from SICAPENT (phosphorus pentoxide on solid support with indicator). Methanol, *N,N*-dimethylformamide and pyridine were purchased from Acros or Aldrich (anhydrous over molecular sieves). All other chemicals were purchased from ABCR, Acros, Aldrich, Alfa Aesar, Fluorochem, TCI Europe and VWR at highest commercially available purity and used as such. Reactions were monitored by thin layer chromatography using Merck silica gel 60 F₂₅₄ TLC aluminium sheets and visualized under an UV lamp and/or with ceric ammonium molybdate, potassium permanganate or vanillin staining solution. Chromatographic purification was performed as flash chromatography on Acros silica gel 35-70, 60 Å, using a forced flow of eluent (method of Still). Concentration under reduced pressure was performed by rotary evaporation at 40 °C at the appropriate pressure. NMR spectra were recorded on a Varian Mercury plus 300 (operating at 300 MHz for ¹H and 75 MHz for ¹³C acquisitions) and a Varian Mercury plus 400 (operating at 400 MHz for ¹H, 100 MHz for ¹³C). Chemical shifts δ are reported in ppm with the solvent resonance as internal standard (chloroform-*d*₁: 7.26 (¹H-NMR), 77.16 (¹³C-NMR); methanol-*d*₄: 3.31 (¹H-NMR), 49.00 (¹³C-NMR)). Coupling constants *J* are given in Hertz (Hz). Multiplicities are classified by the following abbreviations: s = singlet, d = doublet, t = triplet and combinations thereof, m = multiplet or br = broad signal. Indications in quotation marks are to describe the shape of the signal only but do not represent the correct multiplicity due to too low resolution. High resolution mass spectra were obtained on a Bruker Daltonics ESI-FT-ICR-MS APEX II [7 T]. IR spectra were obtained on an ATI/MATTSON Genesis FT-IR as thin film or KBr disk. Absorbance frequencies are reported in reciprocal centimeters (cm⁻¹). UV spectra were measured on a Jasco V-630 photometer in given solvent and concentration. Melting points were measured with a Büchi “Melting Point B-540” and are uncorrected. Optical rotation data was obtained with a Schmidt+Haensch Polartronic MHZ-8 at the sodium-D line (589 nm) using a 50 mm path-length cell in the solvent and concentration indicated.

General Working Procedures

GWP 1 (Alkylation) - Sodium hydride (1.1 eq.) was added to an ice-cooled solution of the 3-hydroxymannopyranoside (1.0 eq.) in *N,N*-dimethylformamide (9 ml/g) and the mixture was stirred for five min. Then, the appropriate alkyl halide (1.5 eq.) was added and the cooling bath was removed. After 90 minutes the reaction was diluted with dichloromethane and quenched with sat. sodium bicarbonate solution. The organic phase was dried over MgSO₄ and the solvent was removed under reduced pressure. The pure alkylated derivative was isolated by column chromatography.

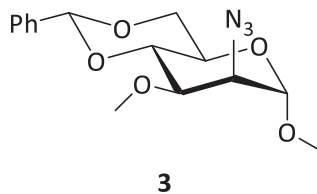
GWP 2 (Azide reduction and acylation) - Palladium on activated charcoal (10% Pd, 150 mg/g) was added to a solution of the mannopyranoside (1.0 eq.) in methanol (15 ml/g). Then, the reaction mixture was stirred in a hydrogen enriched atmosphere (10% H₂ in N₂) for 16 hours. After removal of the catalyst by filtration over Celite the solvent was removed under reduced pressure. The residue was taken up in dichloromethane (20 ml/g) and subsequently treated with triethylamine (3.0 eq.), 4-dimethylaminopyridine (0.1 eq.) and the corresponding acyl chloride (2.0 eq.). After stirring for twelve hours at room temperature the reaction was quenched with sat. sodium bicarbonate solution and washed with brine. The organic phase was dried over MgSO₄ and all volatiles were removed under diminished pressure. Purification was accomplished by means of column chromatography to yield the 2-acylaminomannopyranosides.

GWP 3 (Acetal cleavage) - The 4,6-O-benzylidene-mannopyranoside (1.0 eq.) was dissolved in acetic acid (80% in water, 8 ml/g) and heated to 80°C for three to five hours (until TLC shows disappearance of the starting material). Solvent removal under reduced pressure and purification by column chromatography gave the deprotected diol.

GWP 4 (Hydrogenolysis of the benzyl group) - Palladium on activated charcoal (10% Pd, 200 mg/g) was added to a solution of the benzyl mannopyranoside (1.0 eq.) in methanol (20 ml/g). Then, the mixture was stirred under hydrogen atmosphere (11 bar H₂) at 45°C in a pressure reactor for 50 hours. After removal of the catalyst by filtration over Celite the solvent was removed under reduced pressure. Column chromatography gave the 3-*O*-alkyl-mannosamine derivatives.

COMPOUNDS

Methyl 2-azido-4,6-*O*-benzylidene-2-deoxy-3-*O*-methyl- α -D-mannopyranoside (3)



According to *GWP 1*, methyl 2-azido-4,6-*O*-benzylidene-2-deoxy- α -D-mannopyranoside **1** (842 mg, 2.74 mmol) was reacted with sodium hydride (72.3 mg, 3.01 mmol) and iodomethane (257 μ l, 583 mg, 4.11 mmol). The product (808 mg, 2.51 mmol, 92%) was obtained as colorless oil.

R_f: 0.60 (*n*-hexane/ethyl acetate=3:1 *v/v*)

¹H-NMR: (300 MHz, CDCl₃) δ [ppm] 3.42 (s, 3 H, C-1-O-CH₃), 3.60 (s, 3 H, C-3-O-CH₃), 3.76-3.88 (m, 2 H, **H-3**, **H-6a**), 3.87-3.94 (m, 1 H, **H-4**), 4.05 (“d”, $J_{H,H}$ =9.1 Hz, 1 H, **H-6b**), 4.10 (dd, $^3J_{H,H}$ =3.8, 1.6 Hz, 1 H, **H-2**), 4.28 (“td”, $^3J_{H,H}$ =3.9, 1.9 Hz, 1 H, **H-5**), 4.72 (d, $^3J_{H,H}$ =1.5 Hz, 1 H, **H-1**), 5.64 (s, 1 H, Ph-CH-), 7.35-7.44 (m, 3 H, **H_{ar}-3**, **H_{ar}-3'**, **H_{ar}-4**), 7.48-7.56 (m, 2 H, **H_{ar}-2**, **H_{ar}-2'**).

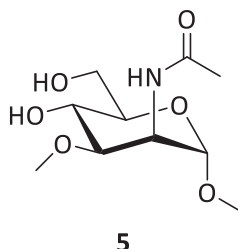
¹³C-NMR: (100 MHz, CDCl₃) δ [ppm] 55.2 (C-1-O-CH₃), 59.2 (C-3-O-CH₃), 61.8 (**C-5**), 63.8 (**C-2**), 68.9 (**C-6**), 77.7 (**C-3**), 79.1 (**C-4**), 100.2 (**C-1**), 101.9 (Ph-CH-), 126.3 (**C_{ar}-3**, **C_{ar}-3'**), 128.4 (**C_{ar}-2**, **C_{ar}-2'**), 129.1 (**C_{ar}-4**), 137.5 (**C_{ipso}**).

HR-MS: (ESI positive, CHCl₃/MeOH) calc. for [C₁₅H₁₉N₃O₅Na]⁺: [M+Na]⁺ 344.12169, found 344.12140

UV: (CHCl₃) λ (lg ϵ)=257 nm (2.916), 263 (2.914), 285 (2.914).

IR: (Film) ν _{max}=2932 cm⁻¹, 2837, 2107, 1773, 1731, 1455, 1379, 1274, 1135, 1102, 1069, 979.

Optical rotation: $[\alpha]_D^{22}$ (° cm³ g⁻¹dm⁻¹)=+53.3 (c=0.8, CHCl₃)

Methyl 2-(acetylamino)-2-deoxy-3-O-methyl- α -D-mannopyranoside (5)

According to *GWP 2* methyl 2-azido-4,6-*O*-benzylidene-2-deoxy-3-*O*-methyl- α -D-mannopyranoside **3** (979 mg, 15.4 mmol) was reduced and then reacted with triethylamine (1.27 ml, 925 mg, 9.14 mmol), 4-dimethylaminopyridine (37.2 mg, 305 μ mol) and acetyl chloride (435 μ l, 478 mg, 6.09 mmol). The intermediate was used without further purification according to *GWP 3*. The product (633 mg, 2.54 mmol, 83%) was obtained as white solid.

R_f: 0.14 (dichloromethane/methanol=10:1 *v/v*)

¹H-NMR: (300 MHz, CD₃OD) δ [ppm] 1.99 (s, 3H, -CO-CH₃), 3.37 (s, 6H, 2 x -O-CH₃), 3.47-3.65 (m, 3H, **H-3**, **H-5**, **H-6a**), 3.81 (“d”, $J_{\text{H,H}}=3.4$ Hz, 2H, **H-4**, **H-6b**), 4.50 (dd, $^3J_{\text{H,H}}=4.3$, 1.4 Hz, 1H, **H-2**), 4.61 (d, $^3J_{\text{H,H}}=1.5$ Hz, 1H, **H-1**).

¹³C-NMR: (100 MHz, DMSO-*d*₆) δ [ppm] 22.5 (-CO-CH₃), 47.9 (**C-2**), 54.0 (-O-CH₃), 56.3 (-O-CH₃), 61.2 (**C-6**), 65.7 (**C-4**), 73.5 (**C-5**), 78.8 (**C-3**), 99.7 (**C-1**), 169.6 (CO).

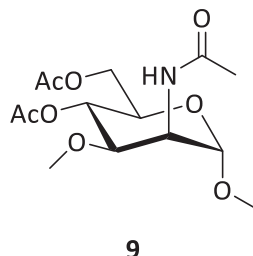
HR-MS: (ESI positive, MeOH) calc. for [C₁₀H₁₉NO₆Na]⁺: [M+Na]⁺ 272.11046, found 272.11034; calc. for [C₂₀H₃₈N₂O₁₂Na]⁺: [2M+Na]⁺ 521.23170, found 521.23183.

UV: (CH₃OH) λ (lg ϵ)=205 nm (3.311).

IR: (KBr) $\nu_{\text{max}}=3427$ cm⁻¹, 2932, 2836, 1654, 1557, 1541, 1378, 1130, 1067, 990, 967.

Optical rotation: $[\alpha]_D^{21}(\text{ }^\circ \text{cm}^3 \text{ g}^{-1} \text{dm}^{-1})=+40.5$ (*c*=0.29, CH₃OH)

Melting point: 64–65 °C

Methyl 4,6-di-O-acetyl-2-(acetylamino)-2-deoxy-3-O-methyl- α -D-mannopyranoside (9)**9**

Methyl 2-(acetylamino)-2-deoxy-3-O-methyl- α -D-mannopyranoside **5** (32.5 mg, 130 μmol , 1.0 eq.) was dissolved in pyridine (0.5 ml) and acetic anhydride (123 μl , 133 mg, 1.30 mmol, 10 eq.) was added. The reaction mixture was stirred at room temperature for 16 hours. Then, the reaction was quenched by addition of sat. sodium bicarbonate solution (1 ml) and diluted with dichloromethane (3 ml). The reaction mixture was washed with cupric sulfate solution twice (2×1 ml) and finally with brine (2 ml). The organic phase was separated and dried over MgSO_4 . Purification by column chromatography afforded the product (39.7 mg, 119 μmol , 91 %) as a hygroscopic white solid.

R_f: 0.11 (*n*-hexane/ethyl acetate=1:2 *v/v*)

¹H-NMR: (400 MHz, CDCl_3) δ [ppm] 2.01 (s, 3 H, -N-CO-CH₃), 2.06 (s, 6 H, 2 \times -O-CO-CH₃), 3.29 (s, 3 H, -O-CH₃), 3.34 (s, 3 H, -O-CH₃), 3.69 (dd, $^3J_{\text{H,H}}=9.8$, 4.9 Hz, 1 H, **H-3**), 3.85 (ddd, $^3J_{\text{H,H}}=10.1$, 5.7, 2.3 Hz, 1 H, **H-5**), 4.04 (dd, $^2J_{\text{H,H}}=12.2$, $^3J_{\text{H,H}}=2.4$ Hz, 1 H, **H-6a**), 4.22 (dd, $^2J_{\text{H,H}}=12.2$, $^3J_{\text{H,H}}=5.7$ Hz, 1 H, **H-6b**), 4.51 (ddd, $^3J_{\text{H,H}}=7.6$, 4.9, 1.5 Hz, 1 H, **H-2**), 4.77 (d, $^3J_{\text{H,H}}=1.4$ Hz, 1 H, **H-1**), 4.93 (dd, $^3J_{\text{H,H}}=10.0$, 10.0 Hz, 1 H, **H-4**), 5.83 (d, $^3J_{\text{H,H}}=7.7$ Hz, 1 H, NH).

¹³C-NMR: (100 MHz, CDCl_3) δ [ppm] 20.8 (-O-CO-CH₃), 20.9 (-O-CO-CH₃), 23.4 (-NH-CO-CH₃), 49.0 (**C-2**), 55.3 (C-1-O-CH₃), 57.1 (C-3-O-CH₃), 62.8 (**C-6**), 67.4 (**C-4**), 67.7 (**C-5**), 76.2 (**C-3**), 100.1 (**C-1**), 170.1 (-NH-CO-), 170.71 (-O-CO-), 170.74 (-O-CO-).

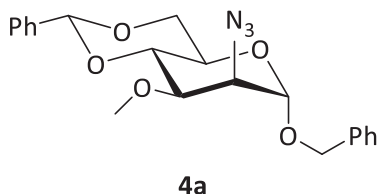
HR-MS: (ESI positive, $\text{CHCl}_3/\text{MeOH}$) calc. for $[\text{C}_{14}\text{H}_{23}\text{NO}_8\text{Na}]^+$: $[\text{M}+\text{Na}]^+$ 356.13159, found 356.13177.

UV: (CH_2Cl_2) λ ($\lg \epsilon$)=236 nm (3.924), 274 (2.896).

IR: (KBr) ν_{max} =3443 cm^{-1} , 2924, 1736, 1637, 1384, 1048, 712.

Optical rotation: $[\alpha]_D^{22} (\text{ }^\circ \text{cm}^3 \text{ g}^{-1} \text{ dm}^{-1}) = +20.8$ ($c=0.32$, CHCl_3)

Melting point: 50–51 °C

Benzyl 2-azido-4,6-O-benzylidene-2-deoxy-3-O-methyl- α -D-mannopyranoside (4a)

According to *GWP 1*, benzyl 2-azido-4,6-O-benzylidene-2-deoxy- α -D-mannopyranoside **2** (2.72 g, 7.09 mmol) was reacted with sodium hydride (187 mg, 7.80 mmol) and iodomethane (665 μ l, 1.51 g, 10.6 mmol). The product (2.48 g, 6.23 mmol, 88%) was obtained as colorless oil.

R_f: 0.66 (*n*-hexane/ethyl acetate=3:1 *v/v*)

¹H-NMR: (300 MHz, CDCl₃) δ [ppm] 3.58 (s, 3H, -O-CH₃), 3.79-3.91 (m, 2H), 3.94 (dd, ³J_{H,H}=9.6, 3.7 Hz, 1H), 4.02-4.14 (m, 2H), 4.18-4.29 (m, 1H), 4.51 (d, ²J_{H,H}=11.7 Hz, 1H, Ph-CH_aH_b-), 4.72 (d, ²J_{H,H}=11.7 Hz, 1H, Ph-CH_aH_b-), 4.88 (d, ³J_{H,H}=1.5 Hz, 1H, H-1), 5.62 (s, 1H, Ph-CH-), 7.30-7.44 (m, 8H, H_{ar}), 7.45-7.53 (m, 2H, H_{ar}).

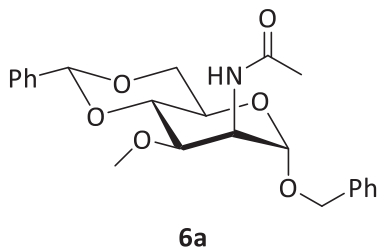
¹³C-NMR: (75 MHz, CDCl₃) δ [ppm] 59.3 (-O-CH₃), 62.0 (**C-5**), 64.1 (**C-2**), 68.8 (**C-6**), 69.7 (Ph-CH₂-), 77.7 (**C-3**), 79.2 (**C-4**), 98.4 (**C-1**), 101.9 (Ph-CH-), 126.2 (C_{ar}), 128.36 (C_{ar}), 128.41 (C_{ar}), 128.8 (C_{ar}), 129.1 (C_{ar}), 136.6 (C_{ipso}), 137.4 (C_{ipso}).

HR-MS: (ESI positive, MeOH) calc. for [C₂₁H₂₃N₃O₅Na]⁺: [M+Na]⁺ 420.15299, found 420.15280.

UV: (CH₃OH) λ (lg ϵ)=239 nm (2.975), 256 (2.863).

IR: (KBr) ν_{max} =3065 cm⁻¹, 2932, 2837, 2107, 1455, 1382, 1275, 1129, 1052, 914, 700.

Optical rotation: $[\alpha]_D^{22} (\text{cm}^3 \text{g}^{-1} \text{dm}^{-1}) = +80.7 (c=1.0, \text{CHCl}_3)$

Benzyl 2-(acetylamino)-4,6-O-benzylidene-2-deoxy-3-O-methyl- α -D-mannopyranoside (6a)

According to *GWP 2* benzyl 2-azido-4,6-O-benzylidene-2-deoxy-3-O-methyl- α -D-mannopyranoside **4a** (6.12 g, 15.4 mmol) was reduced and then reacted with triethylamine (6.45 ml, 4.68 g, 46.2 mmol), 4-dimethylaminopyridine (188 mg, 1.54 mmol) and acetyl chloride (2.19 ml, 2.42 g, 30.8 mmol). The product (5.22 g, 12.6 mmol, 83%) was obtained as white solid.

R_f: 0.33 (*n*-hexane/ethyl acetate=3:1 *v/v*)

¹H-NMR: (300 MHz, CDCl₃) δ [ppm] 2.05 (s, 3H, CO-CH₃), 3.43 (s, 3H, -O-CH₃), 3.68 (dd, J_{H,H}=10.0, 9.5 Hz, 1H, **H-6a**), 3.78 (dd, ³J_{H,H}=10.6, 10.0 Hz, 1H, **H-4**), 3.87-3.99 (m, 1H, **H-5**), 3.92 (dd, ³J_{H,H}=9.7, 4.4 Hz, 1H, **H-6b**), 4.22 (dd, ³J_{H,H}=10.0, 4.6 Hz, 1H, **H-3**), 4.54 (d, ²J_{H,H}=11.7 Hz, 1H, Ph-CH_aH_b-), 4.61 (ddd, ³J_{H,H}=7.2, 5.0, 1.3 Hz, 1H, **H-2**), 4.69 (d, ²J_{H,H}=11.7 Hz, 1H, Ph-CH_aH_b-), 5.05 (d, ³J_{H,H}=1.1 Hz, 1H, **H-1**), 5.58 (s, 1H, Ph-CH-), 5.70 (d, ³J_{H,H}=7.2 Hz, 1H, NH), 7.30-7.41 (m, 8H, H_{ar}), 7.44-7.53 (m, 2H, H_{ar}).

¹³C-NMR: (75 MHz, CDCl₃) δ [ppm] 23.6 (CO-CH₃), 50.6 (**C-2**), 57.7 (-O-CH₃), 63.2 (**C-5**), 69.0 (**C-6**), 70.0 (Ph-CH₂-), 74.9 (**C-3**), 79.0 (**C-4**), 99.4 (**C-1**), 102.3 (Ph-CH-), 126.3 (**C_{ar}**), 128.16 (**C_{ar}**), 128.22 (**C_{ar}**), 128.4 (**C_{ar}**), 128.7 (**C_{ar}**), 129.3 (**C_{ar}**), 136.9 (**C_{ipso}**), 137.2 (**C_{ipso}**), 170.7 (CO).

HR-MS: (ESI positive, MeOH) calc. for [C₂₃H₂₇NO₆Na]⁺: [M+Na]⁺ 436.17306, found 436.17311; calc. for [C₄₆H₅₄N₂O₁₂Na]⁺: [2M+Na]⁺ 849.35690, found 849.35779.

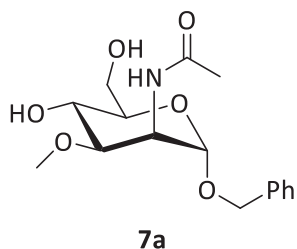
UV: (CHCl₃) λ (lgε)=275 nm (4.415).

IR: (KBr) ν_{max}=3442 cm⁻¹, 2929, 2870, 1655, 1545, 1377, 1121, 1102, 1090, 1038, 700.

Optical rotation: [α]_D²²(° cm³ g⁻¹dm⁻¹)=+50.1 (c=1.0, CHCl₃)

Melting point: 96–97 °C

Benzyl 2-(acetylamino)-2-deoxy-3-*O*-methyl-α-D-mannopyranoside (7a)



Benzyl 2-(acetylamino)-4,6-*O*-benzylidene-2-deoxy-3-*O*-methyl-α-D-mannopyranoside **6a** (2.32 g, 5.61 mmol) was treated according to *GWP 3*. The product (1.55 g, 4.76 mmol, 85%) was obtained as white solid.

R_f: 0.27 (dichloromethane/methanol=15:1 *v/v*)

¹H-NMR: (400 MHz, CD₃OD) δ [ppm] 1.98 (s, 3H, -CO-CH₃), 3.37 (s, 3H, -O-CH₃), 3.55 (dd, ³J_{H,H}=9.8, 4.5 Hz, 1H), 3.58-3.65 (m, 2H), 3.76-3.84 (m, 2H), 4.51 (d, ²J_{H,H}=11.7 Hz, 1H, Ph-CH_aH_b-), 4.53-4.58 (m, 1H), 4.71 (d, ²J_{H,H}=11.7 Hz, 1H, Ph-CH_aH_b-), 4.82 (d, ³J_{H,H}=1.6 Hz, 1H, **H-1**), 7.25-7.40 (m, 5H, H_{ar}), 7.93 (d, ³J_{H,H}=9.2 Hz, 1H, NH).

¹³C-NMR: (100 MHz, DMSO-*d*₆) δ [ppm] 22.6 (-CO-CH₃), 48.0, 56.3, 61.2, 65.8, 67.8, 73.9, 78.8, 98.0 (**C-1**), 127.7 (**C_{ar}-4**), 128.0 (**C_{ar}**), 128.4 (**C_{ar}**), 137.5 (**C_{ar}-1**), 169.6 (CO).

HR-MS: (ESI positive, MeOH) calc. for $[C_{16}H_{23}NO_6Na]^+$: $[M+Na]^+$ 348.14176, found 348.14162; calc. for $[C_{32}H_{46}N_2O_{12}Na]^+$: $[2M+Na]^+$ 673.29430, found 673.29381.

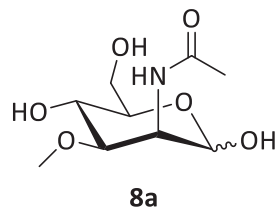
UV: (CH_3OH) λ ($\lg \epsilon$) = 210 nm (3.747), 256 (2.515).

IR: (KBr) $\nu_{\text{max}} = 3365 \text{ cm}^{-1}, 2928, 1655, 1542, 1455, 1125, 1068, 986, 700$.

Optical rotation: $[\alpha]_D^{22} (\text{cm}^3 \text{ g}^{-1} \text{ dm}^{-1}) = +67.7$ ($c=1.0, \text{CHCl}_3$)

Melting point: 53 °C

2-(Acetylamino)-2-deoxy-3-O-methyl-D-mannose (8a)



Benzyl 2-(acetylamino)-2-deoxy-3-O-methyl- α -D-mannopyranoside **7a** (900 mg, 2.77 mmol) was treated according to *GWP 4*. The product (412 mg, 1.75 mmol, 63%) was obtained as white solid.

R_f: 0.20 (dichloromethane/methanol = 5:1 v/v)

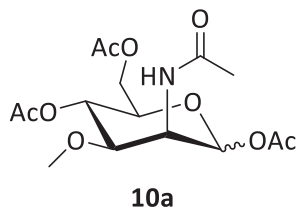
¹H-NMR: (300 MHz, CD_3OD) δ [ppm] 1.98 (s, 3 H, $-\text{CO-CH}_3^*$), 2.02 (s, 3 H, $-\text{CO-CH}_3$), 3.24-3.27 (m, 2 H, **H-3**, **H-5**), 3.39 (s, 3 H, $-\text{O-CH}_3^*$), 3.42 (s, 3 H, $-\text{O-CH}_3$), 3.49-3.53 (m, 1 H, **H-4**), 3.57-3.63 (m, 2 H, **H-3***, **H-4***), 3.72-3.88 (m, 5 H, **H-6a***, **H-6b***, **H-6a**, **H-6b**, **H-5***), 4.48 (dd, $^3J_{\text{H,H}} = 3.7, 1.7$ Hz, 1 H, **H-2***), 4.61 (dd, $^3J_{\text{H,H}} = 4.2, 1.4$ Hz, 1 H, **H-2**), 4.79-4.82 (br, 1 H, **H-1**), 5.03 (d, $^3J_{\text{H,H}} = 1.6$ Hz, 1 H, **H-1***). Signals of the major anomer are marked with an asterisk.

¹³C-NMR: (75 MHz, CD_3OD) δ [ppm] 21.3 ($-\text{CO-CH}_3^*$), 21.5 ($-\text{CO-CH}_3$), 49.5 (**C-2***), 50.3 (**C-2**), 56.3 ($-\text{O-CH}_3^*$), 56.5 ($-\text{O-CH}_3$), 60.9 (**C-6**), 61.0 (**C-6***), 65.7 (**C-4***), 66.0 (**C-4**), 72.2 (**C-5***), 77.0 (**C-5**), 79.2 (**C-3***), 82.7 (**C-3**), 93.87 (**C-1***), 93.92 (**C-1**), 172.23 ($-\text{CO-CH}_3^*$), 173.19 ($-\text{CO-CH}_3$), Signals of the major anomer are marked with an asterisk.

HR-MS: (ESI positive, MeOH) calc. for $[C_9H_{17}NO_6Na]^+$: $[M+Na]^+$ 258.09481, found 258.09460; calc. for $[C_{18}H_{34}N_2O_{12}Na]^+$: $[2M+Na]^+$ 493.20040, found 493.20012.

UV: (CH_3OH) λ ($\lg \epsilon$) = 208 nm (3.110), 281 (2.043).

IR: (KBr) $\nu_{\text{max}} = 3396 \text{ cm}^{-1}, 2930, 1656, 1545, 1382, 1106, 1067, 987$.

1,4,6-Tri-*O*-acetyl-2-(acetylamino)-2-deoxy-3-*O*-methyl-D-mannopyranose (10a)

2-(Acetylamino)-2-deoxy-3-*O*-methyl-D-mannose **8a** (150 mg, 638 µmol, 1.0 eq.) was dissolved in pyridine (1.0 ml) and acetic anhydride (603 µl, 651 mg, 6.38 mmol, 10 eq.) was added. The reaction mixture was stirred at room temperature for 16 hours. Then, the reaction was quenched by addition of sat. sodium bicarbonate solution (2 ml) and diluted with dichloromethane (5 ml). The reaction mixture was washed with cupric sulfate solution twice (2 × 2 ml) and finally with brine (3 ml). The organic phase was separated and dried over MgSO₄. Purification by column chromatography afforded the product (196 mg, 542 µmol, 85%) as a hygroscopic white solid.

R_f: 0.09 (*n*-hexane/ethyl acetate/methanol=20:8:3 v/v/v)

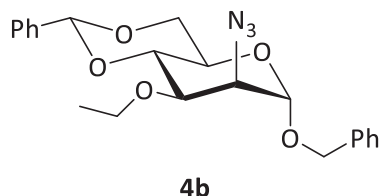
¹H-NMR: (400 MHz, CDCl₃) δ [ppm] 2.05 (s, 3H, -CH₃*), 2.07 (s, 3H, -CH₃*), 2.08 (s, 6H, -CH₃, -CH₃), 2.09 (s, 3H, -CH₃), 2.10 (s, 6H, -CH₃, -CH₃*), 2.13 (s, 3H, -CH₃*), 3.36 (s, 3H, -O-CH₃*), 3.39 (s, 3H, -O-CH₃), 3.49 (dd, ³J_{H,H}=8.4, 4.5 Hz, 1H, **H-3**), 3.71 (dd, ³J_{H,H}=9.1, 4.8 Hz, 1H, **H-3***), 3.79 (ddd, ³J_{H,H}=8.2, 6.0, 3.2 Hz, 1H, **H-5**), 3.96 (ddd, ³J_{H,H}=9.8, 5.3, 2.5 Hz, 1H, **H-5***), 4.04 (dd, ³J_{H,H}=12.3, 2.5 Hz, 1H, **H-6a***), 4.14 (dd, ³J_{H,H}=12.3, 3.1 Hz, 1H, **H-6a**), 4.25 (dd, ³J_{H,H}=12.5, 5.3 Hz, 1H, **H-6b***), 4.30 (dd, ³J_{H,H}=11.3, 5.1 Hz, 1H, **H-6b**), 4.57 (ddd, ³J_{H,H}=8.2, 4.8, 2.4 Hz, 1H, **H-2***), 4.83 (ddd, ³J_{H,H}=9.8, 4.5, 2.2 Hz, 1H, **H-2**), 4.99 (dd, ³J_{H,H}=8.7, 7.9 Hz, 1H, **H-4**), 5.02 (dd, ³J_{H,H}=9.6, 9.2 Hz, 1H, **H-4***), 5.73 (d, ³J_{H,H}=9.6 Hz, 1H, NH), 5.78 (d, ³J_{H,H}=7.8 Hz, 1H, NH*), 5.81 (d, ³J_{H,H}=2.3 Hz, 1H, **H-1**), 6.11 (d, ³J_{H,H}=2.3 Hz, 1H, **H-1***), Signals of the major anomer are marked with an asterisk.

¹³C-NMR: (100 MHz, CDCl₃) δ [ppm] 20.88 (-CH₃*), 20.89 (-CH₃), 20.96 (-CH₃*), 20.98 (-CH₃), 21.01 (-CH₃*), 21.1 (-CH₃), 23.5 (-O-1-CO-CH₃*), 23.6 (-O-1-CO-CH₃), 47.2 (**C-2**), 48.2 (**C-2***), 57.4 (-O-CH₃*), 57.8 (-O-CH₃), 62.4 (**C-6***), 62.6 (**C-6**), 66.5 (**C-4**), 66.8 (**C-4***), 70.0 (**C-5***), 73.3 (**C-5**), 76.4 (**C-3***), 78.4 (**C-3**), 91.5 (**C-1**), 92.0 (**C-1***), 168.4 (O-1-CO), 170.0 (O-4-CO), 170.6 (NH-CO), 170.8 (O-6-CO), Signals of the major anomer are marked with an asterisk.

HR-MS: (ESI positive, MeOH) calc. for [C₁₅H₂₃NO₉Na]⁺: [M+Na]⁺ 384.12650, found 384.12641.

UV: (CHCl₃) λ (lgε)=240 nm (2.454).

IR: (KBr) ν_{max}=3435 cm⁻¹, 2957, 2935, 2832, 1747, 1661, 1541, 1372, 1233, 1135, 1047, 972.

Benzyl 2-azido-4,6-O-benzylidene-2-deoxy-3-O-ethyl- α -D-mannopyranoside (4b)

According to *GWP 1*, benzyl 2-azido-4,6-O-benzylidene-2-deoxy- α -D-mannopyranoside **2** (1.50 g, 3.91 mmol) was reacted with sodium hydride (103 mg, 4.30 mmol) and iodoethane (472 μ l, 915 mg, 5.87 mmol). The product (1.40 g, 3.40 mmol, 87%) was obtained as colorless oil.

R_f: 0.58 (*n*-hexane/ethyl acetate=5:1 *v/v*)

¹H-NMR: (400 MHz, CDCl₃) δ [ppm] 1.24 (t, ³J_{H,H}=7.0 Hz, 3H, -CH₂-CH₃), 3.70 (dq, J_{H,H}=9.4, 7.0 Hz, 1H, -CH_aH_b-CH₃), 3.78-3.90 (m, 3H, -CH_aH_b-CH₃), 4.00-4.08 (m, 3H), 4.19-4.28 (m, 1H), 4.50 (d, ²J_{H,H}=11.7 Hz, 1H, Ph-CH_aH_b-), 4.71 (d, ²J_{H,H}=11.7 Hz, 1H, Ph-CH_aH_b-), 4.86 (d, ³J_{H,H}=1.4 Hz, 1H, **H-1**), 5.62 (s, 1H, Ph-CH-), 7.30-7.44 (m, 6H, **H_{ar}**), 7.45-7.54 (m, 2H, **H_{ar}**).

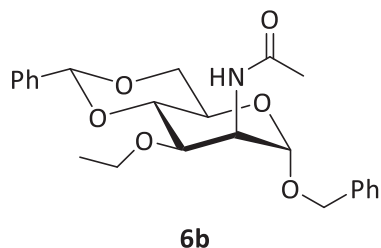
¹³C-NMR: (75 MHz, CDCl₃) δ [ppm] 15.7 (-O-CH₂-CH₃), 62.6 (**C-2**), 64.2 (**C-5**), 67.0 (**C-6**), 68.8 (-O-CH₂-CH₃), 69.6 (Ph-CH₂-), 76.2 (**C-4**), 79.0 (**C-3**), 98.4 (**C-1**), 101.7 (Ph-CH-), 126.2 (**C_{ar}**), 128.32 (**C_{ar}**), 128.34 (**C_{ar}**), 128.4 (**C_{ar}**), 128.7 (**C_{ar}**), 129.0 (**C_{ar}**), 136.6 (**C_{ipso}**), 137.6 (**C_{ipso}**).

HR-MS: (ESI positive, CHCl₃/MeOH) calc. for [C₂₂H₂₅N₃O₅Na]⁺: [M+Na]⁺ 434.16864, found 434.16882; calc. for [C₄₄H₅₀N₆O₁₀Na]⁺: [2M+Na]⁺ 845.34806, found 845.34887.

UV: (CH₃OH) λ (lg ϵ)=235 nm (2.721), 252 (2.524).

IR: (film) ν_{\max} =2976 cm⁻¹, 2927, 2106, 1454, 1383, 1274, 1092, 1053, 750, 698.

Optical rotation: $[\alpha]_D^{22} (\text{ }^\circ \text{cm}^3 \text{ g}^{-1} \text{dm}^{-1}) = +65.9$ (*c*=1.0, CH₂Cl₂)

Benzyl 2-(acetylamino)-4,6-O-benzylidene-2-deoxy-3-O-ethyl- α -D-mannopyranoside (6b)

According to *GWP 2* benzyl 2-azido-4,6-O-benzylidene-2-deoxy-3-O-ethyl- α -D-mannopyranoside **4b** (3.17 g, 7.70 mmol) was reduced and then reacted with triethylamine (3.22 ml, 2.34 g, 23.1 mmol), 4-dimethylaminopyridine (94.1 mg, 770 μ mol) and acetyl chloride (1.10 ml, 1.21 g, 15.4 mmol). The product (2.74 g, 6.41 mmol, 83%) was obtained as white solid.

R_f: 0.33 (*n*-hexane/ethyl acetate=1:1 *v/v*)

¹H-NMR: (300 MHz, CDCl₃) δ [ppm] 1.18 (t, ³J_{H,H}=7.0 Hz, 3H, -CH₂-CH₃), 2.05 (s, 3H, CO-CH₃), 3.50-3.61 (m, 1H), 3.61-3.73 (m, 2H), 3.77 (“t”, ³J_{H,H}=10.2 Hz, 1H), 3.91 (dd, ³J_{H,H}=9.7, 4.5 Hz, 1H), 4.01 (dd, ³J_{H,H}=10.1, 5.0 Hz, 1H, **H-3**), 4.22 (dd, ³J_{H,H}=10.0, 4.6 Hz, 1H, **H-4**), 4.53 (d, ²J_{H,H}=11.6 Hz, 1H, Ph-CH_aH_b-), 4.57 (ddd, ³J_{H,H}=7.4, 5.0, 1.2 Hz, 1H, **H-2**), 4.69 (d, ²J_{H,H}=11.7 Hz, 1H, Ph-CH_aH_b-), 5.05 (d, ³J_{H,H}=1.0 Hz, 1H, **H-1**), 5.59 (s, 1H, Ph-CH-), 5.77 (d, ³J_{H,H}=7.2 Hz, 1H, NH), 7.32-7.40 (m, 6H, **H_{ar}**), 7.46-7.53 (m, 2H, **H_{ar}**).

¹³C-NMR: (75 MHz, CDCl₃) δ [ppm] 15.5 (-CH₂-CH₃), 23.6 (CO-CH₃), 51.2 (**C-2**), 63.4 (**C-5**), 65.6 (-CH₂-CH₃), 69.0 (**CH₂**), 70.0 (**CH₂**), 73.3 (**C-3**), 78.8 (**C-4**), 99.4 (**C-1**), 102.0 (Ph-CH-), 126.2 (**C_{ar}**), 128.1 (**C_{ar}**), 128.2 (**C_{ar}**), 128.4 (**C_{ar}**), 128.7 (**C_{ar}**), 129.1 (**C_{ar}**), 136.9 (**C_{ipso}**), 137.4 (**C_{ipso}**), 170.7 (**CO**).

HR-MS: (ESI positive, CHCl₃/MeOH) calc. for [C₂₄H₃₀NO₆]⁺: [M+H]⁺ 428.20676, found 428.20656; calc. for [C₂₄H₂₉NO₆Na]⁺: [M+Na]⁺ 450.18871, found 450.18882; calc. for [C₄₈H₅₈N₂O₁₂Na]⁺: [2M+Na]⁺ 877.38820, found 877.38925.

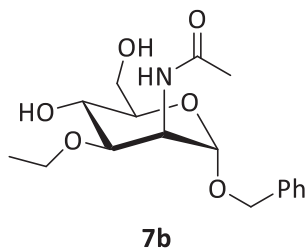
UV: (CH₃OH) λ (lgε)=206 nm (4.238), 261 (3.072), 282 (2.972).

IR: (KBr) ν_{max}=3426 cm⁻¹, 2973, 2928, 1725, 1652, 1550, 1454, 1377, 1117, 1088, 1027, 699.

Optical rotation: [α]_D²⁵(° cm³ g⁻¹dm⁻¹)=+37.6 (*c*=1.0, CH₂Cl₂)

Melting point: 120°C

Benzyl 2-(acetylamino)-2-deoxy-3-*O*-ethyl-α-D-mannopyranoside (**7b**)



Benzyl 2-(acetylamino)-4,6-*O*-benzylidene-2-deoxy-3-*O*-ethyl-α-D-mannopyranoside **6b** (1.30 g, 3.04 mmol) was treated according to GWP 3. The product (901 mg, 2.65 mmol, 87%) was obtained as white solid.

R_f: 0.29 (dichloromethane/methanol=15:1 *v/v*)

¹H-NMR: (300 MHz, D₂O) δ [ppm] 1.01 (t, ³J_{H,H}=7.0 Hz, 3H, -CH₂-CH₃), 1.90 (s, 3H, CO-CH₃), 3.32-3.47 (m, 1H), 3.47-3.68 (m, 4H), 3.68-3.79 (m, 2H), 4.37-4.51 (m, 2H), 4.52-4.61 (m, 1H), 4.82 (d, ³J_{H,H}=1.1 Hz, 1H, **H-1**), 7.24-7.37 (m, 5H, **H_{ar}**).

¹³C-NMR: (75 MHz, D₂O) δ [ppm] 15.6 (-CH₂-CH₃), 23.1 (CO-CH₃), 50.4 (**C-2**), 61.5 (**C-6**), 66.7 (**C-4**), 66.8 (-CH₂-CH₃), 70.8 (Ph-CH₂), 73.8 (**C-5**), 78.3 (**C-3**), 99.7 (**C-1**), 129.75 (**C_{ar}**), 129.83 (**C_{ar}**), 130.1 (**C_{ar}**), 137.8 (**C_{ipso}**), 175.4 (**CO**).

HR-MS: (ESI positive, MeOH) calc. for [C₁₇H₂₆NO₆]⁺: [M+H]⁺ 340.17546, found 340.17509; calc. for [C₁₇H₂₅NO₆Na]⁺: [M+Na]⁺ 362.15741, found 362.15710; calc. for [C₃₄H₅₀N₂O₁₂Na]⁺: [2M+Na]⁺ 701.32560, found 701.32537.

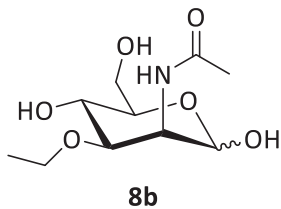
UV: (CH₃OH) λ (lgε)=207 nm (4.101), 259 (2.425).

IR: (KBr) ν_{max}=3418 cm⁻¹, 2975, 2927, 1637, 1541, 1454, 1384, 1125, 980.

Optical rotation: [α]_D²⁴(° cm³ g⁻¹dm⁻¹)=+53.3 (c=1.0, CH₂Cl₂)

Melting point: 99 °C

2-(Acetylamino)-2-deoxy-3-O-ethyl-D-mannose (8b)



Benzyl 2-(acetylamino)-2-deoxy-3-O-ethyl-α-D-mannopyranoside **7b** (640 mg, 1.89 mmol) was treated according to *GWP 4*. The product (470 mg, 1.78 mmol, 94%) was obtained as white solid.

R_f: 0.28 (dichloromethane/methanol=10:1 v/v)

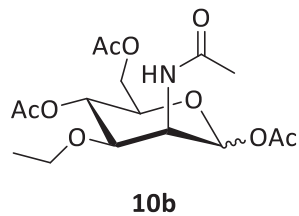
¹H-NMR: (300 MHz, CD₃OD) δ [ppm] 1.15 (t, ³J_{H,H}=7.0 Hz, 3H, -O-CH₂-CH₃), 1.16 (t, ³J_{H,H}=7.0 Hz, 3H, -O-CH₂-CH₃*), 1.98 (s, 3H, CO-CH₃*), 2.02 (s, 3H, CO-CH₃), 3.19-3.39 (m, 1H), 3.40-3.52 (m, 2H), 3.53-3.88 (m, 9H), 4.44 (dd, ³J_{H,H}=4.3, 1.6 Hz, 1H, **H-1***), 4.57 (dd, ³J_{H,H}=4.1, 1.4 Hz, 1H, **H-1**), 4.84 (d, ³J_{H,H}=0.6 Hz, 1H, **H-1**), 5.02 (d, ³J_{H,H}=1.6 Hz, 1H, **H-1***), Signals of the major anomer are marked with an asterisk.

¹³C-NMR: (100 MHz, CD₃OD) δ [ppm] 15.56 (-O-CH₂-CH₃), 15.61 (-O-CH₂-CH₃*), 22.5 (CO-CH₃*), 22.7 (CO-CH₃), 51.3 (**C-2***), 52.0 (**C-2**), 62.1 (**C-6**), 62.2 (**C-6***), 65.7 (**C-4***), 65.8 (**C-4**), 66.8 (-O-CH₂-CH₃), 67.1 (-O-CH₂-CH₃*), 73.4 (**C-5**), 78.2 (**C-5**), 78.5 (**C-3***), 82.0 (**C-3**), 95.0 (**C-1**), 95.1 (**C-1**), 173.4 (**CO***), 174.5 (**CO**), Signals of the major anomer are marked with an asterisk.

HR-MS: (ESI positive, CHCl₃/MeOH) calc. for [C₁₀H₁₉NO₆Na]⁺: [M+Na]⁺ 272.11046, found 272.11044.

UV: (CH₃OH) λ (lgε)=202 nm (3.708).

IR: (KBr) ν_{max}=3388 cm⁻¹, 2977, 2932, 1706, 1645, 1552, 1426, 1384, 1233, 1105, 1071.

1,4,6-Tri-O-acetyl-2-(acetylamino)-2-deoxy-3-O-ethyl-D-mannopyranose (10b)**10b**

2-(Acetylamino)-2-deoxy-3-O-ethyl-D-mannose **8b** (37.2 mg, 149 µmol, 1.0 eq.) was dissolved in pyridine (0.5 ml) and acetic anhydride (141 µl, 152 mg, 1.49 mmol, 10 eq.) was added. The reaction mixture was stirred at room temperature for 16 hours. Then, the reaction was quenched by addition of sat. sodium bicarbonate solution (1 ml) and diluted with dichloromethane (3 ml). The reaction mixture was washed with cupric sulfate solution twice (2 × 1 ml) and finally with brine (2 ml). The organic phase was separated and dried over MgSO₄. Purification by column chromatography afforded the product (47.5 g, 127 µmol, 85%) as a hygroscopic white solid.

R_f: 0.24 (*n*-hexane/ethyl acetate=1:2 v/v)

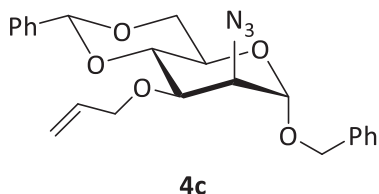
¹H-NMR: (400 MHz, CDCl₃) δ [ppm] 1.128 (t, ³J_{H,H}=7.0 Hz, 3H, -CH₂-CH₃*), 1.131 (t, ³J_{H,H}=7.0 Hz, 3H, -CH₂-CH₃), 2.04 (s, 3H, -CO-CH₃*), 2.056 (s, 3H, -CO-CH₃), 2.060 (s, 3H, -CO-CH₃*), 2.062 (s, 3H, -CO-CH₃), 2.07 (s, 3H, -CO-CH₃), 2.078 (s, 3H, -CO-CH₃*), 2.080 (s, 3H, -CO-CH₃), 2.12 (s, 3H, -CO-CH₃*), 3.38–3.48 (m, 2H, -O-CH_aH_b-, -O-CH_aH_b*), 3.55–3.71 (m, 3H, -O-CH_aH_b-, -O-CH_aH_b*, **H-3**), 3.78 (dd, ³J_{H,H}=9.0, 4.8 Hz, 1H, **H-3***), 3.76–3.80 (m, 1H, **H-5**), 3.95 (ddd, ³J_{H,H}=9.5, 5.2, 2.6 Hz, 1H, **H-5***), 4.04 (dd, ³J_{H,H}=12.3, 2.6 Hz, 1H, **H-6a***), 4.14 (dd, ³J_{H,H}=12.3, 3.4 Hz, 1H, **H-6a**), 4.24 (dd, ³J_{H,H}=12.3, 5.3 Hz, 1H, **H-6b***), 4.29 (dd, ³J_{H,H}=12.2, 6.0 Hz, 1H, **H-6b**), 4.50 (ddd, ³J_{H,H}=8.2, 4.8, 2.5 Hz, 1H, **H-2***), 4.77 (ddd, ³J_{H,H}=9.7, 4.5, 2.3 Hz, 1H, **H-2**), 4.98 (dd, ³J_{H,H}=8.3, 8.3 Hz, 1H, **H-4**), 5.01 (dd, ³J_{H,H}=9.4, 9.4 Hz, 1H, **H-4***), 5.800 (d, ³J_{H,H}=2.3 Hz, 1H, **H-1**), 5.803 (d, ³J_{H,H}=9.6 Hz, 1H, NH), 5.89 (d, ³J_{H,H}=7.9 Hz, 1H, NH*), 6.10 (d, ³J_{H,H}=2.5 Hz, 1H, **H-1***), Signals of the major anomer are marked with an asterisk.

¹³C-NMR: (100 MHz, CDCl₃) δ [ppm] 15.2 (-CH₂-CH₃), 15.3 (-CH₂-CH₃*), 20.84 (-CO-CH₃*), 20.86 (-CO-CH₃), 20.88 (-CO-CH₃*), 20.91 (-CO-CH₃), 20.99 (-CO-CH₃*), 21.04 (-CO-CH₃), 23.4 (-CO-CH₃*), 23.5 (-CO-CH₃), 47.6 (**C-2**), 48.9 (**C-2***), 62.4 (**C-6***), 62.6 (**C-6**), 65.3 (**C-4***), 65.6 (**C-4**), 66.7 (-CH₂-CH₃), 67.0 (-CH₂-CH₃*), 70.1 (**C-5***), 73.3 (**C-5**), 74.6 (**C-3***), 76.5 (**C-3**), 91.5 (**C-1**), 91.9 (**C-1***), 168.4 (CO*), 169.0 (CO), 169.88 (CO*), 169.91 (CO), 170.64 (CO*), 170.685 (CO), 170.694 (CO), 170.75 (CO*), Signals of the major anomer are marked with an asterisk.

HR-MS: (ESI positive, CHCl₃/MeOH) calc. for [C₁₆H₂₅NO₉Na]⁺: [M+Na]⁺ 398.14215, found 398.14196.

UV: (CH₂Cl₂) λ (lgε)=233 nm (4.022), 274 (3.023).

IR: (KBr) ν_{max}=3445 cm⁻¹, 2925, 1746, 1649, 1374, 1235, 1130, 1047, 606.

Benzyl 2-azido-4,6-O-benzylidene-2-deoxy-3-O-prop-2-en-1-yl- α -D-mannopyranoside (4c)

According to *GWP 1*, benzyl 2-azido-4,6-O-benzylidene-2-deoxy- α -D-mannopyranoside **2** (524 mg, 1.37 mmol) was reacted with sodium hydride (36.1 mg, 1.50 mmol) and iodoethane (472 μ l, 915 mg, 5.87 mmol). The product (567 mg, 1.34 mmol, 98%) was obtained as white solid.

R_f: 0.68 (*n*-hexane/ethyl acetate=3:1 *v/v*)

¹H-NMR: (400 MHz, CDCl₃) δ [ppm] 3.80-3.90 (m, 2H), 4.04-4.11 (m, 3H), 4.18 (ddt, ³J_{H,H}=13.1, 5.7, 1.6 Hz, 1H, H_{Propenyl-1a}), 4.21-4.25 (m, 1H), 4.37 (ddt, ³J_{H,H}=13.1, 5.1, 1.5 Hz, 1H, H_{Propenyl-1b}), 4.51 (d, ²J_{H,H}=11.7 Hz, 1H, Ph-CH_aH_b-), 4.71 (d, ²J_{H,H}=11.9 Hz, 1H, Ph-CH_aH_b-), 4.86 (d, ³J_{H,H}=1.2 Hz, 1H, H-1), 5.19 ("dq", ³J_{H,H}=10.5, 1.4 Hz, 1H, H_{Propenyl-3a}), 5.34 ("dq", ³J_{H,H}=17.2, 1.7 Hz, 1H, H_{Propenyl-3b}), 5.62 (s, 1H, Ph-CH-), 5.92 (dddd, ³J_{H,H}=15.6, 15.1, 8.1, 4.9 Hz, 1H, H_{Propenyl-2}), 7.31-7.41 (m, 8H, H_{ar}), 7.46-7.51 (m, 2H, H_{ar}).

¹³C-NMR: (100 MHz, CDCl₃) δ [ppm] 63.0, 64.1, 68.8, 69.6, 72.4, 75.8, 79.3, 98.5 (**C-1**), 101.8 (Ph-CH-), 117.0 (-CH=CH₂), 126.2 (**C_{ar}**), 128.3 (**C_{ar}**), 128.4 (**C_{ar}**), 128.4 (**C_{ar}**), 128.7 (**C_{ar}**), 129.1 (**C_{ar}**), 134.5 (-CH=CH₂), 136.6 (**C_{ipso}**), 137.5 (**C_{ipso}**).

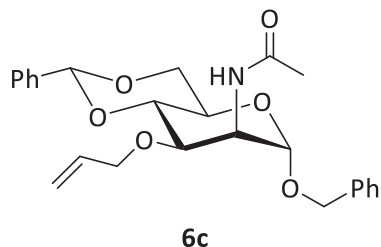
HR-MS: (ESI positive, CHCl₃/MeOH) calc. for [C₂₃H₂₅N₃O₅Na]⁺: [M+Na]⁺ 446.16864, found 446.16858; calc. for [C₄₆H₅₀N₆O₁₀Na]⁺: [2M+Na]⁺ 869.34806, found 869.34727.

UV: (CHCl₃) λ (lg ϵ)=239 (2.695), 258 nm (2.650).

IR: (KBr) ν_{\max} =2921 cm⁻¹, 2872, 2106, 1454, 1378, 1275, 1134, 1094, 734, 699.

Optical rotation: $[\alpha]_D^{23} (\text{ }^\circ \text{cm}^3 \text{ g}^{-1} \text{ dm}^{-1}) = +65.9$ (*c*=1.0, CHCl₃)

Melting point: 58°C

Benzyl 2-(acetylamino)-4,6-O-benzylidene-2-deoxy-3-O-prop-2-en-1-yl- α -D-mannopyranoside (6c)

Triphenylphosphane (139 mg, 531 μ mol, 3.0 eq.) was added to a solution of benzyl 2-azido-4,6-O-benzylidene-2-deoxy-3-O-prop-2-en-1-yl- α -D-mannopyranoside **4c** (75.0 mg, 177 μ mol, 1.0 eq.) in a water/THF mixture (3.0 ml, 1:8 v/v). After stirring for 24 hours at room temperature the mixture was evaporated to dryness and the acylation was carried out according to GWP 2 with triethylamine (74.1 μ l, 53.8 mg, 531 μ mol), 4-dimethylaminopyridine (2.16 mg, 17.7 μ mol) and acetyl chloride (25.3 μ l, 27.8 mg, 354 μ mol). The product (46.0 mg, 105 μ mol, 59%) was obtained as colorless oil.

R_f: 0.21 (*n*-hexane/ethyl acetate=1:1 v/v)

¹H-NMR: (400 MHz, CDCl₃) δ [ppm] 1.58 (s, 3H, -CO-CH₃), 3.71 (t, ³J_{H,H}=9.8 Hz, 1H, **H-6a**), 3.78 (t, ³J_{H,H}=10.3 Hz, 1H, **H-4**), 3.87-3.97 (m, 1H, **H-5**), 4.04-4.16 (m, 3H, **H_{Propenyl}-1a**, **H_{Propenyl}-1b**, **H-6b**), 4.22 (dd, ³J_{H,H}=10.3, 4.6 Hz, 1H, **H-3**), 4.53 (d, ²J_{H,H}=11.8 Hz, 1H, Ph-CH_aH_b-), 4.55-4.59 (m, 1H, **H-2**), 4.68 (d, ²J_{H,H}=11.7 Hz, 1H, Ph-CH_aH_b-), 5.03 (d, ³J_{H,H}=0.5 Hz, 1H, **H-1**), 5.16 (ddd, ³J_{H,H}=4.4, 2.5, 1.4 Hz, 1H, **H_{Propenyl}-3a**), 5.31 ("dq", ³J_{H,H}=3.1, 1.3 Hz, 1H, **H_{Propenyl}-3b**), 5.58 (s, 1H, Ph-CH-), 5.72-5.78 (m, 1H, NH), 5.81-5.93 (m, 1H, **H_{Propenyl}-2**), 7.34-7.39 (m, 2H, **H_{ar}**), 7.42-7.51 (m, 3H, **H_{ar}**), 7.51-7.58 (m, 2H, **H_{ar}**), 7.63-7.72 (m, 3H, **H_{ar}**).

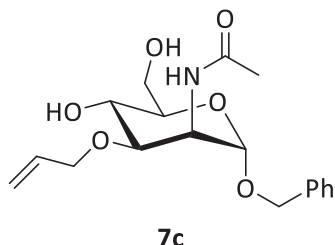
¹³C-NMR: (75 MHz, CDCl₃) δ [ppm] 23.5 (-CO-CH₃), 51.2 (**C-2**), 63.2 (**C-5**), 68.8 (CH₂), 69.9 (CH₂), 70.8 (CH₂), 72.8 (**C-3**), 78.9 (**C-4**), 99.3 (**C-1**), 101.8 (Ph-CH-), 117.4 (-CH=CH₂), 126.1 (**C_{ar}**), 128.4 (**C_{ar}**), 128.6 (**C_{ar}**), 132.0 (**C_{ar}**), 132.1 (**C_{ar}**), 132.2 (**C_{ar}**), 134.3 (-CH=CH₂), 136.8 (**C_{ipso}**), 137.3 (**C_{ipso}**), 170.6 (-CO-CH₃).

HR-MS: (ESI positive, CHCl₃/MeOH) calc. for [C₂₅H₂₉NO₆Na]⁺: [M+Na]⁺ 462.18871, found 462.18900.

UV: (CHCl₃) λ (lg ϵ)=239 nm (3.887), 261 (3.870), 265 (3.883), 372 (3.782).

IR: (film) ν_{\max} =3063 cm⁻¹, 2928, 2868, 1738, 1655, 1546, 1375, 1119, 1038, 698, 542.

Optical rotation: $[\alpha]_D^{22} (\text{ }^\circ \text{cm}^3 \text{ g}^{-1} \text{dm}^{-1}) = +23.7$ (*c*=1.0, CHCl₃)

Benzyl 2-(acetylamino)-2-deoxy-3-O-prop-2-en-1-yl- α -D-mannopyranoside (7c)

Benzyl 2-(acetylamino)-4,6-O-benzylidene-2-deoxy-3-O-prop-2-en-1-yl- α -D-mannopyranoside **6c** (218 mg, 480 μ mol) was treated according to *GWP 3*. The product (141 mg, 386 μ mol, 80%) was obtained as white waxy solid.

R_f: 0.43 (dichloromethane/methanol=10:1 v/v)

¹H-NMR: (300 MHz, CDCl₃) δ [ppm] 2.03 (s, 3H, -CO-CH₃), 3.65-3.77 (m, 2H), 3.81-3.89 (m, 3H), 3.95 (ddt, ³J_{H,H}=12.2, 6.1, 1.2 Hz, 1H, H_{Propenyl-1a}), 4.20 (ddt, ³J_{H,H}=12.2, 5.6, 1.4 Hz, 1H, H_{Propenyl-1b}), 4.53 (d, ²J_{H,H}=11.7 Hz, 1H, Ph-CH_aH_b-), 4.59 (ddd, ³J_{H,H}=8.4, 4.6, 1.5 Hz, 1H, H-2), 4.69 (d, ²J_{H,H}=11.7 Hz, 1H, Ph-CH_aH_b-), 4.97 (d, ³J_{H,H}=1.3 Hz, 1H, H-1), 5.21 (ddd, ³J_{H,H}=10.4, 2.7, 1.2 Hz, 1H, H_{Propenyl-3a}), 5.30 (ddd, ³J_{H,H}=17.2, 3.1, 1.5 Hz, 1H, H_{Propenyl-3b}), 5.74 (d, ³J_{H,H}=8.5 Hz, 1H, NH), 5.90 (dddd, ³J_{H,H}=17.1, 10.3, 6.1, 5.6 Hz, 1H, H_{Propenyl-2}), 7.31-7.42 (m, 5H, H_{ar}).

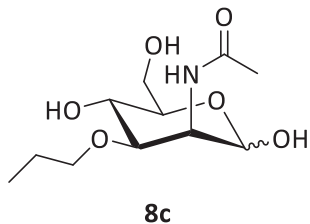
¹³C-NMR: (100 MHz, CDCl₃) δ [ppm] 23.4 (-CO-CH₃), 49.0 (**C-2**), 62.0 (**C-6**), 66.4 (**C-4**), 69.8 (CH₂), 70.1 (CH₂), 71.5 (**C-5**), 76.8 (**C-3**)[†], 99.2 (**C-1**), 118.3 (-CH=CH₂), 128.1 (**C_{ar}**), 128.2 (**C_{ar}**), 128.6 (**C_{ar}**), 134.1 (-CH=CH₂), 137.0 (**C_{ipso}**), 170.5 (-CO-CH₃) †Signal is overlapping with the deuterochloroform signal.

HR-MS: (ESI positive, CHCl₃/MeOH) calc. for [C₁₈H₂₅NO₆Na]⁺: [M+Na]⁺ 374.15741, found 374.15735.

UV: (CHCl₃) λ (lg ϵ)=240 nm (2.769), 254 (2.604).

IR: (KBr) ν_{\max} =3397 cm⁻¹, 3087, 2925, 1733, 1656, 1548, 1128, 1079, 1038, 699.

Optical rotation: $[\alpha]_D^{22} (\text{ }^\circ \text{cm}^3 \text{ g}^{-1} \text{dm}^{-1}) = +51.7 (c=1.0, \text{CHCl}_3)$

2-(Acetylamino)-2-deoxy-3-O-propyl- α -D-mannose (8c)

Benzyl 2-(acetylamino)-2-deoxy-3-O-prop-2-en-1-yl- α -D-mannopyranoside **7c** (6223 mg, 635 μ mol) was treated according to *GWP 4*. The product (137 mg, 518 μ mol, 82%) was obtained as white waxy solid.

R_f: 0.41 (dichloromethane/methanol=10:1 v/v)

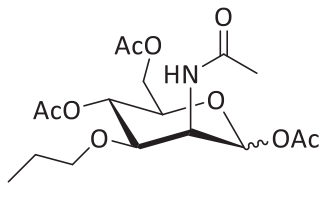
¹H-NMR: (400 MHz, CD₃OD) δ [ppm] 0.91 (t, $^3J_{H,H}$ =7.2 Hz, 6H, -CH₂-CH₃^{*}, -CH₂-CH₃), 1.54-1.59 (m, 4H, -CH₂-CH₃^{*}, -CH₂-CH₃), 1.98 (s, 6H, -CO-CH₃^{*}, -CO-CH₃), 3.36-3.40 (m, 4H), 3.56-3.71 (m, 4H), 3.74-3.85 (m, 6H), 4.45 (dd, $^3J_{H,H}$ =4.4, 1.6 Hz, 1H, **H-2**^{*}), 4.58 (dd, $^3J_{H,H}$ =4.4, 1.6 Hz, 1H, **H-2**), 5.02 (d, $^3J_{H,H}$ =1.6 Hz, 1H, **H-1**^{*}), Signal of **H-1** of the minor anomer is overlapping with the water signal. Signals of the major anomer are marked with an asterisk.

¹³C-NMR: (100 MHz, CD₃OD) δ [ppm] 10.8 (-CH₂-CH₃), 10.9 (-CH₂-CH₃^{*}), 22.5 (-CO-CH₃^{*}), 22.7 (-CO-CH₃), 24.0 (-CH₂-CH₃), 24.1 (-CH₂-CH₃^{*}), 51.2 (**C-2**), 51.3 (**C-2**^{*}), 62.2 (**C-6**), 62.3 (**C-6**^{*}), 66.9 (**C-4**), 67.2 (**C-4**^{*}), 72.05 (-O-CH₂-^{*}), 72.11 (-O-CH₂-), 73.38 (**C-5**^{*}), 73.41 (**C-5**), 78.2 (**C-3**), 78.6 (**C-3**^{*}), 95.1 (**C-1**^{*}), 95.2 (**C-1**), 173.29 (-CO-CH₃^{*}), 173.31 (-CO-CH₃), Signals of the major anomer are marked with an asterisk.

HR-MS: (ESI positive, MeOH) calc. for [C₁₁H₂₁NO₆Na]⁺: [M+Na]⁺ 286.12613, found 286.12585.

UV: (CH₃OH) λ (lg ϵ)=204 nm (3.921), 267 (1.916).

IR: (KBr) ν_{max} =3419 cm⁻¹, 2963, 2934, 2878, 1654, 1550, 1376, 1107, 1070, 1040, 974.

1,4,6-Tri-O-acetyl-2-(acetylamino)-2-deoxy-3-O-propyl-D-mannopyranose (10c)**10c**

2-(Acetylamino)-2-deoxy-3-O-propyl- α -D-mannose **8c** (34.2 mg, 130 μ mol, 1.0 eq.) was dissolved in pyridine (0.5 ml) and acetic anhydride (123 μ l, 133 mg, 1.30 mmol, 10 eq.) was added. The reaction mixture was stirred at room temperature for 16 hours. Then, the reaction was quenched by addition of sat. sodium bicarbonate solution (1 ml) and diluted with dichloromethane (3 ml). The reaction mixture was

washed with cupric sulfate solution twice (2×1 ml) and finally with brine (2 ml). The organic phase was separated and dried over MgSO_4 . Purification by column chromatography afforded the product (41.2 mg, 106 μmol , 81%) as a hygroscopic white solid.

R_f: 0.27 (*n*-hexane/ethyl acetate=1:2 v/v)

¹H-NMR: (400 MHz, CDCl_3) δ [ppm] 0.865 (t, ${}^3J_{\text{H,H}}=7.4$ Hz, 3 H, -CH₂-CH₃^{*}), 0.869 (t, ${}^3J_{\text{H,H}}=7.8$ Hz, 3 H, -CH₂-CH₃), 1.44-1.57 (m, 4 H, -CH₂-CH₃, -CH₂-CH₃^{*}), 2.04 (s, 3 H, -CO-CH₃^{*}), 2.057 (s, 6 H, 2 x -CO-CH₃), 2.062 (s, 3 H, -CO-CH₃^{*}), 2.068 (s, 3 H, -CO-CH₃), 2.073 (s, 3 H, -CO-CH₃^{*}), 2.08 (s, 3 H, -CO-CH₃), 2.12 (s, 3 H, -CO-CH₃^{*}), 3.26-3.33 (m, 2 H, -O-CH_aH_b-, -O-CH_aH_b-^{*}), 3.51-3.63 (m, 3 H, -O-CH_aH_b-, -O-CH_aH_b-^{*}, **H-3**), 3.78 (dd, ${}^3J_{\text{H,H}}=9.2$, 4.9 Hz, 1 H, **H-3**^{*}), 3.77-3.81 (m, 1 H, **H-5**), 3.95 (ddd, ${}^3J_{\text{H,H}}=9.7$, 5.2, 2.6 Hz, 1 H, **H-5**^{*}), 4.04 (dd, ${}^3J_{\text{H,H}}=12.3$, 2.6 Hz, 1 H, **H-6a**^{*}), 4.14 (dd, ${}^3J_{\text{H,H}}=12.2$, 3.3 Hz, 1 H, **H-6a**), 4.24 (dd, ${}^3J_{\text{H,H}}=12.3$, 5.3 Hz, 1 H, **H-6b**^{*}), 4.30 (dd, ${}^3J_{\text{H,H}}=12.2$, 6.0 Hz, 1 H, **H-6b**), 4.51 (ddd, ${}^3J_{\text{H,H}}=7.9$, 4.8, 2.4 Hz, 1 H, **H-2**^{*}), 4.78 (ddd, ${}^3J_{\text{H,H}}=9.7$, 4.5, 2.3 Hz, 1 H, **H-2**), 5.00 (dd, ${}^3J_{\text{H,H}}=8.2$, 8.1 Hz, 1 H, **H-4**), 5.03 (dd, ${}^3J_{\text{H,H}}=9.7$, 9.3 Hz, 1 H, **H-4**^{*}), 5.78 (d, ${}^3J_{\text{H,H}}=9.9$ Hz, 1 H, NH), 5.80 (d, ${}^3J_{\text{H,H}}=2.3$ Hz, 1 H, **H-1**), 5.87 (d, ${}^3J_{\text{H,H}}=7.9$ Hz, 1 H, NH^{*}), 6.11 (d, ${}^3J_{\text{H,H}}=2.3$ Hz, 1 H, **H-1**^{*}), Signals of the major anomer are marked with an asterisk.

¹³C-NMR: (100 MHz, CDCl_3) δ [ppm] 10.53 (-CH₂-CH₃), 10.54 (-CH₂-CH₃^{*}), 20.85 (-CO-CH₃^{*}), 20.87 (-CO-CH₃), 20.88 (-CO-CH₃^{*}), 20.91 (-CO-CH₃), 20.99 (-CO-CH₃^{*}), 21.04 (-CO-CH₃), 22.9 (-CO-CH₃), 23.0 (-CO-CH₃^{*}), 23.4 (-CH₂-CH₃^{*}), 23.5 (-CH₂-CH₃), 47.6 (**C-2**), 48.9 (**C-2**^{*}), 62.4 (**C-6**^{*}), 62.6 (**C-6**), 66.6 (**C-4**), 66.9 (**C-4**^{*}), 70.1 (**C-5**^{*}), 71.4 (-O-CH₂-^{*}), 71.7 (**C-5**), 73.3 (-O-CH₂), 74.8 (**C-3**^{*}), 76.7 (**C-3**), 91.5 (**C-1**), 92.0 (**C-1**^{*}), 168.4 (CO^{*}), 169.1 (CO), 169.87 (CO^{*}), 169.91 (CO), 170.64 (CO^{*}), 170.65 (CO), 170.70 (CO), 170.77 (CO^{*}), Signals of the major anomer are marked with an asterisk.

HR-MS: (ESI positive, $\text{CHCl}_3/\text{MeOH}$) calc. for $[\text{C}_{17}\text{H}_{27}\text{NO}_9\text{Na}]^+$: $[\text{M}+\text{Na}]^+$ 412.15780, found 412.15796.

UV: (CH_2Cl_2) λ ($\lg\epsilon$)=232 nm (3.719), 266 (3.347).

IR: (KBr) ν_{max} =3443 cm^{-1} , 2924, 1637, 1376, 864.

Mouse Siglec-1 Mediates *trans*-Infection of Surface-bound Murine Leukemia Virus in a Sialic Acid N-Acyl Side Chain-dependent Manner*

Received for publication, July 27, 2015, and in revised form, September 2, 2015. Published, JBC Papers in Press, September 14, 2015, DOI 10.1074/jbc.M115.681338

Elina Erikson,^{a,b,1} Paul R. Wratil,^c Martin Frank,^d Ina Ambiel,^a Katharina Pahnke,^e Maria Pino,^f Parastoo Azadi,^g Nuria Izquierdo-Useros,^{f,2} Javier Martinez-Picado,^{f,h} Chris Meier,^e Ronald L. Schnaar,ⁱ Paul R. Crocker,^j Werner Reutter,^c and Oliver T. Keppler^{a,b,3}

From the ^aInstitute of Medical Virology, National Reference Center for Retroviruses, University of Frankfurt, 60596 Frankfurt am Main, Germany, the ^bDepartment of Infectious Diseases, Virology, University of Heidelberg, 69120 Heidelberg, Germany, the ^cInstitut für Laboratoriumsmedizin, Klinische Chemie und Pathobiochemie, Charité Universitätsmedizin Berlin, 12200 Berlin, Germany, ^dBiognos AB, 402 74 Göteborg, Sweden, ^eOrganic Chemistry, Department of Chemistry, Faculty of Sciences, University of Hamburg, 20146 Hamburg, Germany, the ^fAIDS Research Institute IrsiCaixa, Institut d'Investigació en Ciències de la Salut Germans Trias i Pujol, Universitat Autònoma de Barcelona, 08916 Barcelona, Spain, the ^gComplex Carbohydrate Research Center, University of Georgia, Athens, Georgia 30602, the ^hInstitució Catalana de Recerca i Estudis Avançats (ICREA), 08010 Barcelona, Spain, the ⁱDepartments of Pharmacology and Neuroscience, The Johns Hopkins University School of Medicine, Baltimore, Maryland 21218, and the ^jCollege of Life Sciences, University of Dundee, Dundee DD1 5EH, Scotland, United Kingdom

Background: Human Siglec-1 mediates HIV *trans*-infection by interaction with virion-associated sialylated gangliosides.

Results: Here, Siglec-1 on mouse macrophages mediated *trans*-infection of surface-bound MLV. This could be inhibited by biosynthetic modification of sialic acids' N-acyl side chain in virus-producer cells.

Conclusion: The N-acyl side chain is a critical determinant of Siglec-1-dependent MLV *trans*-infection.

Significance: Glycoengineering allows manipulation of sialic acid-dependent virus/receptor interactions.

Siglec-1 (sialoadhesin, CD169) is a surface receptor on human cells that mediates *trans*-enhancement of HIV-1 infection through recognition of sialic acid moieties in virus membrane gangliosides. Here, we demonstrate that mouse Siglec-1, expressed on the surface of primary macrophages in an interferon- α -responsive manner, captures murine leukemia virus (MLV) particles and mediates their transfer to proliferating lymphocytes. The MLV infection of primary B-cells was markedly more efficient than that of primary T-cells. The major structural protein of MLV particles, Gag, frequently co-localized with Siglec-1, and *trans*-infection, primarily of surface-bound MLV particles, efficiently occurred. To explore the role of sialic acid for MLV *trans*-infection at a submolecular level, we analyzed the potential of six sialic acid precursor analogs to modulate the sialylated ganglioside-dependent interaction of MLV particles with Siglec-1. Biosynthetically engineered sialic acids were detected in both the glycolipid and glycoprotein fractions of

MLV producer cells. MLV released from cells carrying N-acyl-modified sialic acids displayed strikingly different capacities for Siglec-1-mediated capture and *trans*-infection; N-butanoyl, N-isobutanoyl, N-glycolyl, or N-pentanoyl side chain modifications resulted in up to 92 and 80% reduction of virus particle capture and *trans*-infection, respectively, whereas N-propanoyl or N-cyclopropylcarbamyl side chains had no effect. In agreement with these functional analyses, molecular modeling indicated reduced binding affinities for non-functional N-acyl modifications. Thus, Siglec-1 is a key receptor for macrophage/lymphocyte *trans*-infection of surface-bound virions, and the N-acyl side chain of sialic acid is a critical determinant for the Siglec-1/MLV interaction.

The cellular lectin Siglec-1 and the sialyl-lactose-containing ganglioside, GM3, in the viral membrane were recently identified as critical determinants for HIV-1 particle capture and storage by human monocyte-derived dendritic cells (DCs)⁴ as well as for DC-mediated *trans*-infection of T-cells (1). The term *trans*-infection refers to a two-step process as follows: the cap-

* This work was supported, in whole or in part, by National Institutes of Health Grant P41GM10349010 (Research Resource for Biomedical Glycomics to Complex Carbohydrate Research Center, University of Georgia) to P. A. and HL107151 to R. L. S. This work was also supported by the Robert Koch-Institute to the National Reference Center for Retroviruses (to O. T. K.), the Sonnenfeld-Stiftung Berlin (to W. R.), Spanish Secretariat for Research Grant SAF2013-49042-R (to N. I. U. and J. M. P.), and Goethe University (to O. T. K.). The authors declare that they have no conflicts of interest with the contents of this article.

¹ Present address: Dept. of Microbiology, Tumor and Cell Biology, Karolinska Institutet, 171 77 Stockholm, Sweden.

² Supported by Mathilde Krim Fellowship 108676 in basic biomedical research founded by "AmFAR," AIDS Research Foundation.

³ To whom correspondence should be addressed: Institute of Medical Virology, National Reference Center for Retroviruses, University of Frankfurt, Paul-Ehrlich Str. 40, 60596 Frankfurt am Main, Germany. Tel.: 49-69-6301-5219; Fax: 49-69-6301-6477; E-mail: oliver.keppler@kgu.de.

⁴ The abbreviations used are: DC, dendritic cell; MLV, murine leukemia virus; BMDM, bone marrow-derived macrophage; PDB, Protein Data Bank; mSiglec, mouse Siglec; But, N-butanoyl; iBut, N-isobutanoyl; Pent, N-pentanoyl; m.o.i., multiplicity of infection; ManNAc, N-acetyl-D-mannosamine; ManNProp, N-propanoyl-D-mannosamine; ManNBut, N-butanoyl-D-mannosamine; ManNiBut, N-isobutanoyl-D-mannosamine; ManNPent, N-pentanoyl-D-mannosamine; ManNCyclo, N-cyclopropylcarbamyl-D-mannosamine; ManNGc, N-glycolyl-D-mannosamine; Neu5G, N-glycolyl-neuraminic acid; ConA, concanavalin A; MD, molecular dynamics; Neu5Ac, N-acetylneuraminic acid; DMB, 1,2-diamino-4,5-methylenedioxobenzene-2HCl.

ture of virus particles by low or non-permissive cells that can retain viruses for a certain period and then mediate viral transmission to permissive neighboring target cells, promoting vigorous infection and spread (2). Siglec-1 is a transmembrane protein belonging to a family of sialic acid-binding immunoglobulin-like lectins. As a group-defining structural characteristic, Siglec proteins consist of an N-terminal V-set domain followed by a variable number of C2-set domains, a transmembrane domain, and a cytoplasmic tail (3). Characterizations of Siglec-1 in humans, mice, rats, and pigs indicate a preferential physiological expression of the lectin receptor on cells of the myeloid lineage. Its expression is mainly restricted to macrophage subsets, and in mice, it is highly exposed on macrophage subsets in the marginal zone of the spleen and in the subcapsular sinus of lymph nodes (4).

The physiological roles of Siglec-1 are still under debate. Although initially proposed to be a regulator of hematopoiesis (5–7), knock-out (KO) mice were viable, displayed no gross developmental abnormalities, and exhibited only subtle changes in B- and T-cell populations (8). Evidence is emerging that Siglec-1 may contribute to shaping various inflammatory and autoimmune responses (4). Furthermore, a role of Siglec-1 for infection, *trans*-infection, or clearance of sialylated pathogens other than HIV has been suggested (3, 9–11). Earlier work indicated a role of Siglec-1 as a receptor for infection of alveolar macrophages by porcine reproductive and respiratory syndrome virus. However, this was called into question in a study using Siglec-1 KO pigs (12). Both human and mouse Siglec-1 (mSiglec-1) expressed on human cells were recently shown to capture ecotropic murine leukemia virus (MLV), a simple retrovirus and mouse pathogen, in a ganglioside-dependent manner (13). Siglec-1 may also function as a recognition and uptake receptor for sialylated bacteria and protozoa, including *Neisseria meningitidis*, *Campylobacter jejuni*, and *Trypanosoma cruzi* (4).

Siglec-1 binds promiscuously to a variety of sialylated molecules (9). For the lectin receptor the molecular basis of carbohydrate binding has been investigated by site-directed mutagenesis (14), crystallography (15), and nuclear magnetic resonance analysis (16). Accordingly, within the critical V-set domain of Siglec-1, arginine 97 and tryptophans at positions 2 and 106 were identified as key residues interacting with sialic acid. Siglec-1 has a preference for *N*-acetylneurameric acid (Neu5Ac), the most abundant of the mammalian sialic acids, in α -2,3-linkage to D-galactose and does apparently not recognize Neu5Gc or Neu5Ac9Ac (17, 18). In line with these results, the sialylated carbohydrate headgroup of gangliosides constitutes the molecular recognition domain of HIV-1 particles as well as liposomes for human Siglec-1 (1). GM3 and possibly also GM2 gangliosides, all built of sialyl-lactose consisting of a sialic acid-D-galactose-D-glucose-trisaccharide linked to ceramide, appear to be critical for the HIV/Siglec-1 interaction (19, 20).

Reutter and co-workers and Bertozzi and co-workers (21, 22) identified biosynthetic engineering as an efficient tool to metabolically incorporate sialic acids with unnatural *N*-acyl side chains into cellular glycoconjugates. Synthetic *N*-acyl-modified D-mannosamines can be metabolized by the promiscuous sialic acid biosynthetic pathway and are incorporated into sialylated

cell surface glycoconjugates replacing ~10–85% of natural sialic acids (23). This approach has enabled studies on sialic acid modifications in their native environment on the surface of living cells (24–27) as well as *in vivo* (16), and it has been exploited to introduce chemically reactive ketone or azide groups (22, 28).

In this study we analyzed the role of the lectin receptor mSiglec-1, endogenously expressed on primary macrophages, for capture of MLV and *trans*-infection of primary lymphocytes *ex vivo*. Furthermore, we explored whether metabolic engineering of sialic acids in virus-producer cells using synthetic *N*-acyl-modified precursor analogs is a feasible approach to modulate sialyl-lactose-containing gangliosides in released MLV particles and, importantly, whether this method can be used to assess the impact of *N*-substituted sialic acids on the functional interaction of viruses with mSiglec-1.

Experimental Procedures

Cell Culture—Cell lines S1A.TB.4.8.2 (S1A.TB; T-cell lymphoma from BALB/c mice), ANA-1 (myelomonocytic cell line established from bone marrow cells of C57BL/6 (H-2^b) mice infected with J2 recombinant retrovirus for immortalization), L929 cells (NCTC clone 929, subcutaneous areolar and adipose tissue of a 100-day-old male C3H/An mouse, secreting M-CSF), and 293T cells (human embryonic kidney cells) were obtained from the American Type Culture Collection and cultivated under standard conditions in Dulbecco's modified Eagle's medium or RPMI 1640 medium supplemented with 10% fetal bovine serum, 1% penicillin/streptomycin, and 1% L-glutamine (all from Gibco). The hybridoma producing rat anti-MLV Gag p30 antibody R184 was a kind gift from Dr. Carol Stocking.

Primary Mouse Cells—The generation of Siglec-1 KO mice on a C57BL/6 background has been reported (8). To prepare bone marrow-derived macrophages (BMDM), mice were sacrificed, and femur and tibia were extracted; bone marrow cells were collected by centrifugation and cultivated overnight in complete RPMI 1640 medium. Next, cells were seeded in BMDM differentiation medium containing 25% L929 supernatant as a source of colony-stimulating factor. 2–3 days later, fresh L929 supernatant was added to the cultures. Cells were reseeded for an experiment 6 days after preparation. For some experiments, 500 IU/ml mouse interferon α (IFN α , PBL Assay Science) was added 2 days prior to the experiment. Spleen and lymph nodes were placed in cold RPMI 1640 medium and gently passed through a 100- μ m cell strainer. Cell suspensions were washed once in PBS, resuspended in complete RPMI 1640 medium, counted, and seeded in 96-well plates at a density of 5×10^6 cells/ml. In case of B- or T-cell activation, lipopolysaccharide (LPS, Sigma; 7.5 μ g/ml) or concanavalin A (ConA, Sigma, 2 μ g/ml) in combination with human interleukin 2 (IL-2, Biomol; 100 IU/ml) was added to the cultures.

Siglec-1 Genotyping—DNA was prepared from tail cuts of newborns using the DNeasy blood and tissue kit (Qiagen) according to the manufacturer's protocol for rodent tails. Following DNA extraction, a PCR, using allele-specific primers NEO (5'-CGTTGGCTACCCGTATTGC), SND1F3 (5'-CACCAAGGTCACTGTGACAA), and SND2R2 (5'-GGC-CATATGTAGGGTCGTCT), was performed in a thermocy-

cler (Eppendorf). PCR products were separated and visualized by agarose gel electrophoresis. The predicted sizes of diagnostic PCR products are as follows: WT(+/+), 495 bp; heterozygous(−/+), 495 and 204 bp; and homozygous KO(−/−), 204 bp.

Virus Preparation—The generation, production, and titration of MLV-GFP and MLV-Gag-GFP have been reported (29, 30).

Generation of MLV-GFP Particles in ManN Analog-treated 293T Cells—293T cells were seeded for virus production in the presence or absence of ManN analogs at non-toxic concentrations (5 mm for ManNAc, ManNProp, ManNBut, ManNiBut, ManNPent, and ManNCyclo or 0.3 mm for Ac₄ManNGc, Ac₄ManNAc, and Ac₄ManNProp). Peracetylated ManN derivatives were used to enhance membrane permeability. After entering the cell, the O-acetyl groups were cleaved by cytosolic esterases, releasing the active sialic acid precursors. After 5 days, cells were re-seeded and transfected with the MLV-GFP proviral plasmid. 4–6 h post-transfection, the medium was changed, and new ManN analogs were added. 48 h post-transfection, supernatants were collected, and viruses were purified by ultracentrifugation through a 20% sucrose cushion. All viral titers were determined on S1A.TB cells and identical titers were used in subsequent (*trans* or direct) infection experiments.

MLV Capture and Transfer Assays—To assess capture of MLV particles, L929-differentiated BMDM were incubated with MLV-GFP for 4 h at 37 °C and then washed extensively in PBS to remove unbound virus. BMDM were either analyzed for MLV p30^{Gag} expression by intracellular flow cytometry using rat anti-MLV Gag p30 antibody R184, an Alexa488-conjugated donkey anti-rat antibody (Invitrogen), and the cytofix/cytoperm protocol (BD Biosciences) or for cell-associated MLV RT activity using a SYBR Green I-based product-enhanced RT assay, as reported previously (31).

In transfer experiments assessing Siglec-1-dependent transfer of MLV particles from macrophages to lymphocytes, BMDM or ANA-1 cells were incubated with virus particles according to the description above (in case of antibody blocking, BMDM were treated with 10 μg/ml anti-mSiglec-1 mAb (clone 3D6.112) or an isotype control mAb (Aviva Systems Biology) for 30 min at 4 °C before virus pulse). After extensive washing, either activated splenocytes or S1A.TB cells were added and co-cultured with macrophages in a ratio of 1:1 for 48 h. S1A.TB cells were harvested and analyzed for GFP expression; splenocytes were stained using phycoerythrin-conjugated anti-mCD19 and allophycocyanin-conjugated anti-mCD3 antibodies (BD Biosciences) and were acquired on a FACSVerse flow cytometer (BD Biosciences) using the FACSuite software and analyzed using FlowJo Software (Tree Star, Inc.).

Pronase Treatment—MLV-exposed BMDM were washed extensively in PBS and treated with increasing concentrations of Pronase (Roche Applied Science) for 30 min at 4 °C. Heat-inactivated Pronase that had been boiled for 10 min served as a control for the enzymatic activity. After extensive washing in medium containing FBS, target cells were added and co-cultured with macrophages in a ratio of 1:1 for 48 h. As an additional control to ensure that the Pronase treatment of the BMDM did not have any effect on splenocyte infectivity *per se*,

a direct infection of LPS-activated splenocytes was carried out in BMDM supernatants that had been treated with Pronase, washed, and then incubated in medium for 1 h.

Immunofluorescence Microscopy—BMDM were seeded onto coverslips 1 day prior to the virus pulse. Washed cells were fixed in 4% paraformaldehyde/PBS for 30 min and then permeabilized with 0.1% Triton X-100/PBS for 2 min. Cells were blocked for 20 min in PBS containing 5% FCS, 0.1% BSA-c (Aurion), and 5% horse serum (Sigma). Cells were incubated with Alexa647-conjugated rat monoclonal anti-mouse Siglec-1 mAb 3D6.112 diluted in blocking buffer for 60 min at room temperature. Coverslips were mounted onto glass slides using DAPI mounting medium (Sigma). Epifluorescence images were acquired using a Nikon eclipse Ti-S microscope and the NIS-Elements imaging software. Acquired images were processed using ImageJ and Adobe Photoshop CS5.

Molecular Dynamics Simulations—Molecular dynamics simulations of Siglec-1 in complex with Neu5Ac, Neu5Gc, Neu5Prop, or Neu5But were performed in explicit solvent for 50 ns at 298 K using YASARA (29). The starting structures were built from the crystal structure of mouse Siglec-1 (PDB code 1OD7) by modifying the ligand using the YASARA graphical interface. Pressure control was performed by scaling the periodic simulation box to keep the water density at 0.997 g/liter. The AMBER03 (32) force field was used for the protein and GAFF parameters with AM1-BCC charges (33) for the carbohydrates. Long range Coulomb interactions were calculated using the Particle Mesh Ewald algorithm (34). Because the side chain of Arg-97 was flexible despite the presence of the ligand, a distance restraint of 100 newton/m was applied between the NH atoms of Arg-97 and the carboxylate oxygens of the ligands to maintain the hydrogen bonds. Simulation snapshots were recorded every 25 ps. The average interaction energy was calculated from all snapshots using a Yanaconda macro based on Equation 1,

$$E = \langle E(\text{receptor}) + E(\text{ligand}) - E(\text{receptor} + \text{ligand}) \rangle \quad (\text{Eq. 1})$$

where $E(\text{receptor})$ = potential energy of siglec-1; $E(\text{ligand})$ = potential energy of Neu5Ac, Neu5Gc, Neu5Prop, or Neu5But, respectively; $E(\text{receptor} + \text{ligand})$ = potential energy of the complex; $\langle \rangle$ means averaging over all snapshots.

The solvation energy was calculated using the boundary element method implemented in YASARA (29). The boundary between solvent (dielectric constant 78) and solute (dielectric constant 1) was formed by the latter's molecular surface, constructed with a solvent probe radius of 1.4 Å, and the following radii for the solute elements: polar hydrogens 0.32 Å; other hydrogens 1.017 Å; carbon 1.8 Å; oxygen 1.344 Å; nitrogen 1.14 Å; sulfur 2.0 Å. The solute charges were assigned based on the AMBER03 force field (32), using GAFF/AM1BCC (35) for the ligands.

Docking and Post-scoring—The receptor was prepared for docking using LeadIT 2.1.7 (BioSolveIT GmbH, Sankt Augustin, Germany) based on the crystal structure of mouse Siglec-1 (PDB code 1OD7). Neu5Ac, Neu5Gc, Neu5Prop, and Neu5But were minimized using YASARA (29) and docked using FlexX

N-Acyl Chain and Siglec-1-dependent MLV trans-Infection

(37). Ten poses were generated for each ligand and scored using SeeSAR (BioSolveIT GmbH, Sankt Augustin, Germany), which uses the HYDE scoring function (38).

Analysis of Modified Sialic Acids—Concentrations of total membrane-bound and glycolipid-bound sialic acids were measured by DMB-HPLC (39). Approximately 100,000 293T cells were cultured in DMEM (10% FBS, 2 mM L-glutamine, 2 mM sodium pyruvate) containing ManNAc or its analogs (5 mM ManNAc, 5 mM ManNProp, 5 mM ManNCyclo, 5 mM ManNBut, 0.3 mM Ac₄ManNAc, or 0.3 mM Ac₄ManNGc). The medium was renewed on day 5. After 7 days the cells were harvested and homogenized by sonication in ice-cold lysis buffer (150 mM NaCl, 10 mM Tris, 5 mM EDTA, 1 mM PMSF, 40 μM leupeptin, 1.5 μM aprotinin, pH 8.0) (40). A stepwise chloroform/methanol precipitation was performed on half of each sample to extract the glycolipid fractions (41). Membrane fractions were isolated from the remaining cell lysates by centrifugation at 21,000 × g and 4 °C for 2 h. Protein concentrations in the supernatants (representing the cytosolic compartment) were measured using the bicinchoninic acid assay (BCA, Pierce). All membrane and glycolipid fractions were hydrolyzed with 1 M trifluoroacetic acid (TFA) for 4 h at 80 °C, as described previously (42). Hydrolyzed samples were dried and subsequently dissolved in 5 μl of TFA (120 mM). Samples were labeled for 2 h at 56 °C with 30 μl of DMB solution (6.9 mM DMB, 0.67 mM β-mercaptopethanol, 0.19% sodium bisulfite).

Labeled samples were analyzed on an Agilent 1200 HPLC system using a Gemini-NX C18 column (110 Å, 3 μm particle size, 4.6 × 150 mm, Phenomenex). Probes were separated at 0.5 ml/min flow rate with methanol/acetonitrile/water (6:8:86) as eluent. The detector was configured with 373 nm for excitation and 448 nm for emission. To quantify the occurring sialic acid species, DMB-labeled standards were injected: Neu5Ac (Sigma), Neu5Gc (a gift from R. Schauer, University of Kiel), and Neu5But (a gift from C. R. Bertozzi, Stanford University). Concentrations of Neu5Prop and Neu5Cyclo were estimated according to the Neu5Ac standard. Unlabeled standards and HPLC retention peaks of interest were further analyzed by LC-electrospray-ionization mass spectrometry (ESI-MS). Therefore, 20 μl of collected sample or 500 ng of the respected standard dissolved in H₂O were injected into an Agilent 1100 series LC/MSD system with 79.9% methanol, 20% isopropyl alcohol, and 0.1% formic acid as eluent, 0.5 ml/min flow rate, 4 kV capillary voltage, and 350 °C capillary temperature.

Statistical Analyses—Plotting of graphs and general statistical analyses were performed using the GraphPad Prism 5 software package (GraphPad Software Inc., La Jolla, CA). This software was also used to calculate Pearson correlation coefficients and significance values by applying the two-tailed, unpaired Student's *t* test.

Results

Mouse Siglec-1 Is Expressed on Macrophages, Up-regulated by IFNα, and Mediates MLV trans-Infection of Lymphocytes—To explore the expression of Siglec-1 on the cell surface of mouse macrophages, macrophage cell line ANA-1 and primary BMDM were stained with either rat anti-mouse Siglec-1 mAb 3D6.112 or an isotype control mAb and processed for flow

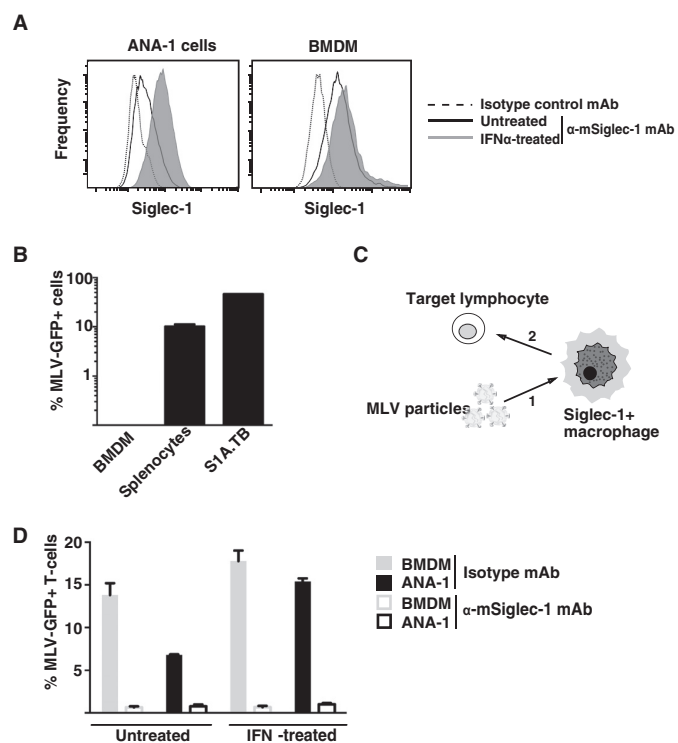


FIGURE 1. Siglec-1 is expressed on mouse macrophages in an IFNα-responsive manner and supports MLV trans-infection. *A*, ANA-1 cells or BMDM were stimulated with mouse IFNα (500 units/ml) for 48 h or left untreated. Mechanically detached cells were stained using a phycoerythrin-conjugated anti-mSiglec-1 mAb or an isotype control mAb and analyzed by flow cytometry. Shown are untreated cells (black lines) or IFNα-treated cells (shaded histograms) stained for mSiglec-1 and untreated cells (dotted line) stained with the isotype mAb. *B*, each of the indicated cell types was infected with MLV-GFP (m.o.i. 0.1) and 2 days later analyzed for GFP expression, indicative of productive infection, by flow cytometry. *C*, experimental setup for assessment of MLV trans-infection. 1, addition of MLV particles to macrophages; 2, addition of target lymphocytes to macrophage culture. *D*, BMDM or ANA-1 cells were stimulated with mouse IFNα (500 units/ml) for 48 h or left untreated. Cells were preincubated with an anti-Siglec-1 mAb or an isotype control mAb at 4 °C, exposed to MLV-GFP (m.o.i. 0.1) for 4 h at 37 °C, and washed three times in PBS. S1A.TB cells were then added in a 1:1 ratio to the virus-pulsed macrophage cultures for 48 h and then analyzed for GFP expression by flow cytometry. Data are expressed as the arithmetic means ± S.D. of triplicate samples from one mouse and are representative of at least two experiments each performed using 2–3 mice.

cytometry. Cells that had either been left untreated or exposed to mouse IFNα for 48 h were analyzed. ANA-1 cells expressed low constitutive levels of Siglec-1 on the surface, the expression of which could be induced 3-fold by IFNα stimulation (Fig. 1*A*). BMDM expressed markedly higher constitutive levels but also INFα-responsive levels of the sialic acid-binding Ig-like receptor on their cell surface (Fig. 1*A*).

For studies on direct infection or *trans*-infection, we employed a replication-competent ecotropic Moloney MLV carrying an IRES-egfp element (MLV-GFP) (67) that had been produced in human 293T cells. The GFP reporter encoded by this recombinant retrovirus is expressed only upon productive infection of target cells. We first characterized the susceptibility of the cell lines and primary cells used in this study for direct, productive MLV-GFP infection. Virus exposure of the S1A.TB.4.8.2 (S1A.TB) T-cell lymphoma or LPS-activated primary mouse splenocytes demonstrated their high level susceptibility, although BMDM were non-permissive (Fig. 1*B*). The

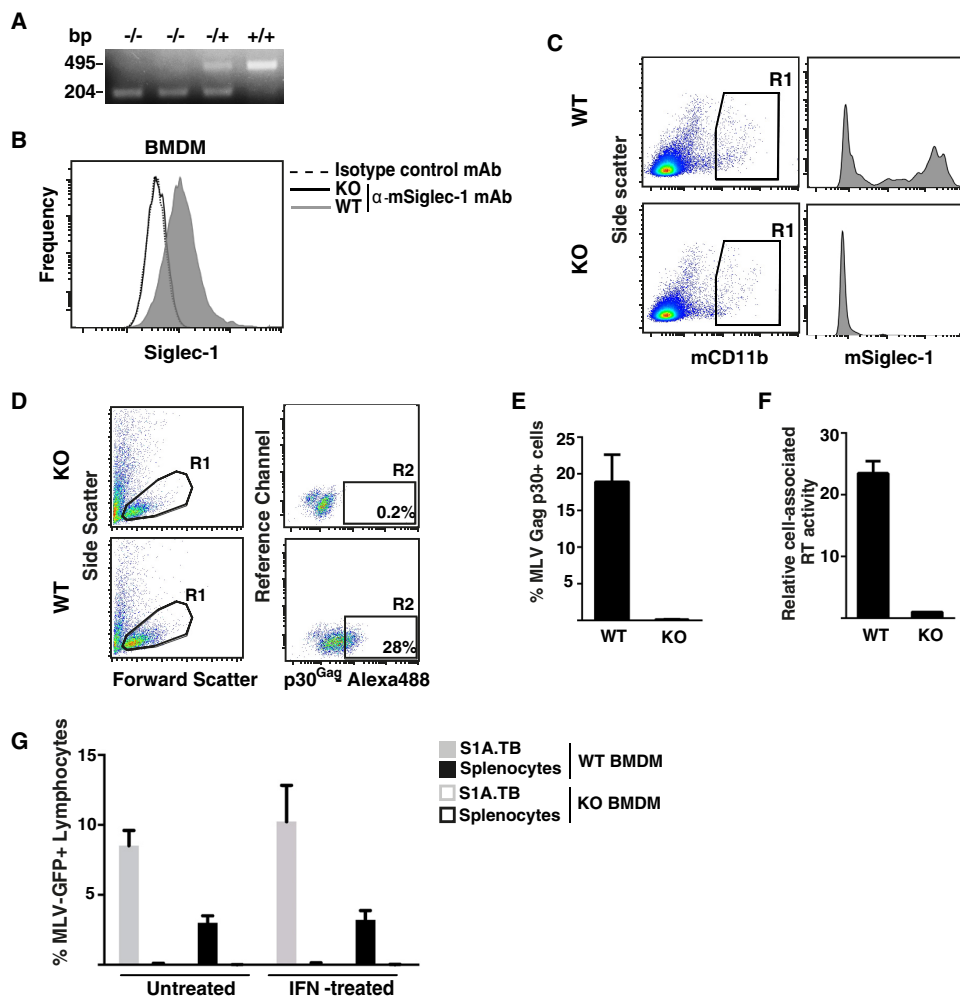


FIGURE 2. BMDM from WT, but not from Siglec-1 KO mice, support MLV capture and trans-infection. *A*, genotyping of KO and heterozygous mice by PCR. DNA extracted from mouse tails was amplified using an allele-specific PCR. Product sizes of 495 or 204 bp are diagnostic for the WT and KO allele, respectively. *B* and *C*, Siglec-1 phenotyping of KO and WT mice. L929-differentiated BMDM (*B*) or freshly isolated, mechanically disrupted inguinal lymph nodes (*C*) were stained for mSiglec-1 surface expression (in *C*, co-stained for mCD11b) and analyzed by flow cytometry. *B*, shown are WT-BMDM (shaded histogram) or KO-BMDM (black line) stained for mSiglec-1 and WT-BMDM (dotted line) stained with the isotype mAb. *D–G*, BMDM from WT and KO mice were exposed to MLV-GFP for 4 h at 37 °C and subsequently washed three times with PBS. *D* and *F*, MLV-GFP-pulsed BMDM were detached and analyzed for MLV capture by two methods. *D*, first, pulsed cells (m.o.i. 0.5) were fixed, permeabilized, and stained with rat anti-p30^{Gag} mAb followed by an Alexa488-conjugated secondary antibody. *D*, dot plots from flow cytometric analyses depicting (*left panels*) the forward and side scattering of light to identify live cells (gate R1) and (*right panels*) Alexa488 staining to identify cell-associated MLV p30^{Gag} (gate R2) are shown. The percentage of viable, p30^{Gag}⁺ cells within R2 is indicated. *E*, chart bars depict the arithmetic means \pm S.D. of the percentage of p30^{Gag}-positive cells from triplicates. *F*, second, pulsed cells (m.o.i. 0.1) were detached, lysed, and analyzed for cell-associated RT activity. *G*, MLV-GFP-pulsed BMDM were co-cultivated with LPS-activated splenocytes or S1A.TB cells at a 1:1 ratio. 48 h later, lymphocytes were analyzed for GFP expression by flow cytometry. Data are expressed as the arithmetic means \pm S.D. of triplicate samples from one KO and one WT mouse and are representative of at least two experiments each performed using 2–3 mice.

inability of MLV to infect non-cycling macrophages is well established (43, 44) and an important characteristic to unambiguously assess their role as a virus donor in MLV trans-infection of lymphocytes in this study.

To explore the ability of mouse macrophages to capture and trans-infect target cells with MLV-GFP in a Siglec-1-dependent manner, BMDM or ANA-1 cells were first pretreated for 30 min at 4 °C with blocking anti-Siglec-1 or isotype control mAbs, then exposed to MLV-GFP particles for 4 h at 37 °C, washed extensively, and subsequently co-cultured with target S1A.TB lymphoma cells (Fig. 1*C*). Two days later, the percentage of GFP-positive S1A.TB cells was analyzed by flow cytometry as a quantitative readout for the efficiency of trans-infection. ANA-1 cells and BMDM, which had been pretreated with an isotype control mAb, mediated a robust MLV-GFP trans-infec-

tion (Fig. 1*D*). Their capacity for trans-infection was increased by IFN α pretreatment (Fig. 1*D*), and this effect largely correlated with their Siglec-1 surface levels (Fig. 1*A* and data not shown). Importantly, MLV trans-infection was efficiently and specifically blocked when macrophages were pretreated with the anti-mouse Siglec-1 mAb 3D6.112 (Fig. 1*D*). Thus, Siglec-1 on the cell surface of BMDM is constitutively expressed, IFN α -responsive, and has the capacity to mediate trans-infection of the retroviral pathogen MLV to permissive lymphocytes.

BMDM from Wild-type, but Not from Siglec-1 KO Mice, Support MLV Capture and trans-Infection—To further corroborate the role of mSiglec-1 in MLV trans-infection, we employed Siglec-1 KO mice (8). The genotype of mice was determined using an allele-specific PCR (Fig. 2*A*). The absence of Siglec-1 expression in KO mice carrying the homozygous(−/−) dele-

N-Acyl Chain and Siglec-1-dependent MLV trans-Infection

tion was demonstrated in cultured BMDM (Fig. 2B) and mCD11b-positive cells of the monocyte/macrophage lineage in a freshly isolated lymph node suspension (Fig. 2C), in line with previous characterizations (45).

In a comparative assessment of Siglec-1 KO and wild-type (+/+, WT) mice, we quantified Siglec-1-dependent capture of MLV particles by BMDM. Two experimental approaches were taken; BMDM from WT and KO mice were incubated with MLV for 4 h at 37 °C, washed with PBS, detached by gentle scraping, and processed for detection of either cell-associated MLV p30^{Gag} structural protein or cell-associated reverse transcriptase (RT) activity. For the first approach, BMDM were fixed, permeabilized, and stained using a rat anti-p30^{Gag} mAb. Although flow cytometric analysis of MLV-exposed KO-BMDM showed only background staining (Fig. 2, D, upper panel (gate R2), and E), BMDM from WT littermates revealed a robust signal for the p30^{Gag} capsid staining (Fig. 2, D, lower panel (gate R2), and E).

For the second approach, BMDM were lysed and processed for a SYBR Green I-based product-enhanced RT assay, a method previously developed for the quantitation of retroviruses in culture supernatants (31, 46). MLV exposure of WT-BMDM, but not of KO-BMDM, resulted in a significant cell-associated RT activity (Fig. 2F).

Next, BMDM derived from WT and KO mice were analyzed side-by-side for their capacity to mediate MLV *trans*-infection. In line with the above antibody-blocking studies (Fig. 1D), WT-BMDM efficiently *trans*-infected S1A.TB T-lymphocytes and LPS-stimulated splenocytes (Fig. 2G). In contrast, KO-BMDM were unable to support MLV *trans*-infection, and IFN α stimulation could not overcome this limitation (Fig. 2G). Together, these results demonstrate that primary macrophages from mice are capable of capturing infectious MLV particles and of mediating a subsequent *trans*-infection of lymphocytes in a Siglec-1-dependent manner.

MLV-GFP trans-Infection Is an Efficient Process That Preferentially Targets Primary Activated B-cells—Next, we sought to assess the relative contribution of direct infection as compared with *trans*-infection to the overall infection of cultured primary lymphocytes in the context of a constant multiplicity of infection. Moreover, we tested the impact of two activation protocols for splenocyte cultures, *i.e.* treatment with either LPS or ConA/IL-2, which preferentially stimulate the proliferation of B-cells and T-cells, respectively (47, 48), on the MLV-GFP susceptibility of lymphocytes under these conditions.

WT splenocyte cultures following LPS activation for 3 days consisted of 64% CD19-positive and 31% CD3-positive cells, expressed as fractions within the viable lymphocyte gate (Fig. 3A, left lower panel). In contrast, stimulation with ConA/IL-2 resulted in 97% CD3-positive T-cells (Fig. 3B, left lower panel). Two interesting observations were made. First, in the absence of BMDM (“splenocytes only”), only LPS stimulation allowed for a robust direct infection of WT splenocytes ($4.0 \pm 0.8\%$, Fig. 3C), the vast majority of which were blasted CD19-positive B-cells (99.8%, data not shown). In comparison, the low level infection of the ConA/IL-2-stimulated culture ($0.2 \pm 0.08\%$, Fig. 3C) represented both T-cells (63%) and B-cells (24%) (data not shown). Second, the experimental setup, in which WT splenocytes (targets for both direct and *trans*-infection) and

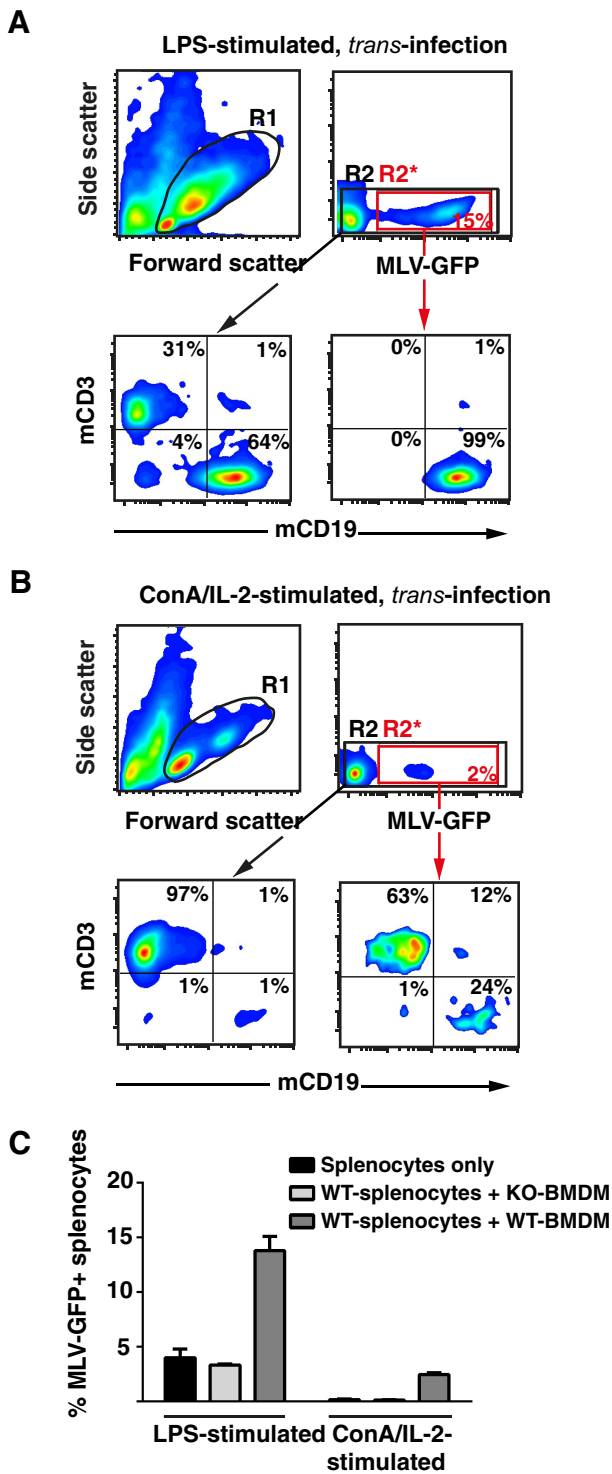


FIGURE 3. BMDM-mediated trans-infection of MLV-GFP efficiently targets activated primary B-cells. Splenocytes from WT mice were activated with either LPS (A) or ConA/IL-2 (B) for 3 days and then seeded either alone or onto BMDM from WT or KO mice in a ratio of 1:1. Cultures were challenged with MLV-GFP (m.o.i. 0.2) and splenocytes analyzed for GFP expression 48 h later by flow cytometry. A and B, effect of activation protocols, and the identity of MLV-GFP-infected splenocytes was determined by co-staining for the lineage markers CD3 (T-cells) and CD19 (B-cells). R1 identifies the viable cells. R2* (red box) identifies the MLV-GFP-positive cells and R2 (black box) all viable cells. Dots plots in the lower panels depict the respective mCD3/mCD19 stainings. C, chart bars depict the arithmetic means \pm S.D. of the percentage of GFP-positive, viable cells from analyses performed in triplicate. Experiments were performed using 2–3 KO or WT mice and were repeated at least twice showing similar results.

BMDM (donor cells for *trans*-infection) were present in the culture at the time of virus addition, revealed that WT-BMDM, but not KO-BMDM, were able to markedly boost the overall infection level of lymphocytes, respectively (Fig. 3C). For LPS-stimulated splenocytes, the co-culture with WT-BMDM raised the percentage of GFP-positive lymphocytes to $14.0 \pm 1.3\%$, representing a 3–5-fold increase over the conditions with splenocytes alone or co-culture with Siglec-1-deficient BMDM (Fig. 3C). Virtually all infected cells were CD19-positive B-cells (Fig. 3A, *lower right panel*). Remarkably, co-culture with WT-BMDM resulted also in a notable infection of ConA/IL-2-activated splenocytes translating to a 15-fold enhancement over the reference conditions (Fig. 3C) with both T-cells and B-cells being infected (Fig. 3B). Collectively, these results indicate that Siglec-1-dependent *trans*-infection via macrophages may contribute to a more efficient infection process of lymphocytes in the context of a limited number of infectious MLV particles. Moreover, activated primary B-cells appear to be a preferential target of direct infection as well as *trans*-infection of MLV.

Mouse Siglec-1 and MLV Gag Partially Co-localize Early after Virus Exposure—Next, we investigated the fate of Siglec-1 and MLV in BMDM early and late after virus exposure by co-immunofluorescence microscopy and *trans*-infection analysis. BMDM derived from WT or KO mice were pulsed with either MLV-GFP or MLV-Gag-GFP for 4 h at 37 °C and then extensively washed. The latter virus carries Gag-GFP fusion proteins within the particle.

BMDM cultured on coverslips were either fixed immediately after pulse (“4 h”) or cultivated for another 20 h (“24 h”) and stained with antibodies to mSiglec-1. At the 4-h time point, mSiglec-1 and Gag-GFP partially co-localized in distinct punctae in WT-BMDM (Fig. 4A, *upper and middle panels*). Here, two phenotypes were frequently observed. A dominant single accumulation of the mSiglec-1 receptor and the viral structural protein was observed in 69% of cells (Fig. 4, A (*upper panels*) and B), resembling the sac-like compartment reported for human Siglec-1 and HIV p24^{Gag} in myeloid dendritic cells (1, 34). In 31% of BMDM, a more scattered cytoplasmic localization of Siglec-1 and Gag-GFP was noted with up to 100 distinct punctae, in which signals for both proteins partially overlapped (Fig. 4, A (*middle panels*) and B). No co-localization of the mSiglec-1/Gag-GFP-positive punctae with a marker for acidic lysosomes was observed (data not shown). BMDM from KO mice displayed only background staining for mSiglec-1 and at most a few small Gag-GFP signals (Fig. 4A (*lower panels*)). Interestingly, at 24 h, the frequency and intensity of the punctae for both mSiglec-1 and Gag-GFP in WT-BMDM were strongly diminished (Fig. 4C).

In parallel to the microscopic analyses, we assessed the ability of BMDM to *trans*-infect S1A.TB cells immediately after the virus pulse (4 h) and after the prolonged storage period of 24 h. Remarkably, delayed addition of target T-cells at only 24 h resulted in a drastic drop in the efficiency of *trans*-infection, levels of 2% compared with the condition in which the S1A.TB cells had been added to the BMDM at the 4-h time point (Fig. 4D). Similarly, levels of cell-associated RT activity were also found to be drastically decreased at the 24-h time point (Fig. 4E). Of note, neither the loss of capsid signal in immunofluo-

rcence nor the drop in *trans*-infection could be rescued by pretreating the BMDM with proteasomal or lysosomal inhibitors at non-toxic concentrations (data not shown). In conclusion, mSiglec-1 and MLV Gag partially co-localize in BMDM early after virus exposure. Within 24 h, the detection of the viral structural protein is greatly diminished coinciding with a marked reduction in the ability of pulsed BMDM to *trans*-infect.

Mainly Surface-bound MLV Particles *trans*-Infect Lymphocytes—To investigate whether the MLV particles responsible for *trans*-infection are internalized into BMDM or are still accessible at the cell surface, we used short term proteolytic digestion to remove surface-bound particles after virus pulse. We found that BMDM that had been treated with Pronase, a protease mixture that digests extracellular proteins, including viral proteins, transferred considerably less MLV particles than untreated BMDMs (Fig. 4F). The reduction was dependent on the Pronase concentration, while BMDM viability was not affected. As controls of specificity, boiled Pronase had no effect on *trans*-infection (Fig. 4F), and supernatants from Pronase-treated and subsequently washed BMDMs, which had not been exposed to MLV, did not affect the ability of MLV-GFP for direct infection of target lymphocytes (Fig. 4G). Collectively, these results indicate that MLV particles that are captured by Siglec-1-positive macrophages and that are responsible for *trans*-infection remain surface-bound and are not internalized into a strictly “intracellular” compartment in BMDM.

Detection of Biosynthetically Modified Sialic Acids in Glycolipids and Glycoproteins in Cells Pretreated with N-Acyl-modified D-Mannosamines—We then sought to functionally explore the role of sialic acid for the Siglec-1-dependent *trans*-infection of MLV at a submolecular level in living cells by employing metabolic glycoengineering (23, 49). This experimental approach is based on the established ability of synthetic *N*-substituted D-mannosamine (ManN) derivatives to act as metabolic precursors for sialic acids with structurally altered *N*-acyl side chains incorporated into cellular glycoconjugates, including sialylated gangliosides that are incorporated into budding retroviruses (50, 51).

We first pretreated 293T cells with six different synthetic *N*-acyl-modified ManN analogs (Fig. 5A) or the most common physiological precursor, *N*-acetyl ManN (ManNAc), for 5 days at non-toxic concentrations. For two analogs (ManNProp and ManNGc) and ManNAc also, peracetylated (Ac4) derivatives were used, which facilitate the cellular uptake of the compounds and therefore require considerably lower concentrations for treatment. Subsequently, re-seeded cells were transfected with MLV-GFP proviral DNA and cultivated in the presence of the respective ManN derivatives for 2 more days. Released MLV-GFP particles were concentrated and purified by ultracentrifugation through a sucrose cushion.

As quality controls for analysis, ESI-MS was used to determine the purity of the sialic acid standards (Fig. 5B), and the presence of the DMB-labeled sialic acid species was verified in the collected retention peaks (Fig. 5C). Chromatograms of glycolipid-bound (Fig. 6A) and total membrane-bound (data not shown) sialic acids were used to quantify their respective concentrations. Alterations of the sialylation pattern of the cells

N-Acyl Chain and Siglec-1-dependent MLV trans-Infection

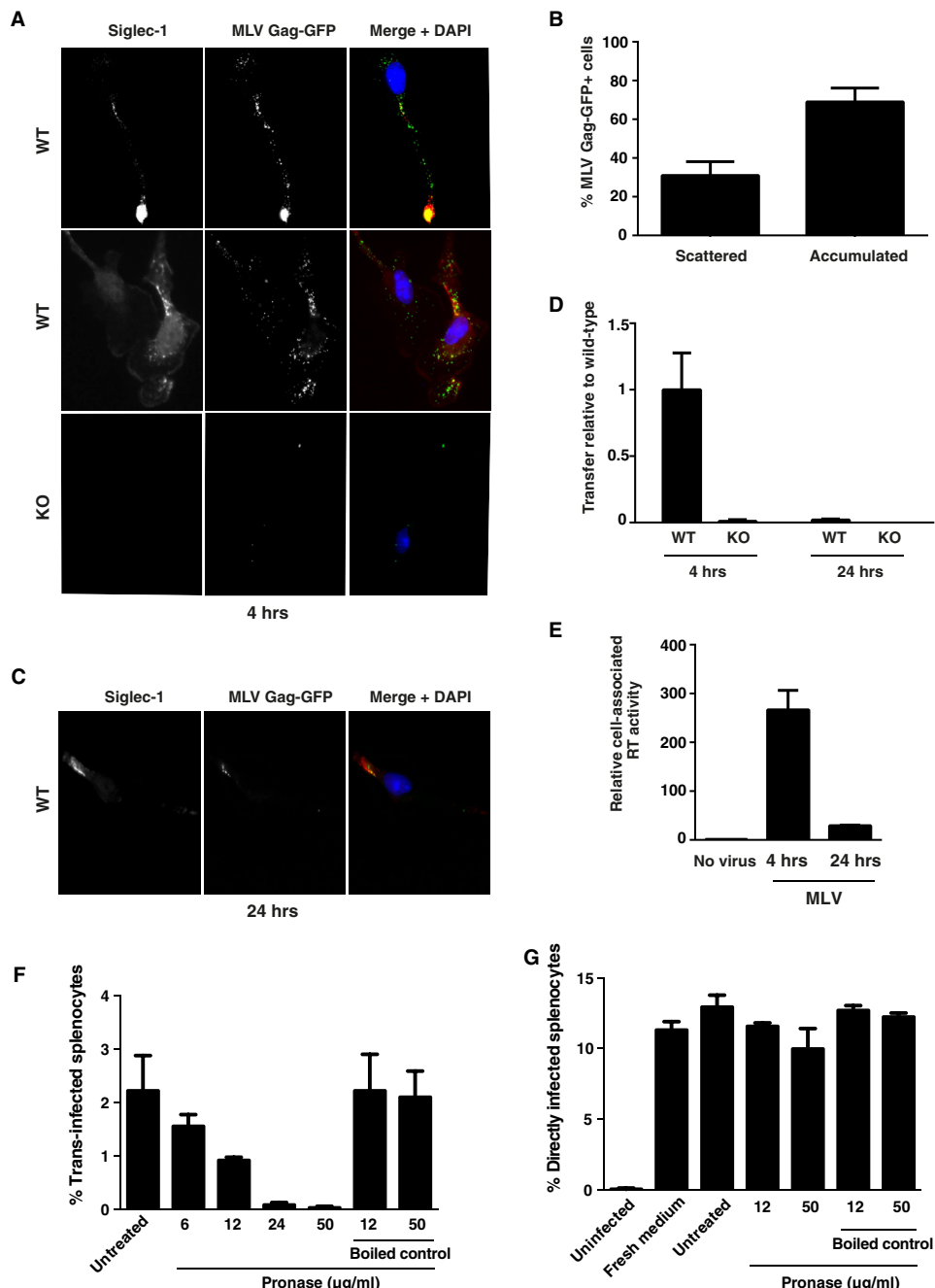


FIGURE 4. Captured MLV particles partially co-localize with Siglec-1 in BMDM early after virus exposure, and surface-bound MLV is the primary source for trans-infection. BMDM derived from either WT or KO mice were pulsed with MLV Gag-GFP, which carries a Gag-GFP fusion protein (A–C), or MLV-GFP, for 4 h at 37 °C (D and E). PBS-washed BMDM were either co-cultivated with S1A.TB-cells added either immediately after washing (4 h) or 20 h later (24 h) (D) or fixed, permeabilized, and stained using an Alexa647-conjugated anti-Siglec-1 mAb (A–C). Representative images for a dominant single accumulated MLV Gag/Siglec-1 signal (A, upper panels, 4 h) or multiple scattered puncta from WT-BMDM (A, middle panels, 4 h) are shown. A, bottom panel, images of MLV-Gag-GFP-pulsed KO-BMDM stained for mSiglec-1. B, MLV Gag pattern ("scattered" or "accumulated") and frequency of WT-BMDM displaying this phenotype were quantified. At least 70 cells from each of three mice were analyzed. E, cell-associated RT activity was quantified using SG-PERT, and values are depicted as activity associated with WT cells relative to KO cells. F and G, BMDM were pulsed with MLV-GFP for 4 h at 37 °C. PBS-washed BMDM were treated with increasing concentrations of cleavage-competent active Pronase for 30 min at 4 °C. After Pronase inactivation through washes in FBS-containing medium, cells were co-cultured with LPS-activated splenocytes for assessment of trans-infection. F, BMDM, in the absence of MLV, were treated as in G, then washed with PBS, and cultivated for 1 h more at 37 °C. These culture supernatants were then mixed with MLV-GFP to assess their potential impact on direct MLV-GFP infection of splenocytes.

were noted for all treatment conditions, both in the total membrane fraction (glycoproteins and glycolipids) and in the glycolipid fraction alone (Fig. 6, A and B). Growth of 293T cells in the presence of either synthetic ManNProp, ManNCyclo, ManN-But, or AcManNGc resulted in the detection of unnatural sialic

acid carrying the corresponding N-acyl substitution. Both the overall concentration of N-acyl-modified sialic acids (Fig. 6B) and their abundance relative to Neu5Ac varied considerably; Neu5But represented 23% of all sialic acids in the total membrane fraction and 48% in the glycolipid fraction of ManNBut-

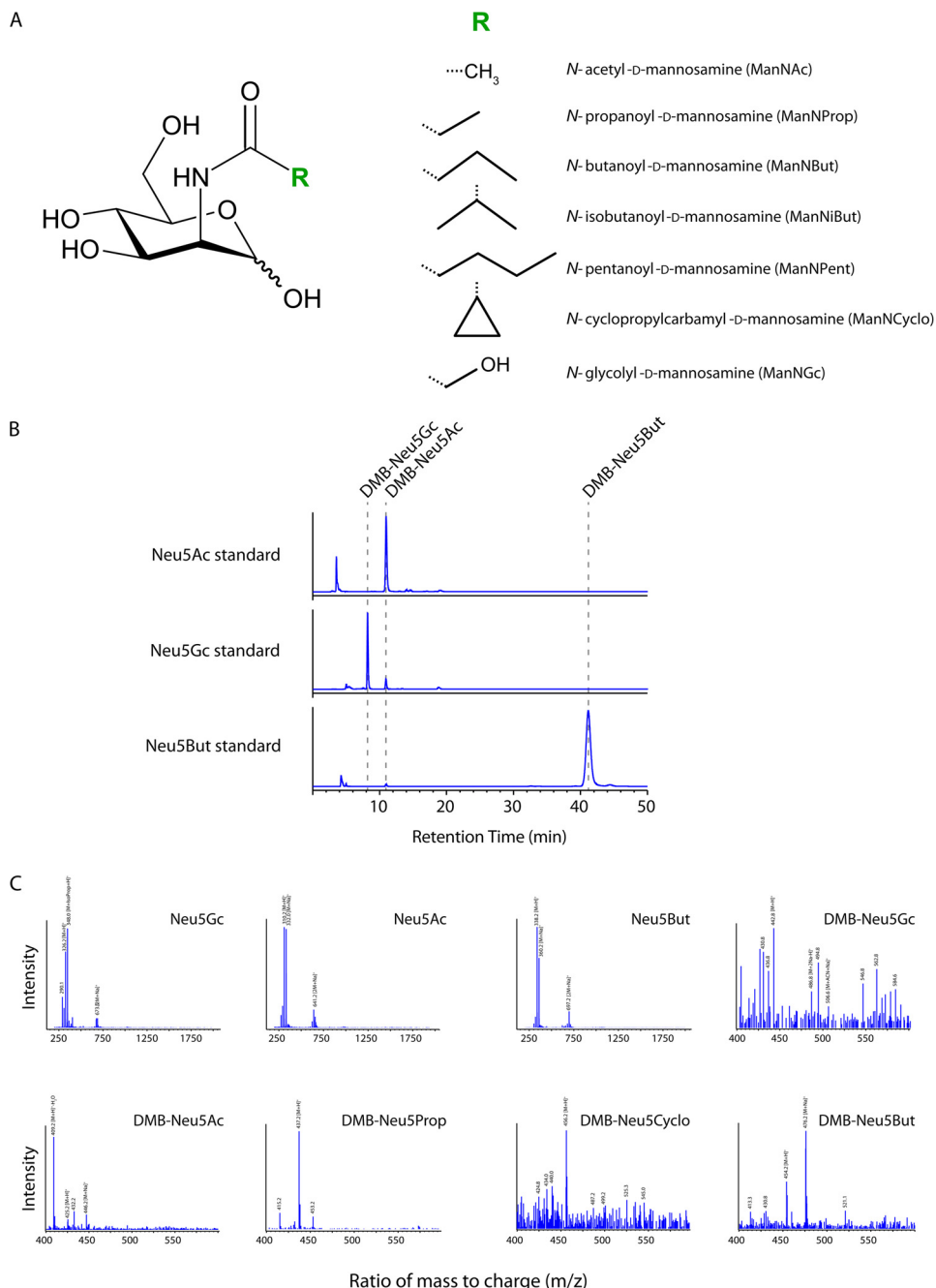


FIGURE 5. Biosynthetic modification of the N-acyl side chain of sialic acids in glycoconjugates of ManN analog-treated virus producer cells. *A*, schematic representation of ManNAc and the applied *N*-substituted ManNs with *R* indicating the modified *N*-acyl group. *B*, representative chromatograms of DMB-labeled sialic acid standards. Retention times (dashed lines) and peak areas of the sialic acid standards were determined after injecting 30 ng of the respected DMB-labeled species into the HPLC system. *C*, mass spectra of standards and DMB-labeled sialic acid species found in the lysates of 293T cells treated with different ManN derivatives. HPLC retention peaks were collected and subsequently analyzed by ESI-MS. 20 μ l of the collected retentions peaks or 500 ng of the respected standard dissolved in H_2O were injected into the LC-MSD system. DMB labeling of sialic acids leads to an increase in the molecular mass of 116.2 Da. Masses of the different sialic acid species are depicted, partly with common adducts. ACN, acetonitrile; IsoProp, isopropyl alcohol.

treated cells. In ManNProp-treated cells, Neu5Prop comprised 76% of the detected sialic acids in the total membrane fraction and 83% in the glycolipid fraction. Representing the most drastic change in sialic acid composition, 91 or 93% of all sialic acids in ManNCyclo-pretreated cells were identified to be Neu5Cyclo in the total membrane or glycolipid fraction, respectively (Fig. 6, *A* and *B*). Overall, there was a trend toward a higher abundance of biosynthetically modified sialic acids in the glycolipid fraction alone as compared with

the total membrane fraction. As a side note, small amounts of Neu5Gc, which is normally not found in human cells (52), were also detected in some of the cells that had not been pretreated with synthetic Ac₄ManNGc (Fig. 6, *A* and *B*). This most likely occurred through a salvage pathway that recruits Neu5Gc from fetal bovine serum sialoglycoconjugates in the media (53). Thus, addition of *D*-ManN analogs carrying *N*-acyl substitutions to cultured 293T cells for several days prior to their use as MLV producer cells resulted in the bio-

N-Acyl Chain and Siglec-1-dependent MLV trans-Infection

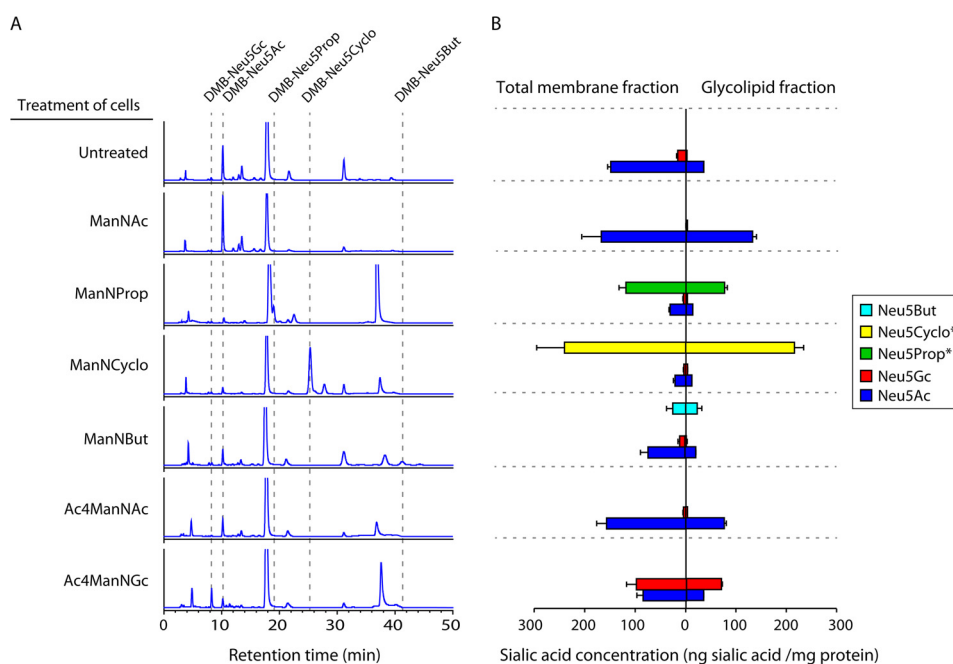


FIGURE 6. High level detection of biosynthetically modified sialic acids in glycoconjugates of N-acyl-modified ManN-treated virus producer cells. *A* and *B*, characterization and quantification of glycolipid-bound sialic acids by DMB-HPLC. 293T cells were treated for 7 days with the respective ManN derivatives. A medium change was performed on day 5. To calculate the concentrations of the occurring sialic acid species, retention peak areas of interest were compared with the retention peak areas of standards (Fig. 5C and data not shown) and normalized to the cytosolic protein concentrations of the respective cell lysates. Internal standards were used for Neu5Ac, Neu5Gc, and Neu5But (Fig. 5B). Concentrations of Neu5Prop and Neu5Cyclo were estimated according to the Neu5Ac standard (*). *B*, data shown represent the mean values and S.D. of two independent experiments ($n = 2$).

synthetic incorporation of up to 93% of unnatural sialic acid in cellular glycoconjugates.

Biosynthetic Modulation of the N-Acyl Side Chain of Sialic Acid in Virus Producer Cells Affects the Ability of Released MLV Particles for Siglec-1-dependent Capture and trans-Infection—

The preparations of MLV-GFP particles released from ManN analog-pretreated 293T cells were first titered on S1A.TB T-cells, the binding and infection process of which is mediated by the mCAT-1 receptor in a sialic acid-independent manner (54).

Employing our standard experimental setup, these MLV-GFP particle preparations were assessed for their functionality to be captured by Siglec-1-positive WT-BMDM and to *trans*-infect S1A.TB T-cells. In parallel, the inocula of the different MLV-GFP stocks were used to infect S1A.TB T-cells directly (Fig. 7A), confirming that comparable infectious titers had indeed been applied.

Striking functional differences were, however, observed for virus capture by BMDM and *trans*-infection. First, MLV-GFP particles released from 293T cells pretreated with *N*-butanoyl, *N*-isobutanoyl, *N*-glycolyl, or *N*-pentanoyl-modified sialic acid precursor analogs were only inefficiently captured by BMDM, whereas ManNProp or ManNCyclo treatments had no or only slight effects (Fig. 7, *B–D*). Levels of cell-associated MLV p30^{Gag} staining and cell-associated RT activity were reduced by up to 92% (Fig. 7, *B* and *C*) and these readouts for virus capture strongly correlated with each other (Fig. 7*E*, $r = 0.91$, $p = 0.0008$).

Second, in support of a cardinal role of virus capture for the efficiency of subsequent *trans*-infection, levels of MLV-GFP infection in S1A.TB cells were markedly reduced for viruses

derived from producer cells exposed to the *N*-butanoyl, *N*-isobutanoyl, *N*-glycolyl, or *N*-pentanoyl ManNs (Fig. 7*D*), and these infection levels correlated with both readouts for virus capture (Fig. 7, *F* and *G*).

Taken together, these results indicate that biosynthetic engineering of glycoconjugates in virus-producer cells is a feasible strategy to alter the composition of sialylated glycolipids and glycoproteins within the envelope of viruses that bud from the plasma membrane allowing their functional characterization. Specifically, this approach allowed us to identify the *N*-acyl side chain of sialic acid as a critical determinant for the interaction of MLV particles with mSiglec-1 in a native environment.

Molecular Modeling of Siglec-1 in Complex with Sialic Acid Derivatives Suggests Altered Interaction Affinities for Specific N-Acyl Side Chain Modifications—To further explore and possibly rationalize the impact of some of these *N*-acyl side chain modifications on the interaction with mSiglec-1, molecular modeling studies were carried out based on the crystal structure of the N terminus of the mouse receptor complexed with ME-A-9-*N*-(naphthyl-2-carbonyl)-amino-9-deoxy-Neu5Ac (PDB code 1OD7). Three-dimensional models of mSiglec-1 in complex with Neu5Ac, Neu5Gc, Neu5Prop, and Neu5But were generated. Notably, all ligands could be accommodated in the binding site without steric clashes (Fig. 8*A*).

Based on these structures two different computational methods were applied to model an influence of the *N*-acyl side chain modifications on the binding affinity. In a molecular dynamics (MD)-based approach, the relative binding strength of the ligands was estimated by calculation of the average potential interaction energy between mSiglec-1 and the respective ligand (Fig. 8*B*, *1st column*). The estimation of the binding free energy

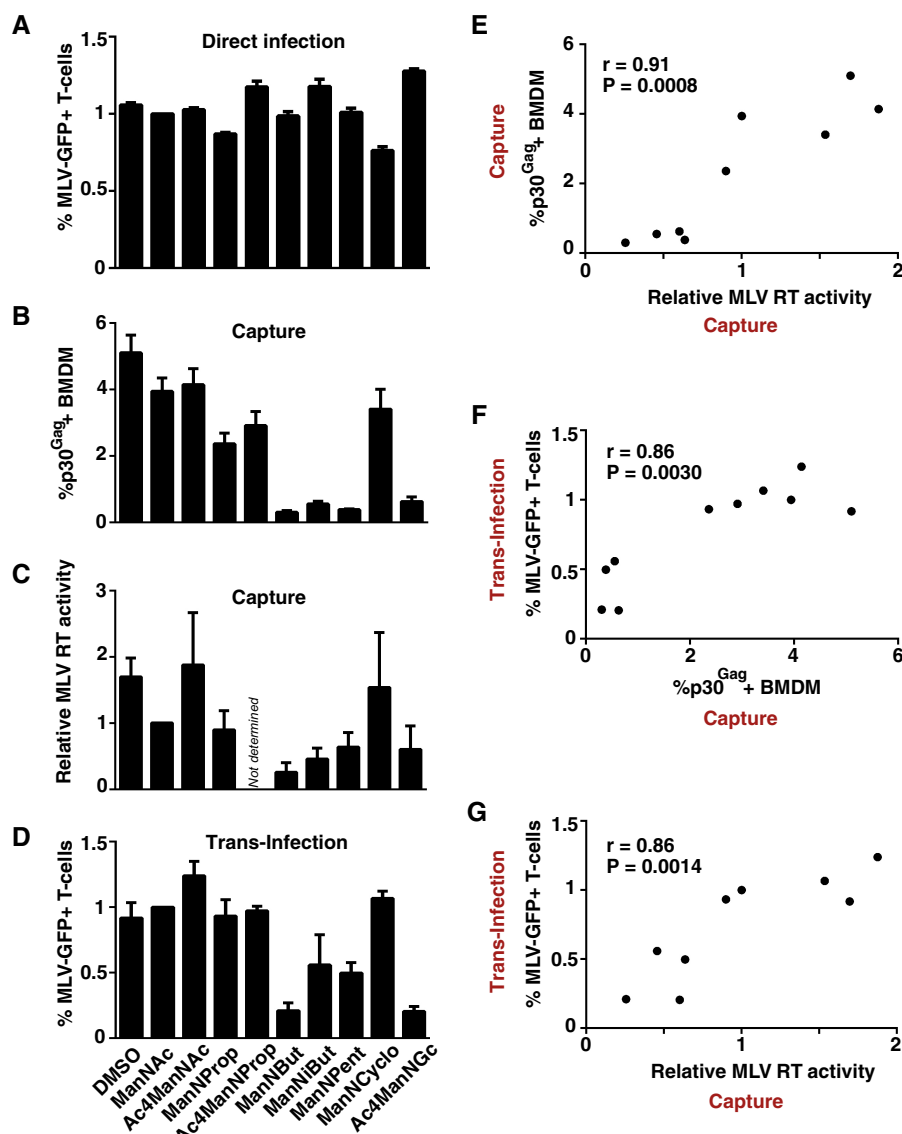


FIGURE 7. Diminished capture and transfer of MLV particles derived from producer cells carrying specific N-acyl-substituted sialic acids. *A*, S1A.TB cells were directly infected with MLV-GFP stocks (m.o.i. 0.1) produced in the absence or presence of the indicated ManN analogs and analyzed 2 days later for GFP expression. *B–D*, WT-BMDM were pulsed for 4 h at 37 °C with MLV-GFP stocks (*B*, m.o.i. 0.5; *C* and *D*, m.o.i. 0.1) produced in the absence or presence of the indicated ManN analogs. Washed cells were then either analyzed for MLV capture by quantification of p30^{Gag}-positive cells by flow cytometry (*B*) or cell-associated RT activity (*C*), or used for *trans*-infection of S1A.TB cells (*D*). *E–G*, correlation analysis between the relative efficiency of virus capture and *trans*-infection (data depicted in *B–D*) for the 10 different MLV-GFP stocks was performed using GraphPad Prism. Data are expressed as the arithmetic means \pm S.D. of triplicate samples from one mouse and are representative of at least two experiments each performed using 2–3 mice. *r* and *p* values are shown.

from the MD data turned out to be difficult because of the significant fluctuations of the solvation free energy related to the protein (data not shown). For the isolated ligands, Neu5Gc and Neu5But, compared with Neu5Ac and Neu5Prop, had a significantly more favorable solvation energy (negative relative potential interaction energy values) indicative of a negative contribution to their binding affinity originating in the solvation.

As an alternative method to predict relative binding affinities of *N*-acyl-modified sialic acids to mSiglec-1, a “docking and post-scoring” approach was applied (for details see under “Experimental Procedures”). The values of the estimated affinity (Fig. 8*B*, 2nd column) showed a similar trend as found in the MD-based approach, *i.e.* Neu5Gc and Neu5But were predicted to have the lowest affinity for mSiglec-1. Thus,

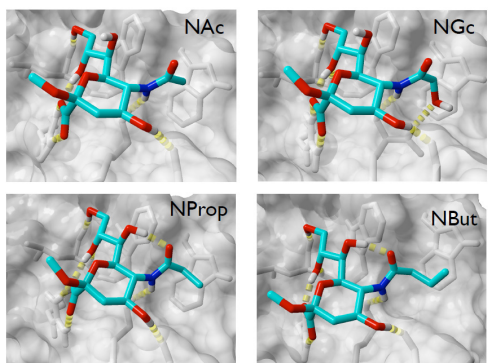
in agreement with the functional analyses, these crystal structure-based molecular modeling studies suggest reduced binding affinities for *N*-butanoyl and *N*-glycetyl, but not for *N*-propanoyl sialic acid side chain modifications, for the interaction with mSiglec-1.

Discussion

In this study, we demonstrate that Siglec-1 is a key receptor on primary mouse macrophages for capture of the retrovirus and mouse pathogen MLV and the efficient *trans*-infection of surface-bound particles to neighboring lymphocytes. Terminal sialic acid residues on plasma membrane-derived sialyl-lactose-containing gangliosides that are incorporated into the envelope of budding retroviral particles are the key interaction moiety with the lectin receptor Siglec-1. Using metabolic glycoengi-

N-Acyl Chain and Siglec-1-dependent MLV trans-Infection

A



B

Relative Potential Interaction Energies and SeeSAR Affinity Scores		
Ligand	Relative Potential Interaction Energy [kcal/mol]	SeeSAR Affinity Score [mM]
Neu5Ac	0	5
Neu5Prop	5.5	12
Neu5But	-6.2	26
Neu5Gc	-5.8	33

The relative average potential interaction energies were calculated from 50 ns MD simulations in water (higher values means better binding) and the average estimated affinity values calculated by SeeSAR (lower values means better binding).

FIGURE 8. Molecular modeling of structural interaction, interaction potentials, and binding affinities of mSiglec-1 in complex with sialic acid derivatives. A, three-dimensional models of mSiglec-1 in complex with Neu5Ac, Neu5Gc, Neu5Prop, or Neu5But were generated. B, relative potential interaction energies and SeeSAR affinity scores.

neering we introduced various *N*-acyl-modified sialic acids into glycoconjugates of virus-producer cells, and we demonstrated that for specific substitutions newly produced MLV particles were functionally impaired for Siglec-1-dependent capture and *trans*-infection. This highlights the use of sialic acid precursor analogs as a feasible approach to study the impact of submolecular modifications in glycoconjugates incorporated into enveloped viruses in a native environment and identifies the *N*-acyl side chain as a critical determinant for the mSiglec-1/MLV interaction. Collectively, mSiglec-1 is an important receptor for the sialic acid-dependent macrophage/lymphocyte *trans*-infection of MLV.

Macrophages and dendritic cells patrol peripheral mucosal sites recognizing, capturing, and processing potential pathogens into antigenic peptides for MHC class II presentation to CD4 T-cells in lymphoid tissue (55). Landmark studies proposed that HIV-1 usurps this natural DC function in the newly infected host by “hiding” inside DCs, which traffic to lymphoid organs, probably taking advantage of the formation of DC/T-cell conjugates to promote its replication and spread (56–58). Today it is widely believed that human DCs capture and internalize infectious HIV particles into clustered “storage” compartments and subsequently transfer these virions to neighboring T-cells at virological synapses (1, 59). In contrast to the virus-promoting scenario proposed for HIV, mSiglec-1-positive sinus macrophages residing underneath the lymph node capsule were shown to act as gatekeepers at the lymph-tissue interface capturing and *trans*-presenting lymph-borne viruses, including vesicular stomatitis virus, to migrating B-cells in the underlying follicles leading to activation of effective antiviral humoral immune responses (11). Furthermore, these macrophages also appear to prevent vesicular stomatitis virus spread and fatal neuroinvasion by additional innate mechanisms (10).

Of note, Siglec-1 in these studies was used as a marker for this subset of macrophages and not explored as a *bona fide* virus-binding receptor.

In contrast to the notion of an intracellular storage compartment for captured viruses that may be capable of efficient *trans*-infection of HIV-1 for up to 4 days (56, 58), Cavrois *et al.* (60) provided evidence that virions bound to the surface of monocyte-derived DCs or CD34-derived Langerhans cells, but not internalized HIV-1, was the major source of infectious virions transmitted in *trans*. This observation was recently confirmed (61). In line with these studies for HIV, our data also show that MLV particles that are still attached to the outside of BMDM, or at least accessible to protease treatment at their surface, are mainly responsible for *trans*-infection of murine lymphocytes. Moreover, we noted a marked drop of MLV *trans*-infection between the 4- and 24-h time points following virus capture by BMDM. Similarly, the HIV-1 *trans*-infection efficiency of monocyte-derived DCs was shown to be most efficient in the 1st h (60, 62). These authors also detected large amounts of internalized HIV-1 particles by confocal microscopy and suggested that this may reflect a “dead end” for functional retroviral particles. However, although neither lysosomal nor proteasomal inhibitors could prevent the apparent loss of MLV structural proteins over time in BMDM, lysosomal inhibitors did prevent the degradation of cell-associated HIV-1 in human macrophages (63).

From another perspective, given the unique subanatomical localization of Siglec-1-positive mouse macrophages in the subcapsular sinus, a “long term storage” of captured infectious virus may not at all be critical for interaction and efficient virus transmission because the preferentially targeted B-lymphocytes in the lymph follicles are closely adjacent (45). Thus, *trans*-infection of retroviruses appears to be mediated by cells of the monocytic lineage by capturing particles via surface-exposed Siglec-1. Retroviral particles that productively infect lymphocytes in *trans* originate primarily from the surface of macrophages/dendritic cells, and this process is most efficient in the 1st h following capture.

A central question for the process of *trans*-infection is its relative efficiency compared with direct infection. For HIV-1, monocyte-derived DC *trans*-infection has been suggested to be particularly effective for minimal virus doses that alone may not be sufficient for productive infection of CD4 T-cells by direct infection (56). Our results for MLV support this notion. The Siglec-1-dependent *trans*-infection of activated primary lymphocytes via BMDM, compared with direct infection, was 4–15-fold more efficient. Thus, it will be highly instructive to compare WT and Siglec-1 KO mice for the ability to support MLV replication and pathogenesis via lymphatic and intravenous challenge routes with low multiplicities of infection.

To our knowledge this study for the first time investigated the functional impact of metabolically modified sialic acids in virus producer cells on newly released viruses carrying cell-derived glycoconjugates. *N*-Substituted sialic acids could be detected and quantified in total membrane fraction and, importantly, in the glycolipid fraction of the 293T virus producer cells by DMB-HPLC and ESI-MS. More than 90% of the total cellular sialic acid content could be replaced by *N*-acyl derivatives pro-

viding a sound basis for the assessment of viruses released from these cells in sialic acid-dependent, functional assays.

Previous analyses of HIV-1 and MLV particles indicated that the overall lipid content of these retroviruses mostly matched that of the plasma membrane, with some lipids being enriched, including cholesterol, ceramide, and GM3 (50, 51). Notably, a single HIV-1 virion was estimated to contain ~12,000 sialyl-lactose-containing GM3 molecules that may constitute the primary interactor with the lectin receptor (1). The rather low millimolar affinity of Siglec-1 for different sialylated ligands was postulated to result in high avidity binding by receptor and ligand clustering (3). This may also be true for the interaction with viruses; HIV-1, bound initially over the entire plasma membrane, subsequently accumulated in many instances at one pole of the cell (64).

Several lines of evidence suggest that metabolically engineered gangliosides carrying *N*-acyl-modified sialic acids were indeed incorporated into MLV particles without inflicting gross structural changes to the infectious virion. First, the sialic acid-independent mCAT-mediated direct infection of lymphocytes was comparable for all MLV preparations, irrespective of the producer cell's pretreatment. In contrast, particles derived from *N*-butanoyl, *N*-isobutanoyl, *N*-glycolyl, or *N*-pentanoyl ManN-treated cells displayed strongly reduced capacities for the sialic acid-dependent mSiglec-1-mediated capture and *trans*-infection. Second, in agreement with these functional analyses, both *in vitro* interaction studies of sialylated ligands with Siglec-1 (4) and our molecular modeling studies of mSiglec-1 in complex with sialic acid derivatives indicated reduced binding affinities for the *N*-glycolyl and *N*-butanoyl, but not for the *N*-propanoyl substitution. This indicates at an atomic level that an elongation of the *N*-acyl side chain by one methyl group is still tolerated, although longer extension (Neu5But and Neu5Pent) strongly reduced the binding affinity. Interestingly, the rather bulky *N*-cyclo-propylcarbamyl side chain in glycoconjugates on MLV particles does not appear to impact the interaction with mSiglec-1, although the replacement of the methyl group (Neu5Ac) by a hydroxyl group (Neu5Gc) abolished capture and *trans*-infection.

Neu5Gc naturally occurs in mice but not in humans (65). Interestingly, it has been reported that both resting T- and B-cells preferentially carry Neu5Gc in α -2,6-linkage. Cell activation, however, results in marked changes in the glycosylation pattern, including a shift to Neu5Ac in α -2,3-linkage (36, 66). As a result, expression of Siglec-1 and Siglec-E ligands is enhanced on these lymphocytes. These changes may of course be highly relevant for MLV. On the one hand, the surface expression of selective ligands fosters the interaction of activated lymphocytes with Siglec-1-positive macrophages, increasing the likelihood for *trans*-infection. On the other hand, MLV replicates in these Neu5Ac-containing proliferating B- and T-cells, leading to the release of "Siglec-1/interaction-competent" virions.

Altogether, our study reports fundamental characteristics of *trans*-infection of the rodent pathogen MLV in primary mouse cells. We describe biosynthetic engineering of the *N*-acyl side chain of cellular sialic acid as a novel approach to study the functional impact of submolecular modifications in sialogly-

cans incorporated into budding enveloped retroviruses. This allowed us to identify critical determinants at atomic resolution for the Siglec-1-dependent MLV *trans*-infection in a native cellular environment.

Author Contributions—W. R. and O. T. K. conceived the study; O. T. K. and E. E. designed the experiments; E. E. performed and analyzed all MLV experiments; P. R. W., P. A., and W. R. analyzed sialic acids; M. F. performed molecular modeling analyses; I. A. assisted with mouse work; K. P., C. M., R. L. S., M. P. C., N. I.-U., and J. M.-P. provided reagents and discussion; P. R. C. provided KO mice; O. T. K. wrote the paper; and all authors commented on the manuscript.

Acknowledgments—We thank Walther Mothes for plasmids; Stephanie A. Archer-Hartmann for technical assistance; Sebenzile Myeni and Nikolas Herold for discussion; Hanna-Mari Baldauf for the coordination of animal work; and Roland Schauer and Carolyn Bertozzi for providing Neu5Gc and Neu5But, respectively.

References

- Izquierdo-Useros, N., Lorizate, M., McLaren, P. J., Telenti, A., Kräusslich, H. G., and Martinez-Picado, J. (2014) HIV-1 capture and transmission by dendritic cells: the role of viral glycolipids and the cellular receptor Siglec-1. *PLoS Pathog.* **10**, e1004146
- Geijtenbeek, T. B., and van Kooyk, Y. (2003) DC-SIGN: a novel HIV receptor on DCs that mediates HIV-1 transmission. *Curr. Top. Microbiol. Immunol.* **276**, 31–54
- Crocker, P. R., Paulson, J. C., and Varki, A. (2007) Siglecs and their roles in the immune system. *Nat. Rev. Immunol.* **7**, 255–266
- Klaas, M., and Crocker, P. R. (2012) Sialoadhesin in recognition of self and non-self. *Semin. Immunopathol.* **34**, 353–364
- Chow, A., Huggins, M., Ahmed, J., Hashimoto, D., Lucas, D., Kunisaki, Y., Pinho, S., Leboeuf, M., Noizat, C., van Rooijen, N., Tanaka, M., Zhao, Z. J., Bergman, A., Merad, M., and Frenette, P. S. (2013) CD169(+) macrophages provide a niche promoting erythropoiesis under homeostasis and stress. *Nat. Med.* **19**, 429–436
- Chow, A., Lucas, D., Hidalgo, A., Méndez-Ferrer, S., Hashimoto, D., Scheiermann, C., Battista, M., Leboeuf, M., Prophete, C., van Rooijen, N., Tanaka, M., Merad, M., and Frenette, P. S. (2011) Bone marrow CD169+ macrophages promote the retention of hematopoietic stem and progenitor cells in the mesenchymal stem cell niche. *J. Exp. Med.* **208**, 261–271
- Crocker, P. R., Werb, Z., Gordon, S., and Bainton, D. F. (1990) Ultrastructural localization of a macrophage-restricted sialic acid binding hemagglutinin, SER, in macrophage-hematopoietic cell clusters. *Blood* **76**, 1131–1138
- Oetke, C., Vinson, M. C., Jones, C., and Crocker, P. R. (2006) Sialoadhesin-deficient mice exhibit subtle changes in B- and T-cell populations and reduced immunoglobulin M levels. *Mol. Cell. Biol.* **26**, 1549–1557
- Hartnell, A. (2001) Characterization of human sialoadhesin, a sialic acid binding receptor expressed by resident and inflammatory macrophage populations. *Blood* **97**, 288–296
- Iannaccone, M., Moseman, E. A., Tonti, E., Bosurgi, L., Junt, T., Henrickson, S. E., Whelan, S. P., Guidotti, L. G., and von Andrian, U. H. (2010) Subcapsular sinus macrophages prevent CNS invasion on peripheral infection with a neurotropic virus. *Nature* **465**, 1079–1083
- Junt, T., Moseman, E. A., Iannaccone, M., Massberg, S., Lang, P. A., Boes, M., Fink, K., Henrickson, S. E., Shayakhmetov, D. M., Di Paolo, N. C., van Rooijen, N., Memel, T. R., Whelan, S. P., and von Andrian, U. H. (2007) Subcapsular sinus macrophages in lymph nodes clear lymph-borne viruses and present them to antiviral B cells. *Nature* **450**, 110–114
- Prather, R. S., Rowland, R. R., Ewen, C., Trible, B., Kerrigan, M., Bawa, B., Teson, J. M., Mao, J., Lee, K., Samuel, M. S., Whitworth, K. M., Murphy, C. N., Egen, T., and Green, J. A. (2013) An intact sialoadhesin (S_n/SIGLEC1/CD169) is not required for attachment/internalization of the

N-Acyl Chain and Siglec-1-dependent MLV trans-Infection

- porcine reproductive and respiratory syndrome virus. *J. Virol.* **87**, 9538–9546
- 13. Puryear, W. B., Akiyama, H., Geer, S. D., Ramirez, N. P., Yu, X., Reinhard, B. M., and Gummuluru, S. (2013) Interferon-inducible mechanism of dendritic cell-mediated HIV-1 dissemination is dependent on Siglec-1/CD169. *PLoS Pathog.* **9**, e1003291
 - 14. Vinson, M., van der Merwe, P. A., Kelm, S., May, A., Jones, E. Y., and Crocker, P. R. (1996) Characterization of the sialic acid-binding site in sialoadhesin by site-directed mutagenesis. *J. Biol. Chem.* **271**, 9267–9272
 - 15. May, A. P., Robinson, R. C., Vinson, M., Crocker, P. R., and Jones, E. Y. (1998) Crystal structure of the N-terminal domain of sialoadhesin in complex with 3' sialyl-lactose at 1.85 Å resolution. *Mol. Cell* **1**, 719–728
 - 16. Gagiannis, D., Gossrau, R., Reutter, W., Zimmermann-Kordmann, M., and Horstkorte, R. (2007) Engineering the sialic acid in organs of mice using *N*-propanoylmannosamine. *Biochim. Biophys. Acta* **1770**, 297–306
 - 17. Kelm, S., Brossmer, R., Isecke, R., Gross, H. J., Strenge, K., and Schauer, R. (1998) Functional groups of sialic acids involved in binding to siglecs (sialoadhesins) deduced from interactions with synthetic analogues. *Eur. J. Biochem.* **255**, 663–672
 - 18. Kelm, S., Schauer, R., Manuguerra, J. C., Gross, H. J., and Crocker, P. R. (1994) Modifications of cell surface sialic acids modulate cell adhesion mediated by sialoadhesin and CD22. *Glycoconj. J.* **11**, 576–585
 - 19. Izquierdo-Useros, N., Lorizate, M., Contreras, F. X., Rodriguez-Plata, M. T., Glass, B., Erkizia, I., Prado, J. G., Casas, J., Fabriàs, G., Kräusslich, H. G., and Martínez-Picado, J. (2012) Sialyllactose in viral membrane gangliosides is a novel molecular recognition pattern for mature dendritic cell capture of HIV-1. *PLoS Biol.* **10**, e1001315
 - 20. Puryear, W. B., Yu, X., Ramirez, N. P., Reinhard, B. M., and Gummuluru, S. (2012) HIV-1 incorporation of host-cell-derived glycosphingolipid GM3 allows for capture by mature dendritic cells. *Proc. Natl. Acad. Sci. U.S.A.* **109**, 7475–7480
 - 21. Kayser, H., Zeitler, R., Kannicht, C., Grunow, D., Nuck, R., and Reutter, W. (1992) Biosynthesis of a nonphysiological sialic acid in different rat organs, using *N*-propanoyl-D-hexosamines as precursors. *J. Biol. Chem.* **267**, 16934–16938
 - 22. Mahal, L. K., Yarema, K. J., and Bertozzi, C. R. (1997) Engineering chemical reactivity on cell surfaces through oligosaccharide biosynthesis. *Science* **276**, 1125–1128
 - 23. Keppler, O. T., Horstkorte, R., Pawlita, M., Schmidt, C., and Reutter, W. (2001) Biochemical engineering of the *N*-acyl side chain of sialic acid: biological implications. *Glycobiology* **11**, 11R–18R
 - 24. Horstkorte, R., Rau, K., Laabs, S., Danker, K., and Reutter, W. (2004) Biochemical engineering of the *N*-acyl side chain of sialic acid leads to increased calcium influx from intracellular compartments and promotes differentiation of HL60 cells. *FEBS Lett.* **571**, 99–102
 - 25. Keppler, O. T., Herrmann, M., von der Lieth, C. W., Stehling, P., Reutter, W., and Pawlita, M. (1998) Elongation of the *N*-acyl side chain of sialic acids in MDCK II cells inhibits influenza A virus infection. *Biochem. Biophys. Res. Commun.* **253**, 437–442
 - 26. Keppler, O. T., Stehling, P., Herrmann, M., Kayser, H., Grunow, D., Reutter, W., and Pawlita, M. (1995) Biosynthetic modulation of sialic acid-dependent virus-receptor interactions of two primate polyoma viruses. *J. Biol. Chem.* **270**, 1308–1314
 - 27. Wieser, J. R., Heisner, A., Stehling, P., Oesch, F., and Reutter, W. (1996) *In vivo* modulated *N*-acyl side chain of *N*-acetylneurameric acid modulates the cell contact-dependent inhibition of growth. *FEBS Lett.* **395**, 170–173
 - 28. Saxon, E., and Bertozzi, C. R. (2000) Cell surface engineering by a modified Staudinger reaction. *Science* **287**, 2007–2010
 - 29. Krieger, E., Darden, T., Nabuurs, S. B., Finkelstein, A., and Vriend, G. (2004) Making optimal use of empirical energy functions: force-field parameterization in crystal space. *Proteins* **57**, 678–683
 - 30. Jin, J., Li, F., and Mothes, W. (2011) Viral determinants of polarized assembly for the murine leukemia virus. *J. Virol.* **85**, 7672–7682
 - 31. Pizzato, M., Erlwein, O., Bonsall, D., Kaye, S., Muir, D., and McClure, M. O. (2009) A one-step SYBR Green I-based product-enhanced reverse transcriptase assay for the quantitation of retroviruses in cell culture supernatants. *J. Virol. Methods* **156**, 1–7
 - 32. Duan, Y., Wu, C., Chowdhury, S., Lee, M. C., Xiong, G., Zhang, W., Yang, R., Cieplak, P., Luo, R., Lee, T., Caldwell, J., Wang, J., and Kollman, P. (2003) A point-charge force field for molecular mechanics simulations of proteins based on condensed-phase quantum mechanical calculations. *J. Comput. Chem.* **24**, 1999–2012
 - 33. Jakalian, A., Jack, D. B., and Bayly, C. I. (2002) Fast, efficient generation of high-quality atomic charges. AM1-BCC model: II. Parameterization and validation. *J. Comput. Chem.* **23**, 1623–1641
 - 34. Shan, Y., Klepeis, J. L., Eastwood, M. P., Dror, R. O., and Shaw, D. E. (2005) Gaussian split Ewald: A fast Ewald mesh method for molecular simulation. *J. Chem. Phys.* **122**, 54101
 - 35. Wang, J., Wolf, R. M., Caldwell, J. W., Kollman, P. A., and Case, D. A. (2004) Development and testing of a general amber force field. *J. Comput. Chem.* **25**, 1157–1174
 - 36. Naito-Matsui, Y., Takada, S., Kano, Y., Iyoda, T., Sugai, M., Shimizu, A., Inaba, K., Nitschke, L., Tsubata, T., Oka, S., Kozutsumi, Y., and Take-matsu, H. (2014) Functional evaluation of activation-dependent alterations in the sialoglycan composition of T cells. *J. Biol. Chem.* **289**, 1564–1579
 - 37. Rarey, M., Kramer, B., Lengauer, T., and Klebe, G. (1996) A fast flexible docking method using an incremental construction algorithm. *J. Mol. Biol.* **261**, 470–489
 - 38. Schneider, N., Lange, G., Hindle, S., Klein, R., and Rarey, M. (2013) A consistent description of HYdrogen bond and DEhydration energies in protein-ligand complexes: methods behind the HYDE scoring function. *J. Comput. Aided Mol. Des.* **27**, 15–29
 - 39. Inoue, S., and Inoue, Y. (2003) Ultrasensitive analysis of sialic acids and oligo/polysialic acids by fluorometric high-performance liquid chromatography. *Methods Enzymol.* **362**, 543–560
 - 40. Galuska, S. P., Geyer, H., Weinhold, B., Kontou, M., Röhricht, R. C., Bernard, U., Gerardy-Schahn, R., Reutter, W., Münster-Kühnel, A., and Geyer, R. (2010) Quantification of nucleotide-activated sialic acids by a combination of reduction and fluorescent labeling. *Anal. Chem.* **82**, 4591–4598
 - 41. Smith, D. F., and Prieto, P. A. (2001) Special considerations for glycolipids and their purification. *Curr. Protoc. Mol. Biol.* Chapter 17, Unit 17.13
 - 42. Wratil, P. R., Rigol, S., Solecka, B., Kohla, G., Kannicht, C., Reutter, W., Giannis, A., and Nguyen, L. D. (2014) A novel approach to decrease sialic acid expression in cells by a C-3-modified *N*-acetylmannosamine. *J. Biol. Chem.* **289**, 32056–32063
 - 43. Lewis, P. F., and Emerman, M. (1994) Passage through mitosis is required for oncoretroviruses but not for the human immunodeficiency virus. *J. Virol.* **68**, 510–516
 - 44. Roe, T., Reynolds, T. C., Yu, G., and Brown, P. O. (1993) Integration of murine leukemia virus DNA depends on mitosis. *EMBO J.* **12**, 2099–2108
 - 45. Kuka, M., and Iannacone, M. (2014) The role of lymph node sinus macrophages in host defense. *Ann. N.Y. Acad. Sci.* **1319**, 38–46
 - 46. Posch, W., Steger, M., Knackmuss, U., Blatzner, M., Baldauf, H. M., Doppler, W., White, T. E., Hörtnagl, P., Diaz-Griffero, F., Lass-Flörl, C., Hackl, H., Moris, A., Keppler, O. T., and Wilflingseder, D. (2015) Complement-opsonized HIV-1 overcomes restriction in dendritic cells. *PLoS Pathog.* **11**, e1005005
 - 47. Coutinho, A., and Möller, G. (1973) B cell mitogenic properties of thymus-independent antigens. *Nat. New Biol.* **245**, 12–14
 - 48. Dwyer, J. M., and Johnson, C. (1981) The use of concanavalin A to study the immunoregulation of human T cells. *Clin. Exp. Immunol.* **46**, 237–249
 - 49. Luchansky, S. J., and Bertozzi, C. R. (2004) Azido sialic acids can modulate cell-surface interactions. *ChemBioChem* **5**, 1706–1709
 - 50. Brügger, B., Glass, B., Haberkant, P., Leibrecht, I., Wieland, F. T., and Kräusslich, H. G. (2006) The HIV lipidome: a raft with an unusual composition. *Proc. Natl. Acad. Sci. U.S.A.* **103**, 2641–2646
 - 51. Chan, R., Uchil, P. D., Jin, J., Shui, G., Ott, D. E., Mothes, W., and Wenk, M. R. (2008) Retroviruses human immunodeficiency virus and murine leukemia virus are enriched in phosphoinositides. *J. Virol.* **82**, 11228–11238
 - 52. Sonnenburg, J. L., Altheide, T. K., and Varki, A. (2004) A uniquely human consequence of domain-specific functional adaptation in a sialic acid-binding receptor. *Glycobiology* **14**, 339–346
 - 53. Oetke, C., Hinderlich, S., Brossmer, R., Reutter, W., Pawlita, M., and Kep-

- pler, O. T. (2001) Evidence for efficient uptake and incorporation of sialic acid by eukaryotic cells. *Eur. J. Biochem.* **268**, 4553–4561
54. Rosenberg, N., and Jolicoeur, P. (1997) in *Retroviruses* (Coffin, J. M., Hughes, S. H., and Varmus, H. E., eds) pp. 475–586, Cold Spring Harbor Laboratory Press, Cold Spring Harbor, NY
 55. Banchereau, J., and Steinman, R. M. (1998) Dendritic cells and the control of immunity. *Nature* **392**, 245–252
 56. Geijtenbeek, T. B., Kwon, D. S., Torensma, R., van Vliet, S. J., van Duijnhoven, G. C., Middel, J., Cornelissen, I. L., Nottet, H. S., KewalRamani, V. N., Littman, D. R., Figdor, C. G., and van Kooyk, Y. (2000) DC-SIGN, a dendritic cell-specific HIV-1-binding protein that enhances trans-infection of T cells. *Cell* **100**, 587–597
 57. Geijtenbeek, T. B., Torensma, R., van Vliet, S. J., van Duijnhoven, G. C., Adema, G. J., van Kooyk, Y., and Figdor, C. G. (2000) Identification of DC-SIGN, a novel dendritic cell-specific ICAM-3 receptor that supports primary immune responses. *Cell* **100**, 575–585
 58. Kwon, D. S., Gregorio, G., Bitton, N., Hendrickson, W. A., and Littman, D. R. (2002) DC-SIGN-mediated internalization of HIV is required for trans-enhancement of T cell infection. *Immunity* **16**, 135–144
 59. Garcia, E., Pion, M., Pelchen-Matthews, A., Collinson, L., Arrighi, J. F., Blot, G., Leuba, F., Escola, J. M., Demaurex, N., Marsh, M., and Piguet, V. (2005) HIV-1 trafficking to the dendritic cell-T-cell infectious synapse uses a pathway of tetraspanin sorting to the immunological synapse. *Traffic* **6**, 488–501
 60. Cavrois, M., Neidleman, J., Kreisberg, J. F., and Greene, W. C. (2007) *In vitro* derived dendritic cells trans-infect CD4 T cells primarily with surface-bound HIV-1 virions. *PLoS Pathog.* **3**, e4
 61. Akiyama, H., Ramirez, N. G., Gudheti, M. V., and Gummuluru, S. (2015) CD169-mediated trafficking of HIV to plasma membrane invaginations in dendritic cells attenuates efficacy of anti-gp120 broadly neutralizing anti-bodies. *PLoS Pathog.* **11**, e1004751
 62. Yu, H. J., Reuter, M. A., and McDonald, D. (2008) HIV traffics through a specialized, surface-accessible intracellular compartment during trans-infection of T cells by mature dendritic cells. *PLoS Pathog.* **4**, e1000134
 63. Pino, M., Erkizia, I., Benet, S., Erikson, E., Fernández-Figueras, M. T., Guerrero, D., Dalmau, J., Ouchi, D., Rausell, A., Ciuffi, A., Keppler, O. T., Telenti, A., Kräusslich, H. G., Martinez-Picado, J., and Izquierdo-Useros, N. (2015) HIV-1 immune activation induces Siglec-1 expression and enhances viral trans-infection in blood and tissue myeloid cells. *Retrovirology* **12**, 37
 64. Izquierdo-Useros, N., Esteban, O., Rodriguez-Plata, M. T., Erkizia, I., Prado, J. G., Blanco, J., García-Parajo, M. F., and Martinez-Picado, J. (2011) Dynamic imaging of cell-free and cell-associated viral capture in mature dendritic cells. *Traffic* **12**, 1702–1713
 65. Brinkman-Van der Linden, E. C., Sjoberg, E. R., Juneja, L. R., Crocker, P. R., Varki, N., and Varki, A. (2000) Loss of N-glycolyneuraminic acid in human evolution. Implications for sialic acid recognition by siglecs. *J. Biol. Chem.* **275**, 8633–8640
 66. Naito, Y., Takematsu, H., Koyama, S., Miyake, S., Yamamoto, H., Fujinawa, R., Sugai, M., Okuno, Y., Tsujimoto, G., Yamaji, T., Hashimoto, Y., Itohara, S., Kawasaki, T., Suzuki, A., and Kozutsumi, Y. (2007) Germinal center marker GL7 probes activation-dependent repression of N-glycolyneuraminic acid, a sialic acid species involved in the negative modulation of B-cell activation. *Mol. Cell. Biol.* **27**, 3008–3022
 67. Goffinet, C., Michel, N., Allespach, I., Tervo, H.-M., Hermann, V., Kräusslich, H.-G., Greene, W. C., and Keppler, O. T. (2007) Primary T-cells from human CD4/CCR5-transgenic rats support all early steps of HIV-1 replication including integration, but display impaired viral gene expression *Retrovirology* **4**, 53

CrossMark
click for updatesCite this: *Chem. Sci.*, 2016, **7**, 3928

Inhibition of the key enzyme of sialic acid biosynthesis by C6-Se modified N-acetylmannosamine analogs†

Olaia Nieto-Garcia,^{‡,a} Paul R. Wratil,^{‡,b} Long D. Nguyen,^b Verena Böhrsch,^a Stephan Hinderlich,^{*,c} Werner Reutter^{*b} and Christian P. R. Hackenberger^{*ad}

Synthetically accessible C6-analogs of *N*-acetylmannosamine (ManNAc) were tested as potential inhibitors of the bifunctional UDP-*N*-acetylglucosamine-2-epimerase/*N*-acetylmannosamine kinase (GNE/MNK), the key enzyme of sialic acid biosynthesis. Enzymatic experiments revealed that the modification introduced at the C6 saccharide position strongly influences the inhibitory potency. A C6-ManNAc diselenide dimer showed the strongest kinase inhibition in the low μM range among all the substrates tested and successfully reduced cell surface sialylation in Jurkat cells.

Received 27th October 2015
Accepted 13th February 2016

DOI: 10.1039/c5sc04082e
www.rsc.org/chemicalscience

Introduction

Sialic acid is an essential component of the periphery of the glycocalyx. Sialylated glycoconjugates are involved in a broad range of cell functions and biological interactions including recognition of pathogens and immune regulation, among others.^{1–3} For instance, it is known that the influenza virus invades host cells through sialic acid recognition.⁴ Many tumor cells show an altered glycosylation pattern with increased expression of sialic acids on their surface.^{5,6} Assumingly, this oversialylation may act as a shield to protect these tumor cells from immune recognition.^{7,8} Nowadays, the elucidation of the precise role of sialic acids in glycan-mediated cellular interactions is a field of growing interest. For studying cell-surface glycosylation metabolic oligosaccharide-engineering (MOE) is a well-established tool to modify and visualize sialic acids on the cell membrane even in living animals.⁹ By this strategy, unnatural *N*-acetylmannosamine (ManNAc) analogs can be efficiently incorporated into membrane glycoconjugates utilizing the sialic acid biosynthetic pathway, which can be subsequently labeled with bioorthogonal reactions.^{9–12} Regarding sialic acid expression, inhibitors of sialyltransferases, a group of enzymes that

facilitate the transfer of sialic acid onto glycoconjugates in the Golgi lumen, were reported to efficiently reduce cell surface sialylation *in vitro*^{13,14} and *in vivo*.¹⁵ Another promising approach for the study of sialic acid related biological processes is the development of inhibitors targeting the *de novo* biosynthesis of this sugar. The key enzyme of sialic acid biosynthesis is the bifunctional UDP-*N*-acetylglucosamine-2-epimerase/*N*-acetylmannosamine kinase (GNE/MNK), which consequently serves as an important regulator of cell surface sialylation in mammals.¹⁶ Specifically, the GNE domain of the enzyme first isomerizes UDP-*N*-acetylglucosamine (UDP-GlcNAc) into ManNAc, which is then phosphorylated at the 6-hydroxy position under consumption of adenosine triphosphate (ATP) by the MNK domain (Scheme 1).

To date, known GNE/MNK inhibitors were synthesized based on unnatural monosaccharides, including *N*-acetylglucosamine (GlcNAc), UDP-GlcNAc and ManNAc analogs (Fig. 1).^{17–23}

Among all reported inhibitors, only 3-*O*-methyl-*N*-acetylglucosamine (**1**) and the methylated ManNAc analog **2** were tested in eukaryotic cells. For instance, the methylated GlcNAc analog **1** at 1 mM final concentration reduced the incorporation rate of *N*-GlcNAc and *N*-ManNAc into glycoproteins by 70% in HepG2 cells.¹⁷ More recently, the methylated ManNAc analog **2** showed reduction of cell surface sialylation to 20% using 500 μM final concentration of the inhibitor in culture medium.²² Other reported inhibitors, including 6-O-Ac-ManNAc (**3**), iminosugars **4–6** and 2',3'-dialdehydo-UDP-*N*-acetylglucosamine (**7**) were tested with either the purified ManNAc kinase (**3** at 5 mM final concentration) or UDP-GlcNAc-2-epimerase/MNK kinase (**4–6** at 1 mM; **7** at 300 μM) and showed an inhibition of the corresponding enzyme by 60%, 70% and 93%, respectively.^{18,20,23} Despite these studies, the need of high inhibitor concentrations for an efficient reduction of cell surface sialylation limits the applicability for further studies, especially for *in*

^aLeibniz-Institut für Molekulare Pharmakologie, Robert-Roessle-Strasse 10, 13125 Berlin, Germany

^bInstitut für Laboratoriumsmedizin, Klinische Chemie und Pathobiochemie, Charité-Universitätsmedizin Berlin, Arnimalee 22, 14195 Berlin, Germany. E-mail: werner.reutter@charite.de

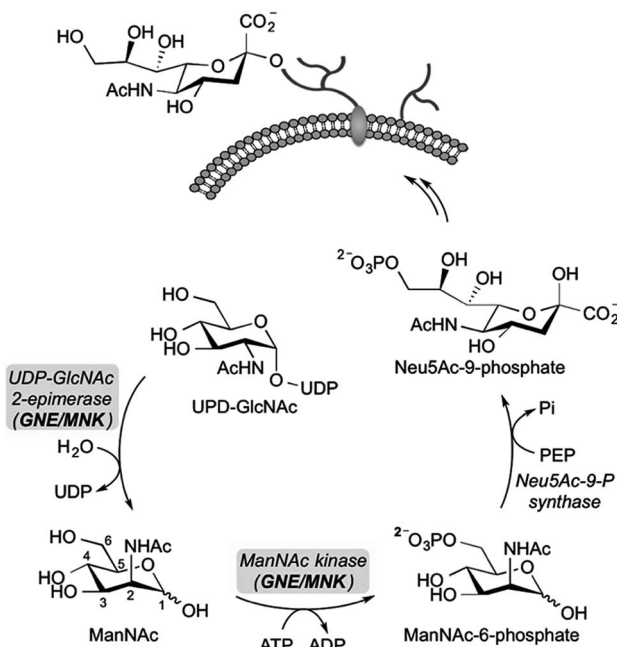
^cBeuth Hochschule für Technik Berlin, Department Life Sciences & Technology, Seestrasse 64, 13347 Berlin, Germany. E-mail: hinderlich@beuth-hochschule.de

^dHumboldt Universität zu Berlin, Department Chemie, Brook-Taylor-Strasse 2, 12489, Berlin, Germany. E-mail: hackenbe@fmp-berlin.de

† Electronic supplementary information (ESI) available. See DOI: 10.1039/c5sc04082e

‡ Both authors contributed equally to this work.





Scheme 1 The bifunctional UDP-*N*-acetylglucosamine-2-epimerase/*N*-acetylmannosamine kinase (GNE/MNK) catalyzes the first two steps in the *de novo* synthesis of sialic acids in cells. UDP-GlcNAc is converted by GNE/MNK to ManNAc-6-phosphate, which is then condensed with phosphoenolpyruvate (PEP) to *N*-acetylneurameric acid-9-phosphate (Neu5Ac-9-P). The latter substrate is further dephosphorylated, activated to CMP-sialic acid and used for the synthesis of sialylated glycans.

vivo experiments, and points towards the need of novel potent inhibitors for sialic acid *de novo* biosynthesis.

In this manuscript, we report the synthesis and evaluation of sulfur and selenium-based C6-derivatives of *N*-acetylmannosamine as potential inhibitors of the human MNK. We hypothesized that C6-ManNAc derivatives cannot be phosphorylated by MNK, making them competitive inhibitors for this enzyme. Our concept was supported by investigating the crystal structure of human MNK in complex with its natural substrate, ManNAc.²³ The geometry of the active site revealed that only the hydroxyl

moiety at the C6 position of ManNAc is sterically accessible for substrate modifications. For this purpose, we planned to access C6-modified ManNAc analogs, in which larger selenium or sulfur atoms replaced the oxygen at position C6, presumably leading to a better blockage of the binding pocket. Furthermore, we reasoned that these C6-modifications would be promising for inhibitory studies in living cells in contrast to compound 3, in which the acetylated C6-hydroxyl group is cleaved by endogenous esterases.

Results and discussion

The synthetic strategy was designed to be versatile and accessible from previously described tosylated ManNAc 8 (Scheme 2),²⁴ which can react with appropriate S- or Se-nucleophiles. Considering the S-derivatives, the peracetylated thiol derivative 9 was obtained from 8 by nucleophilic substitution employing potassium thioacetate. In order to obtain water-soluble compounds suitable for enzymatic *in vitro* assays, simultaneous deprotection of S- and O-acetyl groups was carried out using standard basic conditions; however, to avoid epimerization at position C2 it was crucial to limit the time of basic deprotection with sodium methoxide to 10 min.²⁵ We observed the formation of thiol 11 and the disulfide 12 based on the ¹H-NMR shift of the protons at position C6,²⁶ which were both isolated and employed in further enzymatic MNK-assays. To prepare the corresponding C6-Se-ManNAc-analogues, we employed the same electrophilic building block 8 from above. After reaction with nucleophilic potassium selenocyanate as the Se-source, compound 10 was obtained in 91% yield after purification. The chemoselective reduction of selenocyanate in presence of O-acetyl groups was ensured by using sodium borohydride, followed by acidification and stirring under inert atmosphere. Although the selenol could be observed after the acidification as a minor peak by UPLC-MS analysis, the high oxidation potential of the selenolate prevented the isolation of the corresponding selenol. Instead, the diselenide dimer 14a was obtained in 83% yield and analyzed by ⁷⁷Se NMR, displaying the characteristic shift for diselenides at 319–323 ppm. The treatment with sodium methoxide in methanol and subsequent neutralization afforded the unprotected seleno sugar-dimer 14b in a moderate yield of 47%, most likely due to the cleavage of the labile C–Se bond as previously reported.²⁷ With compounds 11, 12 and 14b in hand we tested the inhibitory effect in an MNK activity assay. Human MNK was expressed in BL21-CodonPlus (DE3)-RIL *Escherichia coli* (Stragene) and purified according to an established method.²³ The half maximal inhibitory concentrations (IC_{50}) of modified ManNAc analogs for MNK activity have been measured *in vitro* using a coupled optical assay based on consumption of nicotinamide adenine dinucleotide (NADH, details in ESI†). Herein, purified enzyme was incubated with ManNAc (125 μ M), the natural substrate for the kinase, ATP and varying concentrations of the previously synthesized C6-modified ManNAc analogs 11, 12 and 14b. With an IC_{50} value of 8.5 μ M, the diselenide 14b showed the strongest inhibition of enzyme activity among all tested substances (Table 1, entries 1–3 and Fig. 2A). Encouraged by these results, we also prepared

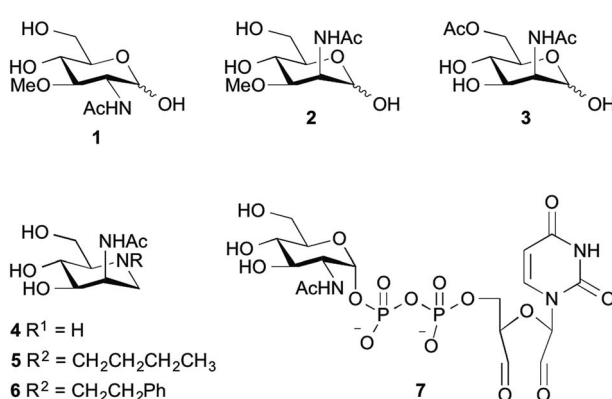


Fig. 1 Some unnatural modified monosaccharides reported as inhibitors of GNE/MNK kinase.



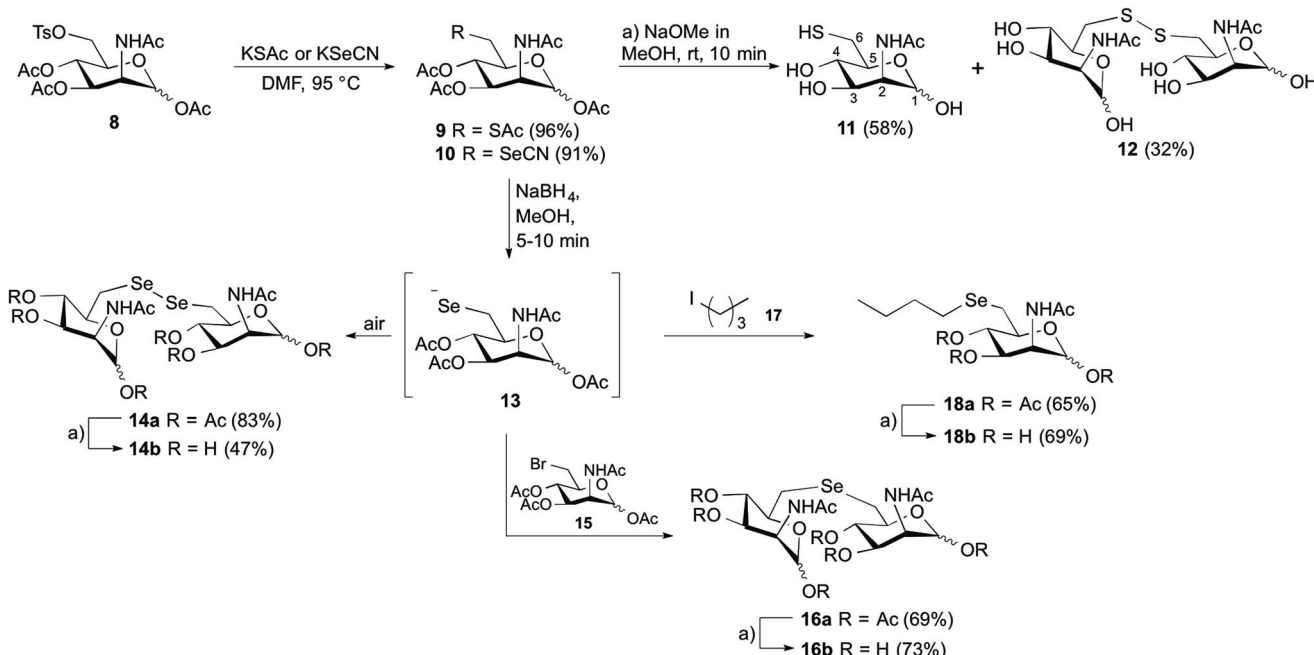
Scheme 2 Synthesis of C6-modified *N*-acetylmannosamine analogs.

Table 1 Half maximal inhibitory concentrations (IC_{50}) of **11**, **12**, **14b**, **16b** and **18b** for MNK inhibition. The data shown represents the means \pm SEM obtained in three independent experiments for **11**, **12**, **16b**, **18b** and five independent experiments for **14b**

Entry	Compound	IC_{50} (mM)
1	11	>10
2	12	4.2 (± 0.7)
3	14b	8.5×10^{-3} ($\pm 1.9 \times 10^{-3}$)
4	16b	3.0 (± 0.7)
5	18b	1.9 (± 0.5)

the selenoethers **16b** and **18b**, to further probe the influence of the second selenium atom as well as the second sugar moiety on enzyme activity. Thereby, we took advantage of the nucleophilic properties of the selenolate anion precursor **13** to access the selenoethers. Seleno cyanate **10** was reductively cleaved with sodium borohydride for 5–10 min (monitored by TLC) and the high reactive selenolate anion **13** was caught *in situ* by Ac₃-6-Br-ManNAc (**15**) or 1-iodopentane (**17**) (Scheme 2). An excess of the electrophiles was used to decrease the formation of the diselenide **14a**. The desired seleno compounds **16a** and **18a** were isolated in 69% and 65%, respectively. The treatment with sodium methoxide delivered unprotected seleno sugars **16b** and **18b** as described for **14b** before. MNK activity studies with selenoethers revealed significantly lower inhibition in comparison to the diselenide **14b** (Table 1, entry 4 and 5).

The performed MNK activity studies for the sulfur and seleno analogs **11**, **12**, **14b**, **16b** and **18b** indicated that a combination of a diselenide bond together with an additional ManNAc unit is highly beneficial for the enzyme inhibition. In the homodimeric

ManNAc derivatives the backbone structure of ManNAc appears twice, giving two potential binding partners for the ManNAc-binding site of MNK. Consequently, this leads to a stoichiometrical advantage for dimeric inhibitors, and therefore increases their inhibitory potential compared to mono-saccharide ManNAc analogs that have been previously reported as MNK inhibitors.^{17–23} Comparing the results of the enzymatic studies with **14b** and **16b**, the length and type of the selenide-linker is apparently of great importance for MNK inhibition. The C-Se-Se-C linker in **14b** is longer, but also could be more flexible than the C-Se-C linker in **16b**. This feature as well as the length and the angle of the C-Se bond could be essential for successful positioning of the inhibitor into the active binding pocket of the MNK.²⁸ In addition, different van der Waals interactions and H-bonding properties of selenium and sulfur atoms could play a role for protein binding.²³ Even though they share a high structural similarity, compound **12** had an approximately 500-fold higher IC_{50} in comparison to **14b**.

With the potent diselenide compound **14b** in hand, we further studied the binding properties of this potent MNK inhibitor, which is to our knowledge the strongest MNK inhibitor reported to date. Diselenide **14b** inhibited MNK activity in a dose dependent manner (Fig. 2A). Additionally, we performed the enzymatic assay in presence of **14b** (25 μ M) and different concentrations of ManNAc and confirmed a competitive inhibition of **14b** for ManNAc. The inhibitor constant (K_i) value obtained was 15.7 μ M (Fig. 2B). Additionally, we tested if diselenide **14b** influenced the GNE activity of the bifunctional GNE/MNK. Analysis of GNE/MNK in mouse liver cytosol revealed an IC_{50} of **14b** for inhibiting the GNE activity in the range of 200 μ M (details in ESI†). This result indicates that the main inhibitory effect of **14b** on sialic acid biosynthesis is due to



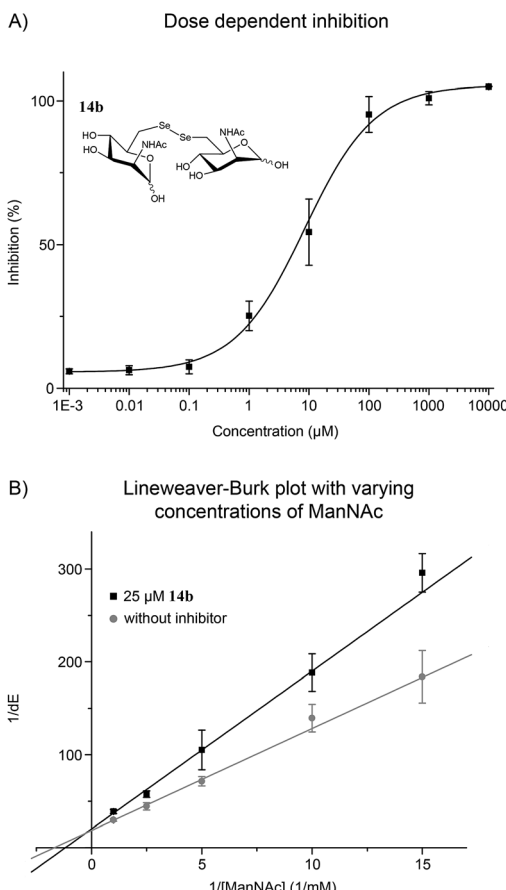


Fig. 2 (A) ManNAc diselenide dimer **14b** inhibited the MNK in dose dependent manner. (B) Lineweaver–Burk plot showed a competitive inhibition of **14b** and ManNAc, the natural substrate of MNK. Sigmoidal (A) and linear (B) approximation curves were used to determine IC_{50} and K_i values. Data shown represent the means \pm SEM from five independent experiments.

MNK inhibition, although the GNE activity appears to be influenced by the diselenide **14b**, likely due to an allosteric effect of the binding of the inhibitor to the MNK domain. To evaluate the specificity of the inhibitor towards other sugar kinases, we performed further inhibition studies using human GlcNAc kinase (GNK) and hexokinase (HK) from yeast (details in ESI†). The IC_{50} of **14b** for GNK activity was about 1.7 mM, and higher than 5 mM for HK activity, respectively, indicating that the effects of **14b** on these other sugar kinases are non-specific and negligible.

At this stage, we also wanted to evaluate the stability of the diselenide **14b** in presence of thiol-containing reducing agents like dithiothreitol (DTT) or glutathione (GSH) to address the application of our compounds in living cells. Therefore, the possible reduction of the diselenide bond was monitored by ^{77}Se NMR using a solution of 60 mM concentration of **14b** in an aqueous saturated DTT solution at room temperature. Immediately after the addition of **14b** to the DTT solution, a characteristic signal for the selenol compound at -48.1 ppm was observed and a major peak at 294 ppm related to the diselenide. Concretely, the integration of diselenide/selenol peaks gave

a 90 : 10 ratio (details in ESI†). Due to the most stable oxidation state, in the time period between 15 min and 5 h, only signals from the diselenide were detected. In the case of saturated GSH solution, using the same procedure as before, only diselenide **14b** was detected after incubation at 60 mM.

Encouraged by the strong *in vitro* inhibition of **14b** and its high stability in the presence of reducing agents, we evaluated the capability of this substance to reduce cell surface sialylation. Due to the fact that peracetylated ManNAc derivatives are known to have better membrane permeability,²⁹ the corresponding peracetylated diselenide **14a** was used as a prodrug like precursor of **14b** for cell experiments. Additionally, selenide **16a** was chosen as a control because it shares high structural similarity to **14a**, but had only weak effects on the enzyme activity of MNK (Table 1). Jurkat cells were treated for 72 h with different concentrations of peracetylated diselenide **14a** and selenide **16a**. First, the cytotoxicity of **14a** as well as **16a** was evaluated using the AlamarBlue® cell viability assay. Up to a concentration of 50 μM in culture medium, diselenide **14a** exposed negligible cytotoxicity (details in ESI†). However, at a final concentration of 100 μM cell viability was reduced by approximately 70%. Therefore, the following experiments on cell surface sialylation were limited to an inhibitor concentration of 50 μM in culture medium. In the same concentration range, selenide **16a** reduced cell viability by up to 25%. Cell surface sialylation was evaluated by measuring the expression of 6'-sialyl-N-acetyllactosamine (6'-sialyl-LacNAc) *via* flow cytometry using fluorescein isothiocyanate-conjugated *Poly-porus squamosus* lectin (FITC-PSL).^{22,30} Only treatment with diselenide **14a** led to a significant reduction of sialic acid expression in tested cells. At a final concentration of 50 μM in cell culture medium, the 6'-sialyl-LacNAc entity was reduced by approximately 85% (Fig. 3).

As expected, selenide **16a** did not alter cell surface sialylation at tested conditions. Total inhibition of cell surface 6'-sialyl-LacNAc expression was not observed. This is most likely due to uptake and reutilization of sialic acids from the serum

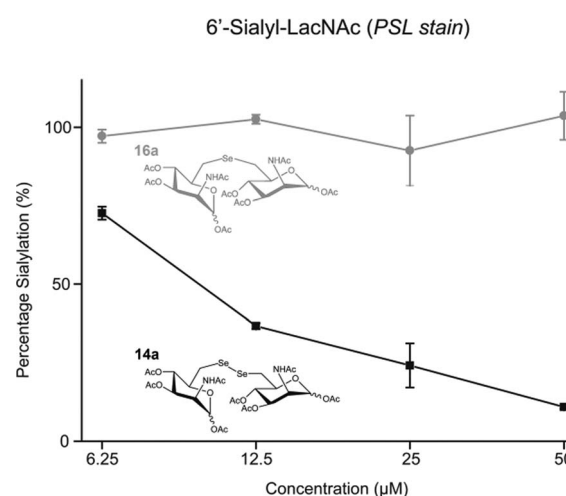


Fig. 3 Diselenide **14a** reduced 6'-sialyl-LacNAc expression in Jurkat cells. Selenide **16a** had no visible effect on cell surface sialylation. Data shown represent the means \pm SEM obtained in a triplicate.

supplement and its conversion to CMP-sialic acid independent of GNE/MNK activity.³¹ A slow turnover of sialylated glycoproteins could additionally contribute to this finding.³²

Conclusions

In summary, the performed enzymatic assays showed that diselenide **14b** is a potent MNK inhibitor both *in vitro* and *in cellulo* with an IC₅₀ value of 8.5 μM, representing the strongest inhibition of all previously reported MNK inhibitors. The homodimeric structure including a diselenide linker introduced at position C6 proved to be highly beneficial for the inhibitory activity of the compound. Finally, we demonstrated that the peracetylated diselenide **14a** was successfully capable of reducing cell surface sialylation in Jurkat cells. With the C6-modified ManNAc analogs presented in this work new insight could be attained into inhibition of the key enzyme of sialic acid biosynthesis, the GNE/MNK. We hope that strong GNE/MNK inhibitors like the described **14a/14b**, pave the way for future studies elucidating the effects of GNE/MNK inhibition *in vivo*.

Acknowledgements

The authors acknowledge support from the DFG (SFB 765 and SPP 1623 to CPRH), the Fonds der Chemischen Industrie (FCI to CPRH), the Einstein Foundation (to CPRH), the DAAD (post-doctoral scholarship to ONG), the Sonnenfeld-Stiftung Berlin (to WR) and the Elfriede and Roland Schauer Stiftung (to WR), Dr Natali Wisbrun for the supply of mouse liver and Prof. H. J. Gabius for providing FITC-conjugated *Polyporus squamosus* lectin.

References

- 1 A. Varki, *FASEB J.*, 1997, **11**, 248.
- 2 S. Kelm and R. Schauer, *Int. Rev. Cytol.*, 1997, **175**, 137.
- 3 R. Schauer, *Curr. Opin. Struct. Biol.*, 2009, **19**, 507.
- 4 C. J. Russell and R. G. Webster, *Cell*, 2005, **123**, 368.
- 5 Y. J. Kim and A. Varki, *Glycoconjugate J.*, 1997, **14**, 569.
- 6 S. Chen and M. Fukuda, *Methods Enzymol.*, 2006, **416**, 371.
- 7 V. P. Bhavanandan, *Glycobiology*, 1991, **1**, 493.
- 8 L. Chen and J. F. Liang, *Eur. J. Pharm. Biopharm.*, 2012, **81**, 339.
- 9 For a review on MOE, see: (a) O. T. Keppler, R. Horstkorte, M. Pawlita, C. Schmidt and W. Reutter, *Glycobiology*, 2001, **11**, 11R–18R; (b) D. H. Dube and C. R. Bertozzi, *Curr. Opin. Chem. Biol.*, 2003, **7**, 616; (c) J. Du, M. A. Meledeo, Z. Wang, H. S. Khanna, V. D. Paruchuri and K. J. Yarema, *Glycobiology*, 2009, **19**, 1382; (d) B. J. Beahm and C. R. Bertozzi, *Imaging Cell-Surface in Animals with Bioorthogonal Chemistry*, ed. T. Endo, P. H. Seeberger, G. W. Hart, C.-H. Wong and T. Taniguchi, *Glycoscience: Biology and Medicine*, Springer, Japan, 2014.
- 10 (a) H. Kayser, R. Zeitler, C. Kannicht, D. Grunow, R. Nuck and W. Reutter, *J. Biol. Chem.*, 1992, **267**, 16934–16938; (b) K. Mahal, K. J. Yarema and C. R. Bertozzi, *Science*, 1997, **276**, 1125.
- 11 (a) E. Saxon and C. R. Bertozzi, *Science*, 2000, **287**, 2007; (b) J. A. Prescher, D. H. Dube and C. R. Bertozzi, *Nature*, 2004, **430**, 873.
- 12 H. Möller, V. Bohrsch, J. Bentrop, J. Bender, S. Hinderlich and C. P. Hackenberger, *Angew. Chem., Int. Ed.*, 2012, **51**, 5986.
- 13 C. D. Rillahan, A. Antonopoulos, C. T. Lefort, R. Sonon, P. Azadi, K. Ley, A. Dell, S. M. Haslam and J. C. Paulson, *Nat. Chem. Biol.*, 2012, **8**, 661.
- 14 C. D. Rillahan, S. J. Brown, A. C. Register, H. Rosen and J. C. Paulson, *Angew. Chem., Int. Ed.*, 2011, **50**, 12534.
- 15 M. S. Macauley, B. M. Arlian, C. D. Rillahan, P. C. Pang, N. Bortell, M. C. G. Marcondes, S. M. Haslam, A. Dell and J. C. Paulson, *J. Biol. Chem.*, 2014, **289**, 35149.
- 16 O. T. Keppler, S. Hinderlich, J. Langner, R. Schwartz-Albiez, W. Reutter and M. Pawlita, *Science*, 1999, **284**, 1372.
- 17 R. Zeitler, A. Giannis, S. Danneschewski, E. Henk, T. Henk, C. Bauer, W. Reutter and K. Sandhoff, *Eur. J. Biochem.*, 1992, **204**, 1165.
- 18 A. Blume, H. Chen, W. Reutter, R. R. Schmidt and S. Hinderlich, *FEBS Lett.*, 2002, **521**, 127.
- 19 F. Stoltz, M. Reiner, A. Blume, W. Reutter and R. R. Schmidt, *J. Org. Chem.*, 2004, **69**, 665.
- 20 S. Al-Rawi, S. Hinderlich, W. Reutter and A. Giannis, *Angew. Chem., Int. Ed.*, 2004, **43**, 4366.
- 21 X. Zhu, F. Stoltz and R. R. Schmidt, *J. Org. Chem.*, 2004, **69**, 7367.
- 22 P. R. Wratil, S. Rigol, B. Solecka, G. Kohla, C. Kannicht, W. Reutter, A. Giannis and L. D. Nguyen, *J. Biol. Chem.*, 2014, **289**, 32056.
- 23 J. Martinez, L. D. Nguyen, S. Hinderlich, R. Zimmer, E. Tauberger, W. Reutter, W. Saenger, H. Fan and S. Moniot, *J. Biol. Chem.*, 2012, **287**, 13656.
- 24 Tosylated ManNAc **8** was prepared according to the protocol reported in: R. Thomson and M. von Itzstein, *Carbohydr. Res.*, 1995, **274**, 29.
- 25 For a proposed mechanism of C-2 base catalyzed epimerization of ManNAc, see: T. Toida, I. R. Vlahov, A. E. Smith, R. E. Hileman and R. J. Linhardt, *J. Carbohydr. Chem.*, 1996, **15**, 351.
- 26 As an example of ¹H NMR assignment for the protons at position 6 of C6-thiol and C6-disulfide modified piranoses, see: M. Guillemineau, S. Singh, M. Grossutti and F. I. Auzanneau, *Carbohydr. Res.*, 2010, **345**, 2723.
- 27 V. Fourniere and I. Cumpstey, *Tetrahedron Lett.*, 2010, **51**, 2127.
- 28 For the values of bond angles and lengths in diselenides and selenoethers, see: (a) C. Paulmier, *Selenium Reagents and Intermediates in Organic Synthesis*, Pergamon Press, Oxford, 1st edn, 1986; to compare the bond angles and lengths in dimethyl ether, thioether and selenoethers, see: (b) D. R. Lide, *Handbook of Chemistry and Physics*, CRC Press, Boca Raton, Florida, 74th edn, 1994; for a discussion of the significant differences between C–O, C–S and C–Se in saccharides, see: (c) S. André, K. E. Kövér, H.-J. Gabius and L. Szilágyi, *Bioorg. Med. Chem. Lett.*, 2015, **25**, 931 and ref. 27.



- 29 M. B. Jones, H. Teng, J. K. Rhee, N. Lahar, G. Baskaran and K. J. Yarema, *Biotechnol. Bioeng.*, 2004, **85**, 394.
- 30 H. Mo, H. C. Winter and I. J. Goldstein, *J. Biol. Chem.*, 2000, **275**, 10623.
- 31 (a) C. Oetke, S. Hinderlich, R. Brossmer, W. Reutter, M. Pawlita and O. T. Keppler, *Eur. J. Biochem.*, 2001, **268**, 4553; (b) C. D. Rillahan, A. Antonopoulos, C. T. Lefort, R. Sonon, P. Azadi, K. Ley, A. Dell, S. M. Haslam and J. C. Paulson, *Nat. Chem. Biol.*, 2012, **8**, 661.
- 32 K. Mendla, J. Baumkötter, C. Rosenau, B. Ulrich-Bott and M. Cantz, *Biochem. J.*, 1988, **250**, 261.



Electronic Supporting Information (ESI)

Inhibition of the key enzyme of sialic acid biosynthesis by C6-Se modified N-acetylmannosamine analogs

O. Nieto-García,^{+,a} P. R. Wratil,^{+,b} L. D. Nguyen,^b Verena Böhrsch,^a S. Hinderlich,^{*,c} W. Reutter,^{*,b} and C. P. R. Hackenberger^{*,a,d}

^aLeibniz-Institut für Molekulare Pharmakologie, Robert-Roessle-Strasse 10, 13125 Berlin, Germany

^bInstitut für Laboratoriumsmedizin, klinische Chemie und Pathobiochemie, Charité-Universitätsmedizin Berlin, Arnimallee 22, 14195 Berlin Germany

^cBeuth Hochschule für Technik Berlin, Department Life Sciences & Technology, Seestrasse 64, 13347 Berlin, German

^dHumboldt Universität zu Berlin, Department Chemie, Brook-Taylor-Strasse 2, 12489, Berlin, Germany

⁺Both authors contributed equally to this work

Email: hinderlich@beuth-hochschule.de, werner.reutter@charite.de
or hackenberger@fmp-berlin.de

Contents:

General Remarks	S1
Experimental procedures for 9 , 10 , 11 , 12 , 14a , 14b , 15 , 16a , 16b , 18a and 18b	S2
N-Acetylmannosamine kinase and N-acetylglucosamine kinase expression and purification	S7
N-Acetylmannosamine kinase, N-acetylglucosamine kinase and yeast hexokinase inhibition experiments	S8
UDP-GlcNAc-2-epimerase activity assays	S9
Cytotoxicity studies	S10
Determination of cell surface sialylation	S10
NMR spectra for new compounds	S13
Evaluation of the stability of the diselenide 14b in presence of Dithiothreitol (DTT)	S27

General Remarks

Reagents and dry solvents were purchased in the highest available commercial quality and used as supplied. Reactions were monitored by TLC with pre-coated silica gel 60 F254 aluminum plates using UV light as the visualizing agent and by dipping the plate into a solution of *p*-anisaldehyde/H₂SO₄ in EtOH, followed by heating. Flash column chromatography was performed with silica gel (0.035-0.070 mm, 60 Å). Concentrations were carried out in a rotary evaporator. ¹H, ¹³C, dept and ⁷⁷Se NMR

were recorded using either Bruker Ultrashield 300 MHz spectrometer or Bruker Ultrashield AV 600 MHz, as indicated. Chemical shifts are reported in ppm and coupling constants in Hz; multiplicities are given as follows: s (singlet), br s (broad singlet), br d (broad doublet), d (doublet), dd (doublet of doublets), ddd (doublet of double doublets), t (triplet), and m (multiplet). The composition (- α,α -,- β,β -, - α,β - or - β,α -) of the disaccharides **12**, **14a**, **14b**, **16a** and **16b** could not be determined. Therefore, NMR data was given for the single anomers: alpha or beta. Mass spectra were recorded on Agilent 6210 ToF LC/MS system and an Acquity UPLC System (Waters) coupled to an ESI-TOF (electrospray-time of flight) unit LCT Premier (Waters Micromass Technologies). Protein purification was carried out on an Äkta™ purifier system (GE Healthcare). Enzyme activity studies were performed using a Multiskan GO plate reader (Thermo Scientific). For fluorescence-activated cell sorting experiments a FACSCANTO II flow cytometer (BD Biosciences) was used. To determine IC₅₀- and K_i-values, sigmoidal and linear curve approximations were performed using Origin 8.5 Pro (Perkin Elmer).

Experimental procedures

2-Acetamido-1,3,4-tri-O-acetyl-6-S-acetyl-2,6-dideoxy-6-thio- α,β -D-mannopyranose (9)

Potassium thioacetate (341 mg, 2.99 mmol) was added to a solution of **8** (500 mg, 0.9 mmol) in dry DMF (8 mL) under argon. After stirring for 20 h at 95 °C (external bath temp), the solvent was removed *in vacuo*. Chromatography (60% EtOAc/hexane) afforded thiosugar **9** as a foam (388 mg, 96%): R_f(80% EtOAc/hexane) = 0.40; *alpha* anomer: ¹H NMR (300 MHz, CDCl₃) δ: 5.95 (d, J = 1.6 Hz, 1H), 5.84 (d, J = 9.2 Hz, 1H), 5.28 (dd, J = 10.1, 4.5 Hz, 1H), 5.07 (t, J = 10.1 Hz, 1H), 4.59 (ddd, J = 9.2, 4.5, 1.6 Hz, 1H), 3.99 (td, J = 10.1, 4.8 Hz, 1H), 3.04-3.16 (m, 2H), 2.34 (s, 3H), 2.14 (s, 3H), 2.10 (s, 3H), 2.06 (s, 3H), 1.98 (s, 3H); ¹³C NMR (75 MHz, CDCl₃) δ: 194.6, 170.3, 170.2, 170.1, 168.4, 91.8, 71.3, 68.9, 67.7, 49.5, 30.6, 30.1, 23.5, 21.0 (2C), 20.9; *beta* anomer: ¹H NMR (300 MHz, CDCl₃) δ: 5.84-5.74 (m, 2H), 5.09-5.02 (m, 2H), 4.78-4.68 (m, 1H), 3.78-3.64 (m, 1H), 3.04-3.16 (m, 2H), 2.34 (s, 3H), 2.14 (s, 3H), 2.10 (s, 3H), 2.06 (s, 3H), 1.98 (s, 3H); ¹³C NMR (75 MHz, CDCl₃) δ: 194.5, 170.8, 170.3, 170.3, 168.5, 90.8, 74.8, 71.5, 67.5, 49.8, 30.6, 30.1, 23.6, 20.9 (3C); HRMS (ESI-TOF, M+H) *m/z*: calcd. for (C₁₆H₂₄NO₉S): 406.1172, found: 406.1165.

2-Acetamido-1,3,4-tri-O-acetyl-6-Se-cyanyl-2,6-dideoxy- α,β -D-mannopyranose (10)

Potassium selenocyanate (190 mg, 1.32 mmol) was added to a solution of **8** (440 mg, 0.88 mmol) in dry DMF (12 mL) under argon. After stirring for 20 h at 95 °C (external bath temp), the solvent was removed *in vacuo*. Chromatography (50% EtOAc/hexane) afforded selenocyanate **10** as a foam (350 mg, 91%): R_f (80% EtOAc/hexane) = 0.38; *alpha*-anomer: ¹H NMR (300 MHz, CDCl₃) δ: 6.02 (d, J = 1.8 Hz, 1H), 5.94 (d, J = 9.1 Hz, 1H), 5.35 (dd, J = 10.0, 4.5 Hz, 1H), 5.10 (t, J = 10.0 Hz, 1H), 4.65 (ddd, J = 9.1, 4.5, 1.8 Hz, 1H), 4.13 (ddd, J = 10.0, 7.6, 3.1 Hz, 1H), 3.35 (dd, J = 12.9, 3.1 Hz, 1H), 3.06 (dd, J = 12.9, 7.6 Hz, 1H), 2.19 (s, 3H), 2.10 (s,

3H), 2.06 (s, 3H), 2.01 (s, 3H); ^{13}C NMR (75 MHz, CDCl_3) δ : 170.4, 170.3, 170.0, 168.2, 101.6, 91.6, 70.4, 68.9, 68.4, 49.4, 30.6, 23.3, 20.9, 20.8 (2C); ^{77}Se NMR (114 MHz, CDCl_3) δ : 176.2; *beta-anomer*: 5.87-5.80 (m, 2H), 5.08-5.01 (m, 2H), 4.78-4.68 (m, 1H), 3.89-3.75 (m, 1H), 3.37-3.30 (m, 1H), 3.14 (dd, $J = 12.9, 7.6$ Hz, 1H), 2.19 (s, 3H), 2.10 (s, 3H), 2.06 (s, 3H), 2.01 (s, 3H); ^{13}C NMR (75 MHz, CDCl_3) δ : 170.9, 170.5, 170.2, 168.5, 101.7, 90.5, 73.8, 71.1, 68.7, 49.6, 30.6, 23.5, 20.9, 20.8 (2C); ^{77}Se NMR (114 MHz, CDCl_3) δ : 175.2; HRMS (ESI-TOF, M+H) *m/z*: calcd. for ($\text{C}_{15}\text{H}_{21}\text{N}_2\text{O}_8\text{Se}$): 437.0463, found: 437.0470.

6-6'-Diselenobis-(2-acetamido-1,3,4-tri-O-acetyl-2,6-dideoxy-D-mannopyranose) (14a)

A mixture of selenocyanate **10** (142 mg, 0.33 mmol) and NaBH_4 (12 mg, 0.33 mmol) in dry MeOH (6 mL) was stirred for 10 min at rt under argon. The pH of the mixture was adjusted to 5 with 5% aqueous AcOH and the solvent was evaporated *in vacuo*. Chromatography (80% EtOAc/hexane \rightarrow 10% MeOH/EtOAc) afforded diselenide **14a** (110 mg, 83%) as a white foam: $R_f = 0.18$ (100% EtOAc); *alpha anomer*: ^1H NMR (600 MHz, CDCl_3) δ : 6.14-6.10 (m, 1H), 5.99 (d, $J = 1.8$ Hz, 1H), 5.31 (dd, $J = 9.9, 4.7$, 1H), 5.08 (t, $J = 9.9$ Hz, 1H), 4.63 (ddt, $J = 9.3, 4.7, 1.8$ Hz, 1H), 4.01 (ddd, $J = 9.9, 6.1, 3.4$ Hz, 1H), 3.24 (dd, $J = 13.0, 3.4$ Hz, 1H), 3.10-3.04 (m, 1H), 2.18 (s, 3H), 2.07 (s, 3H), 2.05 (s, 3H), 2.00 (s, 3H); ^{13}C NMR (75 MHz, CDCl_3) δ : 170.5, 170.2 (2C), 168.7, 91.7, 72.2, 69.1, 68.7, 49.4, 32.9, 23.3, 21.1, 21.0, 20.9; ^{77}Se NMR (114 MHz, CDCl_3) δ : 319.1; *beta anomer*: ^1H NMR (600 MHz, CDCl_3) δ 5.92 (d, $J = 9.2$ Hz, 1H), 5.90 (d, $J = 1.8$ Hz, 1H), 5.31 (dd, $J = 9.5, 4.4$ Hz, 1H), 5.03 (t, $J = 9.5$ Hz, 1H), 4.77 (ddd, $J = 9.2, 4.4, 1.8$ Hz, 1H), 3.84 (ddd, $J = 9.5, 7.9, 3.5$ Hz, 1H), 3.30-3.25 (m, 1H), 3.02 (dd, $J = 12.9, 7.9$ Hz, 1H), 2.16 (s, 3H), 2.10 (s, 3H), 2.06 (s, 3H), 2.00 (s, 3H); ^{13}C NMR (75 MHz, CDCl_3) δ : 170.8, 170.3, 170.2, 168.8, 90.5, 74.3, 71.6, 68.9, 49.7, 33.5, 23.5, 21.0, 21.0, 20.9; ^{77}Se NMR (114 MHz, CDCl_3) δ : 323.9; HRMS (ESI-TOF, M+H) *m/z*: calcd. for ($\text{C}_{28}\text{H}_{41}\text{N}_2\text{O}_{16}\text{Se}_2$): 821.0787, found: 821.0782.

2-Acetamido-1,3,4-tri-O-acetyl-6-bromo-2,6-dideoxy- α,β -D-mannopyranose (15)

Lithium bromide (424 mg, 4.89 mmol) was added to a solution of **8** (700 mg, 1.40 mmol) in dry DMF (12 mL) at rt under argon. After stirring for 24 h at 85 °C, the solvent was evaporated. Chromatography (50% EtOAc/hexane) gave bromide **15** as a white foam (550 mg, 96%): R_f (70% EtOAc/hexane) = 0.45; *alpha anomer*: ^1H NMR (300 MHz, CDCl_3) δ : 6.03 (d, $J = 1.9$ Hz, 1H), 5.95 (d, $J = 9.5$ Hz, 1H), 5.32 (dd, $J = 9.9, 4.4$ Hz, 1H), 5.21 (t, $J = 9.9$ Hz, 1H), 4.62 (ddd, $J = 9.5, 4.4, 1.9$ Hz, 1H), 3.99 (ddd, $J = 9.9, 4.6, 2.9$ Hz, 1H), 3.52 (dd, $J = 11.3, 2.9$ Hz, 1H), 3.38 (dd, $J = 11.3, 4.6$ Hz, 1H), 2.15 (s, 3H), 2.07 (s, 3H), 2.04 (s, 3H), 1.99 (s, 3H); ^{13}C NMR (75 MHz, CDCl_3) δ : 170.3, 170.2, 169.7, 168.3, 91.7, 70.9, 68.8, 67.9, 49.2, 31.9, 23.4, 20.9 (2C), 20.8; *beta anomer*: ^1H NMR (300 MHz, CDCl_3) δ : 5.89 (d, $J = 1.6$ Hz, 1H), 5.87-5.80 (m, 1H), 5.28-5.20 (m, 1H), 5.15-5.05 (m, 1H), 4.74 (dd, $J = 9.8, 4.7$ Hz,

1H), 3.79 (ddd, J = 8.6, 4.7, 3.1 Hz, 1H), 3.61-3.50 (m, 1H), 3.43-3.36 (m, 1H), 2.15 (s, 3H), 2.10 (s, 3H), 2.07 (s, 3H), 1.99 (s, 3H); ^{13}C NMR (75 MHz, CDCl_3) δ : 170.8, 170.3, 169.7, 168.6, 90.4, 73.8, 71.4, 67.5, 49.5, 31.3, 23.5, 21.0, 20.9, 20.8; HRMS (ESI-TOF, M+H) m/z : calcd. for ($\text{C}_{14}\text{H}_{21}\text{BrNO}_8$): 410.0451, found: 410.0452.

6-6'-Selenobis-(2-acetamido-1,3,4-tri-O-acetyl-2,6-dideoxy-D-mannopyranose) (16a)

A solution of selenocyanate **10** (150 mg, 0.34 mmol) in dry THF/MeOH (2:1, 6 mL) was treated with NaBH_4 (20 mg, 0.52 mmol) at rt under argon. After stirring for 15 min, bromide **15** (633 mg, 1.55 mmol) was added and the mixture stirred at rt for 1.5 h. The pH of the mixture was adjusted to 5 with a 1 M aqueous solution of HCl and the solvent evaporated *in vacuo*. Chromatography (80% \rightarrow 100% EtOAc/hexane) gave selenoether **16a** (175 mg, 69%) as a white foam: R_f = 0.24 (100% EtOAc); *alpha anomer*: ^1H NMR (600 MHz, CDCl_3) δ : 6.25-6.13 (m, 1H), 5.93 (d, J = 1.8 Hz, 1H), 5.30 (dd, J = 10.0, 4.5 Hz, 1H), 5.17 (t, J = 10.0 Hz, 1H), 4.62 (ddd, J = 9.4, 4.5, 1.9 Hz, 1H), 4.00 (dt, J = 9.4, 3.7 Hz, 1H), 2.87 (dd, J = 13.3, 3.7 Hz, 1H), 2.76-2.63 (m, 1H), 2.16 (s, 3H), 2.06 (s, 6H), 1.99 (s, 3H); ^{13}C NMR (75 MHz, CDCl_3) δ : 170.5, 170.3, 170.2, 168.6, 91.6, 72.5, 68.9, 68.8, 49.1, 26.4, 23.3, 21.0, 20.9 (2C) ^{77}Se NMR (114 MHz, CDCl_3) δ : 114.5; *beta anomer*: ^1H NMR (600 MHz, CDCl_3) δ : 6.01 (d, J = 9.2 Hz, 1H), 5.83 (d, J = 1.6 Hz, 1H), 5.12-5.05 (m, 1H), 5.03 (dd, J = 9.7, 3.8 Hz, 1H), 4.74 (ddd, J = 9.2, 3.8, 1.6 Hz, 1H), 3.79 (ddd, J = 9.7, 6.2, 3.7 Hz, 1H), 2.91 (dd, J = 13.0, 3.7 Hz, 1H), 2.76-2.63 (m, 1H), 2.16 (s, 3H), 2.09 (s, 3H), 2.08 (s, 3H), 1.97 (s, 3H); ^{13}C NMR (75 MHz, CDCl_3) δ : 170.9, 170.6, 170.3, 168.6, 90.5, 75.2, 72.6, 71.5, 49.7, 26.5, 23.4, 20.9 (2C), 20.8; ^{77}Se NMR (114 MHz, CDCl_3) δ : 118.4; HRMS (ESI-TOF, M+H) m/z : calcd. for ($\text{C}_{28}\text{H}_{41}\text{N}_2\text{O}_{16}\text{Se}$): 741.1621, found: 741.1632.

2-Acetamido-1,3,4-tri-O-acetyl-6-Se-butyl-2,6-dideoxy-6-seleno- α,β -D-mannopyranose (18a)

A solution of **10** (80 mg, 0.18 mmol) in dry THF/MeOH (2:1, 3 mL) was treated with NaBH_4 (10 mg, 0.28 mmol) at rt under argon. After stirring for 15 min, 1-iodopentane (**17**) (63 μL , 0.55 mmol) was added and the mixture stirred at rt for 1 h. The pH of the mixture was adjusted to 5 with a 1 M aqueous solution of HCl and the solvent evaporated *in vacuo*. Chromatography (50% EtOAc/hexane) gave selenide **18a** (55 mg, 65%) as a white foam: R_f = 0.44 (60% EtOAc/hexane); *alpha anomer*: ^1H NMR (600 MHz, CDCl_3) δ : 5.97 (d, J = 1.6 Hz, 1H), 5.96-5.90 (m, 1H), 5.32 (dd, J = 10.5, 3.4 Hz, 1H), 5.22 (t, J = 10.5 Hz, 1H), 4.67-4.55 (m, 1H), 4.06-3.95 (m, 1H), 2.86-2.74 (m, 1H), 2.69-2.59 (m, 3H), 2.15 (s, 3H), 2.05 (s, 6H), 1.99 (s, 3H), 1.60 (p, J = 7.4 Hz, 2H), 1.38 (h, J = 8.1, 7.4 Hz, 2H), 0.90 (t, J = 7.4 Hz, 3H); ^{13}C NMR (75 MHz, CDCl_3) δ : 170.3 (2C), 170.1, 168.4, 91.6, 72.3, 69.0, 68.8, 49.1, 32.7, 32.6, 25.9, 23.4, 23.0, 21.0, 20.9 (2C), 13.7; ^{77}Se NMR (114 MHz, CDCl_3) δ : 131.3; *beta anomer*: ^1H NMR (600 MHz, CDCl_3) δ : 5.91 (d, J = 9.2 Hz, 1H), 5.83 (d, J = 1.4 Hz, 1H), 5.17 (t, J = 10.0 Hz, 1H), 5.02 (dd, J = 10.0, 4.0 Hz, 1H), 4.73 (ddd, J = 9.2, 4.0, 1.4 Hz, 1H), 3.81-3.75 (m, 1H), 2.86-2.74 (m, 1H), 2.69-2.59 (m, 3H), 2.15 (s, 3H),

2.05 (s, 6H), 1.99 (s, 3H), 1.60 (p, $J = 7.4$ Hz, 2H), 1.38 (h, $J = 8.1, 7.4$ Hz, 2H), 0.90 (t, $J = 7.4$ Hz, 3H); ^{13}C NMR (75 MHz, CDCl_3) δ : 170.7, 170.3, 170.0, 168.5, 90.4, 75.3, 71.6, 68.7, 49.7, 32.7, 32.6, 25.7, 23.4, 23.0, 21.0, 20.9 (2C), 13.7; ^{77}Se NMR (114 MHz, CDCl_3) δ : 134.4; HRMS (ESI-TOF, M+H) m/z : calcd. for ($\text{C}_{18}\text{H}_{30}\text{NO}_8\text{Se}$): 468.1137, found: 468.1140.

O-Acetyl deprotection conditions: The corresponding peracetylated precursors **9**, **14a**, **16a** and **18a** were dissolved in MeOH and treated with NaOMe (1 equiv., 5.4 M in MeOH) for 10 min at rt. The pH of the mixture was adjusted to 5 with a 1 M aqueous solution of HCl, the solvent was evaporated and a final silica gel column chromatography (under the elution conditions specified) gave the desired unprotected sugars.

2-Acetamido-6-S-acetyl-2,6-dideoxy- α,β -D-mannopyranose (11)

Thiol **11** [from **9** (150 mg, 0.13 mmol), column eluent (100% EtOAc \rightarrow 10% MeOH/EtOAc \rightarrow 20% MeOH/EtOAc), 50 mg, 58%, white solid, R_f (20% MeOH/EtOAc) = 0.5]; *alpha* anomer: ^1H NMR (300 MHz, D_2O) δ : 5.10 (s, 1H), 4.28 (d, $J = 4.9$ Hz, 1H), 4.02 (dd, $J = 9.8, 4.9$ Hz, 1H), 3.88 (ddd, $J = 9.8, 7.3, 2.8$ Hz, 1H), 3.58 (t, $J = 9.8$ Hz, 1H), 3.07-2.92 (m, 1H), 2.77-2.67 (m, 1H), 2.03 (s, 3H); ^{13}C NMR (75 MHz, D_2O) δ : 174.7, 92.9, 72.2, 69.2, 68.4, 53.2, 25.0, 21.8; *beta* anomer: ^1H NMR (300 MHz, D_2O) δ : 5.02 (d, $J = 1.7$ Hz, 1H), 4.44 (d, $J = 4.5$ Hz, 1H), 3.80 (dd, $J = 9.2, 4.5$ Hz, 1H), 3.50-3.39 (m, 2H), 3.07-2.92 (m, 1H), 2.77-2.67 (m, 1H), 2.07 (s, 3H); ^{13}C NMR (75 MHz, D_2O) δ : 175.6, 92.9, 76.6, 71.6, 69.0, 53.9, 24.9, 21.9; HRMS (ESI-TOF, M+1) m/z : calcd. for ($\text{C}_8\text{H}_{16}\text{NO}_5\text{S}$): 238.0749, found: 238.0755.

6-6'-Dithiobis-(2-acetamido-2-deoxy-D-mannopyranose) (12)

Disulfide **12** [from **9** (150 mg, 0.13 mmol), column eluent (100% EtOAc \rightarrow 10% MeOH/EtOAc \rightarrow 20% MeOH/EtOAc), 25 mg, 28%, white solid, R_f (20% MeOH/EtOAc) = 0.14]; *alpha* anomer: ^1H NMR (600 MHz, D_2O) δ : 5.15 (d, $J = 1.5$ Hz, 1H), 4.35 (dd, $J = 4.7, 1.5$ Hz, 1H), 4.20-4.11 (m, 1H), 4.12-4.02 (m, 1H), 3.40-3.33 (m, 1H), 2.99-2.87 (m, 2H), 2.09 (s, 3H). ^{13}C NMR (151 MHz, D_2O) δ : 174.8, 93.0, 71.8, 70.0, 68.6, 53.4, 39.9, 22.0; *beta* anomer: ^1H NMR (600 MHz, D_2O) δ : 5.07 (d, $J = 1.5$ Hz, 1H), 4.52-4.48 (m, 1H), 3.89-3.82 (m, 1H), 3.68-3.58 (m, 1H), 3.49 (t, $J = 9.7$ Hz, 1H), 2.99-2.87 (m, 2H), 2.13 (s, 3H); ^{13}C NMR (151 MHz, D_2O) δ : 175.7, 93.1, 74.5, 70.2, 69.8, 54.1, 39.7, 22.1; HRMS (ESI-TOF, M+H) m/z : calcd. for ($\text{C}_{16}\text{H}_{29}\text{N}_2\text{O}_{10}\text{S}_2$): 473.1264, found: 473.1269.

6-6'-Diselenobis-(2-acetamido-2-deoxy-D-mannopyranose) (14b)

Diselenide **14b** [from **14a** (110 mg, 0.13 mmol), column eluent (100% EtOAc \rightarrow 20% MeOH/EtOAc), 36 mg, 47%, white solid, R_f (20% MeOH/EtOAc) = 0.14]; *alpha* anomer: ^1H NMR (600 MHz, D_2O) δ : 5.14 (s, 1H), 4.39-4.28 (m, 1H), 4.12-4.04 (m, 1H), 3.65-3.51 (m, 2H), 3.49-3.40 (m, 1H), 3.15-3.05 (m, 1H), 2.09 (s, 3H);

¹³C NMR (151 MHz, D₂O) δ 174.3, 92.5, 71.3, 70.2, 68.0, 52.9, 30.8, 21.5; ⁷⁷Se NMR (114 MHz, D₂O) δ: 282.8, 280.3; *beta anomer*: ¹H NMR (600 MHz, D₂O) δ: 5.06 (s, 1H), 4.52-4.41 (m, 1H), 3.89-3.83 (m, 1H), 3.65-3.51 (m, 2H), 3.49-3.40 (m, 1H), 3.15-3.05 (m, 1H) 2.13 (s, 3H); ¹³C NMR (151 MHz, D₂O) δ 175.2, 92.6, 71.1, 70.1, 69.9, 53.7, 30.6, 21.7; ⁷⁷Se NMR (114 MHz, D₂O) δ: 288.2, 285.5; HRMS (ESI-TOF, M+H) *m/z*: calcd. for (C₁₆H₂₉N₂O₁₀Se₂): 569.0153, found: 569.0155.

6-6'-Selenobis-(2-acetamido-2,6-dideoxy-D-mannopyranose) (**16b**)

Selenoether **16b** [from **16a** (125 mg, 0.17 mmol), column eluent (100% EtOAc → 10% MeOH/EtOAc), 60 mg, 73%, oil, R_f (10% MeOH/EtOAc) = 0.12]; *alpha anomer*: ¹H NMR (600 MHz, D₂O) δ: 5.13 (d, *J* = 1.5 Hz, 1H), 4.33 (d, *J* = 4.8 Hz, 1H), 4.07 (dd, *J* = 9.9, 4.8 Hz, 1H), 4.05-3.98 (m, 1H), 3.58 (t, *J* = 9.9 Hz, 1H), 3.25-3.17 (m, 1H), 2.94-2.84 (m, 1H), 2.09 (s, 3H); ¹³C NMR (75 MHz, D₂O) δ: 174.7, 92.9, 71.5, 70.4, 68.4, 53.2, 25.4, 21.8; ⁷⁷Se NMR (114 MHz, D₂O) δ: 98.1; *beta anomer*: ¹H NMR (600 MHz, D₂O) δ: 5.06 (d, *J* = 1.8 Hz, 1H), 4.49 (dd, *J* = 4.5, 1.8 Hz, 1H), 4.05-3.99 (m, 1H), 3.84 (dd, *J* = 9.8, 4.5 Hz, 1H), 3.47 (t, *J* = 9.8 Hz, 1H), 3.25-3.17 (m, 1H), 2.94-2.84 (m, 1H), 2.09 (s, 3H); ¹³C NMR (75 MHz, D₂O) δ: 175.5, 92.8, 76.2, 71.4, 70.7, 53.9, 25.7, 22.0; ⁷⁷Se NMR (114 MHz, D₂O) δ: 91.9; HRMS (ESI-TOF, M+H) *m/z*: calcd. for (C₁₆H₂₉N₂O₁₀Se): 489.0987, found: 489.0987.

2-Acetamido-6-*Se*-butyl-2,6-dideoxy-6-seleno- α,β -D-mannopyranose (**18b**)

Selenoether **18b** [from **18a** (180 mg, 0.38 mmol), column eluent (100% EtOAc → 10% MeOH/EtOAc), 90 mg, 69%, oil, R_f (10% MeOH/EtOAc) = 0.40]; *alpha anomer*: ¹H NMR (600 MHz, D₂O) δ : 5.12 (d, *J* = 1.5 Hz, 1H), 4.32 (dd, *J* = 4.8, 1.5 Hz, 1H), 4.05 (dd, *J* = 9.8, 4.8 Hz, 1H), 3.98 (td, *J* = 9.8, 2.8 Hz, 1H), 3.55 (t, *J* = 9.8 Hz, 1H), 3.15-3.08 (m, 1H), 2.81 (ddd, *J* = 13.2, 8.3, 6.9 Hz, 1H), 2.78-2.65 (m, 2H), 2.08 (s, 3H), 1.70 (p, *J* = 7.4 Hz, 2H), 1.42 (h, *J* = 7.4 Hz, 2H), 0.92 (t, *J* = 7.4 Hz, 3H); ¹³C NMR (151 MHz, D₂O) δ: 174.3, 92.5, 71.1, 70.4, 68.0, 52.9, 31.4, 24.1, 21.8, 21.6, 21.5, 12.3; ⁷⁷Se NMR (114 MHz, D₂O) δ: 110.5; *beta anomer*: ¹H NMR (600 MHz, D₂O) δ: 5.04 (d, *J* = 1.5 Hz, 1H), 4.49-4.42 (m, 1H), 3.95-3.90 (m, 1H), 3.83 (dd, *J* = 9.7, 4.8 Hz, 1H), 3.54-3.50 (m, 1H), 3.15-3.08 (m, 1H), 2.81 (ddd, *J* = 13.2, 8.3, 6.9 Hz, 1H), 2.78-2.65 (m, 2H), 2.08 (s, 3H), 1.70 (p, *J* = 7.4 Hz, 2H), 1.42 (h, *J* = 7.4 Hz, 2H), 0.92 (t, *J* = 7.4 Hz, 3H); ¹³C NMR (151 MHz, D₂O) δ: 175.2, 92.5, 75.8, 71.3, 70.1, 53.6, 31.4, 24.3, 21.8, 21.6, 21.5, 12.3; ⁷⁷Se NMR (114 MHz, D₂O) δ: 115.9; HRMS (ESI-TOF, M+H) *m/z*: calcd. for (C₁₂H₂₄NO₅Se): 342.0820, found: 342.0816.

N-Acetylmannosamine kinase and N-acetylglucosamine kinase expression and purification

Human *N*-acetylmannosamine kinase (MNK) was expressed and purified using an established method.¹ Therefore, his-tagged MNK was expressed in BL21-CodonPlus (DE3)-RIL *Escherichia coli* (Stragene). Purification was performed by Ni-NTA affinity chromatography, and subsequently size exclusion chromatography on a SuperdexTM HighLoad 16/600 column (GE Healthcare).

GST-Tagged human *N*-acetylglucosamine kinase (GNK) was expressed in BL21-CodonPlus(DE3)-RIL *Escherichia coli* (Stragene) as described.² Purification was performed by glutathione affinity chromatography, followed by size exclusion chromatography on a SuperdexTM HighLoad 16/600 column (GE Healthcare).

To evaluate their purity, protein samples were mixed with SDS-PAGE sample buffer, denatured at 90 °C for 1 min and separated by a 10% SDS-PAGE gel. Proteins were visualized with Coomassie G-250 staining solution (Biorad), and PageRuler Prestained Plus (Biorad) was used as a marker (Figure S1).

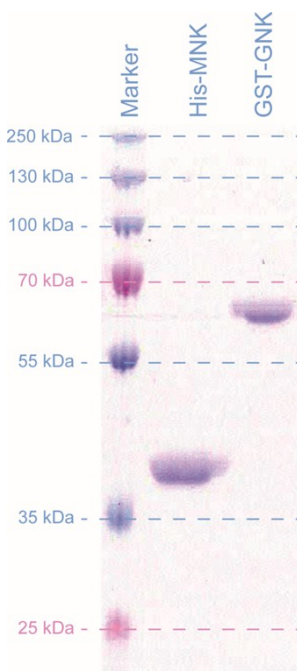


Figure S1. SDS-PAGE of His-tagged MNK (His-MNK) and GST-tagged GNK (GST-GNK) after affinity chromatography and size exclusion chromatography. Apparent molecular masses given by the marker are indicated on the left side.

¹ J. Martinez, L. D. Nguyen, S. Hinderlich, R. Zimmer, E. Tauberger, W. Reutter, W. Saenger, H. Fan and S. Moniot, *J. Biol. Chem.*, 2012, **287**, 13656.

² W.A. Weihofen, M. Berger, H. Chen, W. Saenger, and S. Hinderlich, *J. Mol. Biol.*, 2006, **364**, 388.

Enzyme activity and inhibition studies using *N*-acetylmannosamine kinase, *N*-acetylglucosamine kinase and yeast hexokinase

Evaluation MNK activity in presence of the compounds **11**, **12**, **14b**, **16b** and **18b**

The effects of compounds **11**, **12**, **14b**, **16b**, or **18b** on MNK enzyme activity were evaluated using a coupled optical assay. 55 µl reaction mixture contained the following buffers and reagents: 39.5 µl buffer A (65 mM MgCl₂, 200 mM Tris-HCl, pH 8.1), 5 µl ATP (50 mM), 3.5 µl NADH (30 mM), 2 µl phosphoenolpyruvate (100 mM), 2 U pyruvate-kinase, 2 U lactate-dehydrogenase, 5 µl ManNAc of varying concentrations. Subsequently, 10 µl of the compounds **11**, **12**, **14b**, **16b** and **18b** were added in varying concentrations. The reaction was initiated by adding 0.6 µg MNK in 35 µL buffer B (10 mM Tris-HCl, 150 mM NaCl, pH 8.0). Samples were incubated at 37°C. Spectrophotometric measurements of NADH concentration was performed at 340 nm. Results obtained were normalized to blanks, consisting of 55 µl reaction mixture, 10 µl H₂O and 35 µl buffer B without MNK.

GNK and hexokinase inhibition assays using compound **14b**

To evaluate the specificity of the inhibitor **14b** towards other sugar kinases, we performed further inhibition experiments using human GNK and hexokinase (HK) from yeast (Sigma, H-5000). 39.5 µl Buffer A (see above), 5 µl ATP (50 mM), 3.5 µl NADH (30 mM), 2 µl phosphoenolpyruvate (100 mM), 2 U pyruvate-kinase, 2 U lactate-dehydrogenase, 5 µl GlcNAc (7.5 mM, for GNK experiments), or 5 µl ManNAc (7.5 mM, for GNK experiments), or glucose (5 mM, for HK experiments), and 10 µl **14b** (varying concentrations) were mixed with either 1 µg GNK or 0.2 µg HK in 35 µL buffer B. The decrease of NADH was measured in a spectrophotometer as described above. The IC₅₀ of **14b** for GNK activity was 1.7 mM (\pm 0.7 mM), and > 5 mM for HK activity, respectively (Figure S2).

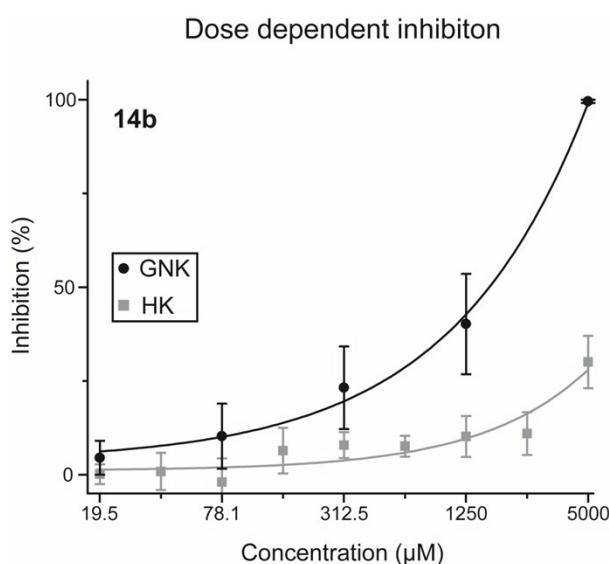


Figure S2. Inhibition of GNK and HK activity by **14b**. Values are means \pm SEM of triplicates

Evaluation of the influence of **14b** on UDP-GlcNAc-2-epimerase activity

To study, if diselenide **14b** interferes with the activity of the GNE domain of the bifunctional enzyme, we used enzymes from mouse liver homogenates. Herein, 5 ml of buffer D (10 mM sodium phosphate, pH 7.1, 1 mM EDTA, 1 mM DTT and cOmplete Protease inhibitor cocktail (Roche) were added to shock-frozen mouse liver (\approx 1 g). The sample was disrupted using an Ultra-Turrax T25 (IKA Labortechnik) twice for 10 s, followed by centrifugation at 35.000 x g for 20 min. The cytosolic supernatant was used for a colorimetric GNE activity assay as reported.³ In brief, a total volume of 200 μ L contained 45 mM sodium phosphate, pH 7.5, 10 mM MgCl₂, 1 mM UDP-GlcNAc and 100 μ L of mouse liver cytosol. The assay was incubated for 45 min at 37 °C and stopped by incubation at 95 °C for 3 min. After a short centrifugation to precipitate insoluble compounds 150 μ L of the supernatant were mixed with 30 μ L of 0.8 M borate, pH 9.1, and boiled for 10 min. Then, 800 μ L of 1% (w/v) 4-dimethylamino benzaldehyde and 1.25% (v/v) 10 M HCl in acetic acid were added. The sample was incubated at 37 °C for 20 min and the absorbance was measured at 578 nm. The IC₅₀ of **14b** for inhibiting GNE activity was determined to be $182 \pm 13 \mu\text{M}$ (Figure S3).

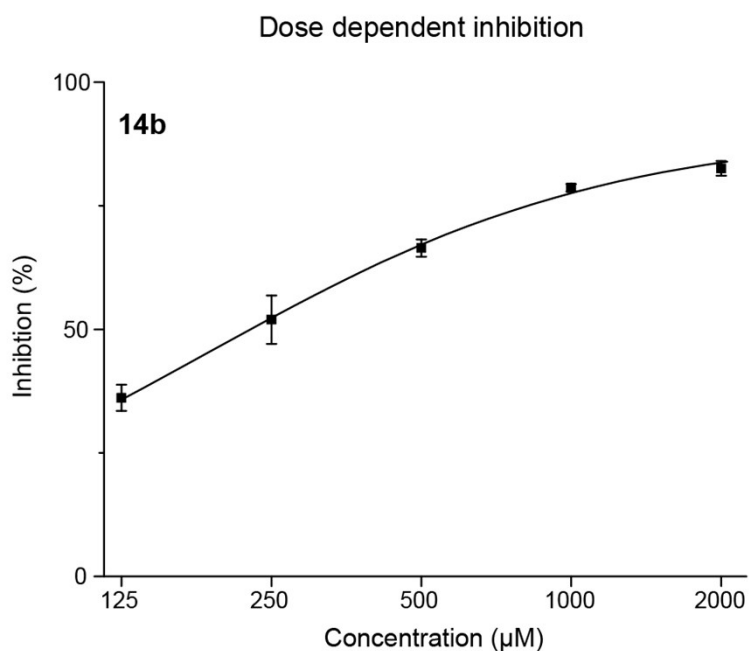


Figure S3. Inhibition of UDP-GlcNAc-2 epimerase activity by **14b**. Values are means \pm SEM of four experiments.

³ W. Reutter, S. Hinderlich and W. Kemmner “UDP-GlcNAc-2-epimerase/ManNAc kinase (GNE), section XV, pp 1511-1522 in N. Taniguchi, K. Honke, M. Fukuda, H. Narimatsu, Y. Yamaguchi and T. Angata eds., *Handbook of Glycosyltransferases and Related Genes*, 2nd edn., Springer Japan, Japan, 2014.

Cytotoxicity studies

The cytotoxicity of compounds **14a** and **16a** in Jurkat cells was evaluated utilizing the AlamarBlue[©] assay (AbD Serotec). Approximately 20,000 Jurkat cells (ATCC) were cultured for 72 h in RPMI 1640 medium (10 % FBS, 2 mM L-glutamine) containing different concentrations of the peracetylated compounds **14a** and **16b**. 10 µl AlamarBlue[©] solution was added, and the cells were incubated for another 4 h. Samples were analyzed in a spectrophotometer at wavelengths of 570 and 620 nm. Experiments were performed in triplicate and normalized to untreated cells (100 % viability) as well as blanks (0 % viability) consisting of cell culture medium without cells (Figure S4).

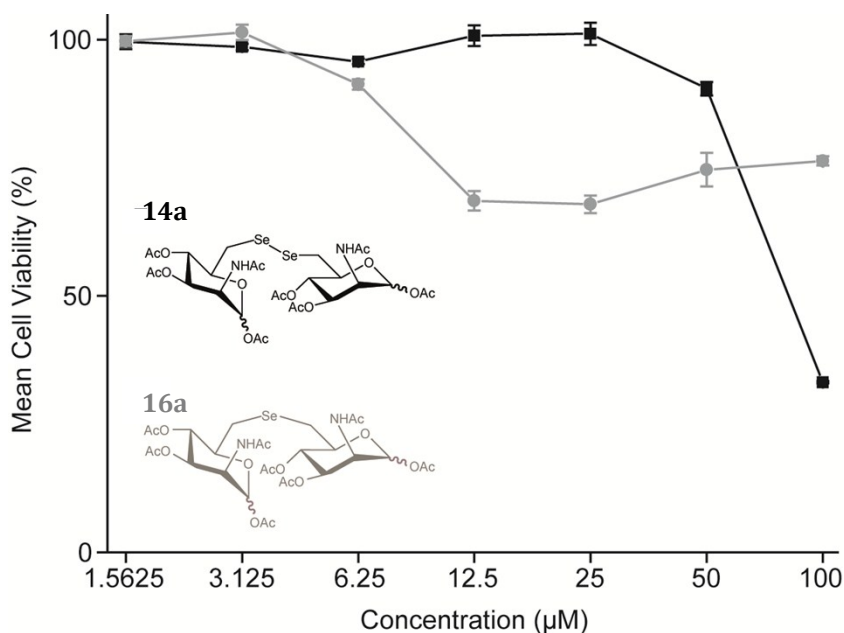


Figure S4. Evaluation of cytotoxicity effects of diselenide **14a** and selenide **16a** in Jurkat cells. Data shown represent the mean values and S.E.M obtained in a triplicate.

Determination of cell surface sialylation

Approximately 20,000 Jurkat cells (ATCC) were cultured for 72 h in 100 µl RPMI 1640 medium with 10 % FBS and 2 mM L-glutamine, containing **14b** or **16b** in varying concentrations. After incubation cells were washed three times with PBS containing 0.5 % bovine serum albumin (PBS + 0.5 % BSA) and labeled for 1 h at 4°C with FITC-conjugated *Polyporus squamosus* lectin (PSL, 0.1 µg/ml). Subsequently, cells were washed three times with PBS + 0.5 % BSA and analyzed on a FACSCanto II flowcytometer (BD Biosciences). Obtained data was normalized to untreated cells and cells treated for 60 min with 0.2 U/ml sialidase from *Clostridium perfringens* (Sigma Aldrich). In order to minimize errors caused by dead cells, only intact cells have been included into the data evaluation, whereas dead cells, small debris and large clumps have been excluded using a probe of untreated cells stained with propidium iodide. Experiments were performed in a triplicate

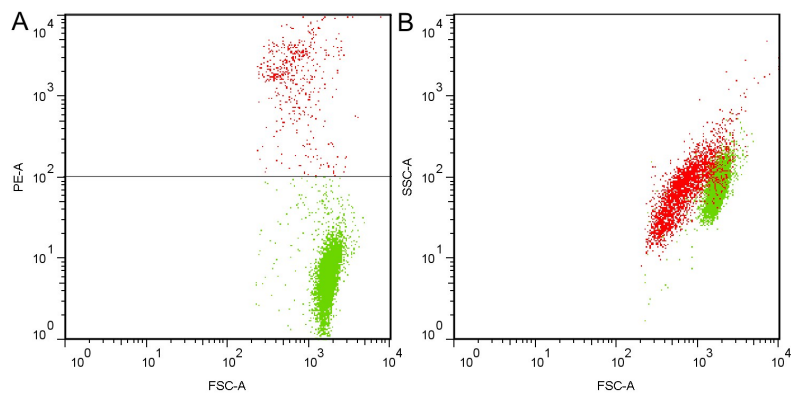


Figure S5. Differentiation between live and dead cells in flow cytometry experiments. In order to exclude dead cells from analysis, a probe of untreated Jurkat cells was stained with propidium iodide (PI) and injected into the flow cytometer. Dot plot (A) depicts forward scattering of light against PE fluorescence (FSC/PE). Red dots represent highly fluorescent dead cells, whereas green dots represent cells that are low fluorescent and therefore considered as being alive. (B) Shows the distribution of PI stained live and dead cells with forward- against side scattering of light (FSC/SSC). To analyze the experiments with FITC-conjugated *Polyporus squamosus* lectin, gates have been used that exclude most of the dead cell population based on this experiment with PI stained untreated cells (see **figure S6**).

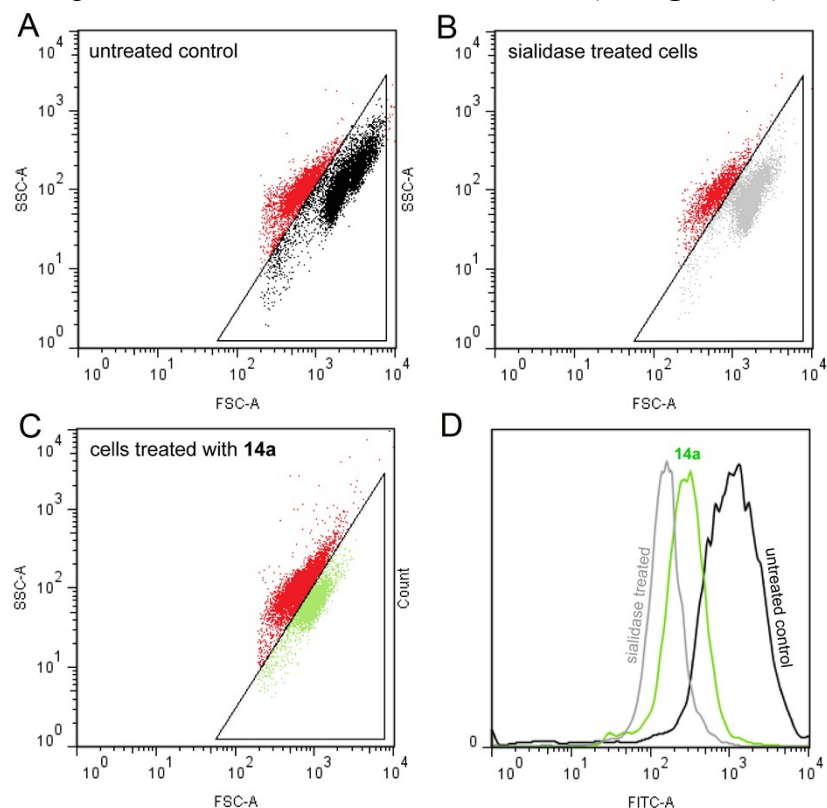
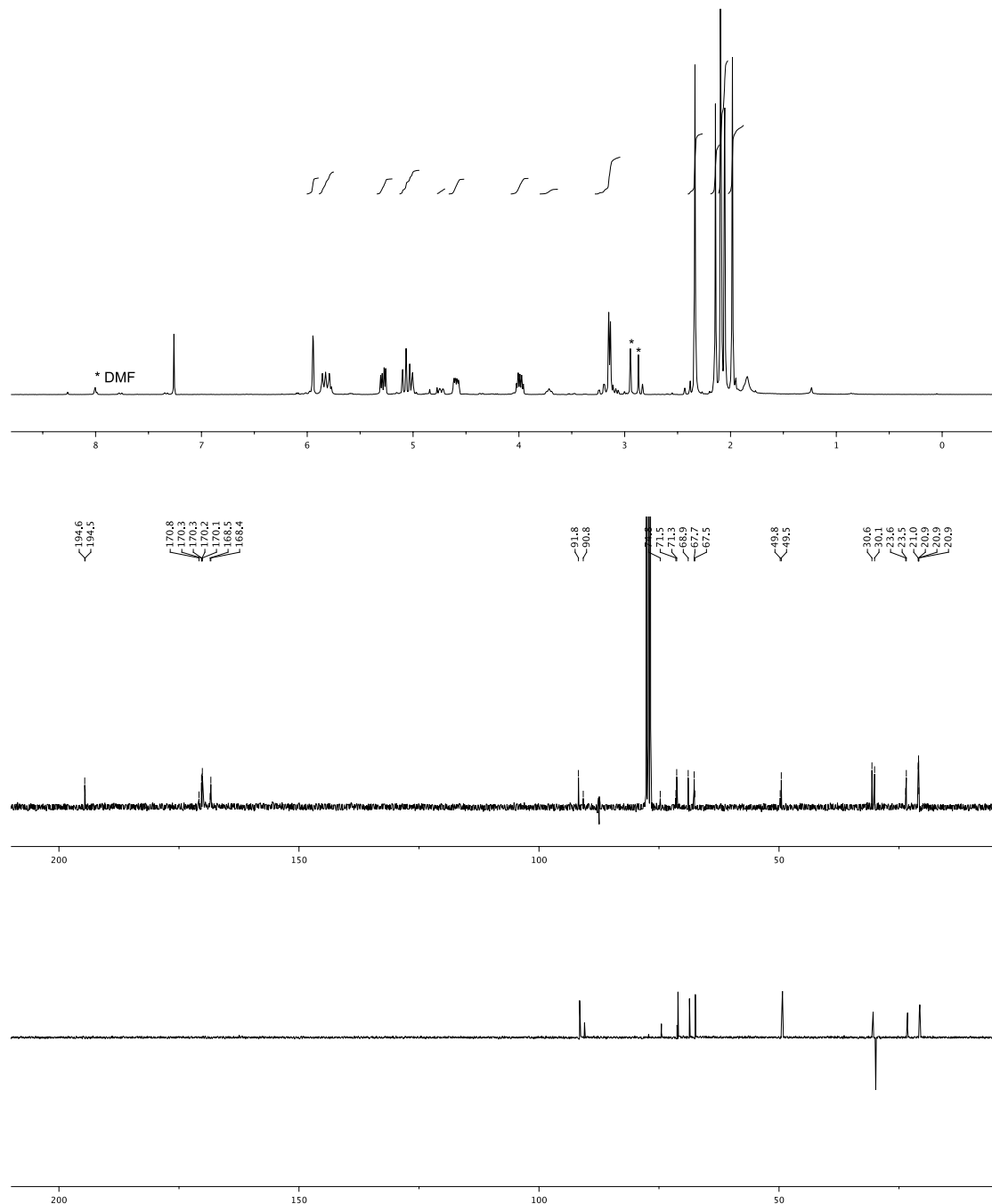
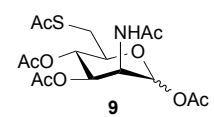
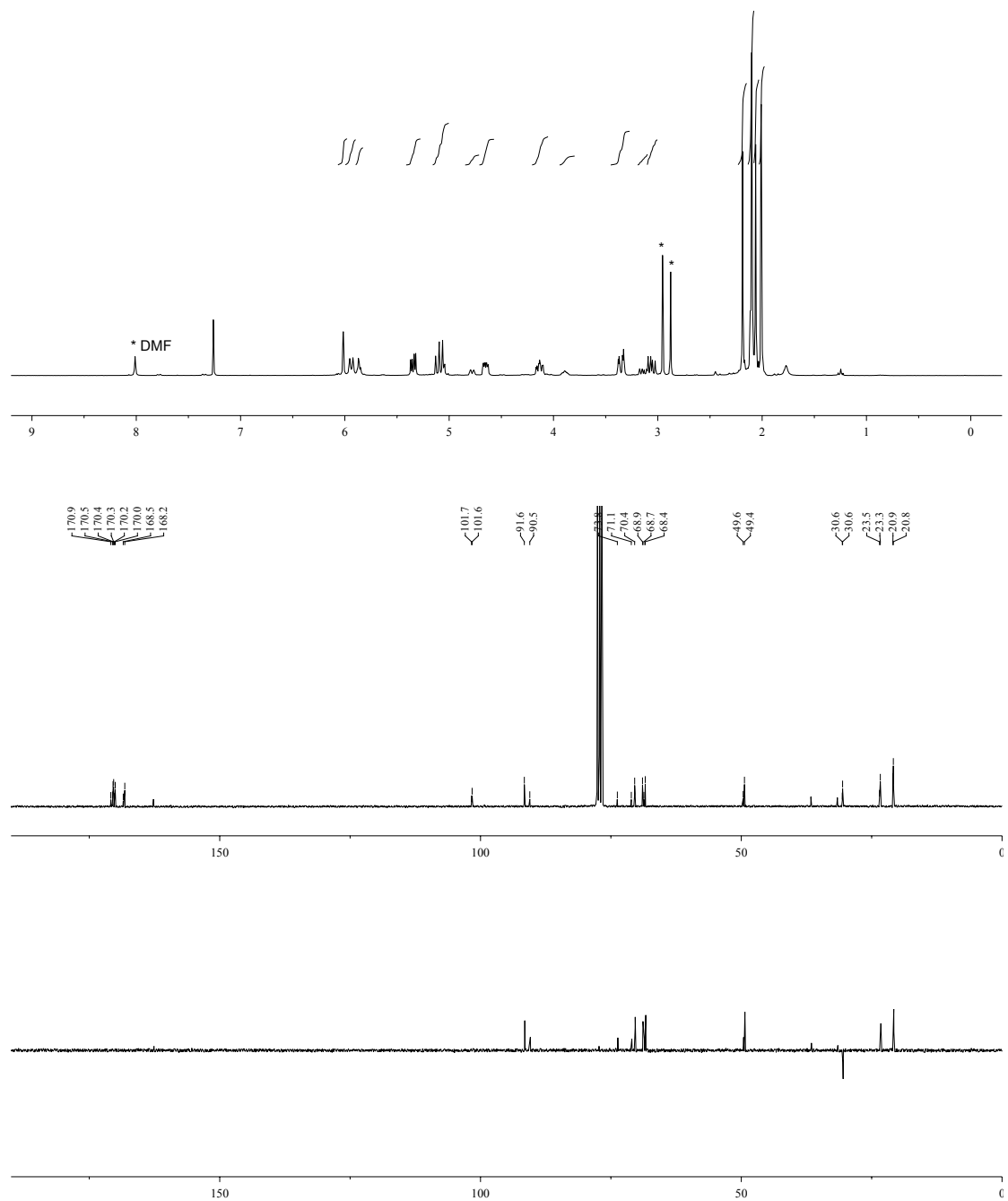
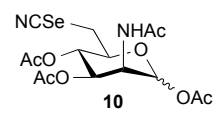


Figure S6. Flow cytometry analysis of Jurkat cells stained with FITC-conjugated *Polyporus squamosus* lectin (PSL). (A) untreated cells, (B) cells treated with sialidase, and (C) cells treated with 50 μ M 14a (C). Triangular gates have been used

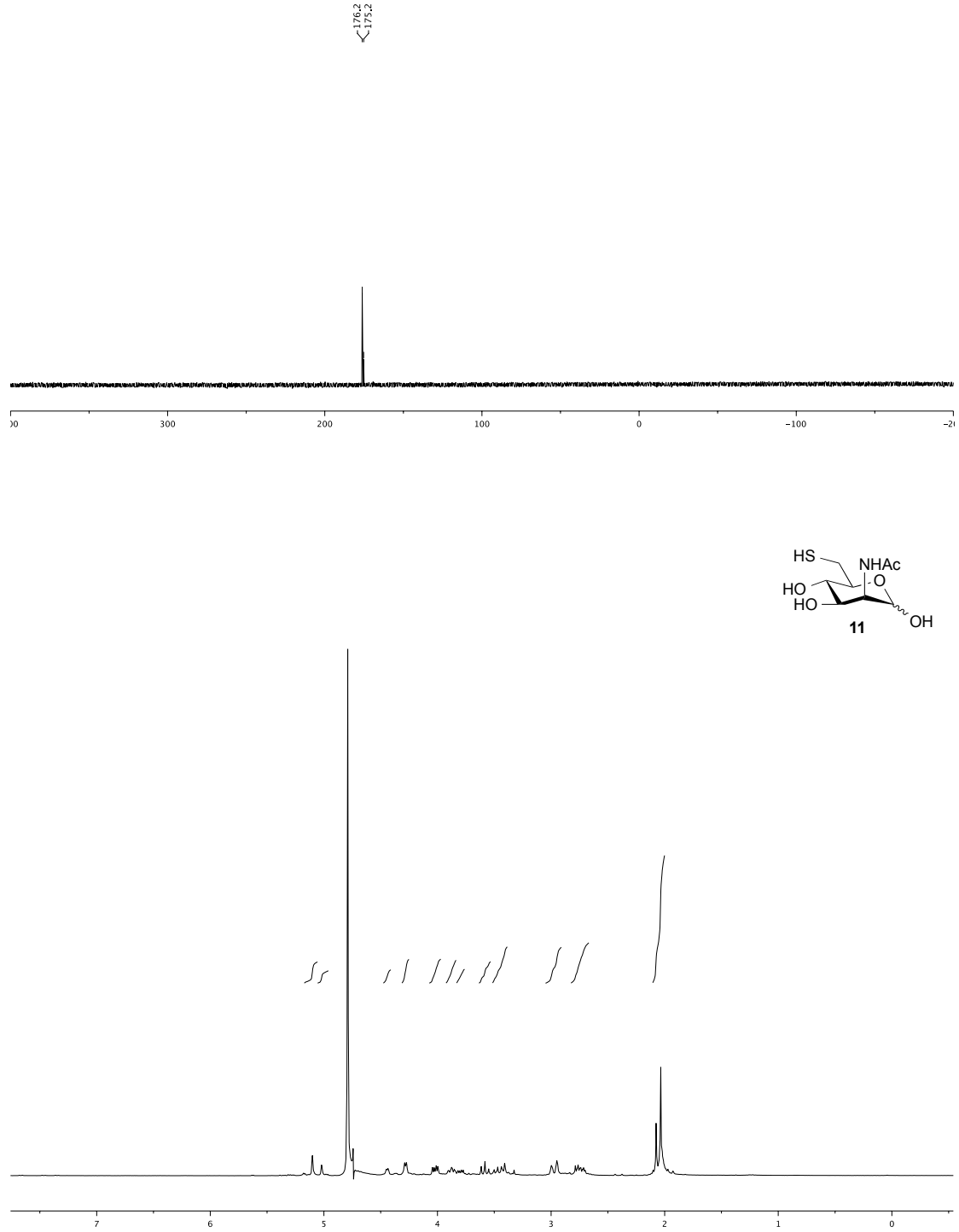
to exclude dead cells, small debris and large clumps (red dots, see **figure S5**). Representative histogram (D) shows that cells treated with 50 μ M **14a** expose less fluorescence than untreated control cells, which indicates lower levels of cell surface sialylation in these inhibitor treated cells.

NMR spectra

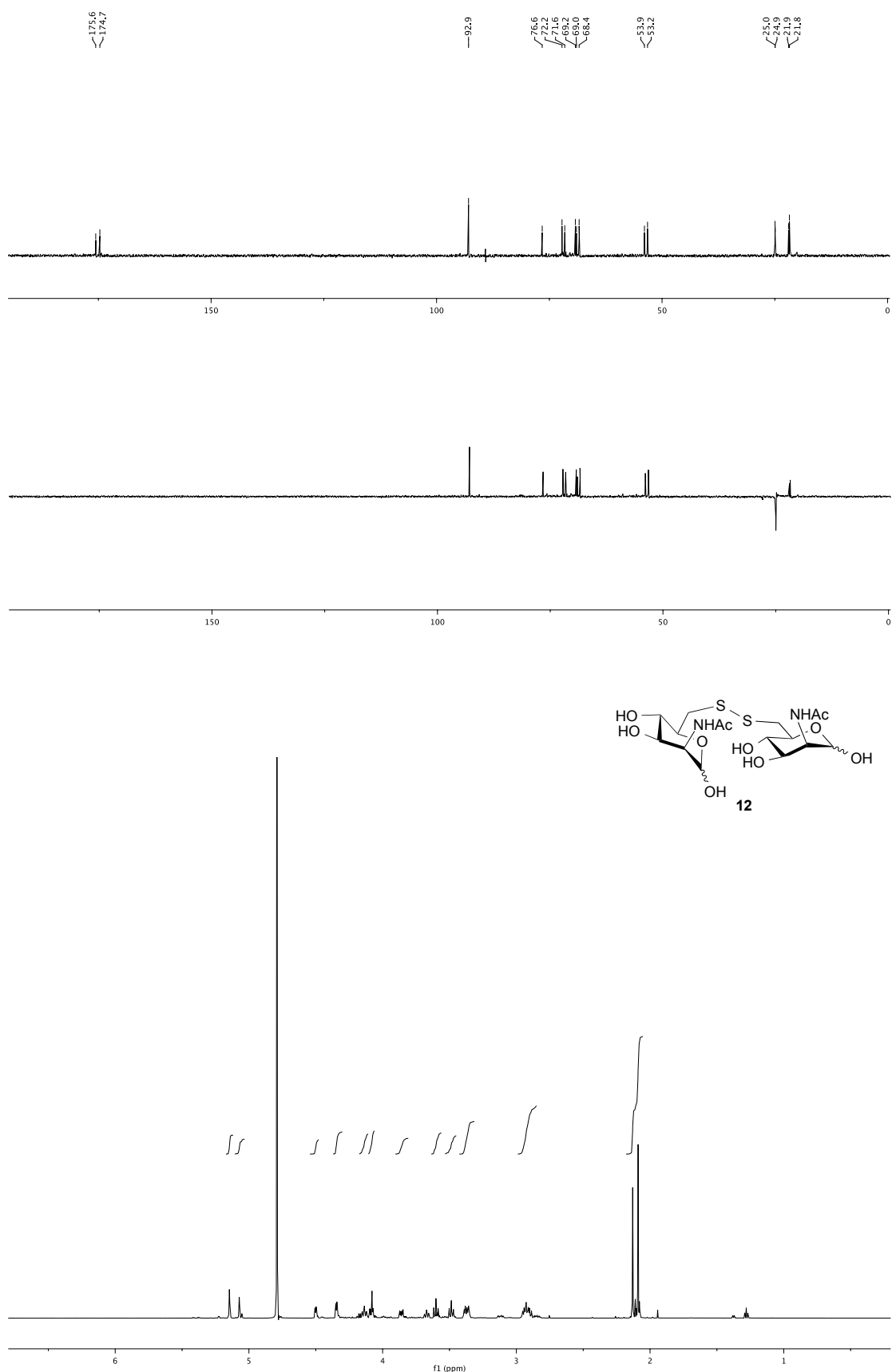




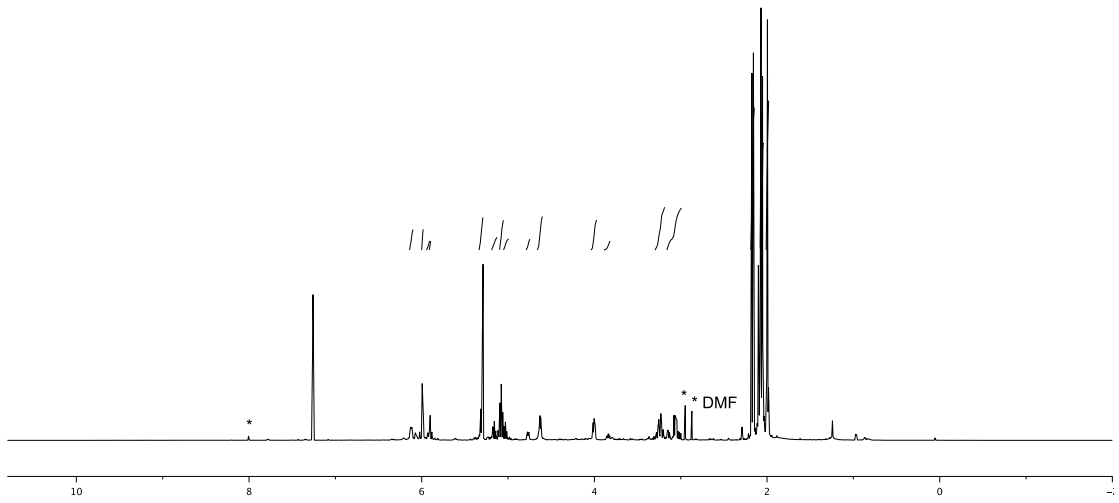
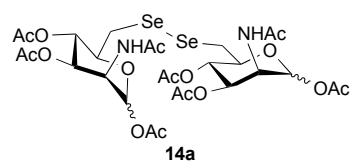
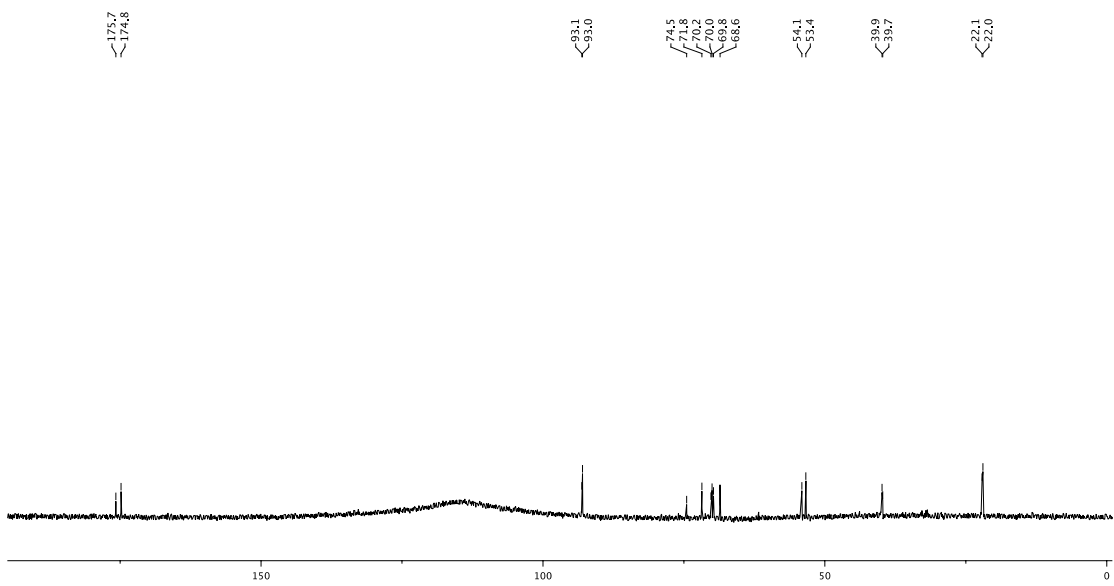
14
(85)

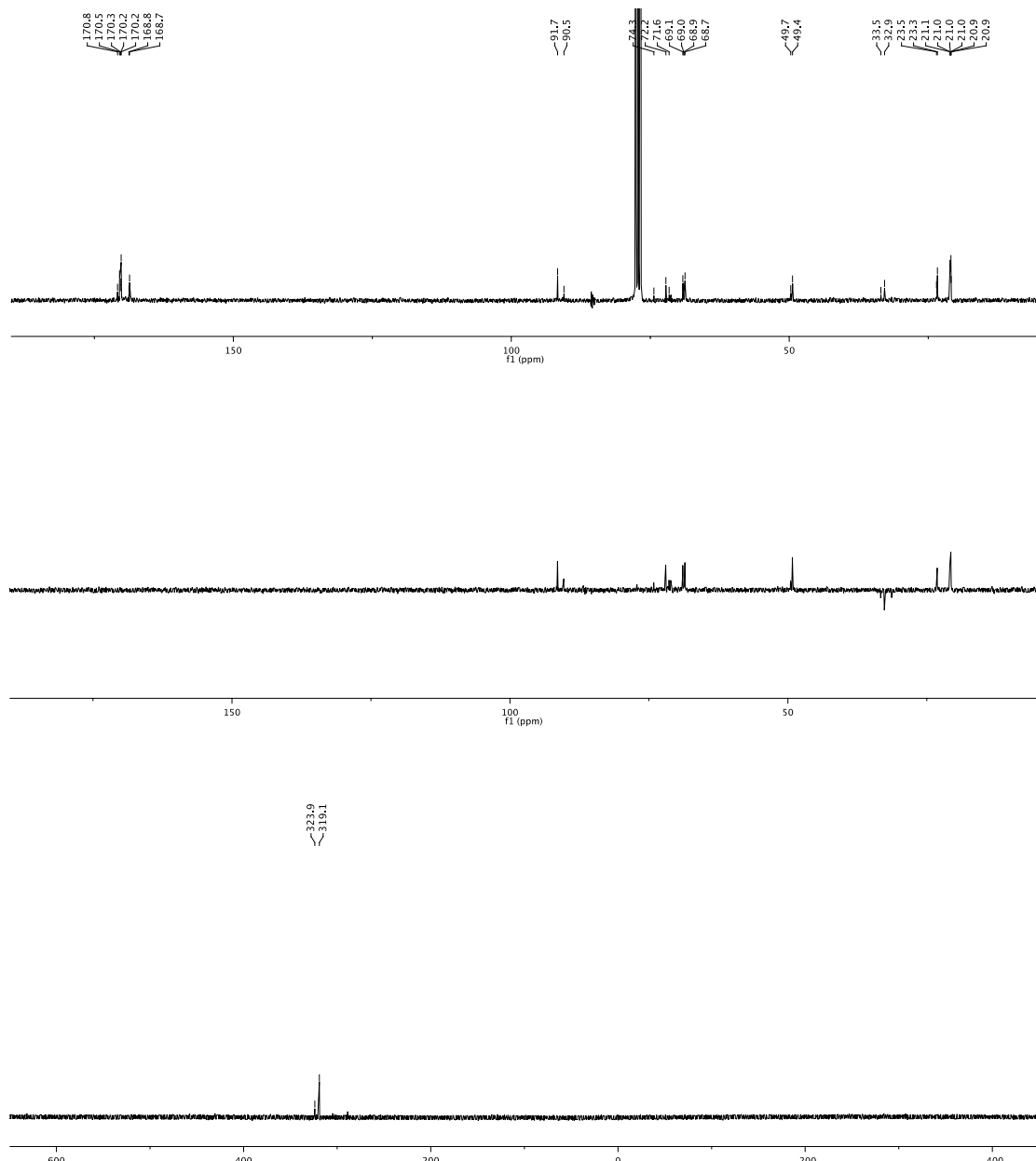


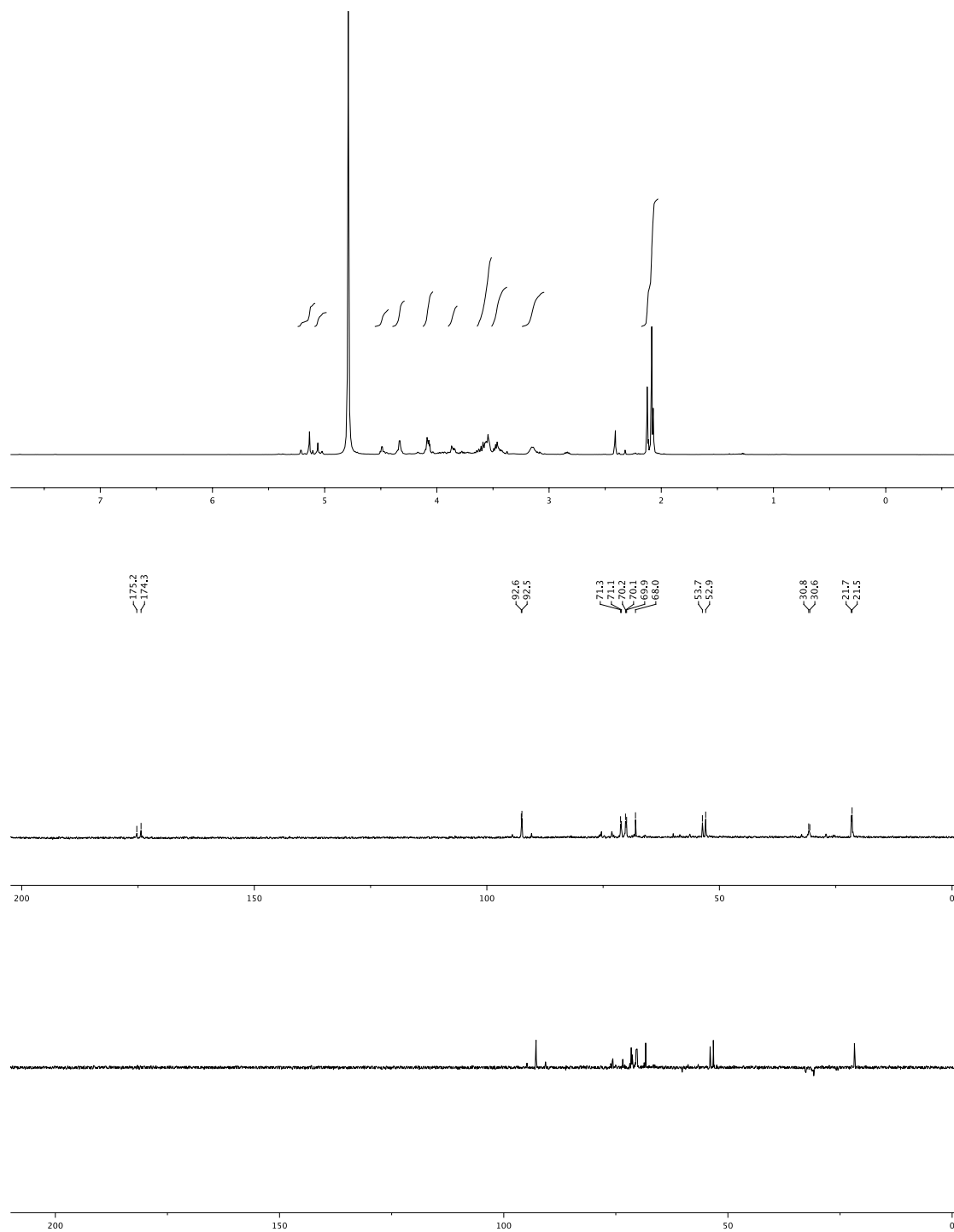
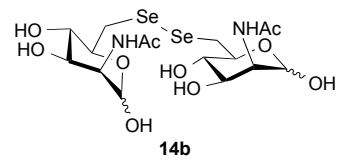
15
(86)



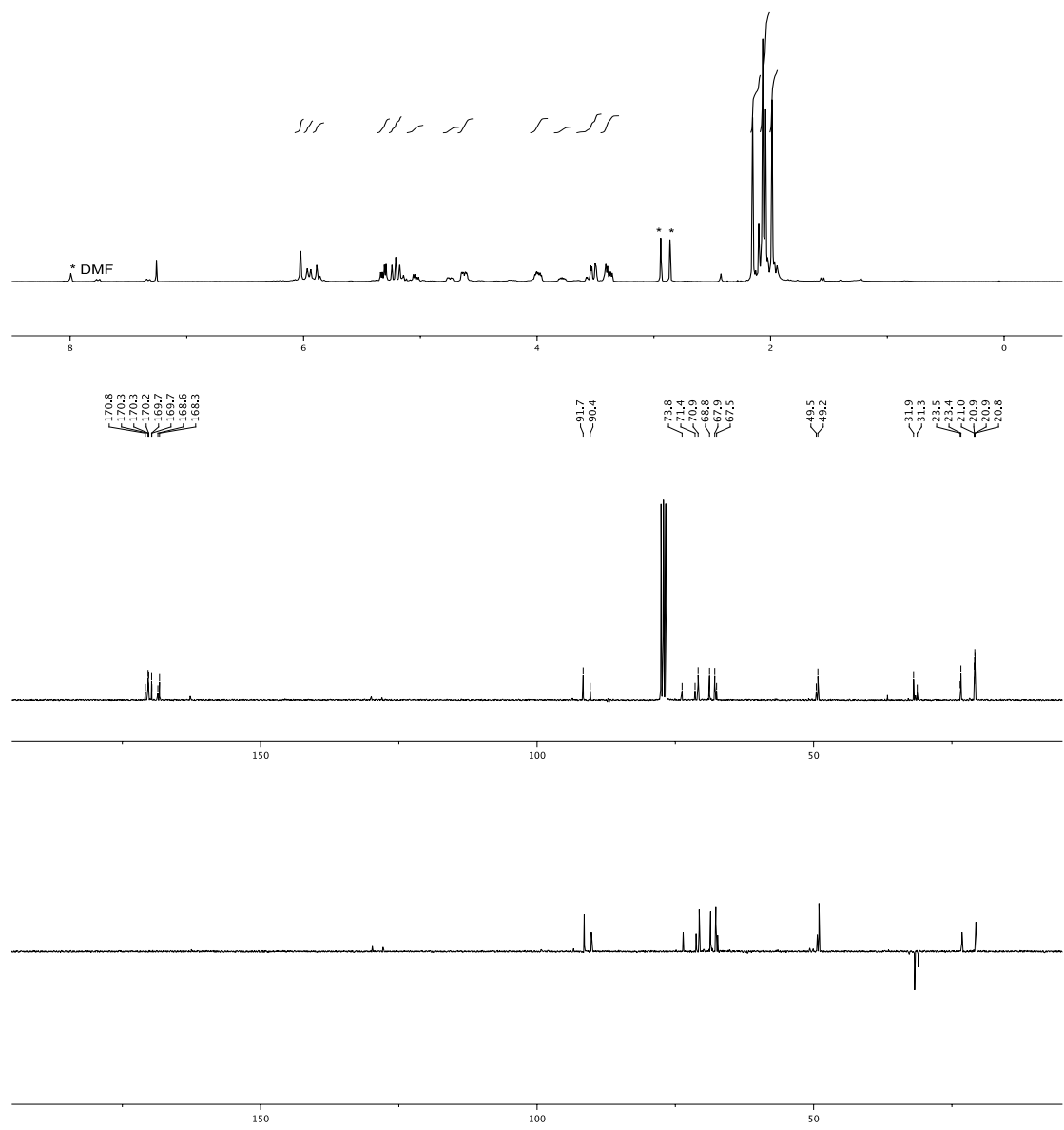
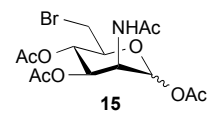
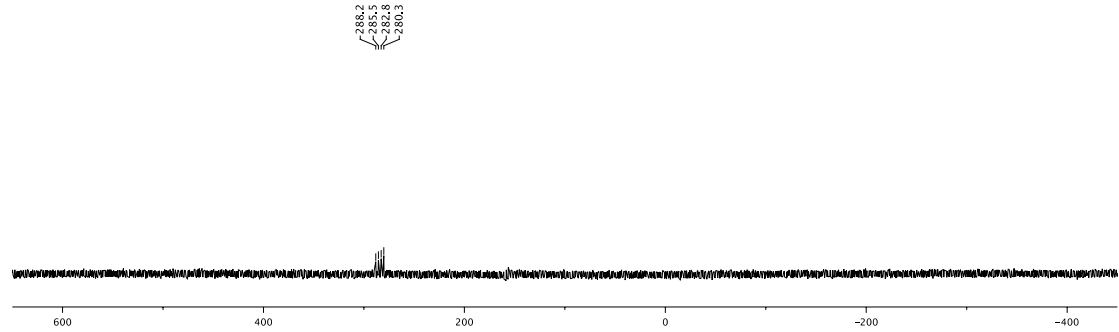
16
(87)



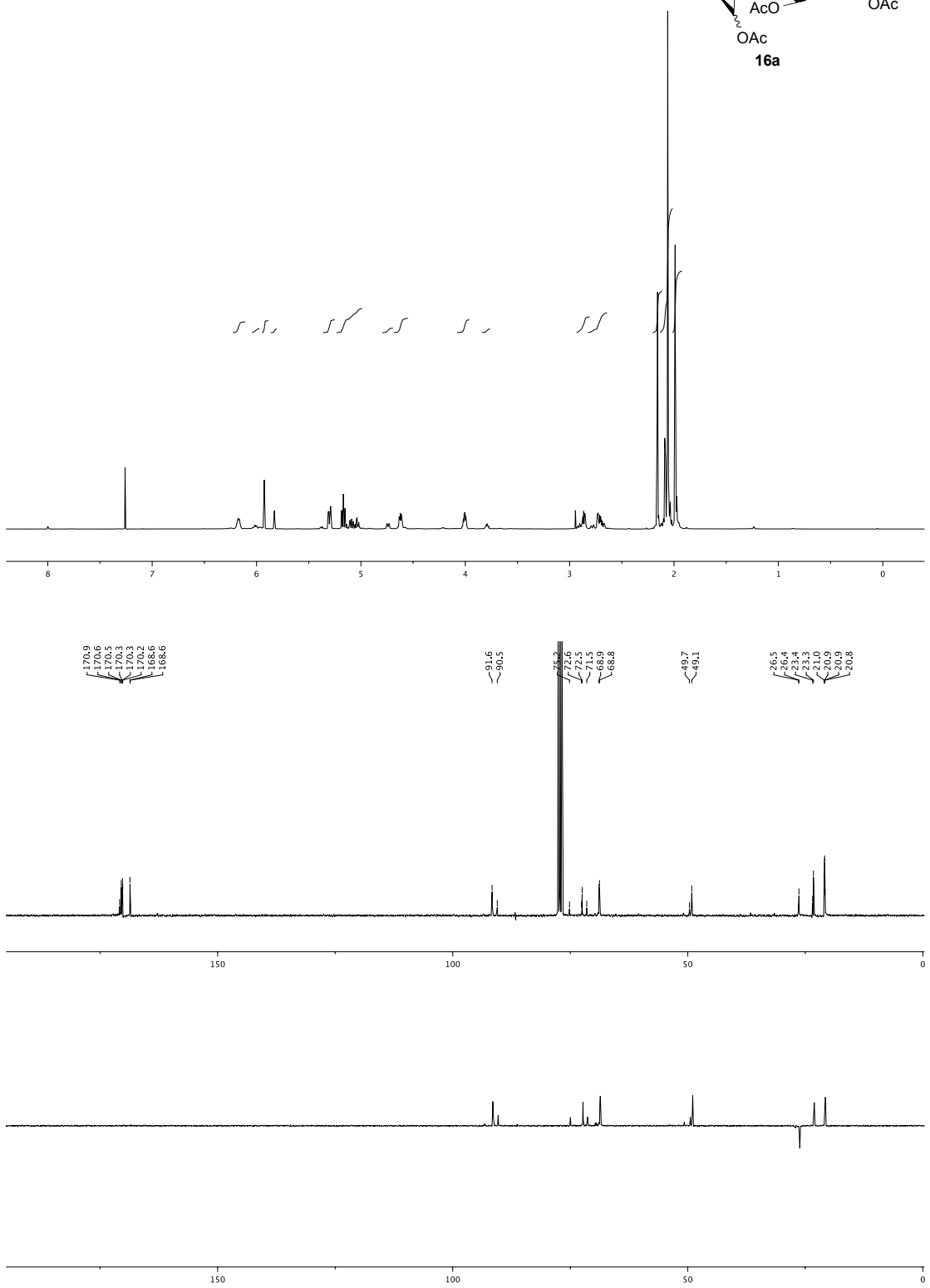
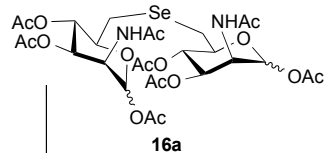


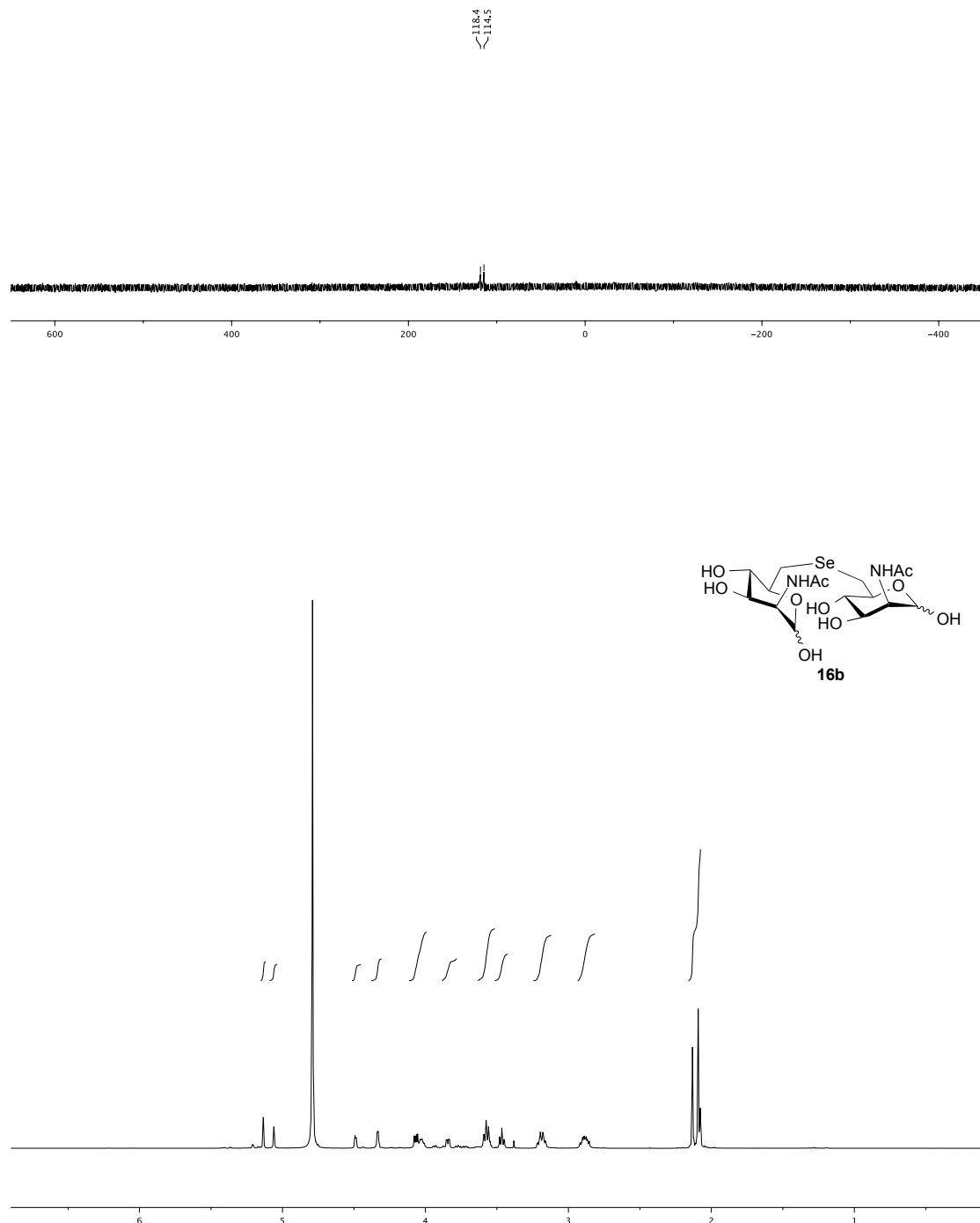


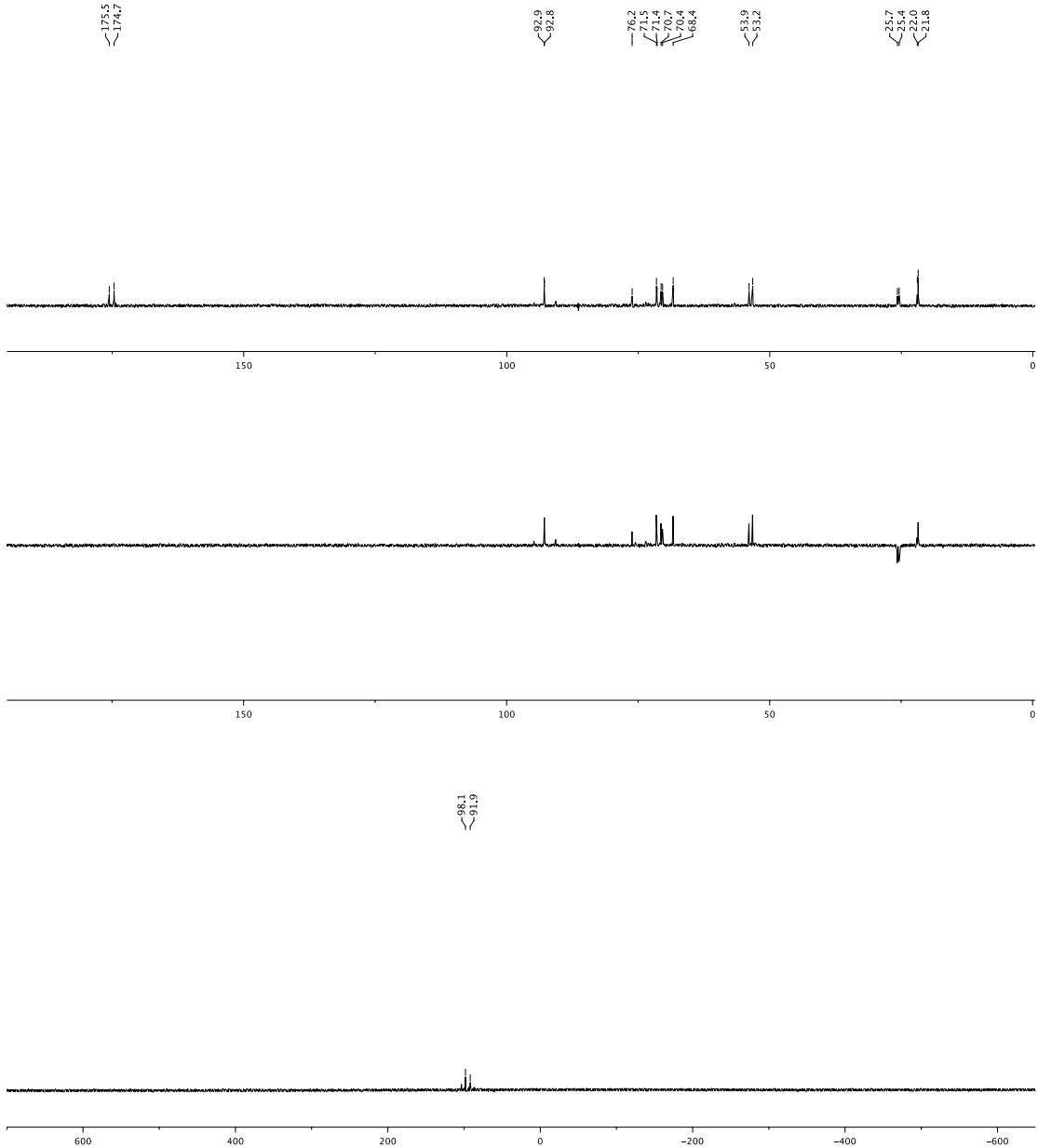
**19
(90)**

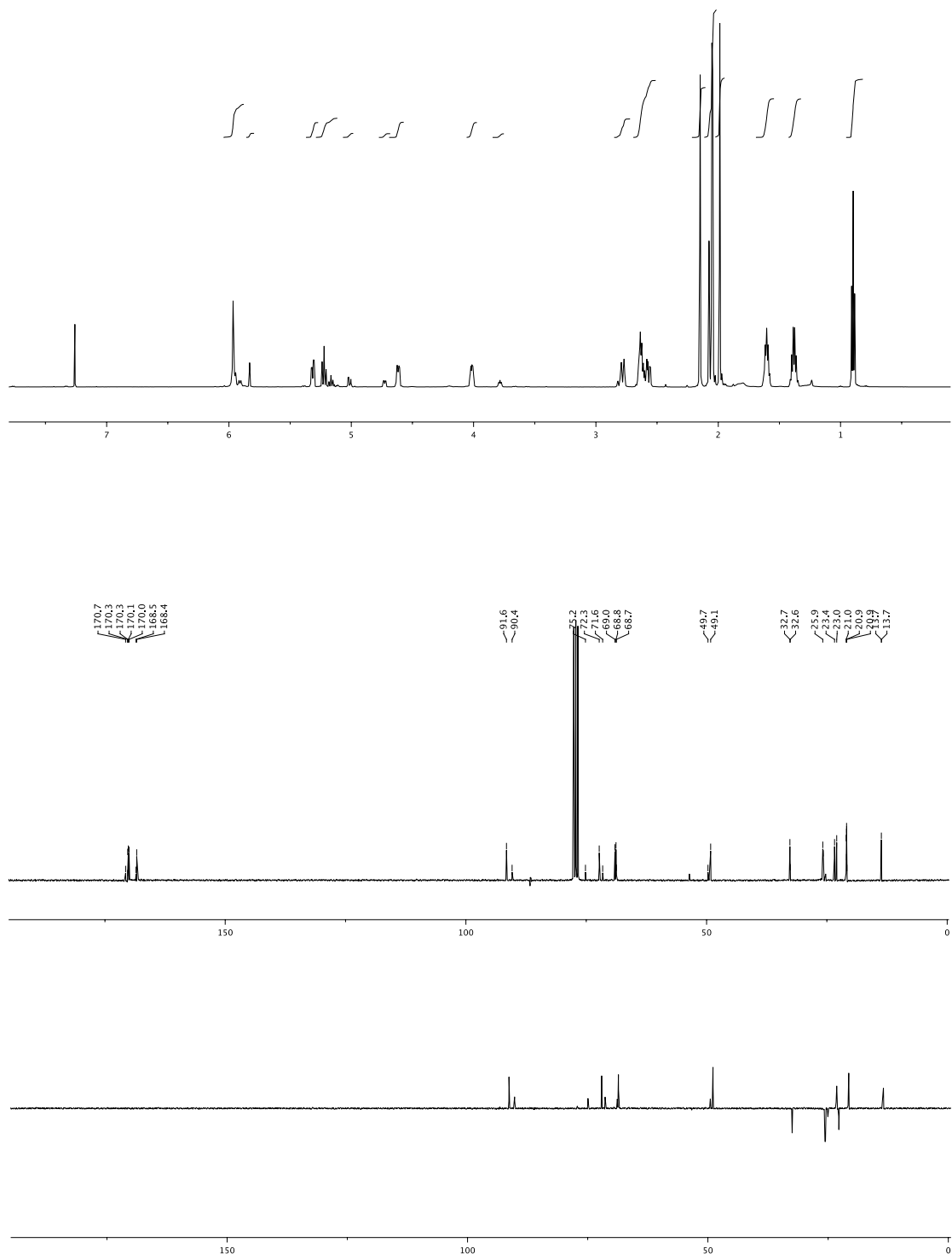
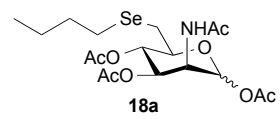


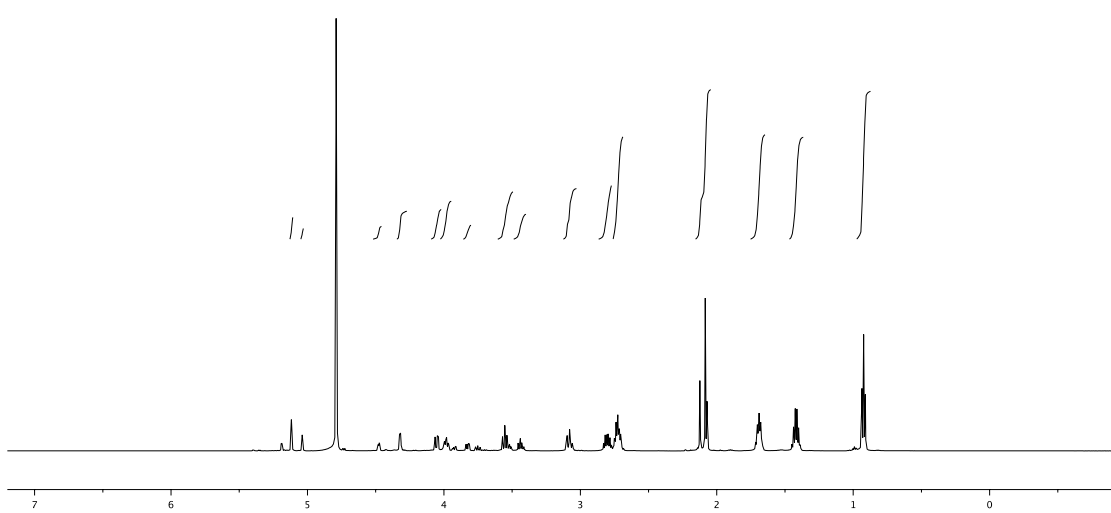
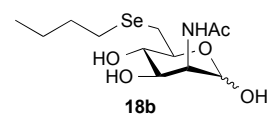
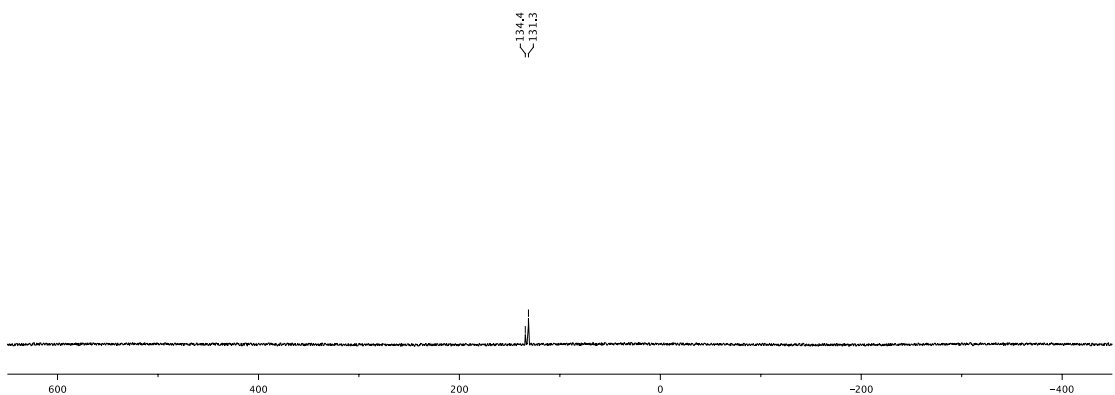
20
 (91)

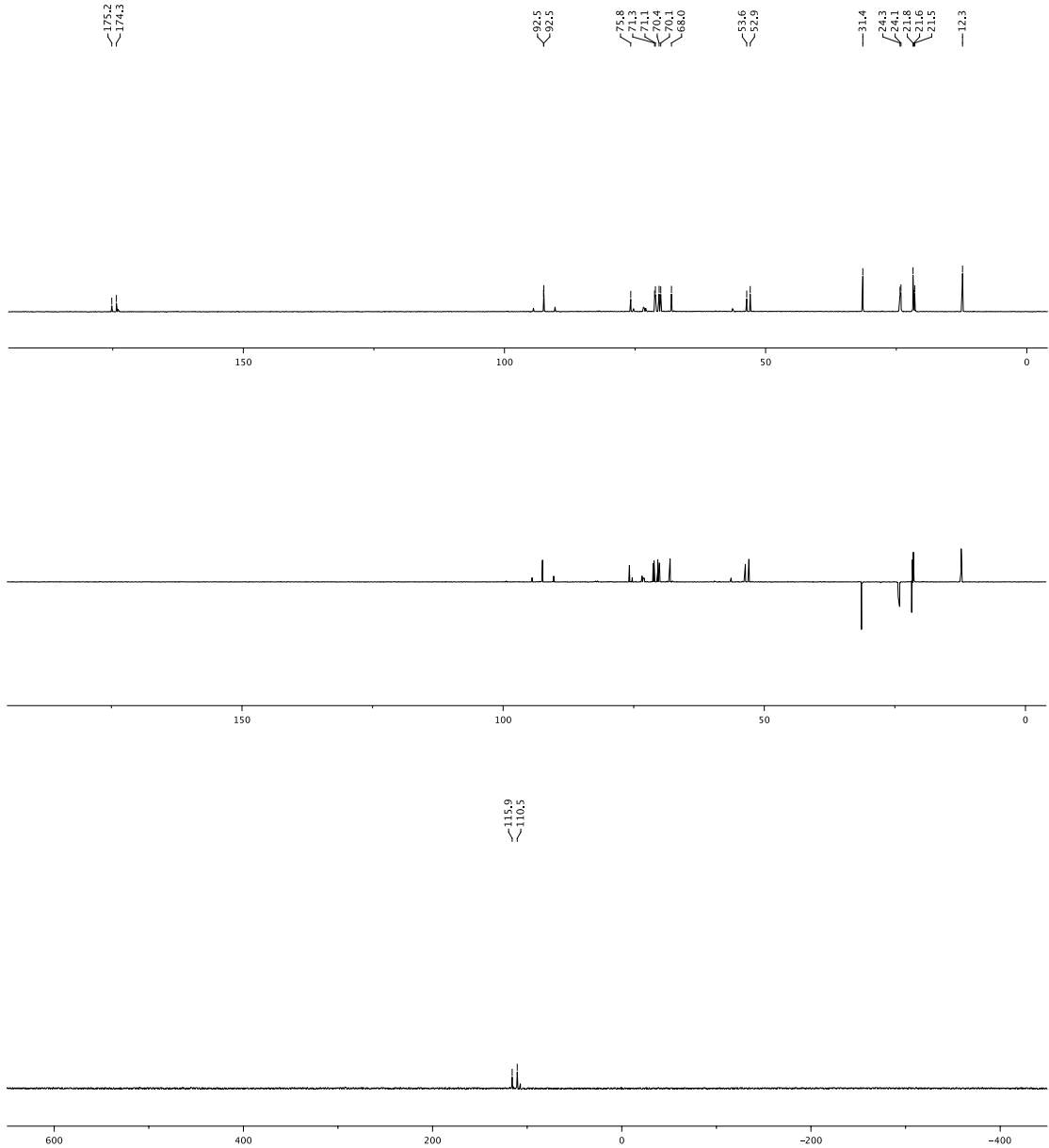










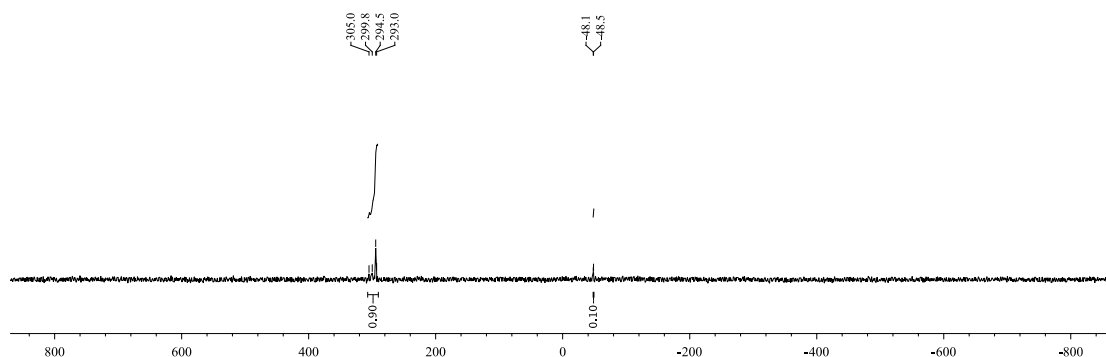


Evaluation of the stability of the diselenide **14b** in presence of dithiothreitol (DTT)

The possible reduction of diselenide bond was monitored by ^{77}Se NMR using a 60 mM solution of diselenide **14b** in aqueous saturated DTT solution at room temperature.

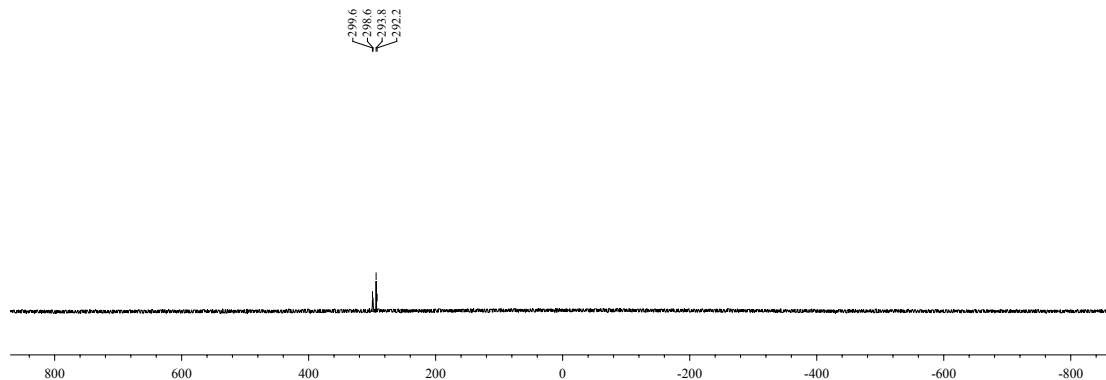
Immediately after the addition of **14b** to the DTT solution:

Diselenide **14b**/selenol (90:10): ^{77}Se NMR (114 MHz, D_2O) δ : 305.0, 299.8, 294.5, 293.0/-48.1, -48.5.



Time period between 15 min and 5 h:

Diselenide **14b**: ^{77}Se NMR (114 MHz, D_2O) δ : 299.6, 298.6, 293.8, 292.2.



The same experiment was performed using saturated glutathione solution instead of saturated DTT solution. In this case, only diselenide **14b** was detected.

Lebenslauf

Mein Lebenslauf wird aus datenschutzrechtlichen Gründen in der elektronischen Version meiner Arbeit nicht veröffentlicht.

Publikationsliste

Wratil PR, Horstkorte R, Reutter W. Metabolic glycoengineering with N-acyl side chain modified mannosamines. *Angew Chem Int Ed*. 2016, Aug 8;55(33):9482-512. *IF: 11.709*

Nieto-Garcia O*, **Wratil PR***, Nguyen LD, Böhrsch V, Hinderlich S, Reutter W, Hackenberger CPR. Inhibition of the key enzyme of sialic acid biosynthesis by C6-Se modified N-acetylmannosamine analogs. *Chem Sci*. 2016, 7, 3928 – 3933. *IF: 9.144*

Aretz J*, **Wratil PR***, Wamhoff EC, Nguyen HG, Reutter W, Rademacher C. Fragment-screening of N-acetylmannosamine kinase reveals non-carbohydrate inhibitors. *Can J Chem*. 2016, DOI: 10.1139/cjc-2015-0603. *IF: 1.003*

Erikson E, **Wratil PR**, Frank M, Ambiel I, Pahnke K, Pino M, Azadi P, Izquierdo-Useros N, Martinez-Picado J, Meier C, Schnaar RL, Crocker PR, Reutter W, Keppler OT. Mouse Siglec-1 Mediates trans-Infection of Surface-bound Murine Leukemia Virus in a Sialic Acid N-Acyl Side Chain-dependent Manner. *J Biol Chem*. 2015 Nov 6;290(45). *IF: 4.258*

Lorenz M, Koschate J, Kaufmann K, Kreye C, Mertens M, Kuebler WM, Baumann G, Gossing G, Marki A, Zakrzewicz A, Miéville C, Benn A, Horbelt D, **Wratil PR**, Stangl K, Stangl V. Does cellular sex matter? Dimorphic transcriptional differences between female and male endothelial cells. *Atherosclerosis*. 2015 May;240(1). *IF: 3.942*

Wratil PR*, Rigol S*, Solecka B, Kohla G, Kannicht C, Reutter W, Giannis A, Nguyen LD. A novel approach to decrease sialic acid expression in cells by a C-3-modified N-acetylmannosamine. *J Biol Chem*. 2014 Nov 14;289(46). *IF: 4.258*

*geteilte Erstautorenschaft

IF, Journal Impact Factor (InCites™ Journal Citation Reports®, Thomson Reuters, 2015)

Danksagung

Diese Arbeit ist Werner Reutter gewidmet. Er war von 2011 bis zum Frühling dieses Jahres der Betreuer meiner Doktorarbeit. Herr Prof. Reutter hat mich immer in meinen Vorhaben unterstützt. Er setzte sich für mich ein und ermöglichte es mir, in die Welt der Forschung einzutauchen. Werner Reutter war stets ein guter Gesprächspartner und wir führten unzählige Diskussionen, viele davon über meine Doktorarbeit, die Forschung und meine Zukunft. Ich sehe in ihm ein Vorbild und einen väterlichen Freund. Werner Reutter starb im Mai 2016 nach kurzer, schwerer Krankheit. Die Erinnerungen an ihn werden mich ein Leben lang begleiten.

Ich danke Herrn Prof. Tauber, dass er sich sofort und ohne Umstände dazu bereit erklärt hat, die Betreuung meiner Doktorarbeit zu übernehmen.

Ganz besonders möchte ich Long Duc Nguyen danken, der mich während meiner gesamten Doktorarbeit begleitet hat und von dem ich einen Großteil meiner technisch-experimentellen und didaktischen Fähigkeiten erlernt habe. Er hat meine Ergebnisse stets kritisch hinterfragt und mir dadurch gezeigt, was gute experimentelle Forschung ausmacht.

Den anderen Mitgliedern unseres Labors und befreundeter Arbeitsgruppen, Yujing Yao, Hoang Giang Nguyen, Felix Bröcker, Paulina Kaplonek, Jonas Aretz, Eike Wamhoff, Christoph Rademacher, Daniel Kolarich, Jonas Hanske und Anika Reinhardt danke ich für die gute Zusammenarbeit und dafür, dass sie immer hilfsbereit waren.

Ich möchte auch den Kooperationspartnern aus anderen Laboren und Instituten danken – im Besonderen Stephan Hinderlich, Rüdiger Horstkorte, Christian Hackenberger, Oliver Keppler, Athanassios Giannis, Olaia Nieto-Garcia, Stephan Rigol, Tomas Trnka, Christoph Kannicht, Guido Kohla, Barbara Solecka, Mario Lorenz, Christian Mieville, Verena Böhrsch und Martin Frank.

Des Weiteren möchte ich Herrn Prof. Seeberger dafür danken, dass ich immer und ohne jede Einschränkung Geräte des Max-Planck-Instituts für Kolloid- und Grenzflächenforschung nutzen durfte.

Ich danke Herrn Prof. Scherer für unzählige ergiebige Diskussionen und dafür, dass er mich an seiner eigenen Forschung teilhaben ließ.

Zuletzt danke ich meinen Eltern für ihre Unterstützung. Ohne sie wäre mir ein Einblick in die Grundlagenforschung verwehrt geblieben.